universität wien

DISSERTATION

Titel der Dissertation

Drug metabolising enzymes and cellular uptake transporters as key factors for the efficacy of anti-cancer agents

Verfasst von

Mag.pharm. Stefan Brenner

angestrebter akademischer Grad

Doktor der Naturwissenschaften (Dr.rer.nat)

Wien, 2014

Acknowledgements

TABLE OF CONTENTS

1 Summary

As cancer represents one of the leading diseases and causes of death world-wide drugs focusing on prolonging life, symptom relief, minimizing side effects and improving quality of life are highly required. For that reason it is crucial to understand interactions of anti-cancer agents with the human body and in particular with cancer tissue. Absorption is the first interaction of anti-cancer agents and the human body. Considering e.g. oral or topical drug application it is necessary to understand that drugs have to enter the bloodstream before any medical effects can take place. For that reason it plays a major role in drug development. In the next step the drug is distributed in several tissues or so called compartments to reach interstitial and intracellular fluids. This distribution is influenced by several factors e.g. vascular permeability, regional blood flow, cardiac output and perfusion rate of the tissue lipid solubility and the ability of the drug to bind tissue and plasma proteins. Furthermore, expression of active and passive transporters in specific tissue types and the affinity of drugs for these transporters can make the difference between effective treatment or severe side effects. Metabolism can be divided into phase I and phase II and is mainly carried out in the liver where xenobiotics are (in the first step) made more polar and (in the second step) are conjugated with e.g. glucuronides or sulphates. This metabolising process can on the one hand detoxify or on the other hand generate more potent substrates. Therefore, in drug therapy and development it is crucial to understand the way a specific drug is metabolised. In this thesis we therefore investigated metabolic and cellular uptake mechanisms of natural and synthetic compounds and their effect on anti-cancer activity.

Additionally we also investigated the specific expression of OATPs and their role in drug distribution in SCLC. **Lung cancer** is the leading cause of cancer-related death in Western countries and small-cell lung cancer (SCLC) accounts for 15% to 20% of all lung cancer types. SCLC is characterized by rapid tumor doubling time, a high growth fraction and the development of widespread metastases, especially to the brain, at a rather early stage in the disease. In contrast to the majority of non-small cell lung cancers (NSCLC), SCLCs express neuroendocrine markers (e.g., chromogranin A, synaptophysin) and are thought to originate from lung neuronal precursor cells, from which other neuroendocrine tumors in the lung (e.g., carcinoids) are also derived. Importantly, SCLC cells, but not carcinoids, are usually highly responsive to initial chemotherapy, usually with a platin derivative-containing regimen

in combination with etoposide. However, a subsequent relapse of SCLC often occurs within 2 years that is often resistant or has only a mild response to further treatment. Only 10% of advanced patients survive longer than 2 years, leading to a five-year survival rate of only 3% to 7%. Therefore, clues to a more effective treatment for primary SCLC and its metastases are of utmost interest. In lung cancer, transporter effects on absorption, distribution and elimination of xenobiotics as well as in drug-drug interactions is increasingly being recognized. For that reason, this study aimed to investigate SCLC cell lines for their OATP expression. We used cell lines from primary and metastatic SCLC tumors as well as pulmonary carcinoid cells and performed immunofluorescence and immunohistochemistry on paraffin-embedded SCLC samples. Furthermore, the mRNA expression of OATP4A1, OATP5A1 and OATP6A1 was assessed in cell lines that were exposed to the chemotherapeutic drugs cisplatin, etoposide and topotecan, which are all applied in SCLC therapy. Chromogranin A and synaptophysin were used as markers for neuroendocrine differentiation of the tumor cells, and cadherin-1 was applied as a marker for the epithelial origin of cells.

The next study focused on **Resveratrol** (trans-3,5,4´-trihydroxystilbene) which is a natural occurring compound found at high levels in grapes, berries, peanuts and red wine. Over the last decade, it has been shown that resveratrol exhibits a wide variety of biological and pharmacological properties. In several in vitro and animal models, resveratrol has been found to be active in the prevention and treatment of cancer, cardiovascular diseases, inflammation, ischemic injuries and neurodegenerative diseases, and resveratrol may also act as an anti-obesity and anti-aging compound. These effects are observed despite the extremely low bioavailability of resveratrol and its rapid clearance from the circulation due to extensive glucuronidation and sulfation in the intestine and liver. It is unknown whether resveratrol and its metabolites can accumulate to bioactive levels in organs and tissues through active transport mechanisms or if resveratrol's transport is carried out solely passively. However, passive diffusion does not explain the accumulation of resveratrol to bioactive levels in targeted organs. Following intravenous application of resveratrol to mice and rats, resveratrol is distributed into various organs, such as the liver, kidney, lungs and spleen, whereas moderate concentrations are found in the heart, testes and brain. Furthermore, in all of the analysed organs, conjugated metabolites are detected at concentrations that are higher than the concentrations of the parent

resveratrol, which strongly suggests the existence of active uptake transport mechanisms.

In addition we investigated **Flavopiridol** (FLAP) which is a semi-synthetic analog of rohitukin, a main constituent of the herbal drug Dysoxylum binectariferum which is used in traditional indian folk medicine, presently undergoing clinical phase II trials It is a selective inhibitor of cyclin dependent kinases (cdk1, cdk2, cdk4, cdk7). Due to the crucial role of CDK activity for cells during the phases of the cell cycle the CDK inhibition with flavopiridol leads to a block in cell cycle progression at the G1 to S and G2 to M interface which has been proofen in several cell lines. In other cell lines, it has been demonstrated to induce apoptosis and to exhibit proapoptotic and antiangiogenic properties. FLAP also exerts pronounced antitumor activity in a variety of cells. Clinical trials with FLAP as a single agent or in combination with anticancer drugs, including taxanes and gemcitabine, also showed tumor responses in most phase I and phase II studies on different types of progressive tumors refractory to conventional treatment. However, therapeutic success rates for flavopiridol show different response rates during therapy. Therefore, the aim of our study was to investigate the uptake kinetics and interactions of flavopiridol in OATP1B1, OATP1B3 and OATP2B1 transfected Chinese hamster ovary cells (CHO) with wild type cells as a control. Furthermore we wanted to determine uptake kinetics in human ZR-75-1 breast cancer cells versus OATP1B1 knock-out ZR-75-1 breast cancer cells to elucidate the role of OATP transporters in the uptake of flavopiridol and therefore, in cancer therapy. We also demonstrated uptake inhibition of flavopiridol with the known OATP substrate rifampicin and showed by FACS, analyses a clear incidence for a higher cell cycle arrest in the G2/M phase for ZR-75-1 wild type cells compared to OATP1B1 knock-out cells

In addition we investigated the effect of **anthocyans,** ingredients of common food supplements, on human hepatocytes. Food supplements and other products promising health benefits, prolonging of life and in general an improved life quality have become more and more popular in the last decades,(especially in the western society). This lifestyle trend has become a huge, still growing market where benefits for the consumer have not always highest priority as dose toxicity and proof of biological effectiveness are concerned. Especially due to the fact that food supplements and products obtained from food are by the FDA classified as food and not as drugs although concentrations of food ingredients are many times higher in

food supplements than in actual food. Therefore, in this study we investigated the effect of anthocyanidins and anthocyanins, found in fruit extracts, on OATP1B1 and OATP1B3 expression in human hepatocytes (LH45, LH46, LH47, LH49, HEP220670). Anthocyans are widespread natural flavonoids that occur in all tissues of higher plants and are therefore widely-found in food of plant origin. PH and their ability of forming chelating complexes with metal ions are responsible for their colour schema ranging from blue to red. Among anthocyans glycosides from the aglycons cyanidin, delphinidin, malvidin, pelargonidin, peonidin, and petunidin represent the most abundant group in fruits. This substance class displays a plethora of biological effects, including antiproliferative, antiapoptotic, antitumor, antimutagenic, antioxidant, antiradical, and nitric oxide inhibitory effects. In our investigation we screened a broad variety of anthocyanidins and anthocyanins, via real time qPCR and western blotting. We could show effects on OATP1B1 and OATP1B3 mRNA up and down regulation. For this reason we think that recent effects of these substances on the uptake of drugs which are substrates for OATP1B and OATP1B3 are immanent.

In addition plant extracts containing **Lobatin B and Neurolenin B** were studied to investigate their anti-tumor potential. Traditionally, plants have been used as remedies to treat and cure diseases including tumours. In fact, more than 60% of the currently used anti-cancer agents are derivatives of natural products. We investigated the Central American plant Neurolaena lobata (L.) R.Br. ex Cass. (Asteraceae), which is pharmacologically active and used against ulcers, inflammatory skin disorders, malaria, ringworm, dysentery and fungal infections. For this, it was important that the dichloromethane phase fractions of the metanolic leaf extract and the ethanolic leaf extract were active in the carrageenan-induced mouse paw oedema model, indicating that the extracts still contained the in vivo active principles. It has recently been shown that the apolar extract of N. lobata inhibited the expression of the fusion onco-protein NPM/ALK, which is generated by the t(2;5)(p23;q35) translocation and responsible for the development of ALCL occurring mostly in patients at young age. The standard combination therapy (consisting of cyclophosphamide, doxorubicine, vincristine and prednisone) does not directly target the oncogenes that are involved in ALCL (NPM/ALK, JunB, PDGFR) and is known to damage DNA. This increases the likelihood of developing secondary malignancies later in life. To provide more specificity and reducing the risk of recurrent disease and

consecutive cancers synthetic inhibitors particularly targeting ALK, Critozinib and NVP-TAE-684, have been developed and tested in clinical trials. Here we studied natural products that interfere with NPM/ALK expression to decide about the feasibility of the development of a new drug from the isolated leads.

2 Zusammenfassung

Da Krebs eine der führenden Krankheiten und Todesursachen weltweit repräsentiert, werden Medikamente mit dem Schwerpunkt auf Linderung, Lebensverlängerung der mit Krebs assoziierte Symptomen, auf Therapie bezogene Toxizitäts-Minimierung und Verbesserung der Lebensqualität dringend gebraucht. Aus diesem Grund ist es wichtig, das Zusammenspiel von Krebstherapie und dem menschlichen Körper, im speziellen in Bezug auf das Krebsgewebe, zu verstehen. Absorption, welche die erste Interaktion zwischen einem Medikament und dem menschlichen Körper repräsentiert, ist besonders wichtig für die Beispiele der oralen und topische Anwendung von Medikamenten, da jede Substanz vorerst das Blutsystem erreichen muss um eine medizinische Wirkung zu entfalten, (woraus sich auch die Wichtigkeit dieses Punktes auf die Medikamentenentwicklung erschließt). Im nächsten Schritt wird das Medikament in verschiedene Gewebe verteilt, auch sogenannte Kompartimente um interstitielle und intrazelluläre Flüssigkeiten zu erreichen. Diese Verteilung wird von verschiedenen Faktoren beeinflusst, wie zum Beispiel vaskuläre Permeabilität, regionaler Blutfluss, Herzleistung und Perfusionsrate des Gewebes ihrer Fettlöslichkeit, die Fähigkeit des Medikaments an Gewebe und Plasmaproteine zu binden. Weiters kann das Vorhandsein von aktiven und passiven Transportern in bestimmten Gewebetypen und die Affinität von Medikamenten zu diesen den Unterschied zwischen einer wirksamen Behandlung oder schweren Nebenwirkungen machen. Metabolismus in der Leber wird hauptsächlich in Phase I und II unterteilt, wobei Fremdstoffe in Phase I polarer und in Phase II beispielsweise mit Glucuroniden oder Sulfate konjugiert werden. Durch diesen Vorgang können Substrate entweder entgiftet oder in ihrer Wirkung verstärkt werden. Für die medikamentöse Therapie und die Entwicklung neuer Arzneistoffe ist es wichtig zu verstehen, auf welche Art und Weise das Medikament metabolisiert wird. Aus diesem Grund wurde in dieser Arbeit untersucht, inwiefern Metabolismus und zellulärer Aufnahme von natürlichen und synthetischen Verbindungen die Wirkung gegen

Krebs beeinflussen. Auch die spezifische Verteilung von OATPs in SCLC wurde untersucht.

Lungenkrebs ist die führende krebsbezogene Todesursache in der westlichen Welt, wobei kleinzelliges Lungenkarzinom (SCLC) 15% bis 20% aller Lungenkrebsarten ausmacht. SCLC zeichnet sich durch eine hohe Tumorverdopplungsrate, ein hohe Wachstumsrate und einer weit verbreitete Metastasierung, vor allem in frühen Krankheitsstadien ins Gehirn, aus. Im Vergleich zu dem wesentlich häufiger auftretenden nicht kleinzelligem Lungenkarzinom (NSCLC), weist SCLC neuroendokrine Marker auf (z.B.: Chromogranin A, Synaptophysin), welche vermutlich von neuronalen Vorläuferzellen in der Lunge stammen und von denen andere neuroendokrine Tumore in der Lunge (z.B. Karzinoide) ebenfalls abgeleitet werden. Wichtig hierbei ist, dass SCLC-Zellen, nicht aber Karzinoide, normalerweise sehr gut auf die initiale Chemotherapie ansprechen, welche normalerweise aus einem platinhaltigen Derivat in Kombination mit Etoposid besteht. Dieser anfängliche Therapieerfolg wird aber durch ein sehr hohes Wiederauftreten von SCLC nach ca. 2 Jahren überschattet, wobei diese Krebszellen zusätzlich meist wenig bis gar nicht auf die initiale Therapie reagieren. Nur 10% der Patienten überleben länger als 2 Jahre was zu einer Überlebensrate von nur 3% bis 7% führt. Daher sind Ansätze für eine wirksamere Behandlung von primärem SCLC und dessen Metastasen von höchstem Interesse. Im Bereich Lungenkrebs wird die Rolle von Transportern im Bezug auf Absorption, Verteilung und Ausscheidung sowie bei Medikamenten-Interaktionen zunehmend anerkannt. Aus diesem Grund wurde in dieser Studie die Verteilung von OATPs in SCLC Zelllinien untersucht. Es wurden Zelllinien von primären und metastatischen SCLC Tumoren sowie Lungen Karzinoid-Zellen verwendet um Immunfloreszenz und immunhistochemische Untersuchungen durchzuführen. Ferner wurde die mRNA-Expression von OATP4A1, OATP5A1 und OATP6A1 in Ziellinien, welche mit den normalerweise in der SCLC Therapie angewendeten Chemotherapeutikan Cisplatin, Etoposid und Topotecan behandelt wurden, untersucht. Chromogranin A und Synaptophysin wurden als Marker für neuroendokrine Differenzierung der Tumorzellen untersucht und Cadherin-1 wurde als ein Marker für den epithelialen Ursprung der Zellen angelegt.

Eine weitere Studie bezog sich auf **Resveratrol**, eine natürlich vorkommende Verbindung, welche in hohen Konzentrationen in Weintrauben, Beeren, Erdnüssen und Rotwein vorkommt. In den letzten Jahrzenten wurde bewiesen, dass Resveratrol

eine weite biologische und pharmakologische Wirkungspalette aufweist. In mehreren in vitro und Tiermodeln wurde die Wirksamkeit von Resveratrol gegen Krebs, kardiovaskulären Erkrankungen, Entzündungen, ischämischen Verletzungen und neuroendokrinen Erkrankungen gezeigt. Weiters könnte Resveratrol auch als ein Mittel gegen Fettleibigkeit und im Anti –Ageing Bereich eingesetzt werden. Interessanterweise können diese Effekte trotz der sehr geringen Bioverfügbarkeit von Resveratrol und der hohen Clearance aufgrund extensiver Glucuronidierung und Sulfatierung im Darm und in der Leber beobachtet werden. Es ist bislang nicht bekannt, ob Resveratrol oder dessen Metabolite in Geweben oder Organen durch aktiven Transport soweit akkumulieren können, um bioative Level zu erreichen, oder, ob der Transport ausschließlich passiv erfolgt. Jedenfalls erklärt passive Diffusion nicht die Akkumulation von Resveratrol in verschiedenen Gewebetypen. Aufgrund von Studien mit Mäusen und Ratten weiß man, dass sich Resvertrol in hohem Maße in Leber, Niere, Lunge und Milz anlagert, wohingegen beispielsweise in Herz , Hoden und Gehirn vergleichsweise geringe Konzentrationen zu finden sind. Weiters wurde in allen analysierten Organen eine wesentlich höhere Konzentration an Metaboliten gefunden, die höher als die verabreichte Resveratrol-Konzentration war, was auf aktiven Transport schließen lässt.

Zusätzlich wurde **Flavopiridol**, ein semi-synthetisches Analog von Rohitukin, welches ein Hauptbestandteil der pflanzliche Droge *Dysoxylum binectariferum* ist und in der indischen Volksmedizin Verwendung findet untersucht. Diese Substanz befindet sich im Moment in klinischer Testphase II und ist ein selektiver Inhibitor der cyklin abhängigen Kinasen (CDK1, CDK2, CDK4, CDK7). Aufgrund der wichtigen Rolle von CDK Aktivität für Zellen während des Zellzykluses bewirkt eine Inhibition mit Flavopiridol eine Blockade des Zellzykluses im Bereich der Interphase G1 zu S und G2 zu M, was in verschiedene Zelllinien bewiesen wurde. Weiters konnten Apoptose induzierende, proapoptotische, antiangiogenische und eine anti-Tumor-Aktivität nachgewiesen werden. Klinische Studien mit FLAP als Einzelmedikation oder in Kombination mit Krebsmedikamenten wie zum Beispiel Taxanen und Gemcitabin zeigten gute Ergebnisse in Phase I und Phase II in verschiedenen Tumoren, welche Resistenz gegen normale Therapie zeigten. Flavopiridol jedoch weist unterschiedliche Ansprechraten während der Therapie auf. Aus diesem Grund war das Ziel unserer Studie, die Aufnahme-kinetik und Interaktionen von Flavopiridol mit OATP1B1, OATP1B3 und OATP2B1 in transfizierten Chinese hamster ovary cells

(CHO) mit untransfizierten Zellen als Kontrolle zu erforschen. Des weiteren wollten wir die Aufnahme-kinetik in humanen ZR-75-1 Brustkrebszellen OATP1B1 knock out ZR-75-1 Brustkrebszellen gegenüberstellen, um die wichtige Rolle der OATPs für die Aufnahme von Flavopiridol und demzufolge, in der Krebstherapie hervorzuheben. Wir konnten außerdem demonstrieren, dass die Flavopiridol-Aufnahme durch den bekannten Inhibitor Rifampicin gehemmt wird. Eine FACS-Analyse zeigte, dass einen wesentlich größeren Zellzyklusarrest in der G2/M Phase in ZR-75-1 Zellen, verglichen zu den OATP1B1 knock-out Varianten.

Eine weitere Studie befasste sich mit dem Effekt von **Anthocyanen**, welche Teil von Nahrungsergänzungsmitteln sind, auf humane Hepatozyten. Nahrungsergänzungsmittel und andere Produkte, welche positive Gesundheitseffekte, Lebensverlängerung und im Allgemeinen eine Verbesserung der Lebensqualität versprechen wurden in den letzten Jahrzenten vor allem in den westlichen Ländern immer beliebter. Dieser Trend ist in der Zwischenzeit zu einem großen, immer noch wachsenden Markt geworden, in welchem der Konsumentenschutz, im speziellen bezogen auf Dosistoxizität und Beweis von biologischen Effekten nicht immer höchste Priorität hat. Dieser Missstand lässt sich unter anderem auf die Tatsache zurückführen, dass Nahrungsergänzungsmittel durch die FDA als Nahrungsmittel klassifiziert sind und nicht als Medikamente, obwohl die Inhaltsstoffe in diesen um ein Vielfaches konzentrierter vorkommen können als in den tatsächlichen Nahrungsmitteln. Aus diesem Grund untersuchten wir den Effekt von Anthocyaninen und Anthoyanidinen, welche in Fruchtextrakten vorkommen, auf die OATP1B1 und OATP1B3 Expression in humanen Hepatozyten (LH45, LH46, LH47, LH49, HEP220670). Anthocyane sind weit verbreitete Flavonoide, welche in allen Geweben höherer Pflanzen vorkommen und daher sehr oft in Nahrungsmittel auf Pflanzenbasis zu finden sind. Der pH-Wert und Metall-Chelat-Komplexe sind verantwortlich für deren blaue bis rote Farbgebung. Unter den Anthocyanen repräsentieren Glycoside der Aglyca Cyanidin, Delphinidin, Malvidin, Pelargonidin, Peonidin und Petunidin die größte Gruppe. Diese Substanzklasse zeigt eine Vielzahl an biologischen Effekten wie zum Beispiel antiproliferative, antiapoptotische, antitumorale, antimutagene, antioxidative und Stickstoffmonoxid-hemmende Wirkung. In dieser Studie wurde eine breite Palette von Anthocyanen mittels qPCR und Western Blotting untersucht und konnten auf-und-ab Regulation von OATP1B1 und OATP1B3 feststellen. Aus diesem Grund sind wir der Meinung,

dass Auswirkungen dieser Substanzen auf die Aufnahme von Medikamenten, welche OATP1B1 und OATP1B3 Substrate sind immanent sind.

Zusätzlich wurden Pflanzenextrakte, welche **Lobatin B und Neurolenin B** beinhalten, auf deren Wirkung gegen Krebs untersucht. In der Volksmedizin wurden hauptsächlich Pflanzen eingesetzt, um Krankheiten zu heilen, darunter auch Krebs. Tatsächlich sind 60% der heute eingesetzten Medikamente gegen Krebs pflanzlichen Ursprungs. Unter Berücksichtigung dieser Umstände untersuchten wir die zentralamerikanische Pflanze Neurolaena lobata (L.) R.Br. ex Cass. (Asteraceae), welche pharmakologisch aktiv ist und gegen Geschwüre, entzündliche Hauterkrankungen, Malaria, Flechten, Ruhr und Pilzinfektionen eingesetzt wird. Für diese Untersuchungen war es wichtig, dass die Dichlormethanfraktion des Methanolextraktes der Blätter und der Ethanolextrakt der Blätter in den Carrageeninduzierten Maus-Pfotenödem-Modellen aktiv waren, was darauf hinweist, dass die Extrakte noch die in vivo wirksamen Bestandteile enthalten. Es wurde gezeigt, dass der apolare Extrakt von N. lobata die Expression des Fusions-Onko-proteins NPM/ALK, welches durch eine t(2;5)(p23;q35)-Translokation gebildet wird und für die Ausbildung von ALCL verantwortlich ist, was hauptsächlich in jungen Patienten vorkommt. Die Standardkombinationstherapie (bestehend aus Cyclophosphamid, Doxorubicin, Vincristin und Prednison) beeinflusst nicht direkt die Onkogene, welche in ALCL involviert sind (NPM/ALK, JunB, PDGFR) und für DNS-Schäden bekannt sind. Dies erhöht die Chance von Sekundärerkrankungen im weiteren Lebensverlauf. Um mehr Spezifität und das Risiko von wiederkehrenden Krankheiten und Krebserkrankungen zu minimieren wurden synthetische Inhibitoren im Besonderen auf ALK, Critozinib und NVP - TAE -684 gerichtet entwickelt und in klinischen Studien getestet. Darum untersuchten wir natürliche Produkte, welche mit NPM / ALK interferieren und deren Expression stören, um über die Durchführbarkeit der Entwicklung eines neuen Medikaments aufgrund der gefunden Leadstrukturen des Extraktes zu entscheiden.

3 Introduction

3.1 Cancer

Cancer is still one of the major health issues in western countries and ranges among the top 4 causes of death. New Cancer incidences in Europe estimated for 40 countries in 2012 for male population was highest for prostate (22.8%), lung (15.9%), and colorectum (13.2%) with a mortality rate of lung (26.1%), colorectum (11.6%) and prostate (9.5%). For female population new incidence were highest for breast (28.8%), colorectum (12.7%) and lung (7.4%) with a mortality rate for breast (16.8%), colorectum (13.0%) and lung (12.7%) for female [2]. The major problems in cancer therapy are severe side effects, low patient compliance and active efflux transporters lowering the availability of anti-cancer drugs resulting in therapy resistance [3]. This active efflux transport represents the first defense of cells against xenobiotics which explains the crucial role of upregulated ABC transporters in cancerous tissue during therapy resulting in low therapy effects [3, 4]. Therefore new drugs evading AET systems or inhibiting them and using transporter systems in tumor tissue to increase drug concentrations are needed [3].

3.2 Cellular Drug Transport

Besides paracellular, transcellular and intracellular vesiculation pathways for xenobiotics as they can be seen in figure 1[5] also active ways of drug transport have
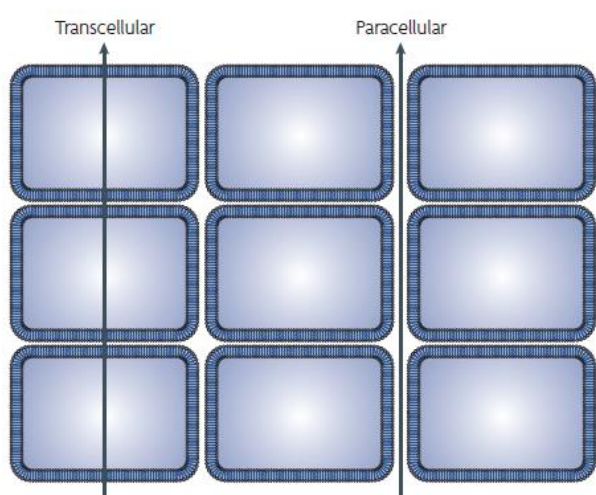
Figure 1 Molecular transmembrane transport [1]

to be considered especially concerning drug distribution into specific tissue, occurrence of specific altered drug concentrations throughout the human body and accumulation of substances in levels exceeding intracellular binding sides [1, 6]. Furthermore based on Lipinski's 'rule of 5' some administered drugs like antibiotics, antifungals, vitamins and cardiac glycosides do exceed at least two of the following parameters: molecular mass >500 Daltons, octanol–water partition coefficient t cLogP >5, number of hydrogen-bond donors >5, and number of hydrogen-bond
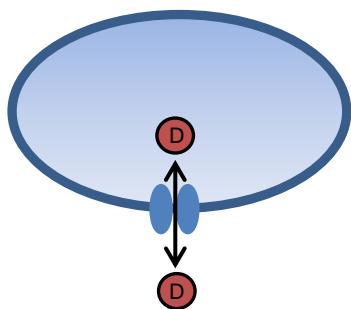
Figure2 Transmembrane transport of drugs via transporters

acceptors >10 and are therefore considered to have poor absorption which is in fact not the case [1, 7]. To explain these facts it is assumed that drug transport is partly carried out via transporters in the membrane which normally transport endogenous cellular and extracellular metabolites. [1, 5]. Figure 2 describes the membrane associated compartment which consists of a lipid membrane where transport proteins are embedded. The drug (D) can diffuse into the lipid bilayer of the membrane and re dissolves in the intracellular compartment where it can also be actively taken up or carried out via a transporter of the ABC or SLC family [1, 5].

3.2.1 ABC – Transporters

ABC (ATP – binding cassette) transporters are a large transporter protein family which needs ATP hydrolysis to implement their function as transporters of endogenous substrates and drugs across various membranes in the human body [8]. They are found to be associated with many important biological processes in prokaryotes where they act as importers and exporters and in eukaryotes where they act as exporters solely [9, 10]. Their physiological function in defending the human body against cytotoxic activity from xenobiotics by actively carrying them out of the cell is one main reason for their role in drug resistance during therapy against microorganisms and cancer [11]. Especially the well characterised P – glycoprotein (P-gp), multidrug resistance protein (MRP) and breast cancer resistance protein (BCRP) transporters play a crucial role in multidrug resistance in cancer [3].

P – Glycoprotein

As a member of the ABC – transporter family P-gp is an ATP powered efflux pump with multiple substrate specificity and no apparent structural similarity among them [3, 9, 12]. Under physiological conditions the role of P-gp is the protection of sensitive organs and tissues from xenobiotics and toxins [13]. This fact also arises from its distribution in tissue types/organs with excretory function like bile canalicular membranes of hepatocytes in the liver, proximal tubules in the kidney and enterocytes lining the wall of the intestine [14]. Besides their role in protecting tissue

from the influence of toxins P-gp transporters are thought to play a major role in production and secretion of cortisol and other steroids due to their expression in tissue responsible for steroid hormone biosynthesis [15-17]. Furthermore due to their importance in determining blood levels of its substrate drugs P-gp transporters are crucial in cancer therapy and play a major role in resistance development of many cancer types [18-21]. This theory was approved as mice with P-gp deficits show dramatically increased levels of paclitaxel [22], etoposide (ETP) [23], erlotinib [24], and sorafenib [25], which are approved anticancer drugs and P-gp substrates [21, 26].

Multidrug resistance proteins

Apart from multidrug resistance protein P-gp other efflux transporters also have an impact on resistance development in cancer therapy such as multidrug resistance associated proteins MRP 1-9 [27-29]. Besides a wide range of endogenous substrates and toxins studies confirmed their ability to transport many anti-cancer drugs like etoposide, cisplatin, doxorubicin, epirubicin, 6-mercaptopurine, topotecan, and methotrexate [30-35]. MRP7 confers resistance to docetaxel, paclitaxel, and vincristine [36]. This fact makes the MRP transporter family crucial to consider in cancer therapy and a valuable target for new therapy approaches especially for inhibitors of MRPs [3, 37]. They are generally expressed an basolateral membranes in polarized epithelial cells [3]. Most investigated and responsible for resistance development multidrug resistance associated proteins are MRP1-3 [3] which exhibit a specific tissue expression as follows: MRP1 shows highest expression in testes, lung, heart, bladder, spleen, adrenal glands, placenta, kidney, peripheral blood mononuclear cells, and skeletal muscle [38-40]. MRP2 mRNA is highly expressed in liver, followed by the duodenum where it decreases along the intestinal tract with lower detection in the colon compared with the duodenum, ileum and kidney [37, 40, 41] Levels of human MRP3 mRNA are highest in liver and also detectable in duodenum, colon, pancreas, adrenal glands, kidney, and lung [40-45].

Breast cancer resistance protein

Resistant cancer cell lines lacking MDR/MRP expression suggest an additional efflux transporter responsible for drug removal namely breast cancer resistance protein (BCRP) [37, 46-49]. Like the name indicates the BCRP transporter was originally

discovered in a breast cancer cell line and was long thought to be linked only with cancer resistance, chemotherapeutic response and transporter development linked survival of patients with breast cancer [50]. Recent studies proved that this transporter is not exclusively present in breast cancer but also in variable tumor types like adenocarcinomas of the intestinal tract, endometrium, and lung [51]. Furthermore its role as a marker for therapy progression and survival remains elusive [52]. In addition BCRP is not only expressed in cancerous tissue given that it is also found in a number of organs associated with drug absorption, metabolism, and excretion [37] like placenta, brain, liver, kidneys, small intestine, colon, duodenum and decreasing towards the rectum [53], prostate, spinal cord, adrenal gland, uterus, and testes [46, 54]. Like MDR/MRP transporters BCRPs cover a broad range of endogenous substances and xenobiotics, for example anticancer drugs (mitoxantrone, topotecan, methotrexate, docetaxel, paclitaxel, saquinavir, flavopiridol) and is therefore responsible for less effective cancer therapy and resistance in some cases [3, 37].

3.2.2 SLC – Transporters

In addition to active ABC transporters solute carriers (SLCs) comprise a further family of membrane transport proteins in the human organism. Like as ABCs SLCs regulate the transport of a broad variety of substrates including endogenous substrates and xenobiotics across biological membranes [55]. The SLC gene family are in contrast to ABC transporters energy-independent passive or secondary active transporters which generally are responsible for uptake with only few exceptions where efflux transport is reported [3, 37, 56, 57]. Due to their importance in drug uptake and their far spread distribution this largest transporter family is a major target for drug design in improving selectivity, minimizing side effects and increasing patient compliance by utilizing SLCs for transport which enables cell type-specific drug delivery [57, 58].

Organic anion transporting proteins

Organic anion transporting proteins (OATPs) belong to the superfamily of transmembrane carrier transporters and are classified as carriers of the solute carrier transport protein (SLCO) gene family [59]. 11 members of the OATP family have currently been identified in humans which are further divided into six families, based on 40% amino acid sequence identity. Classification into subfamilies is done on the basis of a 60% amino acid sequence identity [59]. OATPs consist of 643-722 amino

acids with a predicted in Figure3 shown 12 transmembrane helices structure termed H1-H12, separated by 6 extracellular and 5 intracellular loops with both the C- and the N-terminal end of the polypeptide chain at the cytoplasmic side of the cell [60]. In this for OATP1B3 and OATP2B1 established model, 6 N-terminal and 6 C-terminal helices are located around the central pore with a positive electrostatic potential which eases binding and transport of negatively charged compounds [56, 61].
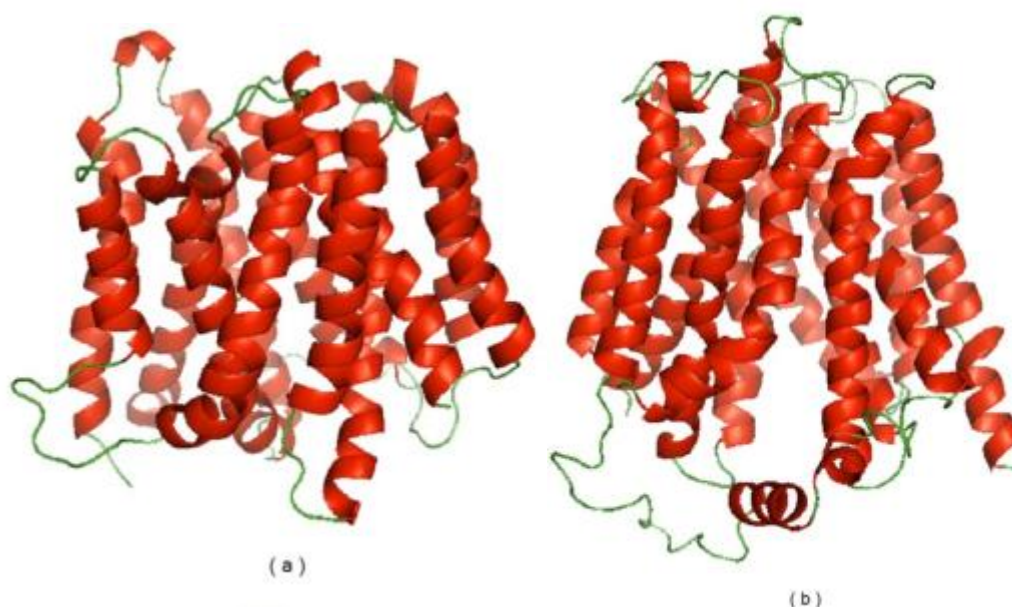
Figure3 Model of (a) OATP2B1 and in (b) of OATP1B3 [62].

At the border of the extracellular domain E3 and the transmembrane domain VI the conserved amino acid sequence [D-X-RW-(I,V)-GAWW-X-G-(F,L)-L] used for identification of the OATP family is found [63]. The structural characteristic large extracellular loop is located between the transmembrane domains IX and X and is important for the levels of OATPs in cell membranes and their transport activity [60, 64]. Hanggi et all proved the importance of cysteine as specific structural feature in this loop by generating nine cysteine-to alanin substitutions in the extracellular loop 5 to investigate their cellular location and transport activity for estrone-3-sulfate in transfected CHO-K1 cells [65]. In these experiments it was shown that except for the control all mutants were located intracellular and had a decreased uptake for the substrate [65]. Within the large extracellular loop 5 a Kazal-2-type serine protease inhibitor (Kazal_SLC21) domain is found [61]. The function of this hydrophilic region is still unclear, and it may regulate the presentation of the substrate to the transporter or interaction with other proteins [61]. Interestingly, members of the Kazal-type serine

14

protease inhibitor family affect various physiological processes, for example, blood coagulation, inflammation, immune response, and development, and they might contribute to tumor invasion and metastasis [66-68]. In addition a protein interaction module called PDZ (P: post-synaptic protein, PSD-95, D: the Drosophila septate junction protein, Discs-large, and Z: the tight junction protein, ZO-1) binding to the carboxy terminus is considered to be involved in the uptake mechanism by recruiting and stabilizing OATPs in the plasma membrane and modulating their function via direct interaction with amino acids located at the C-terminus [69]. Besides the PDZ domain transmembrane domains 8, 9 and 10 show an important role for uptake and function for OATP1B1and OATP1B3 which was investigated in HEK293 cells transfected with chimeric OATP1B1 transporters, generated by substitution of different OATP1B1 transmembrane domains with those from OATP1B3 [70, 71]. In general it is theorised that OATP mediated uptake works as a rocker-switch-type mechanism where substrates are brought through a central, positively-charged pore. However this model has to be verified experimentally [61]. Contrary to many other active transporters ion-gradients like Na^+, K^+ and Cl^- [60, 72-76], the replacement of Na + with other cations or ATP hydrolysis has comparatively little effect on the function of OATPs [77]. Additionally experiments with the common OATP substrate estrone-3-sulfate showed that depolarisation of the membrane had no effect on the transport via OATP1B1 and OATP1B3 leading to the conclusion that the OATP transport is membrane potential independent [78, 79].

Substrates for members of the OATP family cover a wide range of endogenous and exogenous substances like bile salts, hormones, and steroid conjugates for example estrone-3-sulfate as well as drugs like HMG-CoA-reductase inhibitors, cardiac glycosides, anticancer agents as well as various antibiotics. In general characteristics for OATP substrates are: anionic amphipathic organic compounds of high molecular weight beyond 450 Da, steroidal structures, linear structures, cyclic peptides normally bound to proteins, neutral compounds and some cations [59, 63]. Due to the specific distribution of OATPs in organs with barrier function like for example liver, kidney and blood brain barrier, members of the organic anion-transporting polypeptide family are considerd one of the most important cellular drug uptake mechanisms in humans [56, 62]

OATP1A2 mRNA levels are highest in the brain, kidney, liver, lung, testis, and placenta according to Northern blot analysis [73, 80]. Highest protein levels were

found in the blood-brain barrier [81, 82], at the apical membrane of distal nephrons [81] and the apical membrane of enterocytes [83]. It mediates the transport of a wide range of endogenous and exogenous, mainly amphipathic compounds, including bile acids, steroid hormones and their conjugates, cyclic and linear peptides, numerous drugs and toxins. For that reason its expression at the membrane of enterocytes and cholangiocytes (liver) is thought to be critical [56, 83, 84]. OATP1A2 expression in cancer was detected for gliomas, colon polyps and tumors, cancers of the breast and bone [84]. Via immunofluorescence microscopy, OATP1A2 was localized in the luminal membrane of the blood-brain barrier endothelium and in the blood-tumor barrier but not in the glioma cells [85]. By using RT-PCR, OATP1A2 expression was confirmed in patient samples suffering from breast cancer with significantly higher levels in malignant breast tissue than they were in adjacent nonmalignant breast tissue and was furthermore localized to the cell membrane and cytoplasm of breast carcinoma cells [86]. However contrary results were found by Wlcek et al. [87]. OATP1A2 was detected in bone metastases from primary kidney cancer and in the malignant osteosarcoma cell lines [84, 88].

OATP1B1 is a tissue specific OATP under physiological conditions. Its mRNA was detected highest expressed in liver by western blot analysis. This expression was confirmed at the protein level and localized at the basolateral membrane of hepatocytes. [89] It is best characterized according to its substrate specificity and various endogenous compounds (table…) [56, 84, 90]. Under non physiological conditions for both OATP1B1 and OATP1B3 a trend towards reduction of their expression was observed in hepatocellular carcinomas [91, 92].

OATP1B3 is also an example for a tissue-specific OATP which is only found at the basolateral membrane of hepatocytes [56, 89]. However its expression is much higher in the pericentral region compared to the periportal region [93, 94]. The main difference between OATP1B1 and OATP1B3 who share 80% amino acid identity is its high expression in hepatocytes around the central vein [89, 94]. Due to the homology of these two transporters OATP1B3 mediates nearly the same substances as OATP1B1 including cardiac glycoside digoxin [56, 84, 95]. OATP1B3 is upregulated in a wide range of cancer tissue eg. gastric, pancreatic, colon, colon cancer metastatic of lymph node [94], prostate cancer [84] and cancer cell lines eg. : gastrointestinal, colon, pancreatic, gallbladder, lung and glioblastoma cell lines [94].

Furthermore OATP1B3 expression in colorectal tumor showed that it was highest in earlier-stage and lower-grade tumors [96].

OATP1C1 is most expressed in the brain and testis and its mRNA is highest in the blood-brain barrier and in Leydig cells of the testis [97, 98]. In addition OATP1C1 was localized to ciliary body epithelium [99]. Due to its high affinity to thyroid hormones OATP1C1 is thought to be crucial for delivering serum thyroid hormones to the brain [56, 84]. For this thyroid hormone specific transporter no affinity for cancer drugs were reported and its only expression in cancer is confirmed in bone tumors [88].

OATP2A1 mRNA was found in brain, colon, heart, liver, kidney, ovary, lung, pancreas, prostate, skeletal muscle, spleen, and small intestine [100]. At the protein level expression was found in neurons in the frontal gyrus of the brain [101], in the pyloric glands of the antrum and parietal cells in the gastrointestinal tract [102], and in the luminal and glandular epithelium of the endometrium [103]. Furthermore this OATP has a substrate specificity for prostaglandins (PGs) and is therefore known as prostaglandin transporter (PGT) [104]. According to literature OATP2A1 might be very important for the regulation of pericellular PG levels, directing PGs towards and/or away from specific sets of PG receptors to nuclear receptors and participate in the regulation of body fluid homeostasis by influencing PG signal termination [56, 84, 105, 106]. This prostaglandin transporter was detected with high mRNA levels in tumor tissue of breast, liver, ovary, lung and bone [62, 87, 88].

OATP2B1 is like OATP2A1 widely expressed in organs of the human body with highest levels in basolateral membrane of the liver [97, 107] and at the apical membrane of enterocytes [108], at the endothelium of the blood-brain barrier [85], at the endothelial cells of the heart [109], at the myoepithelium of mammary ducts [110], and in the placenta [111]. At a physiological pH OATP2B1 transports only a narrow range of substrates (estrone sulfate, and dehydroepiandrosterone sulfate) though at an acid pH, more compounds become OATP2B1 substrates for example statins and steroid sulfates. In addition this ubiquitously expressed transporter showed expression in bone cysts higher than in osteosarcoma tissues [88] and human gliomas localised in endothelial cells at the blood-brain barrier and blood-tumor barrier [85] and breast tumor specimens with linked expression increased with higher tumor grade [112].

OATP3A1 is the most highly conserved OATP among all species. However, two splice variants (OATP3A1_v1 and OATP3A1_v2) were detected [113]. Besides a lack

of 18 amino acids at the COOH-terminal end OATP3A1_v2 is similar in sequence to OATP3A1_v1 [113]. OATP3A1_v1 sows a wide distribution among various tissue types, with expression in the testis, brain, heart, lung, spleaen, peripheral blood leukocytes, and thyroid gland, [113, 114] in comparison OATP3A1_v2 is mainly expressed in the testis and brain. Both variants show similar substrate specificity and transport PGs, thyroid hormones and vasopressin [113]. Interestingly recent findings reported OATP3A1 expression in epithelial cells of the lactiferous ducts in normal breast tissue [56, 84, 115]. Further analysis showed OATP3A1 expression in osteosarcoma [88], breast carcinoma, lung carcinoma, colon adenocarcinoma, ovarian carcinoma, and pancreatic adenocarcinoma cell lines [97]. A very recent study also detected this OATP in the membrane and cytoplasm of breast cancer species [115].

OATP4A1 is another ubiquitously expressed OATP, with highest mRNA levels in the heart and placenta, lung, liver, skeletal muscle, kidney, and pancreas [97, 116]. Thus far, OATP4A1 protein expression has been confirmed only at the apical membrane of syncytiotrophoblasts in the placenta [56, 84, 117]. In cancerous tissue OATP4A1 shows a similar expression pattern compared to OATP3A1 with highest levels in breast carcinoma, lung carcinoma, colon adenocarcinoma, ovarian carcinoma, and pancreatic carcinoma cell lines [97]. Further expression was found with increased levels in bone cysts compared to osteosarcoma tissues, with significantly higher expression in the malignant osteosarcoma cell lines [88]. OATP4A1 expression was also significantly higher in the colon of patients suffering from bowel disease than in normal colon which is an indication for developing colon cancer where OATP4A1 is found in high levels [62, 118].

OATP4C1 is considered a kidney-specific OATP due to its only expression in the kidney, as shown by Northern blot analysis [119]. Substrate specificity of OATP4C1 is rather low, and it only transports digoxin, ouabain, thyroid hormones, methotrexate, and cAMP [56, 84, 119, 120]. OATP4C1 expression was only detected in cancerous breast tissue [87], but this transporter might play an important role for patients with chronic kidney disease referring to its specific expression in the kidney [119, 121]

OATP5A1 shows high mRNA levels in the brain, heart, skeletal muscle, and ovary [122, 123]. OATP5A1 proteins where found at the plasma membrane of the epithelial cells that line the lactiferous ducts in normal breast tissue [115]. As an OATP not comparable with other OATPs in its function it might be involved in biological

processes like reorganization of the cell shape, with a special focus on differentiation and migration and therefore may play an important role in cancer development [124, 125]. However, the substrate for OATP5A1 mediated transport is still not known but its transport might be coupled to the uptake via other OATPs [56, 84, 124]. As stated before little is known about the expression of OATP5A1 and less concerning its distribution in cancer tissue. mRNA levels of OATP5A1 were found in cancers of the liver, bone, and breast [62].

OATP6A1 mRNA expression has been detected in the testes, with low levels in the spleen, brain, fetal brain, and placenta [126, 127]. However, substrates for OATP6A1 have not been assessed [56, 84]. First identification of OATP6A1 was as a cancer-testis antigen by serological screening of recombinant expression libraries of human cancer with human serum (SEREX) [126]. Furthermore OATP6A1 mRNA is expressed in mesotheliomas, tumors from bladder and esophageal tumors [128].

Because of this broad spectrum of substrates and their tissue distribution in membranes and physiological barriers under normal conditions and their altered tissue expression in cancer tissue OATPs are of particular interest for drug pharmacokinetics and for the prediction of interactions with drugs that are substrates for the same OATP [129, 130].

Organic Cation Transporters

Organic Cation Transporters (OCTs) are polyspecific cationic transporters of the SLC22 family distributed in subfamilies (OCT1-3) which are associated with the interaction of cationic drugs that are positively charged at physiological pH and represent about half of the substances used in therapy [37, 131] OCT uniporters are sodium independent with the electrochemical gradient of the transported organic cation, typically an inside-negative membrane potential, as its driving force [132]. OCT1 is primarily expressed in the sinusoidal membrane of hepatocytes in liver leading to the conclusion of its affliction in the first step of hepatic exertion of cationic drugs [37, 133, 134]. Highest expression for OCT2 mRNA is found within renal proximal tubule cells of the kidney at the basolateral membrane indicating its role for renally excreted cationic drugs, the kidneys [37, 133, 135-138]. Contrary to OCT1 and OCT2, OCT3 shows a broader expression among organs which is highest in placenta, ovaries, and uterus [37, 135, 136, 139-142].

Organic cation/carnitine transporters

Organic cation/carnitine (OCTN) transporters, as indicated by their name are protein transports of carnitine and cationic chemicals, are members of the SLC22 family and are distributed in 3 subfamilies (OCTN1-3) [37]. Besides the uptake of cationic substances they play a crucial role in the breakdown of lipids through oxidation because carnitine is required for the transport of fatty acids from the cytosol into the mitochondria [37, 143]. OCTN1 is most prominently expressed in kidney, skeletal muscle, placenta, prostate, heart, fetal liver, eyes and lung [144, 145]. Besides typical OCTN1 expression on the plasma membrane, intracellular localization in mitochondria has been reported where it may be responsible for carnitine accumulation [37, 146]. Human OCTN2 is expressed in kidneys and placenta and to a minor extent in other tissues [143, 145, 147, 148]. OCTN3 is found in many cell types. This transporter is also localized at peroxisomes where it may be important in supplying carnitine for peroxisomal lipid metabolism [37, 149].

Organic anion transporters

Organic anion transporters (OATs) are located in the solute carrier family SLC22A , divided in 7 subfamilies (OAT1-7) where they function as organic anion exchangers by a sodium and dicarboxylate gradient, generated by the sodium-dicarboxylate cotransporter and the sodium-potassium ATPase [37]. Due to coupling of a sodium-potassium-ATPase pump to the gradient of this transporter family this way of transport is referred as tertiary transport [150]. OAT transport displays a wide substrate range including endogenous substrates and xenobiotics [37]. OAT1 is highest expressed in kidneys with specific location on the basolateral membranes of renal proximal tubules [151]. OAT2 is found mostly in the liver with lower levels in kidneys [152, 153]. OAT3 is primary located in the kidneys, with specific location on the basolateral membranes of renal proximal tubules [154]. OAT4 mRNA is highest expressed in kidneys and placenta [155]. Not much is known About OAT5–7 whether neither their expression nor their substrate specify [37].

Peptide Transporters

Peptide Transporters PEPT1 and PEPT2 belong to the solute carrier family (SLC15A) and transport di- and tripeptides into cells [37]. PEPT1 and PEPT2 are most prominently expressed in kidneys, lung, colon, pancreas and liver [156, 157]

Concentrative Nucleoside Transporters

Contrary to other SLC family member's nucleoside uptake transporters are classified according to their transport properties of concentrative (high-affinity sodium-dependent transport using a physiologic sodium gradient) (SLC28A) and equilibrative (low-affinity facilitated carrier transport) (SLC29A) ability [158, 159]. Nucleosides are glycosylamines consisting of a sugar moiety and a purine or pyrimidine base, (cytidine, uridine, adenosine, guanosine, thymidine, and inosine) which are needed by hematopoietic and other cell types for nucleotide synthesis. Furthermore nucleoside analogs have been designed against viral infections and cancers as they are actively taken up by these kind of transporters [37]. CNT1 and CNT2 show specific location in liver and kidneys. Furthermore CNT2 was also detected in heart, brain, placenta, skeletal muscle, small intestine and pancreas [160-162]. CNT3 is found in various tissues [162] with a specific expression at the apical surface of proximal tubules and the thick ascending loops of Henle loop [162].

Equilibrative Nucleoside Transporters

Equilibrative Nucleoside Transporters (ENTs) transport their substrates down concentration gradients in a bidirectional way [37]. Interestingly, ENTs, typically transporting endogenous nucleosides as well as cancer and antiviral nucleoside analogs, are also expressed in the mitochondria, where they may be involved in the cellular toxicity of antiviral nucleoside drugs [163-168]. ENT1 exhibits a broad tissue range including liver, lungs, heart, ovaries, brain, kidneys, erythrocytes, fetal liver and placenta [162, 165, 169, 170]. The profile of ENT2 is located in skeletal muscle and heart but there are detectable amounts in other organs [169]. ENT3 is known to be broadly expressed in tissue with specific expression in placenta, lung, ovaries, spleen and bone marrow [171]. About ENT4 neither tissue distribution nor transport properties are known [172].

3.3 Metabolising Enzymes

As SLC carriers interoperate with enzymes responsible for metabolism both with phase 1 (cytochrome P450 isoenzymes) and phase 2 (glucuronosyltransferases, sulfotransferases, glutathione transferases, and others) as well as with efflux transporters (P-glycoprotein and breast cancer resistance protein ABCG2) interplays

between uptake, reuptake after metabolism, biotransformation, and efflux strongly affect the distribution of drugs [56, 62]. During phase 1 substrates are metabolised most prominently by various CYP450 enzymes via oxidation, reduction, hydrolysis, cyclization, decyclization and addition of oxygen or removal of hydrogen which is important for the detoxication and conversion of xenobiotics for further metabolomic reactions [173]. Phase II uses completely contrary chemical reactions compared to phase I because in this step substrates are made more polar by adding for example sulfates or glucuronides by sulfotransferases or glucuronosyltransferases. These metabolites are characterised usually by an increased molecular weight and lower activity than their substrates [174]. Besides drug uptake and specific distribution the metabolic profile of drugs is crucial for good therapy outcomes. Furthermore substances co-administered during for example cancer therapy can cause severe drug-drug interactions which can lead to significant side effects by inducing or blocking phase 1 or phase 2 metabolisms. In addition effects of FDA drugs are recognised for their impact on lipoxigenases. Lipoxygenases and CYP450 show strong effects on arachidonic acid metabolic cascade leading for example to higher levels of 12(S)-HETE which are linked with circular chemorepellent induced defects on cells (CCID) [175]. CCID and its link to arachidonic acid metabolite 12(S)-HETE is especially crucial due to its retractionary effect on endothelial cells abetting tumor metastasis [175-177]. Therefore understanding of drug enzyme interaction is crucial for therapy, drug-drug interaction and drug disease interaction [56, 62, 178].

3.3.1 Cytochrome P450 enzymes

Cytochrome P450 is one of the most prominent proteins metabolising xenobiotics, for example anti-cancer drugs, within the human body and furthermore is responsible for the oxidation of unsaturated fatty acids, biosynthesis of steroid hormones and much more [173, 179]. Referring to CYP450 metabolising ability interestingly 60% of FDA drugs is metabolised via this protein which underlines its crucial role in drug therapy and drug-drug interactions [180]. The CYP450 superfamily is subdivided in 18 subfamilies whose distribution is controlled on the one hand by age, sex and organ type and on the other hand by hormonal status, diet and exposure to chemicals [178, 181, 182]. Subfamilies CYP1-4 hold the fast majority of genes in the CYP450 family and are encoding enzymes responsible for eicosanoids, foreign chemicals and drug metabolism [178]. The way CYP450 works can be summed up as a simple enzymatic reaction where molecular oxygen is cleaved followed by the insertion of a single

oxygen atom into the substrate while water remains [183]. The most prominent cytochroms responsible for metabolism of the top 200 drugs are CYPs 1A2, 2B6, 2C8, 2C9, 2C19, 2D6, and 3A4/5 which will be further discussed.

CYP1A1 is an important member of the CYP450 family that is involved in the initial hydroxylation of many xenobiotics and endogenous substrates [184, 185]. In general the expression of CYP1A1 is linked with heterodimeric transcription factors [186]

CYP1A2 is predominantly expressed in liver, where it covers an amount of ~10% of the total microsomal P450 pool [187]. The substrate specifity of the CYP1 enzymes include many polycyclic aromatic hydrocarbons and endogenous substrates like prostaglandins, estrogens and retinoic acid. Interestingly this CYP family is widely expressed in cancer, because of its substrates occurring in cigarette smoke and charred food which are known to be carcinogenic or to be converted into carcinogens [187, 188].

CYP1B1 shows approximately 40% identity with CYP1A1 and plays a key role in the metabolism of various carcinogens [189]. Interestingly typical skin expression of CYP1B1 shows strong interindividual correlation with cutaneous 8-MOP metabolism correlated with PUVA sensitivity [190].

CYP2B6 represents ~3–6% of the total microsomal P450 pool in the liver with a great interindividual variability [191] induced by several clinical important xenobiotics [187, 192, 193].

CYP2C8 member of CYP450 shows a main selectivity for antidiabetic, antiarrhythmic and anti-cancer drugs and is inhibited by e.g. cerivastatin where the clinical relevance of CYP2C8 showed for the first time [187].

CYP2C9 shows high expression in the liver with a selectivity for weakly acidic substances like e.g. several nonsteroidal anti-inflammatory drugs having a narrow therapeutic range. This makes CYP2C9 and especially its polymorphisms a crucial enzyme for drug therapy [187].

CYP2C19 which was the first CYP2C isozyme discovered shows substance specificity for proton-pump inhibitors and other important drugs [187].

CYP2D6, which is highly genetically and less environmentally influenced in its expression, is very well-known and is usually found in the liver and in brain neurons [187]. CYP2D6 catalyses phase 1 reactions for many substrates and furthermore plays an important role in breast cancer therapy where it is responsible for tamoxifen

metabolism in antiestrogenic metabolites crucial for positive therapy outcomes [187, 194].

The CYP3A subfamily (3A4,3A5, 3A7, and 3A43) covers the widest range of substances and shows due to their large and flexible active side, metabolic capability for many preferentially lipophilic and large substances including several endogenous compounds [195, 196] with no specificity for a certain structure type [187]. Within the family, CYP3A5, CYP3A7 and CYP3A43 are found at much lower levels than CYP3A4. Interestingly the expression of CYP3A4 is besides e.g. inflammatory signaling pathways linked to sex difference whereat women show 1.5- to 2-fold higher levels [187, 197].

3.3.2 Arachidonic Acid Metabolising Enzymes

The arachidonic acid metabolic cascade consists of cyclooxygenases, lipoxygenases, and cytochrome P-450. These enzymes create prostaglandins (PG), prostacyclin (PGI2), thromboxane A2 (TxA2), hydroxyeicosatetraenoic acids (HETEs), epoxyeicosatrienoic acids (EETs), and dihydroxyeicosatrienoic acids (DiHETEs) [179, 181]. In general lipids play important functional roles as components of cell signaling cascades. Hence molecular and functional characterization of these mediators is crucial for understanding and therapy of many diseases [181].

The P450 branch of this cascade holds the key for many biological properties and mechanism of action so that it is important to keep in mind that P450 plays an established role in the oxygenated metabolism of eicosanoids [181]. The catalysis of AA epoxidation by P450 was shown by recent studies, indicating a metabolite formation by incubation of CYP450, arachidonic acid and microsomes [198, 199]. These findings showed P450 as an active arachidonic acid epoxygenase with biochemical and physiological implications [181]. The role of CYP450 in lipoxygenase-like reactions is shown in the formation of six regioisomeric allylic alcohols containing a characteristic *cis, trans*-conjugated dienol functionality [181, 200]. Interestingly lipoxigenase and lipoxygenase-like reactions differ in the stero-enantiomer product as 12-lipoxygenases is known to be selective for 12(S)-HETE and P450 forms 12(R)-HETE with enantioselective Na^+/K^+ ATPase inhibition activity [181, 201].

ω and/or ω -1 hydroxylation is the best examined role of P450s in the arachidonic acid cascade where it is in general responsible for mid-chain fatty acids prior to degradation by β-oxidation and/or urinary excretion [181].
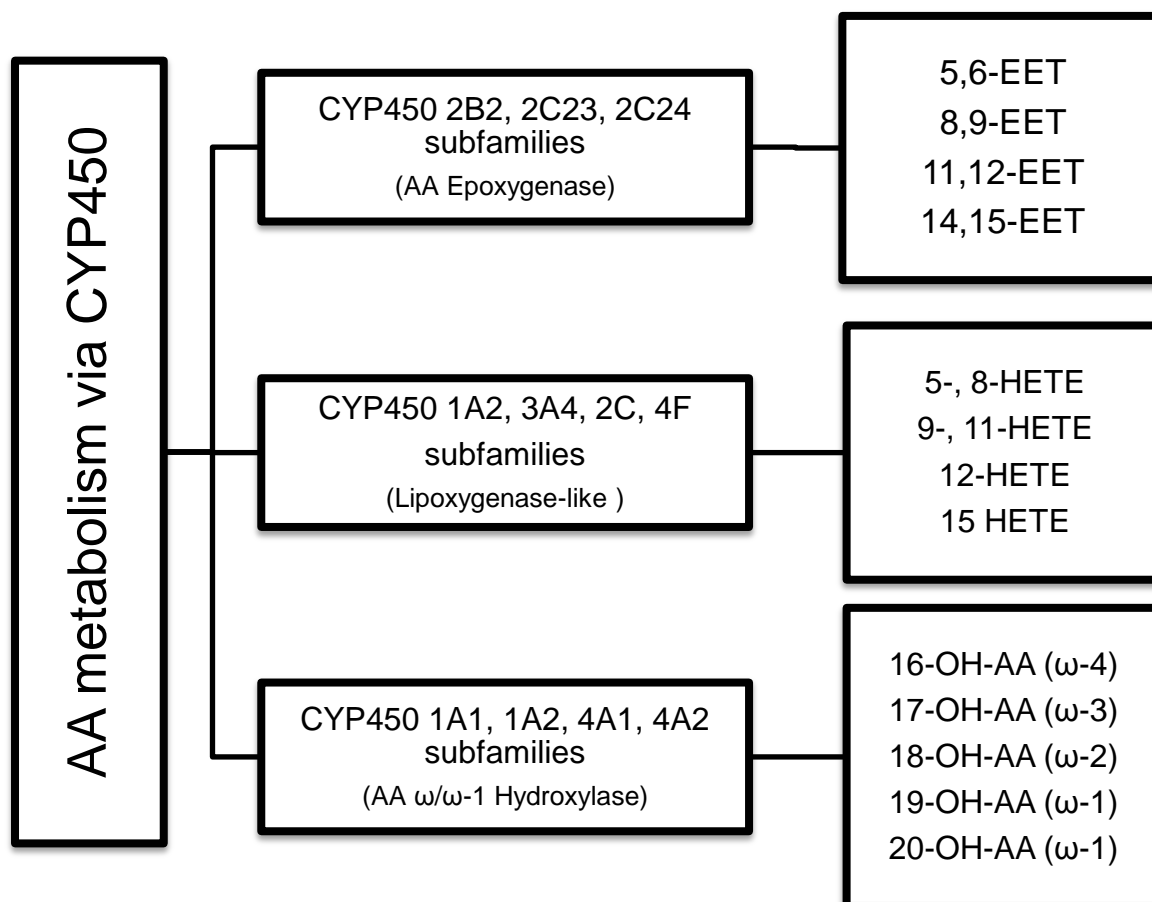
AA metabolism via CYP450	CYP450 2B2, 2C23, 2C24 subfamilies (AA Epoxygenase)	5,6-EET 8,9-EET 11,12-EET 14,15-EET
	CYP450 1A2, 3A4, 2C, 4F subfamilies (Lipoxygenase-like)	5-, 8-HETE 9-, 11-HETE 12-HETE 15 HETE
	CYP450 1A1, 1A2, 4A1, 4A2 subfamilies (AA ω/ω-1 Hydroxylase)	16-OH-AA (ω-4) 17-OH-AA (ω-3) 18-OH-AA (ω-2) 19-OH-AA (ω-1) 20-OH-AA (ω-1)

Figure4 **"**Reactions catalyzed by the cytochrome P450 monooxygenase pathway of AA metabolism. Only the primary oxygenation products of the AA monooxygenase are shown (products derived from the P450-catalyzed oxygenation of AA)." [181]

Furthermore cyclooxygenase, is essential for the conversion of arachidonic acid (AA) to PG. Two different enzyme isoforms (COX-1 and COX-2) are known which are responsible for diverse functions in the human body [202]. Cyclooxygenase-1 is constitutively expressed throughout the body in nearly all tissues where it mediates a variety of normal physiologic processes including preservation of renal blood flow and function, platelet aggregation and hemostasis, and cytoprotection of the gastrointestinal mucosa [202, 203]. In contrast to COX-1 COX-2 is not similarly expressed but is especially active in inflammatory cells and synoviocytes inducing response to hypoxia and tissue injury [202]. COX-2 metabolises arachidonic acid to proinflammatory prostanoids, which are responsible for the mediation of acute and chronic response to inflammation, pain and other actions where cellular repair and

proliferation like for example colon carcinomas that show an enhanced COX-2 expression compared with normal intestinal mucosa [202, 204-207].

Lipoxygenases, classified as 5-, 8-, 12, and 15-lipoxygenases hence to their selectivity to oxygenate fatty acids, are oxidative enzymes which are involved in the inflammatory process generating pro-inflammatory mediators (leukotrienes) and anti-inflammatory mediators (lipoxins) [208-210]. These enzymes catalyse the formation of hydroperoxy eicosatetraenoic acids (HPETEs) which are afterwards reduced and transformed to eicosanoids that play an important regulatory role for immune responses [209]. Besides prominent acute and chronic inflammatory diseases like asthma, atherosclerosis, rheumatoid arthritis etc. linked with over-expression of lipoxygenases Shureiqi and Lippman [211] reported that 5-LOX and 12-LOX are procarcinogenic, through their LTs and HETEs production, [206, 209]. Furthermore for asthma, cardiovascular diseases, rheumatoid arthritis and cancer activation of the NF-κB pathway linked with lipoxygenase activity was reported [209, 212-216].
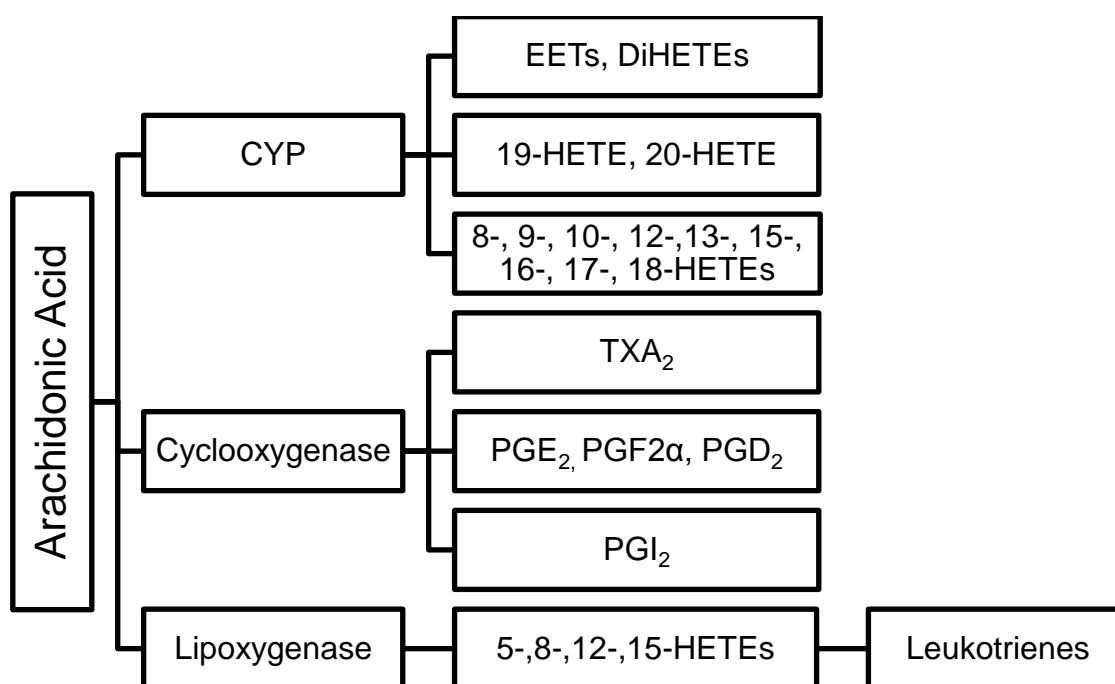

Figure5. Pathways for the metabolism of arachidonic acid [179]

7 References

1   Dobson, P. D., Kell, D. B., Carrier-mediated cellular uptake of pharmaceutical drugs: an exception or the rule? *Nature reviews. Drug discovery* 2008, *7*, 205-220.

2   Ferlay, J., Steliarova-Foucher, E., Lortet-Tieulent, J., Rosso, S*., et al.*, Cancer incidence and mortality patterns in Europe: estimates for 40 countries in 2012. *European journal of cancer (Oxford, England : 1990)* 2013, *49*, 1374-1403.

3   Pavan, B., Paganetto, G., Rossi, D., Dalpiaz, A., Multidrug resistance in cancer or inefficacy of neuroactive agents: innovative strategies to inhibit or circumvent the active efflux transporters selectively. *Drug discovery today* 2014.

4   Aller, S. G., Yu, J., Ward, A., Weng, Y*., et al.*, Structure of P-glycoprotein reveals a molecular basis for poly-specific drug binding. *Science (New York, N.Y.)* 2009, *323*, 1718-1722.

5   Sugano, K., Kansy, M., Artursson, P., Avdeef, A*., et al.*, Coexistence of passive and carrier-mediated processes in drug transport. *Nature reviews. Drug discovery* 2010, *9*, 597-614.

6   Kell, D. B., Dobson, P. D., Oliver, S. G., Pharmaceutical drug transport: the issues and the implications that it is essentially carrier-mediated only. *Drug discovery today* 2011, *16*, 704-714.

7   Lipinski, C. A., Lombardo, F., Dominy, B. W., Feeney, P. J., Experimental and computational approaches to estimate solubility and permeability in drug discovery and development settings. *Advanced drug delivery reviews* 2001, *46*, 3-26.

8   Klein, I., Sarkadi, B., Varadi, A., An inventory of the human ABC proteins. *Biochimica et biophysica acta* 1999, *1461*, 237-262.

9   Higgins, C. F., ABC transporters: from microorganisms to man. *Annual review of cell biology* 1992, *8*, 67-113.

10   Dean, M., Hamon, Y., Chimini, G., The human ATP-binding cassette (ABC) transporter superfamily. *Journal of lipid research* 2001, *42*, 1007-1017.

11   Lage, H., ABC-transporters: implications on drug resistance from microorganisms to human cancers. *International journal of antimicrobial agents* 2003, *22*, 188-199.

12 Zakeri-Milani, P., Valizadeh, H., Intestinal transporters: enhanced absorption through P-glycoprotein-related drug interactions. *Expert opinion on drug metabolism & toxicology* 2014, *10*, 859-871.

13 Nies, A. T., The role of membrane transporters in drug delivery to brain tumors. *Cancer Letters* 2007, *254*, 11-29.

14 Cordon-Cardo, C., O'Brien, J. P., Boccia, J., Casals, D*., et al.*, Expression of the multidrug resistance gene product (P-glycoprotein) in human normal and tumor tissues. *The journal of histochemistry and cytochemistry : official journal of the Histochemistry Society* 1990, *38*, 1277-1287.

15 Thiebaut, F., Tsuruo, T., Hamada, H., Gottesman, M. M*., et al.*, Cellular localization of the multidrug-resistance gene product P-glycoprotein in normal human tissues. *Proceedings of the National Academy of Sciences of the United States of America* 1987, *84*, 7735-7738.

16 Sugawara, I., Kataoka, I., Morishita, Y., Hamada, H*., et al.*, Tissue distribution of P-glycoprotein encoded by a multidrug-resistant gene as revealed by a monoclonal antibody, MRK 16. *Cancer research* 1988, *48*, 1926-1929.

17 Borst, P., Elferink, R. O., Mammalian ABC transporters in health and disease. *Annual review of biochemistry* 2002, *71*, 537-592.

18 Marchetti, S., Mazzanti, R., Beijnen, J. H., Schellens, J. H., Concise review: Clinical relevance of drug drug and herb drug interactions mediated by the ABC transporter ABCB1 (MDR1, P-glycoprotein). *The oncologist* 2007, *12*, 927-941.

19 Fojo, A. T., Ueda, K., Slamon, D. J., Poplack, D. G*., et al.*, Expression of a multidrug-resistance gene in human tumors and tissues. *Proceedings of the National Academy of Sciences of the United States of America* 1987, *84*, 265-269.

20 Ueda, K., Cardarelli, C., Gottesman, M. M., Pastan, I., Expression of a full-length cDNA for the human "MDR1" gene confers resistance to colchicine, doxorubicin, and vinblastine. *Proceedings of the National Academy of Sciences of the United States of America* 1987, *84*, 3004-3008.

21 Kobori, T., Harada, S., Nakamoto, K., Tokuyama, S., Mechanisms of p-glycoprotein alteration during anticancer treatment: role in the pharmacokinetic and pharmacological effects of various substrate drugs. *Journal of pharmacological sciences* 2014, *125*, 242-254.

22 Sparreboom, A., van Asperen, J., Mayer, U., Schinkel, A. H.*, et al.*, Limited oral bioavailability and active epithelial excretion of paclitaxel (Taxol) caused by P-glycoprotein in the intestine. *Proceedings of the National Academy of Sciences of the United States of America* 1997, *94*, 2031-2035.

23 Allen, J. D., Van Dort, S. C., Buitelaar, M., van Tellingen, O., Schinkel, A. H., Mouse breast cancer resistance protein (Bcrp1/Abcg2) mediates etoposide resistance and transport, but etoposide oral availability is limited primarily by P-glycoprotein. *Cancer research* 2003, *63*, 1339-1344.

24 Marchetti, S., de Vries, N. A., Buckle, T., Bolijn, M. J.*, et al.*, Effect of the ATP-binding cassette drug transporters ABCB1, ABCG2, and ABCC2 on erlotinib hydrochloride (Tarceva) disposition in in vitro and in vivo pharmacokinetic studies employing Bcrp1-/-/Mdr1a/1b-/- (triple-knockout) and wild-type mice. *Molecular cancer therapeutics* 2008, *7*, 2280-2287.

25 Lagas, J. S., van Waterschoot, R. A., Sparidans, R. W., Wagenaar, E.*, et al.*, Breast cancer resistance protein and P-glycoprotein limit sorafenib brain accumulation. *Molecular cancer therapeutics* 2010, *9*, 319-326.

26 Cornwell, M. M., Molecular biology of P-glycoprotein. *Cancer treatment and research* 1991, *57*, 37-56.

27 Barrand, M. A., Heppell-Parton, A. C., Wright, K. A., Rabbitts, P. H., Twentyman, P. R., A 190-kilodalton protein overexpressed in non-P-glycoprotein-containing multidrug-resistant cells and its relationship to the MRP gene. *Journal of the National Cancer Institute* 1994, *86*, 110-117.

28 Grant, C. E., Valdimarsson, G., Hipfner, D. R., Almquist, K. C.*, et al.*, Overexpression of multidrug resistance-associated protein (MRP) increases resistance to natural product drugs. *Cancer research* 1994, *54*, 357-361.

29 Stride, B. D., Grant, C. E., Loe, D. W., Hipfner, D. R.*, et al.*, Pharmacological characterization of the murine and human orthologs of multidrug-resistance protein in transfected human embryonic kidney cells. *Molecular pharmacology* 1997, *52*, 344-353.

30 Schuetz, J. D., Connelly, M. C., Sun, D., Paibir, S. G.*, et al.*, MRP4: A previously unidentified factor in resistance to nucleoside-based antiviral drugs. *Nature medicine* 1999, *5*, 1048-1051.

31   Lee, K., Klein-Szanto, A. J., Kruh, G. D., Analysis of the MRP4 drug resistance profile in transfected NIH3T3 cells. *Journal of the National Cancer Institute* 2000, *92*, 1934-1940.

32   Chen, Z. S., Lee, K., Kruh, G. D., Transport of cyclic nucleotides and estradiol 17-beta-D-glucuronide by multidrug resistance protein 4. Resistance to 6-mercaptopurine and 6-thioguanine. *The Journal of biological chemistry* 2001, *276*, 33747-33754.

33   Reid, G., Wielinga, P., Zelcer, N., De Haas, M.*, et al.*, Characterization of the transport of nucleoside analog drugs by the human multidrug resistance proteins MRP4 and MRP5. *Molecular pharmacology* 2003, *63*, 1094-1103.

34   Tian, Q., Zhang, J., Tan, T. M., Chan, E.*, et al.*, Human multidrug resistance associated protein 4 confers resistance to camptothecins. *Pharmaceutical research* 2005, *22*, 1837-1853.

35   El-Sheikh, A. A., van den Heuvel, J. J., Koenderink, J. B., Russel, F. G., Interaction of nonsteroidal anti-inflammatory drugs with multidrug resistance protein (MRP) 2/ABCC2- and MRP4/ABCC4-mediated methotrexate transport. *The Journal of pharmacology and experimental therapeutics* 2007, *320*, 229-235.

36   Hopper-Borge, E., Xu, X., Shen, T., Shi, Z.*, et al.*, Human multidrug resistance protein 7 (ABCC10) is a resistance factor for nucleoside analogues and epothilone B. *Cancer research* 2009, *69*, 178-184.

37   Klaassen, C. D., Aleksunes, L. M., Xenobiotic, bile acid, and cholesterol transporters: function and regulation. *Pharmacological reviews* 2010, *62*, 1-96.

38   Cole, S. P., Bhardwaj, G., Gerlach, J. H., Mackie, J. E.*, et al.*, Overexpression of a transporter gene in a multidrug-resistant human lung cancer cell line. *Science (New York, N.Y.)* 1992, *258*, 1650-1654.

39   Flens, M. J., Zaman, G. J., van der Valk, P., Izquierdo, M. A.*, et al.*, Tissue distribution of the multidrug resistance protein. *The American journal of pathology* 1996, *148*, 1237-1247.

40   Kool, M., de Haas, M., Scheffer, G. L., Scheper, R. J.*, et al.*, Analysis of expression of cMOAT (MRP2), MRP3, MRP4, and MRP5, homologues of the multidrug resistance-associated protein gene (MRP1), in human cancer cell lines. *Cancer research* 1997, *57*, 3537-3547.

41   Uchiumi, T., Hinoshita, E., Haga, S., Nakamura, T*., et al.*, Isolation of a novel human canalicular multispecific organic anion transporter, cMOAT2/MRP3, and its expression in cisplatin-resistant cancer cells with decreased ATP-dependent drug transport. *Biochemical and biophysical research communications* 1998, *252*, 103-110.

42   Zimmermann, C., Gutmann, H., Hruz, P., Gutzwiller, J. P*., et al.*, Mapping of multidrug resistance gene 1 and multidrug resistance-associated protein isoform 1 to 5 mRNA expression along the human intestinal tract. *Drug metabolism and disposition: the biological fate of chemicals* 2005, *33*, 219-224.

43   Belinsky, M. G., Bain, L. J., Balsara, B. B., Testa, J. R., Kruh, G. D., Characterization of MOAT-C and MOAT-D, new members of the MRP/cMOAT subfamily of transporter proteins. *Journal of the National Cancer Institute* 1998, *90*, 1735-1741.

44   Kiuchi, Y., Suzuki, H., Hirohashi, T., Tyson, C. A., Sugiyama, Y., cDNA cloning and inducible expression of human multidrug resistance associated protein 3 (MRP3). *FEBS letters* 1998, *433*, 149-152.

45   Konig, J., Rost, D., Cui, Y., Keppler, D., Characterization of the human multidrug resistance protein isoform MRP3 localized to the basolateral hepatocyte membrane. *Hepatology (Baltimore, Md.)* 1999, *29*, 1156-1163.

46   Doyle, L. A., Yang, W., Abruzzo, L. V., Krogmann, T*., et al.*, A multidrug resistance transporter from human MCF-7 breast cancer cells. *Proceedings of the National Academy of Sciences of the United States of America* 1998, *95*, 15665-15670.

47   Miyake, K., Mickley, L., Litman, T., Zhan, Z*., et al.*, Molecular cloning of cDNAs which are highly overexpressed in mitoxantrone-resistant cells: demonstration of homology to ABC transport genes. *Cancer research* 1999, *59*, 8-13.

48   Ross, D. D., Yang, W., Abruzzo, L. V., Dalton, W. S*., et al.*, Atypical multidrug resistance: breast cancer resistance protein messenger RNA expression in mitoxantrone-selected cell lines. *Journal of the National Cancer Institute* 1999, *91*, 429-433.

49   Allikmets, R., Schriml, L. M., Hutchinson, A., Romano-Spica, V., Dean, M., A human placenta-specific ATP-binding cassette gene (ABCP) on chromosome

4q22 that is involved in multidrug resistance. *Cancer research* 1998, *58*, 5337-5339.

50   Faneyte, I. F., Kristel, P. M., Maliepaard, M., Scheffer, G. L.*, et al.*, Expression of the breast cancer resistance protein in breast cancer. *Clinical cancer research : an official journal of the American Association for Cancer Research* 2002, *8*, 1068-1074.

51   Diestra, J. E., Scheffer, G. L., Catala, I., Maliepaard, M.*, et al.*, Frequent expression of the multi-drug resistance-associated protein BCRP/MXR/ABCP/ABCG2 in human tumours detected by the BXP-21 monoclonal antibody in paraffin-embedded material. *The Journal of pathology* 2002, *198*, 213-219.

52   Tanaka, Y., Slitt, A. L., Leazer, T. M., Maher, J. M., Klaassen, C. D., Tissue distribution and hormonal regulation of the breast cancer resistance protein (Bcrp/Abcg2) in rats and mice. *Biochemical and biophysical research communications* 2005, *326*, 181-187.

53   Gutmann, H., Hruz, P., Zimmermann, C., Beglinger, C., Drewe, J., Distribution of breast cancer resistance protein (BCRP/ABCG2) mRNA expression along the human GI tract. *Biochemical pharmacology* 2005, *70*, 695-699.

54   Fetsch, P. A., Abati, A., Litman, T., Morisaki, K.*, et al.*, Localization of the ABCG2 mitoxantrone resistance-associated protein in normal tissues. *Cancer Lett* 2006, *235*, 84-92.

55   Hediger, M. A., Romero, M. F., Peng, J. B., Rolfs, A.*, et al.*, The ABCs of solute carriers: physiological, pathological and therapeutic implications of human membrane transport proteinsIntroduction. *Pflugers Archiv : European journal of physiology* 2004, *447*, 465-468.

56   Svoboda, M., Riha, J., Wlcek, K., Jaeger, W., Thalhammer, T., Organic anion transporting polypeptides (OATPs): regulation of expression and function. *Current drug metabolism* 2011, *12*, 139-153.

57   Rask-Andersen, M., Masuram, S., Fredriksson, R., Schioth, H. B., Solute carriers as drug targets: current use, clinical trials and prospective. *Molecular aspects of medicine* 2013, *34*, 702-710.

58   Nakanishi, T., Tamai, I., Solute carrier transporters as targets for drug delivery and pharmacological intervention for chemotherapy. *Journal of pharmaceutical sciences* 2011, *100*, 3731-3750.

59 Hagenbuch, B., Meier, P. J., Organic anion transporting polypeptides of the OATP/ SLC21 family: phylogenetic classification as OATP/ SLCO superfamily, new nomenclature and molecular/functional properties. *Pflugers Archiv : European journal of physiology* 2004, *447*, 653-665.

60 Hagenbuch, B., Gui, C., Xenobiotic transporters of the human organic anion transporting polypeptides (OATP) family. *Xenobiotica; the fate of foreign compounds in biological systems* 2008, *38*, 778-801.

61 Meier-Abt, F., Mokrab, Y., Mizuguchi, K., Organic anion transporting polypeptides of the OATP/SLCO superfamily: identification of new members in nonmammalian species, comparative modeling and a potential transport mode. *The Journal of membrane biology* 2005, *208*, 213-227.

62 Hagenbuch, B., Meier, P. J., The superfamily of organic anion transporting polypeptides. *Biochimica et biophysica acta* 2003, *1609*, 1-18.

63 Gui, C., Miao, Y., Thompson, L., Wahlgren, B.*, et al.*, Effect of pregnane X receptor ligands on transport mediated by human OATP1B1 and OATP1B3. *European journal of pharmacology* 2008, *584*, 57-65.

64 Hanggi, E., Grundschober, A. F., Leuthold, S., Meier, P. J., St-Pierre, M. V., Functional analysis of the extracellular cysteine residues in the human organic anion transporting polypeptide, OATP2B1. *Molecular pharmacology* 2006, *70*, 806-817.

65 Schlott, B., Wohnert, J., Icke, C., Hartmann, M.*, et al.*, Interaction of Kazal-type inhibitor domains with serine proteinases: biochemical and structural studies. *Journal of molecular biology* 2002, *318*, 533-546.

66 Rawlings, N. D., Tolle, D. P., Barrett, A. J., Evolutionary families of peptidase inhibitors. *The Biochemical journal* 2004, *378*, 705-716.

67 Zheng, Q. L., Sheng, Q., Zhang, Y. Z., [Progresses in the structure and function of Kazal-type proteinase inhibitors]. *Sheng wu gong cheng xue bao = Chinese journal of biotechnology* 2006, *22*, 695-700.

68 Wang, P., Wang, J. J., Xiao, Y., Murray, J. W.*, et al.*, Interaction with PDZK1 is required for expression of organic anion transporting protein 1A1 on the hepatocyte surface. *The Journal of biological chemistry* 2005, *280*, 30143-30149.

69 Miyagawa, M., Maeda, K., Aoyama, A., Sugiyama, Y., The eighth and ninth transmembrane domains in organic anion transporting polypeptide 1B1 affect

the transport kinetics of estrone-3-sulfate and estradiol-17beta-D-glucuronide. *The Journal of pharmacology and experimental therapeutics* 2009, *329*, 551-557.

70   Gui, C., Hagenbuch, B., Role of transmembrane domain 10 for the function of organic anion transporting polypeptide 1B1. *Protein science : a publication of the Protein Society* 2009, *18*, 2298-2306.

71   Jacquemin, E., Hagenbuch, B., Stieger, B., Wolkoff, A. W., Meier, P. J., Expression cloning of a rat liver Na(+)-independent organic anion transporter. *Proceedings of the National Academy of Sciences of the United States of America* 1994, *91*, 133-137.

72   Kullak-Ublick, G. A., Hagenbuch, B., Stieger, B., Schteingart, C. D.*, et al.*, Molecular and functional characterization of an organic anion transporting polypeptide cloned from human liver. *Gastroenterology* 1995, *109*, 1274-1282.

73   Walters, H. C., Craddock, A. L., Fusegawa, H., Willingham, M. C., Dawson, P. A., Expression, transport properties, and chromosomal location of organic anion transporter subtype 3. *American journal of physiology. Gastrointestinal and liver physiology* 2000, *279*, G1188-1200.

74   Shi, X., Bai, S., Ford, A. C., Burk, R. D.*, et al.*, Stable inducible expression of a functional rat liver organic anion transport protein in HeLa cells. *The Journal of biological chemistry* 1995, *270*, 25591-25595.

75   Noe, B., Hagenbuch, B., Stieger, B., Meier, P. J., Isolation of a multispecific organic anion and cardiac glycoside transporter from rat brain. *Proceedings of the National Academy of Sciences of the United States of America* 1997, *94*, 10346-10350.

76   Sai, Y., Kaneko, Y., Ito, S., Mitsuoka, K.*, et al.*, Predominant contribution of organic anion transporting polypeptide OATP-B (OATP2B1) to apical uptake of estrone-3-sulfate by human intestinal Caco-2 cells. *Drug metabolism and disposition: the biological fate of chemicals* 2006, *34*, 1423-1431.

77   Kullak-Ublick, G. A., Hagenbuch, B., Stieger, B., Wolkoff, A. W., Meier, P. J., Functional characterization of the basolateral rat liver organic anion transporting polypeptide. *Hepatology (Baltimore, Md.)* 1994, *20*, 411-416.

78   Mahagita, C., Grassl, S. M., Piyachaturawat, P., Ballatori, N., Human organic anion transporter 1B1 and 1B3 function as bidirectional carriers and do not

mediate GSH-bile acid cotransport. *American journal of physiology. Gastrointestinal and liver physiology* 2007, *293*, G271-278.

79   Buxhofer-Ausch, V., Secky, L., Wlcek, K., Svoboda, M*., et al.*, Tumor-specific expression of organic anion-transporting polypeptides: transporters as novel targets for cancer therapy. *Journal of drug delivery* 2013, *2013*, 863539.

80   Steckelbroeck, S., Nassen, A., Ugele, B., Ludwig, M*., et al.*, Steroid sulfatase (STS) expression in the human temporal lobe: enzyme activity, mRNA expression and immunohistochemistry study. *Journal of neurochemistry* 2004, *89*, 403-417.

81   Gao, B., Hagenbuch, B., Kullak-Ublick, G. A., Benke, D*., et al.*, Organic anion-transporting polypeptides mediate transport of opioid peptides across blood-brain barrier. *The Journal of pharmacology and experimental therapeutics* 2000, *294*, 73-79.

82   Lee, W., Glaeser, H., Smith, L. H., Roberts, R. L*., et al.*, Polymorphisms in human organic anion-transporting polypeptide 1A2 (OATP1A2): implications for altered drug disposition and central nervous system drug entry. *The Journal of biological chemistry* 2005, *280*, 9610-9617.

83   Glaeser, H., Bailey, D. G., Dresser, G. K., Gregor, J. C*., et al.*, Intestinal drug transporter expression and the impact of grapefruit juice in humans. *Clinical pharmacology and therapeutics* 2007, *81*, 362-370.

84   Obaidat, A., Roth, M., Hagenbuch, B., The expression and function of organic anion transporting polypeptides in normal tissues and in cancer. *Annual review of pharmacology and toxicology* 2012, *52*, 135-151.

85   Bronger, H., Konig, J., Kopplow, K., Steiner, H. H*., et al.*, ABCC drug efflux pumps and organic anion uptake transporters in human gliomas and the blood-tumor barrier. *Cancer research* 2005, *65*, 11419-11428.

86   Meyer zu Schwabedissen, H. E., Kim, R. B., Hepatic OATP1B transporters and nuclear receptors PXR and CAR: interplay, regulation of drug disposition genes, and single nucleotide polymorphisms. *Molecular pharmaceutics* 2009, *6*, 1644-1661.

87   Wlcek, K., Svoboda, M., Thalhammer, T., Sellner, F*., et al.*, Altered expression of organic anion transporter polypeptide (OATP) genes in human breast carcinoma. *Cancer biology & therapy* 2008, *7*, 1450-1455.

88   Liedauer, R., Svoboda, M., Wlcek, K., Arrich, F.*, et al.*, Different expression patterns of organic anion transporting polypeptides in osteosarcomas, bone metastases and aneurysmal bone cysts. *Oncology reports* 2009, *22*, 1485-1492.

89   Konig, J., Cui, Y., Nies, A. T., Keppler, D., A novel human organic anion transporting polypeptide localized to the basolateral hepatocyte membrane. *American journal of physiology. Gastrointestinal and liver physiology* 2000, *278*, G156-164.

90   Tirona, R. G., Kim, R. B., Pharmacogenomics of organic anion-transporting polypeptides (OATP). *Advanced drug delivery reviews* 2002, *54*, 1343-1352.

91   Monks, N. R., Liu, S., Xu, Y., Yu, H.*, et al.*, Potent cytotoxicity of the phosphatase inhibitor microcystin LR and microcystin analogues in OATP1B1- and OATP1B3-expressing HeLa cells. *Molecular cancer therapeutics* 2007, *6*, 587-598.

92   Libra, A., Fernetti, C., Lorusso, V., Visigalli, M.*, et al.*, Molecular determinants in the transport of a bile acid-derived diagnostic agent in tumoral and nontumoral cell lines of human liver. *The Journal of pharmacology and experimental therapeutics* 2006, *319*, 809-817.

93   Hsiang, B., Zhu, Y., Wang, Z., Wu, Y.*, et al.*, A novel human hepatic organic anion transporting polypeptide (OATP2). Identification of a liver-specific human organic anion transporting polypeptide and identification of rat and human hydroxymethylglutaryl-CoA reductase inhibitor transporters. *The Journal of biological chemistry* 1999, *274*, 37161-37168.

94   Abe, T., Unno, M., Onogawa, T., Tokui, T.*, et al.*, LST-2, a human liver-specific organic anion transporter, determines methotrexate sensitivity in gastrointestinal cancers. *Gastroenterology* 2001, *120*, 1689-1699.

95   Tsujimoto, M., Dan, Y., Hirata, S., Ohtani, H., Sawada, Y., Influence of SLCO1B3 gene polymorphism on the pharmacokinetics of digoxin in terminal renal failure. *Drug metabolism and pharmacokinetics* 2008, *23*, 406-411.

96   Lockhart, A. C., Harris, E., Lafleur, B. J., Merchant, N. B.*, et al.*, Organic anion transporting polypeptide 1B3 (OATP1B3) is overexpressed in colorectal tumors and is a predictor of clinical outcome. *Clinical and experimental gastroenterology* 2008, *1*, 1-7.

97 Tamai, I., Nezu, J., Uchino, H., Sai, Y.*, et al.*, Molecular identification and characterization of novel members of the human organic anion transporter (OATP) family. *Biochemical and biophysical research communications* 2000, *273*, 251-260.

98 Pizzagalli, F., Hagenbuch, B., Stieger, B., Klenk, U.*, et al.*, Identification of a novel human organic anion transporting polypeptide as a high affinity thyroxine transporter. *Molecular endocrinology (Baltimore, Md.)* 2002, *16*, 2283-2296.

99 Gao, B., Huber, R. D., Wenzel, A., Vavricka, S. R.*, et al.*, Localization of organic anion transporting polypeptides in the rat and human ciliary body epithelium. *Experimental eye research* 2005, *80*, 61-72.

100 Schuster, V. L., Prostaglandin transport. *Prostaglandins & other lipid mediators* 2002, *68-69*, 633-647.

101 Choi, K., Zhuang, H., Crain, B., Dore, S., Expression and localization of prostaglandin transporter in Alzheimer disease brains and age-matched controls. *Journal of neuroimmunology* 2008, *195*, 81-87.

102 Mandery, K., Bujok, K., Schmidt, I., Wex, T.*, et al.*, Influence of cyclooxygenase inhibitors on the function of the prostaglandin transporter organic anion-transporting polypeptide 2A1 expressed in human gastroduodenal mucosa. *The Journal of pharmacology and experimental therapeutics* 2010, *332*, 345-351.

103 Kang, J., Chapdelaine, P., Parent, J., Madore, E.*, et al.*, Expression of human prostaglandin transporter in the human endometrium across the menstrual cycle. *The Journal of clinical endocrinology and metabolism* 2005, *90*, 2308-2313.

104 Bao, Y., Pucci, M. L., Chan, B. S., Lu, R.*, et al.*, Prostaglandin transporter PGT is expressed in cell types that synthesize and release prostanoids. *American journal of physiology. Renal physiology* 2002, *282*, F1103-1110.

105 Chi, Y., Pucci, M. L., Schuster, V. L., Dietary salt induces transcription of the prostaglandin transporter gene in renal collecting ducts. *American journal of physiology. Renal physiology* 2008, *295*, F765-771.

106 Nomura, T., Lu, R., Pucci, M. L., Schuster, V. L., The two-step model of prostaglandin signal termination: in vitro reconstitution with the prostaglandin transporter and prostaglandin 15 dehydrogenase. *Molecular pharmacology* 2004, *65*, 973-978.

107 Kullak-Ublick, G. A., Ismair, M. G., Stieger, B., Landmann, L.*, et al.*, Organic anion-transporting polypeptide B (OATP-B) and its functional comparison with three other OATPs of human liver. *Gastroenterology* 2001, *120*, 525-533.

108 Kobayashi, D., Nozawa, T., Imai, K., Nezu, J.*, et al.*, Involvement of human organic anion transporting polypeptide OATP-B (SLC21A9) in pH-dependent transport across intestinal apical membrane. *The Journal of pharmacology and experimental therapeutics* 2003, *306*, 703-708.

109 Grube, M., Kock, K., Oswald, S., Draber, K.*, et al.*, Organic anion transporting polypeptide 2B1 is a high-affinity transporter for atorvastatin and is expressed in the human heart. *Clinical pharmacology and therapeutics* 2006, *80*, 607-620.

110 Pizzagalli, F., Varga, Z., Huber, R. D., Folkers, G.*, et al.*, Identification of steroid sulfate transport processes in the human mammary gland. *The Journal of clinical endocrinology and metabolism* 2003, *88*, 3902-3912.

111 St-Pierre, M. V., Hagenbuch, B., Ugele, B., Meier, P. J., Stallmach, T., Characterization of an organic anion-transporting polypeptide (OATP-B) in human placenta. *The Journal of clinical endocrinology and metabolism* 2002, *87*, 1856-1863.

112 Al Sarakbi, W., Mokbel, R., Salhab, M., Jiang, W. G.*, et al.*, The role of STS and OATP-B mRNA expression in predicting the clinical outcome in human breast cancer. *Anticancer research* 2006, *26*, 4985-4990.

113 Huber, R. D., Gao, B., Sidler Pfandler, M. A., Zhang-Fu, W.*, et al.*, Characterization of two splice variants of human organic anion transporting polypeptide 3A1 isolated from human brain. *American journal of physiology. Cell physiology* 2007, *292*, C795-806.

114 Adachi, H., Suzuki, T., Abe, M., Asano, N.*, et al.*, Molecular characterization of human and rat organic anion transporter OATP-D. *American journal of physiology. Renal physiology* 2003, *285*, F1188-1197.

115 Kindla, J., Rau, T. T., Jung, R., Fasching, P. A.*, et al.*, Expression and localization of the uptake transporters OATP2B1, OATP3A1 and OATP5A1 in non-malignant and malignant breast tissue. *Cancer biology & therapy* 2011, *11*, 584-591.

116 Fujiwara, K., Adachi, H., Nishio, T., Unno, M*., et al.*, Identification of thyroid hormone transporters in humans: different molecules are involved in a tissue-specific manner. *Endocrinology* 2001, *142*, 2005-2012.

117 Sato, K., Sugawara, J., Sato, T., Mizutamari, H*., et al.*, Expression of organic anion transporting polypeptide E (OATP-E) in human placenta. *Placenta* 2003, *24*, 144-148.

118 Wojtal, K. A., Eloranta, J. J., Hruz, P., Gutmann, H*., et al.*, Changes in mRNA expression levels of solute carrier transporters in inflammatory bowel disease patients. *Drug metabolism and disposition: the biological fate of chemicals* 2009, *37*, 1871-1877.

119 Mikkaichi, T., Suzuki, T., Onogawa, T., Tanemoto, M*., et al.*, Isolation and characterization of a digoxin transporter and its rat homologue expressed in the kidney. *Proceedings of the National Academy of Sciences of the United States of America* 2004, *101*, 3569-3574.

120 Yamaguchi, H., Sugie, M., Okada, M., Mikkaichi, T*., et al.*, Transport of estrone 3-sulfate mediated by organic anion transporter OATP4C1: estrone 3-sulfate binds to the different recognition site for digoxin in OATP4C1. *Drug metabolism and pharmacokinetics* 2010, *25*, 314-317.

121 Toyohara, T., Suzuki, T., Morimoto, R., Akiyama, Y*., et al.*, SLCO4C1 transporter eliminates uremic toxins and attenuates hypertension and renal inflammation. *Journal of the American Society of Nephrology : JASN* 2009, *20*, 2546-2555.

122 Okabe, M., Szakacs, G., Reimers, M. A., Suzuki, T*., et al.*, Profiling SLCO and SLC22 genes in the NCI-60 cancer cell lines to identify drug uptake transporters. *Molecular cancer therapeutics* 2008, *7*, 3081-3091.

123 Sainis, I., Fokas, D., Vareli, K., Tzakos, A. G*., et al.*, Cyanobacterial cyclopeptides as lead compounds to novel targeted cancer drugs. *Marine drugs* 2010, *8*, 629-657.

124 Sebastian, K., Detro-Dassen, S., Rinis, N., Fahrenkamp, D*., et al.*, Characterization of SLCO5A1/OATP5A1, a solute carrier transport protein with non-classical function. *PloS one* 2013, *8*, e83257.

125 Olszewski-Hamilton, U., Svoboda, M., Thalhammer, T., Buxhofer-Ausch, V*., et al.*, Organic Anion Transporting Polypeptide 5A1 (OATP5A1) in Small Cell

Lung Cancer (SCLC) Cells: Possible Involvement in Chemoresistance to Satraplatin. *Biomarkers in cancer* 2011, *3*, 31-40.

126   Lee, S. Y., Williamson, B., Caballero, O. L., Chen, Y. T.*, et al.*, Identification of the gonad-specific anion transporter SLCO6A1 as a cancer/testis (CT) antigen expressed in human lung cancer. *Cancer immunity* 2004, *4*, 13.

127   Suzuki, T., Onogawa, T., Asano, N., Mizutamari, H.*, et al.*, Identification and characterization of novel rat and human gonad-specific organic anion transporters. *Molecular endocrinology (Baltimore, Md.)* 2003, *17*, 1203-1215.

128   Oba-Shinjo, S. M., Caballero, O. L., Jungbluth, A. A., Rosemberg, S.*, et al.*, Cancer-testis (CT) antigen expression in medulloblastoma. *Cancer immunity* 2008, *8*, 7.

129   Fahrmayr, C., Fromm, M. F., Konig, J., Hepatic OATP and OCT uptake transporters: their role for drug-drug interactions and pharmacogenetic aspects. *Drug metabolism reviews* 2010, *42*, 380-401.

130   Kalliokoski, A., Niemi, M., Impact of OATP transporters on pharmacokinetics. *British journal of pharmacology* 2009, *158*, 693-705.

131   Pochini, L., Scalise, M., Galluccio, M., Indiveri, C., OCTN cation transporters in health and disease: role as drug targets and assay development. *Journal of biomolecular screening* 2013, *18*, 851-867.

132   Koepsell, H., Endou, H., The SLC22 drug transporter family. *Pflugers Archiv : European journal of physiology* 2004, *447*, 666-676.

133   Gorboulev, V., Ulzheimer, J. C., Akhoundova, A., Ulzheimer-Teuber, I.*, et al.*, Cloning and characterization of two human polyspecific organic cation transporters. *DNA and cell biology* 1997, *16*, 871-881.

134   Zhang, L., Dresser, M. J., Gray, A. T., Yost, S. C.*, et al.*, Cloning and functional expression of a human liver organic cation transporter. *Molecular pharmacology* 1997, *51*, 913-921.

135   Slitt, A. L., Cherrington, N. J., Hartley, D. P., Leazer, T. M., Klaassen, C. D., Tissue distribution and renal developmental changes in rat organic cation transporter mRNA levels. *Drug metabolism and disposition: the biological fate of chemicals* 2002, *30*, 212-219.

136   Alnouti, Y., Petrick, J. S., Klaassen, C. D., Tissue distribution and ontogeny of organic cation transporters in mice. *Drug metabolism and disposition: the biological fate of chemicals* 2006, *34*, 477-482.

137 Karbach, U., Kricke, J., Meyer-Wentrup, F., Gorboulev, V*., et al.*, Localization of organic cation transporters OCT1 and OCT2 in rat kidney. *American journal of physiology. Renal physiology* 2000, *279*, F679-687.

138 Motohashi, H., Sakurai, Y., Saito, H., Masuda, S*., et al.*, Gene expression levels and immunolocalization of organic ion transporters in the human kidney. *Journal of the American Society of Nephrology : JASN* 2002, *13*, 866-874.

139 Kekuda, R., Prasad, P. D., Wu, X., Wang, H*., et al.*, Cloning and functional characterization of a potential-sensitive, polyspecific organic cation transporter (OCT3) most abundantly expressed in placenta. *The Journal of biological chemistry* 1998, *273*, 15971-15979.

140 Wu, X., Kekuda, R., Huang, W., Fei, Y. J*., et al.*, Identity of the organic cation transporter OCT3 as the extraneuronal monoamine transporter (uptake2) and evidence for the expression of the transporter in the brain. *The Journal of biological chemistry* 1998, *273*, 32776-32786.

141 Wu, X., Huang, W., Ganapathy, M. E., Wang, H*., et al.*, Structure, function, and regional distribution of the organic cation transporter OCT3 in the kidney. *American journal of physiology. Renal physiology* 2000, *279*, F449-458.

142 Verhaagh, S., Schweifer, N., Barlow, D. P., Zwart, R., Cloning of the mouse and human solute carrier 22a3 (Slc22a3/SLC22A3) identifies a conserved cluster of three organic cation transporters on mouse chromosome 17 and human 6q26-q27. *Genomics* 1999, *55*, 209-218.

143 Tamai, I., Ohashi, R., Nezu, J., Yabuuchi, H*., et al.*, Molecular and functional identification of sodium ion-dependent, high affinity human carnitine transporter OCTN2. *The Journal of biological chemistry* 1998, *273*, 20378-20382.

144 Tamai, I., Yabuuchi, H., Nezu, J., Sai, Y*., et al.*, Cloning and characterization of a novel human pH-dependent organic cation transporter, OCTN1. *FEBS letters* 1997, *419*, 107-111.

145 Garrett, Q., Xu, S., Simmons, P. A., Vehige, J*., et al.*, Expression and localization of carnitine/organic cation transporter OCTN1 and OCTN2 in ocular epithelium. *Investigative ophthalmology & visual science* 2008, *49*, 4844-4849.

146 Lamhonwah, A. M., Tein, I., Novel localization of OCTN1, an organic cation/carnitine transporter, to mammalian mitochondria. *Biochemical and biophysical research communications* 2006, *345*, 1315-1325.

147 Tokuhiro, S., Yamada, R., Chang, X., Suzuki, A.*, et al.*, An intronic SNP in a RUNX1 binding site of SLC22A4, encoding an organic cation transporter, is associated with rheumatoid arthritis. *Nature genetics* 2003, *35*, 341-348.

148 Lahjouji, K., Elimrani, I., Lafond, J., Leduc, L.*, et al.*, L-Carnitine transport in human placental brush-border membranes is mediated by the sodium-dependent organic cation transporter OCTN2. *American journal of physiology. Cell physiology* 2004, *287*, C263-269.

149 Lamhonwah, A. M., Ackerley, C. A., Tilups, A., Edwards, V. D.*, et al.*, OCTN3 is a mammalian peroxisomal membrane carnitine transporter. *Biochemical and biophysical research communications* 2005, *338*, 1966-1972.

150 Srimaroeng, C., Perry, J. L., Pritchard, J. B., Physiology, structure, and regulation of the cloned organic anion transporters. *Xenobiotica; the fate of foreign compounds in biological systems* 2008, *38*, 889-935.

151 Hosoyamada, M., Sekine, T., Kanai, Y., Endou, H., Molecular cloning and functional expression of a multispecific organic anion transporter from human kidney. *The American journal of physiology* 1999, *276*, F122-128.

152 Sekine, T., Cha, S. H., Tsuda, M., Apiwattanakul, N.*, et al.*, Identification of multispecific organic anion transporter 2 expressed predominantly in the liver. *FEBS letters* 1998, *429*, 179-182.

153 Sun, W., Wu, R. R., van Poelje, P. D., Erion, M. D., Isolation of a family of organic anion transporters from human liver and kidney. *Biochemical and biophysical research communications* 2001, *283*, 417-422.

154 Cha, S. H., Sekine, T., Fukushima, J. I., Kanai, Y.*, et al.*, Identification and characterization of human organic anion transporter 3 expressing predominantly in the kidney. *Molecular pharmacology* 2001, *59*, 1277-1286.

155 Cha, S. H., Sekine, T., Kusuhara, H., Yu, E.*, et al.*, Molecular cloning and characterization of multispecific organic anion transporter 4 expressed in the placenta. *The Journal of biological chemistry* 2000, *275*, 4507-4512.

156 Liang, R., Fei, Y. J., Prasad, P. D., Ramamoorthy, S.*, et al.*, Human intestinal H+/peptide cotransporter. Cloning, functional expression, and chromosomal localization. *The Journal of biological chemistry* 1995, *270*, 6456-6463.

157 Zhang, E. Y., Emerick, R. M., Pak, Y. A., Wrighton, S. A., Hillgren, K. M., Comparison of human and monkey peptide transporters: PEPT1 and PEPT2. *Molecular pharmaceutics* 2004, *1*, 201-210.

158 Pastor-Anglada, M., Cano-Soldado, P., Errasti-Murugarren, E., Casado, F. J., SLC28 genes and concentrative nucleoside transporter (CNT) proteins. *Xenobiotica; the fate of foreign compounds in biological systems* 2008, *38*, 972-994.

159 Young, J. D., Yao, S. Y., Sun, L., Cass, C. E., Baldwin, S. A., Human equilibrative nucleoside transporter (ENT) family of nucleoside and nucleobase transporter proteins. *Xenobiotica; the fate of foreign compounds in biological systems* 2008, *38*, 995-1021.

160 Wang, J., Su, S. F., Dresser, M. J., Schaner, M. E.*, et al.*, Na(+)-dependent purine nucleoside transporter from human kidney: cloning and functional characterization. *The American journal of physiology* 1997, *273*, F1058-1065.

161 Shin, H. C., Landowski, C. P., Sun, D., Vig, B. S.*, et al.*, Functional expression and characterization of a sodium-dependent nucleoside transporter hCNT2 cloned from human duodenum. *Biochemical and biophysical research communications* 2003, *307*, 696-703.

162 Damaraju, V. L., Elwi, A. N., Hunter, C., Carpenter, P.*, et al.*, Localization of broadly selective equilibrative and concentrative nucleoside transporters, hENT1 and hCNT3, in human kidney. *American journal of physiology. Renal physiology* 2007, *293*, F200-211.

163 Lai, Y., Tse, C. M., Unadkat, J. D., Mitochondrial expression of the human equilibrative nucleoside transporter 1 (hENT1) results in enhanced mitochondrial toxicity of antiviral drugs. *The Journal of biological chemistry* 2004, *279*, 4490-4497.

164 Govindarajan, R., Leung, G. P., Zhou, M., Tse, C. M.*, et al.*, Facilitated mitochondrial import of antiviral and anticancer nucleoside drugs by human equilibrative nucleoside transporter-3. *American journal of physiology. Gastrointestinal and liver physiology* 2009, *296*, G910-922.

165 Griffiths, M., Beaumont, N., Yao, S. Y., Sundaram, M.*, et al.*, Cloning of a human nucleoside transporter implicated in the cellular uptake of adenosine and chemotherapeutic drugs. *Nature medicine* 1997, *3*, 89-93.

166 Damaraju, V. L., Visser, F., Zhang, J., Mowles, D.*, et al.*, Role of human nucleoside transporters in the cellular uptake of two inhibitors of IMP dehydrogenase, tiazofurin and benzamide riboside. *Molecular pharmacology* 2005, *67*, 273-279.

167 Nagai, M., Furihata, T., Matsumoto, S., Ishii, S.*, et al.*, Identification of a new organic anion transporting polypeptide 1B3 mRNA isoform primarily expressed in human cancerous tissues and cells. *Biochemical and biophysical research communications* 2012, *418*, 818-823.

168 Govindarajan, R., Endres, C. J., Whittington, D., LeCluyse, E.*, et al.*, Expression and hepatobiliary transport characteristics of the concentrative and equilibrative nucleoside transporters in sandwich-cultured human hepatocytes. *American journal of physiology. Gastrointestinal and liver physiology* 2008, *295*, G570-580.

169 Pennycooke, M., Chaudary, N., Shuralyova, I., Zhang, Y., Coe, I. R., Differential expression of human nucleoside transporters in normal and tumor tissue. *Biochemical and biophysical research communications* 2001, *280*, 951-959.

170 Govindarajan, R., Bakken, A. H., Hudkins, K. L., Lai, Y.*, et al.*, In situ hybridization and immunolocalization of concentrative and equilibrative nucleoside transporters in the human intestine, liver, kidneys, and placenta. *American journal of physiology. Regulatory, integrative and comparative physiology* 2007, *293*, R1809-1822.

171 Baldwin, S. A., Yao, S. Y., Hyde, R. J., Ng, A. M.*, et al.*, Functional characterization of novel human and mouse equilibrative nucleoside transporters (hENT3 and mENT3) located in intracellular membranes. *The Journal of biological chemistry* 2005, *280*, 15880-15887.

172 Barnes, K., Dobrzynski, H., Foppolo, S., Beal, P. R.*, et al.*, Distribution and functional characterization of equilibrative nucleoside transporter-4, a novel cardiac adenosine transporter activated at acidic pH. *Circulation research* 2006, *99*, 510-519.

173 Hasler, J. A., Pharmacogenetics of cytochromes P450. *Molecular aspects of medicine* 1999, *20*, 12-24, 25-137.

174 Jakoby, W. B., Ziegler, D. M., The enzymes of detoxication. *The Journal of biological chemistry* 1990, *265*, 20715-20718.

175 Kretschy, N., Teichmann, M., Kopf, S., Atanasov, A. G.*, et al.*, In vitro inhibition of breast cancer spheroid-induced lymphendothelial defects resembling intravasation into the lymphatic vasculature by acetohexamide, isoxsuprine, nifedipin and proadifen. *British journal of cancer* 2013, *108*, 570-578.

176 Madlener, S., Saiko, P., Vonach, C., Viola, K.*, et al.*, Multifactorial anticancer effects of digalloyl-resveratrol encompass apoptosis, cell-cycle arrest, and inhibition of lymphendothelial gap formation in vitro. *British journal of cancer* 2010, *102*, 1361-1370.

177 Honn, K. V., Tang, D. G., Grossi, I., Duniec, Z. M.*, et al.*, Tumor cell-derived 12(S)-hydroxyeicosatetraenoic acid induces microvascular endothelial cell retraction. *Cancer research* 1994, *54*, 565-574.

178 Nebert, D. W., Wikvall, K., Miller, W. L., Human cytochromes P450 in health and disease. *Philosophical transactions of the Royal Society of London. Series B, Biological sciences* 2013, *368*, 20120431.

179 Roman, R. J., P-450 metabolites of arachidonic acid in the control of cardiovascular function. *Physiological reviews* 2002, *82*, 131-185.

180 Venkatakrishnan, K., Von Moltke, L. L., Greenblatt, D. J., Human drug metabolism and the cytochromes P450: application and relevance of in vitro models. *Journal of clinical pharmacology* 2001, *41*, 1149-1179.

181 Capdevila, J. H., Falck, J. R., Harris, R. C., Cytochrome P450 and arachidonic acid bioactivation. Molecular and functional properties of the arachidonate monooxygenase. *Journal of lipid research* 2000, *41*, 163-181.

182 Nelson, D. R., Koymans, L., Kamataki, T., Stegeman, J. J.*, et al.*, P450 superfamily: update on new sequences, gene mapping, accession numbers and nomenclature. *Pharmacogenetics* 1996, *6*, 1-42.

183 Ortiz de Montellano, P. R., Oxygen activation and reactivity. In Cytochrome P450: Structure, Mechanism, and Biochemistry (2nd edition). *Plenum Press, New York* 1995, 245–304.

184 Vorrink, S. U., Hudachek, D. R., Domann, F. E., Epigenetic determinants of CYP1A1 induction by the aryl hydrocarbon receptor agonist 3,3',4,4',5-pentachlorobiphenyl (PCB 126). *International journal of molecular sciences* 2014, *15*, 13916-13931.

185 Beresford, A. P., CYP1A1: friend or foe? *Drug metabolism reviews* 1993, *25*, 503-517.

186 Ma, Q., Lu, A. Y., CYP1A induction and human risk assessment: an evolving tale of in vitro and in vivo studies. *Drug metabolism and disposition: the biological fate of chemicals* 2007, *35*, 1009-1016.

187 Zanger, U. M., Turpeinen, M., Klein, K., Schwab, M., Functional pharmacogenetics/genomics of human cytochromes P450 involved in drug biotransformation. *Analytical and bioanalytical chemistry* 2008, *392*, 1093-1108.

188 Landi, M. T., Sinha, R., Lang, N. P., Kadlubar, F. F., Human cytochrome P4501A2. *IARC scientific publications* 1999, 173-195.

189 Liu, Y., Lin, C. S., Zhang, A. M., Song, H., Fan, C. C., The CYP1B1 Leu432Val polymorphism and risk of urinary system cancers. *Tumour biology : the journal of the International Society for Oncodevelopmental Biology and Medicine* 2014, *35*, 4719-4725.

190 Deeni, Y. Y., Ibbotson, S. H., Woods, J. A., Wolf, C. R., Smith, G., Cytochrome P450 CYP1B1 interacts with 8-methoxypsoralen (8-MOP) and influences psoralen-ultraviolet A (PUVA) sensitivity. *PloS one* 2013, *8*, e75494.

191 Hofmann, M. H., Blievernicht, J. K., Klein, K., Saussele, T.*, et al.*, Aberrant splicing caused by single nucleotide polymorphism c.516G>T [Q172H], a marker of CYP2B6*6, is responsible for decreased expression and activity of CYP2B6 in liver. *The Journal of pharmacology and experimental therapeutics* 2008, *325*, 284-292.

192 Saussele, T., Burk, O., Blievernicht, J. K., Klein, K.*, et al.*, Selective induction of human hepatic cytochromes P450 2B6 and 3A4 by metamizole. *Clinical pharmacology and therapeutics* 2007, *82*, 265-274.

193 Turpeinen, M., Raunio, H., Pelkonen, O., The functional role of CYP2B6 in human drug metabolism: substrates and inhibitors in vitro, in vivo and in silico. *Current drug metabolism* 2006, *7*, 705-714.

194 Johnson, M. D., Zuo, H., Lee, K. H., Trebley, J. P.*, et al.*, Pharmacological characterization of 4-hydroxy-N-desmethyl tamoxifen, a novel active metabolite of tamoxifen. *Breast cancer research and treatment* 2004, *85*, 151-159.

195 Scott, E. E., Halpert, J. R., Structures of cytochrome P450 3A4. *Trends in biochemical sciences* 2005, *30*, 5-7.

196 Yamazaki, H., Shimada, T., Progesterone and testosterone hydroxylation by cytochromes P450 2C19, 2C9, and 3A4 in human liver microsomes. *Archives of biochemistry and biophysics* 1997, *346*, 161-169.

197 Wolbold, R., Klein, K., Burk, O., Nussler, A. K.*, et al.*, Sex is a major determinant of CYP3A4 expression in human liver. *Hepatology (Baltimore, Md.)* 2003, *38*, 978-988.

198 Oliw, E. H., Guengerich, F. P., Oates, J. A., Oxygenation of arachidonic acid by hepatic monooxygenases. Isolation and metabolism of four epoxide intermediates. *The Journal of biological chemistry* 1982, *257*, 3771-3781.

199 Chacos, N., Falck, J. R., Wixtrom, C., Capdevila, J., Novel epoxides formed during the liver cytochrome P-450 oxidation of arachidonic acid. *Biochemical and biophysical research communications* 1982, *104*, 916-922.

200 Capdevila, J., Marnett, L. J., Chacos, N., Prough, R. A., Estabrook, R. W., Cytochrome P-450-dependent oxygenation of arachidonic acid to hydroxyicosatetraenoic acids. *Proceedings of the National Academy of Sciences of the United States of America* 1982, *79*, 767-770.

201 Capdevila, J., Yadagiri, P., Manna, S., Falck, J. R., Absolute configuration of the hydroxyeicosatetraenoic acids (HETEs) formed during catalytic oxygenation of arachidonic acid by microsomal cytochrome P-450. *Biochemical and biophysical research communications* 1986, *141*, 1007-1011.

202 Pruthi, R. S., Wallen, E. M., Cyclooxygenase-2: a therapeutic target for prostate cancer. *Clinical genitourinary cancer* 2005, *4*, 203-211.

203 Koki, A. T., Masferrer, J. L., Celecoxib: a specific COX-2 inhibitor with anticancer properties. *Cancer control : journal of the Moffitt Cancer Center* 2002, *9*, 28-35.

204 Smith, W. L., Garavito, R. M., DeWitt, D. L., Prostaglandin endoperoxide H synthases (cyclooxygenases)-1 and -2. *The Journal of biological chemistry* 1996, *271*, 33157-33160.

205 Futaki, N., Takahashi, S., Yokoyama, M., Arai, I.*, et al.*, NS-398, a new anti-inflammatory agent, selectively inhibits prostaglandin G/H synthase/cyclooxygenase (COX-2) activity in vitro. *Prostaglandins* 1994, *47*, 55-59.

206 Cabral, M., Martin-Venegas, R., Moreno, J. J., Role of arachidonic acid metabolites on the control of non-differentiated intestinal epithelial cell growth. *The international journal of biochemistry & cell biology* 2013, *45*, 1620-1628.

207 Eberhart, C. E., Coffey, R. J., Radhika, A., Giardiello, F. M.*, et al.*, Up-regulation of cyclooxygenase 2 gene expression in human colorectal adenomas and adenocarcinomas. *Gastroenterology* 1994, *107*, 1183-1188.

208 Haining, J. L., Axelrod, B., Induction period in the lipoxidase-catalyzed oxidation of linoleic acid and its abolition by substrate peroxide. *The Journal of biological chemistry* 1958, *232*, 193-202.

209 Wisastra, R., Dekker, F. J., Inflammation, Cancer and Oxidative Lipoxygenase Activity are Intimately Linked. *Cancers* 2014, *6*, 1500-1521.

210 Brash, A. R., Lipoxygenases: occurrence, functions, catalysis, and acquisition of substrate. *The Journal of biological chemistry* 1999, *274*, 23679-23682.

211 Shureiqi, I., Lippman, S. M., Lipoxygenase modulation to reverse carcinogenesis. *Cancer research* 2001, *61*, 6307-6312.

212 Liu, C., Xu, D., Liu, L., Schain, F.*, et al.*, 15-Lipoxygenase-1 induces expression and release of chemokines in cultured human lung epithelial cells. *American journal of physiology. Lung cellular and molecular physiology* 2009, *297*, L196-203.

213 Yla-Herttuala, S., Rosenfeld, M. E., Parthasarathy, S., Sigal, E.*, et al.*, Gene expression in macrophage-rich human atherosclerotic lesions. 15-lipoxygenase and acetyl low density lipoprotein receptor messenger RNA colocalize with oxidation specific lipid-protein adducts. *The Journal of clinical investigation* 1991, *87*, 1146-1152.

214 Li, J., Rao, J., Liu, Y., Cao, Y.*, et al.*, 15-Lipoxygenase promotes chronic hypoxia-induced pulmonary artery inflammation via positive interaction with nuclear factor-kappaB. *Arteriosclerosis, thrombosis, and vascular biology* 2013, *33*, 971-979.

215 Wu, M. Y., Lin, T. H., Chiu, Y. C., Liou, H. C.*, et al.*, Involvement of 15-lipoxygenase in the inflammatory arthritis. *Journal of cellular biochemistry* 2012, *113*, 2279-2289.

216 Zhao, Y., Wang, W., Wang, Q., Zhang, X., Ye, L., Lipid metabolism enzyme 5-LOX and its metabolite LTB4 are capable of activating transcription factor NF-

kappaB in hepatoma cells. *Biochemical and biophysical research communications* 2012, *418*, 647-651.

8 Aims of the Thesis

Cancer is still one of the major health issues in western countries and ranges among the top 4 causes of death. The major problems in cancer therapy are severe side effects, low patient compliance and active efflux transporters lowering the availability of anti-cancer drugs resulting in therapy resistance. This active efflux transport represents the first defense of cells against xenobiotics which explains the crucial role of upregulated ABC-transporters in cancerous tissues during therapy resulting in low therapy effects. Therefore new drugs evading or inhibiting AET systems and using transporter systems in tumor tissue to increase drug concentrations are needed.

Considering drug transport we wanted to focus on active transport via OATPs which are known to be expressed in various cancer tissues and strongly affecting intracellular drug concentrations as they form a superfamily of sodium-independent transport systems and mediate the cellular uptake of many endogenous and exogenous chemicals including drugs in clinical use. Although multi-specificity and wide tissue distribution are common characteristics of many OATPs, some members have a high substrate specificity and exhibit unique cellular expression in distinct organs. For that reason we wanted to elucidate specific expression of OATPs in SCLC and, furthermore, their alteration during therapy. In addition, we planned to highlighte the role of OATPs in the transport of resveratrol and flavopiridol in breast cancer cell lines.

As SLC carriers interoperate with cellular metabolizing enzymes of phase 1 and phase II as well as with efflux transporters, interplays between uptake, reuptake after metabolism, biotransformation and efflux strongly affect the distribution of drugs. Besides drug uptake and specific distribution the metabolic profile of drugs is crucial for good therapy outcomes. In addition, effects of FDA drugs are recognised for their impact on lipoxigenases. We wanted to elucidate the role of lipoxygenases and CYP450 on the arachidonic acid metabolic cascade with a special focus on 12(S)-HETE. Therefore understanding of drug enzyme interaction is crucial for therapy, drug-drug interaction and drug disease interaction.

9 Results

9.1 Original Papers and Manuscripts

Stefan Brenner, Lukas Klameth, Juliane Riha, Madeleine Schölm, Gerhard Hamilton, Erika Bajna, Christoph Ausch, Angelika Reiner, Walter Jäger, Theresia Thalhammer and Veronika Buxhofer-Ausch; Specific expression of OATPs in primary small cell lung cancer (SCLC) cells as novel biomarkers for diagnosis and therapy; Cancer Lett. (Impact factor 5.016) 2014 Oct 6. pii: S0304-3835(14)00552-7.

Juliane Riha, **Stefan Brenner**, Michaela Böhmdorfer, Benedikt Giessrigl, Marc Pignitter, Katharina Schueller, Theresia Thalhammer, Bruno Stieger, Veronika Somoza, Thomas Szekeres and Walter Jäger; Resveratrol and its major sulfated conjugates are substrates of organic anion transporting polypeptides (OATPs): impact on growth of ZR-75-1 breast cancer cells; Mol Nutr Food Res. (Impact factor 4.909) 2014 Sep;58(9):1830-42.
      I performed cell assay experiments

Stefan Brenner, Juliane Riha, Benedikt Giessrigl, Theresia Thalhammer, Michael Grusch, Georg Krupitza, Bruno Stieger and Walter Jäger; The effect of organic anion-transporting polypeptides 1B1, 1B3 and 2B1 on the antitumor activity of flavopiridol against breast cancer cells; Int J Oncol. (Impact factor 2.773) October 2014

Juliane Riha, **Stefan Brenner**, Alzbeta Srovnalova, Lukas Klameth, Zdenek Dvorak, Walter Jäger and Theresa Thalhammer; Effects of anthocyans on the expression of organic anion transporting polypeptides (OATPs) in primary human hepatocytes; Food Funct. (Impact factor 2.907) Submitted October 2014
      I performed Western Blot experiments and statistical analyses

Kiss Izabella, Unger Christine,Nguyen Huu Chi, Atanasov Atanas Georgiev, Kramer Nina, Chatuphonprasert Waranya, **Brenner Stefan**, McKinnon Ruxandra, Peschel Andrea, Vasas Andrea, Lajter Ildikó, Kain Renate, Saiko Philipp, Szekeres Thomas, Kenner Lukas, Hassler Melanie R., Diaz Rene, Frisch Richard, Dirsch Verena M., Jäger Walter, de Martin Rainer, Bochkov Valery N., Passreiter Claus M., Peter-Vörösmarty Barbara, Mader Robert M., Grusch Michael, Dolznig Helmut, Kopp

Brigitte, Zupko Istvan, Hohmann Judit, Krupitza Georg; Lobatin B inhibits NPM/ALK and NF-κB attenuating anaplastic-large-cell-lymphomagenesis and lymphendothelial tumour intravasation; Cancer Lett. (Impact factor 5.016) Submitted October 2014

     I performed 12(S)-HETE ELISA assays

Unger Christine, Kiss Izabella, Vasas Andrea, Lajter Ildikó, Kramer Nina, Atanasov Atanas Georgiev, Chi Nguyen Huu, Chatuphonprasert Waranya, **Brenner Stefan**, McKinnon Ruxandra, Peschel Andrea, Kain Renate, Saiko Philipp, Szekeres Thomas, Kenner Lukas, Hassler Melanie R., Diaz Rene, Frisch Richard, Dirsch Verena M., Jäger Walter, de Martin Rainer, Bochkov Valery N., Passreiter Claus M., Peter-Vörösmarty Barbara, Mader Robert M., Grusch Michael, Dolznig Helmut, Kopp Brigitte, Zupko Istvan, Hohmann Judit, Krupitza Georg; The germacranolide sesquiterpene lactone neurolenin B of the medicinal plant Neurolaena lobata inhibits NPM/ALK-driven cell expansion and NF-κB-driven tumour; Intravasation; Arch Toxicol. (Impact factor 5.078) Submitted October 2014

     I performed 12(S)-HETE ELISA assays

Robert Mader, Daniel Senfter, Silvio Holzner, Maria Kalipciyan, Anna Staribacher, Angelika Walzl, Nicole Huttary, Sigurd Krieger, **Stefan Brenner**, Walter Jäger, Georg Krupitza, and Helmut Dolznig; Loss of miR-200 family in 5-fluorouracil resistant colon cancer drives lymphendothelial invasiveness in vitro; Oncogene (Impact factor 8.559) Submitted October 2014

     I performed 12(S)-HETE ELISA assays

Specific expression of OATPs in primary small cell lung cancer (SCLC) cells as novel biomarkers for diagnosis and therapy

Stefan Brenner, Lukas Klameth, Juliane Riha, Madeleine Schölm, Gerhard Hamilton, Erika Bajna, Christoph Ausch, Angelika Reiner, Walter Jäger, Theresia Thalhammer, Veronika Buxhofer-Ausch.

Original Articles

Specific expression of OATPs in primary small cell lung cancer (SCLC) cells as novel biomarkers for diagnosis and therapy

Stefan Brenner [a], Lukas Klameth [b,d], Juliane Riha [a], Madeleine Schölm [b], Gerhard Hamilton [d], Erika Bajna [b], Christoph Ausch [c,d], Angelika Reiner [d,e], Walter Jäger [a], Theresia Thalhammer [b,*], Veronika Buxhofer-Ausch [d,f]

[a] Department of Clinical Pharmacy and Diagnostics, University of Vienna, Vienna, Austria
[b] Department of Pathophysiology and Allergy Research, Medical University of Vienna, Vienna, Austria
[c] Department of Surgery, Donauspital, Vienna, Austria
[d] Cluster for Translational Oncology, Ludwig Boltzmann Society, Vienna, Austria
[e] Department of Pathology, Donauspital, Vienna, Austria
[f] Department of Internal Medicine 2, Donauspital, Vienna, Austria

ARTICLE INFO

ABSTRACT

The expression of organic anion transporting polypeptides (OATPs) was elucidated in cell lines from small cell lung cancer (SCLC) and lung carcinoids and in paraffin-embedded samples from primary and metastatic SCLCs. We found a strong relationship between OATP expression and the origin of the cells, as cells from primary or metastatic SCLC and carcinoid tumors differ with respect to OATP levels. OATP4A1 is most prominent in non-malignant lung tissue and in all SCLC and carcinoid cell lines and tissues, OATP5A1 is most prominent in metastatic cells, and OATP6A1 is most prominent in SCLC cell lines and tumors. Treatment with topotecan, etoposide and cisplatin caused significant changes in the expression patterns of OATP4A1, OATP5A1, OATP6A1, chromogranin and synaptophysin. This effect was also evident in GLC-14 cells from an untreated SCLC patient before chemotherapy compared to GLC-16/-19 chemoresistant tumor cells from this patient after therapy. mRNA expression of OATP4A1, 5A1 and 6A1 correlates with protein expression as confirmed by quantitative microscopic image analysis and Western blots. OATPs might be novel biomarkers for tumor progression and the development of metastasis in SCLC patients.

© 2014 Published by Elsevier Ireland Ltd.

Introduction

Lung cancer is the leading cause of cancer-related death in western countries and small-cell lung cancer (SCLC) accounts for 15%–20% of all lung cancer types [1]. SCLC is characterized by rapid tumor doubling time, a high growth fraction and the development of widespread metastases, especially to the brain, at a rather early stage [2]. In contrast to the majority of non-small cell lung cancers (NSCLC), SCLCs express neuroendocrine markers (e.g., chromogranin A, synaptophysin) and are thought to originate from lung neuronal precursor cells, from which other neuroendocrine lung tumors (e.g., carcinoids) are also derived [3,4]. Importantly, SCLC cells, but not carcinoids, are usually highly responsive to initial chemotherapy, usually with a platin derivative-containing regimen in combination with etoposide. However, a subsequent relapse of SCLC mostly occurs within 2 years. Recurrent tumors are than often resistant or has only a mild response to further treatment [5,6]. Only

10% of patients with advanced tumors survive longer than 2 years, leading to a five-year survival rate of only 3%–7% [7–9]. Therefore, clues to a more effective treatment for primary SCLC and its metastases are of utmost interest. In lung cancer, the role of transporters in drug absorption, distribution and elimination processes as well as in drug–drug interactions is increasingly being recognized [10]. One of the most important cellular uptake mechanisms for anticancer drugs and endogenous compounds is via the organic anion-transporting polypeptides (OATP proteins/*SLCO* genes) [11,12]. The term OATP is used for both genes and proteins throughout the manuscript [13–18]. Eleven human OATPs, divided into six distinct subfamilies (OATP1-6) [19], were found in human tissues mainly at biological barriers with a specific pattern [16,20]. Some OATPs, such as OATP4A1, are widely expressed in the human body and were also identified at the mRNA level in bronchial epithelial cell models and might contribute to the uptake of solutes into lung cells [10,21–23]. The malignant transformation of cells is known to alter the OATP expression pattern in organs. Indeed, the gonad-specific OATP6A1 was identified as a cancer-testis antigen in lung tumors and lung tumor cell lines. The altered uptake of OATP substrates including anticancer drugs may lead to changes in the activity of drugs

* Corresponding author. Tel.: +43140400–51280; fax: 43140400–51300.
  E-mail address: theresia.thalhammer@meduniwien.ac.at (T. Thalhammer).

and may therefore play a role in the chemosensitivity of cancer cells. For example, OATP5A1 seems to play a role in the resistance of lung cancer cell lines to satraplatin [20,24]. Otherwise, treatment with chemotherapeutic agents alters the expression pattern of OATPs in the cells, which again influences the response to specific cancer chemotherapies. Therefore, this study aimed to investigate the OATP expression of SCLC cell lines. We used cell lines from primary and metastatic SCLC tumors as well as pulmonary carcinoid cells and performed immunofluorescence and immunohistochemistry on paraffin-embedded SCLC samples. Furthermore, the mRNA expression of OATP4A1, OATP5A1 and OATP6A1 was assessed in cell lines that were exposed to the chemotherapeutic drugs cisplatin, etoposide and topotecan, which are all applied in SCLC therapy [10,21,23]. Chromogranin A and synaptophysin were applied as markers for neuroendocrine differentiation of the tumor cells, and cadherin-1 was applied as a marker for the epithelial origin of cells [25,26].

Materials and methods

Reagents

Cisplatin, etoposide, and topotecan were obtained from Eubio (Vienna, Austria). Other reagents and solvents (if not otherwise stated), obtained from Sigma (Munich, Germany), were of analytical grade.

Cancer cell lines and treatment

NCI-H417 cells, the NSCLC cell line A549 [25] and the two pulmonary carcinoid cell lines NCI-H727 and NCI-H835 [26] were obtained from the American Type Culture Collection (Manassas, VA, USA), DMS-153 cells from ECACC (Porton Down, Salisbury, UK). Other SCLC cell lines were obtained from Dr. Nina Pedersen, Department of Radiation Biology, The Finsen Center, National University Hospital, Copenhagen, Denmark [27]. The DMS-114 and NCI-H417 cells were originally established from untreated SCLC patients undergoing lung biopsy [28–31]. The DMS-153 cell line was established from an SCLC metastasis in the liver of a patient treated with cytoxan and methotrexate [28], whereas NCI-H526 was derived from a bone marrow metastasis of an untreated SCLC patient [32]. NCI-H69 cells were established from the pleural effusions of an untreated SCLC patient [33]. The SCLC-26A line was previously established in our lab from a pleural effusion of an untreated SCLC patient [34]. NCI-H727 and NCI-H835 were derived from lung carcinoid patients prior to therapy [35,36]. Cells were grown in RPMI-1640 bicarbonate medium (Seromed, Berlin, Germany) supplemented with 10% fetal bovine serum (Seromed), 4 mM glutamine and antibiotics (penicillin/streptomycin) under previously described tissue culture conditions [37]. All cells were checked regularly for mycoplasma contamination using a Mycoplasma PCR ELISA Kit (Roche Diagnostics, Vienna, Austria). For cell treatments, stock solutions were prepared in DMSO (0.1%), which was used as the control. 1×10^6 cells in six-well plates were incubated with the compound for 3 days and washed with PBS before RNA isolation.

RNA extraction

RNA was extracted from cells using TRI Reagent® (Applied Biosystems, Foster City, CA, USA). The concentration, purity, and integrity of the RNA samples were determined by UV absorbance and electrophoresis. RNA from normal human lung tissue (5 donor pool) was purchased from BioCat (Heidelberg, Germany). RNA from human bronchial epithelial (HBE) cells was obtained from ScienCell Research Lab (Carlsbad, CA).

Reverse transcription and real-time RT-PCR

One microgram of total RNA was reverse transcribed to cDNA with a high capacity cDNA reverse transcription kit (Life Technologies, Carlsbad, CA, USA). For reference genes, expression of 12 housekeeping genes was analyzed using a geNorm reference gene selection kit with PerfectProbeTM (PrimerDesign Ltd., South Hampton, UK). GAPDH (glyceraldehyde-3 phosphate dehydrogenase), YWHAZ (14-3-3 protein zeta/delta) and TOP1 (DNA topoisomerase 1) were used for TaqMan® real-time RT-PCR analysis. Real-time RT-PCR was performed [38] using the TaqMan® Gene Expression Assays containing intron-spanning primers: OATP1A2: Hs00245360_m1, OATP1B1: Hs00272374_m1, OATP1B3: Hs00251986_m1, OATP1C1: Hs00213714_m1, OATP2A1: Hs00194554_m1, OATP2B1: Hs00200670_m1, OATP3A1: Hs00203184_m1, OATP4A1: Hs00249583_m1, OATP4C1: Hs00698884_m1, OATP5A1: Hs00229597_m1, OATP6A1: Hs00542846_m1 and the endogenous controls GAPDH, YWHAZ and TOP1 (PrimerDesign Ltd., South Hampton, UK).

Western blotting

Western blotting was performed as described previously [39] using 30 μg of protein as determined with an assay kit from Bio-Rad Laboratories (Hercules, CA, USA). To control equal sample loading, protein on the membranes was stained with glycerol-3-phosphate dehydrogenase. 5% non-fat dry milk/PBS/0.05% Tween 20 was used for blocking. The following primary antibodies in blocking solution were applied: rabbit anti-human OATP4A1 (LSBio; dilution 1:500), rabbit anti-human OATP5A1 (LSBio; dilution 1:100) and rabbit anti-human OATP6A1 (LSBio; dilution 1:500). Peroxidase-conjugated species-specific IgG was used as secondary antibody (dilution 1:5000). Detection was performed with an ECL detection kit from Thermo Scientific (Portsmouth, NH, USA) using a Versa-Doc Gel Imaging system (Biorad, Hercules, CA).

Paraffin-embedded tumor sections

Archived paraffin-embedded sections from SCLC tumors, SCLC metastases to the brain and non-malignant (emphysema) lung tissue, provided by the Institute of Pathology and Bacteriology, Vienna, Austria (head: Dr. Angelika Reiner) at the Donauspital-Sozialmedizinisches Zentrum Ost, are derived from patients undergoing diagnostic biopsy or surgery. None of them received preoperative chemo- or radiotherapy prior to surgery. The study was performed in accordance with local ethical regulations.

Immunofluorescence and immunohistochemistry in cancer specimens

Double immunofluorescence staining was performed as previously described [40]. For antigen retrieval, 10 mM citric acid (pH 6.0) was used. Antibodies: Rabbit anti-SLCO4A1, anti-SLCO5A1 (Atlas Antibodies, Stockholm, Sweden) 1:50, anti-SLCO6A1 (Novus Biologicals, Littleton, CO, USA) 1:1000 and for double immunofluorescence, mouse polyclonal antibody Anti-CD34 (Lab Vision – Neo Markers, Fremont, CA, USA) as endothelial cell marker were used (1:50). In negative controls, OATP antibodies were replaced by non-immunogenic IgG. Thereafter, samples were incubated with a secondary Alexa Fluor 488 antibody (Invitrogen, Carlsbad, CA, USA) and the cell nuclei were stained with 0.5 μg/ml Hoechst 33342 (Sigma-Aldrich, St. Louis, MO). The slides were monitored on a TissueFAXS System with a Zeiss Fluorescence Microscope [41]. For immunohistochemical stainings, sections were processed with the Envision+ System-HRP (DAB) kit (Dako, Glostrup, Denmark). Immunostaining intensity was first evaluated by two experienced researchers. Thereafter, quantitative evaluation of the percentage of stained cells and the intensity of cell staining per area given as immunoreactive score (IRS) was performed by using the HistoQUEST program (TissueGnostics, Vienna, Austria) as described in detail by Kounnis et al [42].

Statistical analyses

A paired t-test (treated vs. non-treated sample) was applied to calculate the significance of mRNA expression data. Significance: $p < 0.05$.

Results

OATP mRNA expression studies in lung tumor cell lines

The relative mRNA expression of OATPs was assessed in cells from primary SCLC tumors (DMS-114, NCI-H417), SCLC metastatic tumors (DMS-153, NCI-526), carcinoid cell lines (NCI-H727, NCI-H835) and cells isolated from pleural SCLC effusions (NCI-H69, SCLC26A) (Fig. 1A and 1B). Normal lung tissue, human bronchial epithelia (HBE) and the NSCLC cell line A549 [43] were used for comparison. We showed that the OATP4A1 gene was the most abundant OATP in normal lung tissue and in cancer cells (Fig. 1B, Supplementary Table S1). In normal lung, the relative OATP4A1 mRNA expression levels were 2.9-fold higher than that of the housekeeping gene YWHAZ. High levels were also found for the OATP2A1 gene (2.2-fold). The OATP1A2, OATP2B1, OATP3A1, OATP4C1, and OATP5A1 genes were also clearly expressed, but the levels were lower than that of YWHAZ (ranging between 0.33-fold for OATP2B1 and 0.005-fold for OATP5A1). Compared to normal lung, OATP gene expression was greatly reduced in non-malignant HBE. While OATP4A1 mRNA expression was reduced by 66%, a 99% reduction was observed for OATP2A1. Therefore, OATP4A1 was still the highest expressed OATP gene in these cells (Fig. 1B). A rather uniform expression pattern for OATP4A1 was observed in all tumor cell lines although the OATP4A1 gene levels were lower than in lung (up to 13%). Similarly, OATP2A1, OATP2B1,
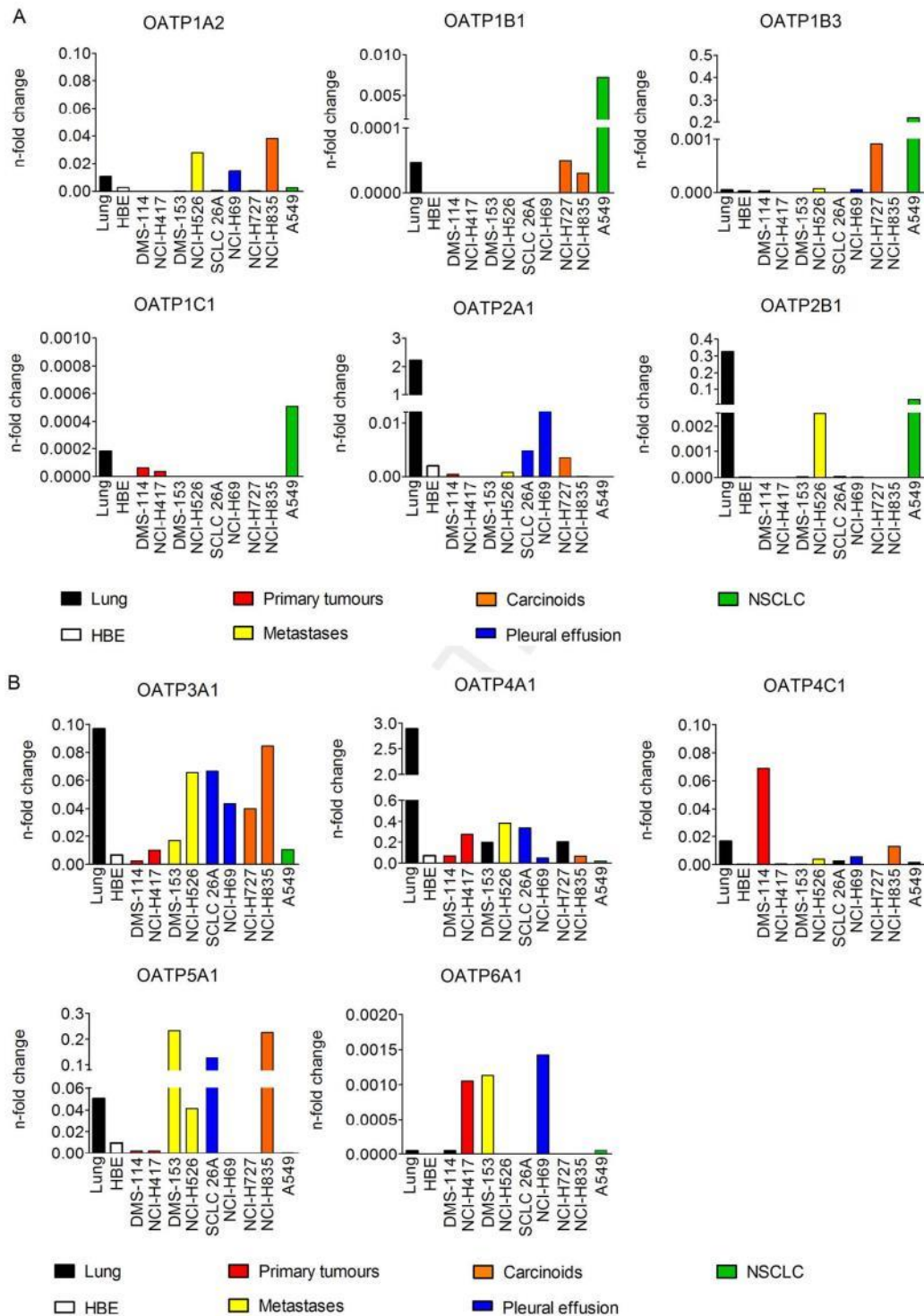
Fig. 1. (A and B) Relative mRNA expression of all known 11 OATPs in SCLC cell lines. 1 μg RNA isolated from non-malignant lung tissue, human bronchial epithelia (HBE), and cell lines from primary SCLC tumors and SCLC metastasis, lung carcinoid cell lines, and a non-small cell lung cancer cell line was reverse transcribed. qPCR studies were performed using TaqMan Assays as described in the Materials and Methods section. SCLC cell lines were either derived from biopsy specimens or from pleural effusions.

mRNA expression levels of OATP1A2, OATP 1B1, OATP1B3, OATP1C1, OATP 2A1 OATP 2B1 (A) and OATP3A1, OATP4A1, OATP4C1, OATP5A1 and OATP6A1 (B) are expressed as n-fold changes related to the most stable expressed reference gene YWHAZ.

and OATP3A1 were expressed at lower levels in SCLC and carcinoid tumor cell lines compared to normal lung tissue, but higher expression levels in SCLC cell lines than in normal human lung were observed for OATP1A2, OATP1B3, OATP4C1, OATP5A1 and OATP6A1. Cells also differed according to whether they originated from primary and metastatic SCLC tumors or from lung carcinoids. Particularly, OATP5A1 levels were highest in DMS-153 cells from metastatic tumors (approximately 2.5-fold higher than in normal lung tissue). Although OATP5A1 was also expressed in SCLC-26A cells and in the carcinoid cell line NCI-H835, it was expressed at lower levels than in the metastatic cell lines (0.13- and 0.23-fold of YWHAZ, respectively). Similar to OATP5A1, OATP1A2 transcripts were found at 2-fold elevated levels in NCI-H526 and 3.7-fold higher levels in NCI-H835 cells compared to normal lung (0.028- and 0.038-fold over YWHAZ). Additionally, OATP3A1 gene expression was highest in these two cell lines and in SCLC-26A cells, in which its expression nearly approached that of normal lung tissue (0.084- vs. 0.097-fold of YWHAZ). In the primary SCLC cell lines, NCI-H417 and DMS-114, the mRNA expression of two OATPs, namely OATP4C1 and OATP6A1, was evident. This finding is remarkable as OATP6A1, which was identified as a cancer-testis antigen, was also proposed as a lung cancer marker [45]. Compared to SCLC cells, the NSCLC cell line A549 showed a contrasting OATP expression pattern. In SCLC cells highly expressed OATP genes (e.g., the OATP4A1 gene) were expressed at low levels in A549 cells. The highest mRNA levels (0.219 x YWHAZ) were observed for OATP1B3 in NCI-H727 cells. Whereas OATP2B1 mRNA is considerably expressed in normal lung and A549 cells, it is reduced in SCLC and carcinoid cell lines (apart from metastatic NCI-H526 SCLC cells).

OATP and neuroendocrine marker mRNA expression in cell lines in response to chemotherapy

To study the changes in the OATP mRNA expression pattern during development of resistance to chemotherapy and subsequent tumor progression, GLC-14, GLC-16 and GLC-19 cells were assessed [44]. GLC cells expressed OATP1A2, 2A1, 2B1, 3A1, 4A1, 4C1, 5A1 and OATP6A1 genes. Relative values of OATP gene expression (related to lung) are shown in Table 1. OATP4A1 gene expression was up-regulated by 120% and 80% in later stage GLC-16 und GLC-19 cell lines, respectively, compared to chemosensitive GLC-14 cells, while

Table 1
mRNA expression of OATPs, neurogenic markers and cadherin-1 in GLC-14, GLC-16 and GLC-19 cell lines.

	GLC-14 [n-fold]	GLC-16 [n-fold]	GL-C19 [n-fold]
OATP1A2	0.002	n.d.	0.002
OATP1B1	n.d.	n.d.	n.d.
OATP1B3	n.d.	n.d.	n.d.
OATP1C1	n.d.	n.d.	n.d.
OATP2A1	0.066	0.037	0.023
OATP2B1	0.045	n.d.	n.d
OATP3A1	0.254	0.198	0.148
OATP4A1	0.013	0.029	0.025
OATP4C1	0.136	0.049	0.005
OATP5A1	23.0	13.3	8.5
OATP6A1	8.75	0.011	n.d.
CHGA	25.7	33.3	60.2
SYP	7.33	3.94	11.6
CDH1	0.082	0.115	0.261

The cell lines were derived from an SCLC patient before treatment (GLC-14), during (GLC-16) and after (GLC-19) surgical removal of the tumor, chemo- and radiation therapy [44]. From sub-confluent (80%) cell lines, RNA was extracted using Trizol. One microgram of total RNA was subjected to reverse transcription and TaqMan Assays were applied to monitor mRNA expression of the OATPs. mRNA levels were calculated as n-fold changes relative to normal lung. n.d.: values are below the detection limit. CHGA: chromogranin; SYP: synaptophysin; CDH1: cadherin-1.

all other OATP genes were down-regulated. GLC cell lines expressed the epithelial cell marker cadherin-1 and both neurogenic markers chromogranin and synaptophysin. The cadherin-1 gene expression was increased by approximately 3-fold in GLC-19 cells compared to GLC-14 cells. Chromogranin expression was also increased by 29% in GLC-16 and by 134% in GLC19. Synaptophysin levels were increased by 58% in GLC-19 cells. We also studied whether changes in the mRNA levels of neurogenic peptides might be related to altered OATP gene expression. We selected OATP4A1 (high levels in normal lung, low in tumor cells), OATP5A1 (low levels in primary SCLC cell lines, high in metastatic SCLC), and OATP6A1 (expressed in SCLC cells, but not found in normal lung tissue) to study the effect of in vitro treatment with chemotherapeutic agents on primary SCLC cells (NCI-H417) and the metastatic DMS-153 cells (Fig. 2), both expressing chromogranin and synaptophysin. Cisplatin dosages of 0.6 and 1.25 μM enhanced OATP5A1 mRNA expression by 75%, whereas OATP4A1 and OATP6A1 gene expression levels were increased only at a higher cisplatin dose (1.25 μM) by 45% and 54%, respectively, in NCI-H417. Cisplatin showed no effect on DMS-153 cells. Similar to the effects of cisplatin on OATPs, both marker transcripts were up-regulated by 2- to 2.5-fold in the NCI-H417 cells only. Etoposide had little effect on OATP4A1 and OATP5A1 mRNA levels, but influenced OATP6A1 expression in both cell lines by 60% stimulation in NCI-H417 cells and by 50% reduction in DMS-153 cells at low-dosage. Chromogranin and synaptophysin gene expression, which was more pronounced in DMS-153 cells, was reduced. Topotecan increased OATP4A1 mRNA expression at 1.25 and 2.5 μM by up to 180 and 250%, respectively. It also stimulated OATP5A1 mRNA expression, but only in NCI-H417 cells. OATP6A1 gene expression was down-regulated by topotecan in both cell lines at 1.25 and 2.5 μM (to approximately 25%). Topotecan also increased chromogranin mRNA expression by 2- to 3-fold in both cell lines, whereas the expression of synaptophysin was less influenced.

OATP protein expression

Western blotting was also performed to confirm OATP4A1-, OATP5A1-, and OATP6A1-expression in GLC-14, GLC-16 and GLC-19 cells from the SCLC patient. We found a clear correlation between protein and mRNA expression during tumor progression. While OAT4A1 was strongly induced, OATP5A1 and OATP6A1 decreased in the later stage GLC-16 and GLC-19 cell lines (see Fig. 3). As topotecan was most efficient to modulate OATP mRNA expression, we further studied cellular protein levels of OATP4A1, OATP5A1 and OATP6A1 in topotecan treated NCI-H417 and DMS-153 cells. Up-regulation was again observed for OATP4A1 and in NCI-H417 cells after treatment with 1.25 μM and 2.5 μM topotecan. In DMS-153 cells, OATP4A1 was also up-regulated whereas OATP6A1 protein expression was down-regulated in both cell lines. This corresponds to PCR-data shown in Fig. 2 and Table 1.

Studies in lung tumor specimens

The cellular localization of OATP4A1, OATP5A1 and OATP6A1 was studied in paraffin-embedded SCLC specimens first by immuno-histochemistry and then by immunofluorescence with positive staining for the transporters in non-malignant lung tissue and in primary and metastatic SCLC tumor specimens. Fig. 4 shows a representative picture of SCLC metastatic tissue, in which brown cytoplasmic and membrane staining of OATP4A1, OATP5A1 and OATP6A1 is visible in tumor cells. For quantitative analysis of the OATP levels in different samples, we used the immunohistochemical stained sections for which the TissueQuest program was found to be suitable [42].

Data from five non-malignant lung tissues, SCLC primary and metastatic tumors, respectively, revealed that the pattern of OATP4A1,
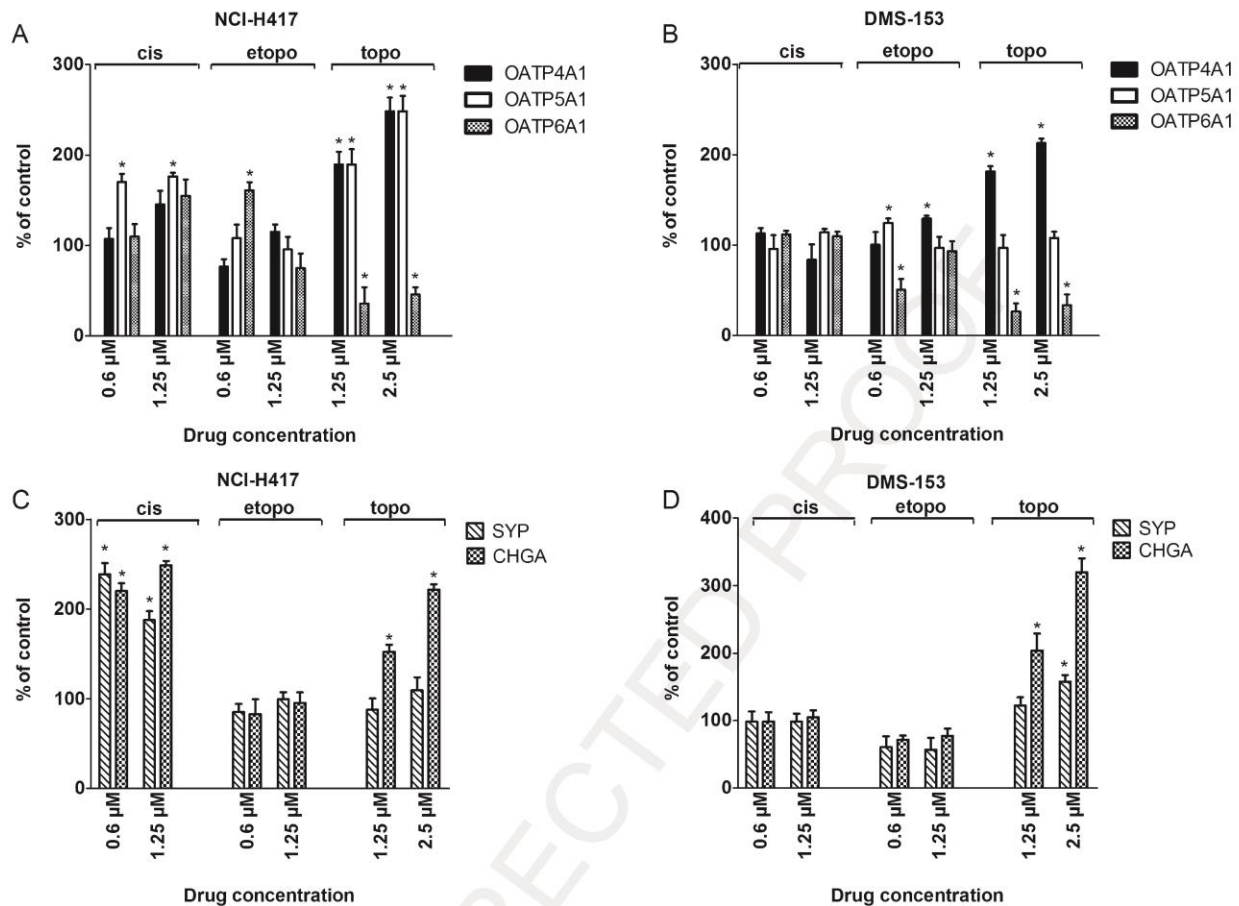
Fig. 2. mRNA expression of OATP4A1, OATP5A1, OATP6A1, synaptophysin and chromogranin in NCI-H417 and DMS-153 SCLC cell lines treated with anticancer agents. NCI-H417 and DMS-153 cell lines were treated with cisplatin (0.6 and 1.25 μM), etoposide (0.6 and 1.25 μM), and topotecan (1.25 and 2.5 μM), respectively, for 48 h, before RNA was isolated. Then, 1 μg RNA was reverse-transcribed and TaqMan Assays were applied in the quantitative PCR. Expression levels in untreated cells line were set to 100% and changes in the expression levels were calculated as % of control (*p < 0.05; n = 3).

OATP5A1 and OATP6A1 corresponds to the data in normal lung and SCLC cell lines, respectively. OATP4A1 is the most abundant OATP in SCLC tumors and in the surrounding non-cancerous tissue (Table 2). As expected OATP4A1 levels (given as immunoreactive scores)

Table 2
Immunoreactive OATP4A1, OATP5A1 and OATP6A1 levels in paraffin-embedded specimens from non-malignant and SCLC tumor samples.

	OATP levels in paraffin-embedded tissue sections IRS (arbitrary units)		
	Non-malignant	Primary tumor	Metastasis
OATP4A1	105.5 ± 60.4	46.2 ± 47.8	49.3 ± 30.1*
OATP5A1	3.4 ± 3.1	8.9 ± 4.7	15.3 ± 5.4 *
OATP6A1	1.3 ± 4.2	10.4 ± 5.1 *	6.9 ± 4.5

OATPs were stained by immunohistochemistry and quantitative microscopic image analysis was performed on specimens with >3% positive cells (compared to the negative control staining with non-specific IgG) to evaluate the immunoreactive score (IRS) for individual samples (n = 5). IRS values were calculated from the number of cells with positive staining multiplied with the mean OATP staining intensity in an area. Immunohistochemistry was performed as described in the Materials and Methods section. Values (means ± SD) are from 5 samples (n = 5). A paired t-test (primary tumor/metastasis vs. non-malignant sample) was applied to calculate the significance *p < 0.05.
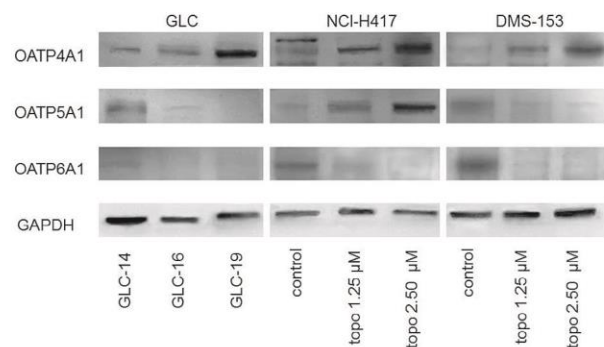

Fig. 3. Effect of anticancer chemotherapy on cellular OATP4A1, OATP5A1 and OATP6A1 levels in SCLC cancer cell lines. Protein extracts (30 μg) isolated from GLC-14 (before), GLC-16 (during) and GLC-19 (after therapy) cell lines derived from one SCLC patient, and in the NCI-H417 and the DMS-153 SCLC cancer cell line treated with topotecan (1.25 μM and 2.5 μM), respectively, were separated on a 12% PAGE and proteins were blotted onto nitrocellulose membranes. Blots were probed with antibodies against OATP4A1, OATP5A1 and OATP6A1, respectively. GAPDH was used as loading control.
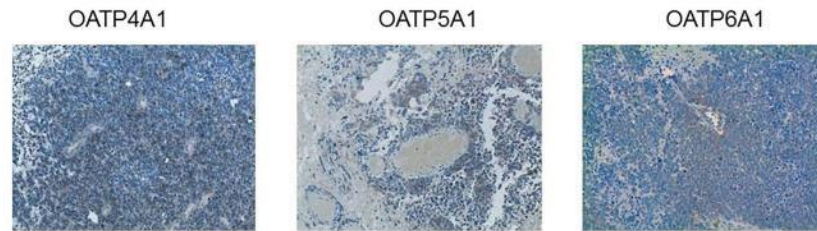
Fig. 4. Immunohistochemical staining of OATP4A1, OATP5A1 and OATP6A1 in paraffin-embedded SCLC metastatic SCLC tissue section. 4 μm sections were probed with polyclonal rabbit anti OATP antibodies and immunoreactive proteins were visualized with the Envision + System HRP system. Nuclei were counterstained (blue) with hematoxylin (magnification ×200). Brown staining for the OATPs is visible in the tumor cells within the metastases. (For interpretation of the references to color in this figure legend, the reader is referred to the web version of this article.)

are reduced (by approximately 50%) in the tumor sections compared to the non-cancerous tissue. OATP5A1 levels are highest in the metastatic tumors, while OATP6A1 levels are near the detection limit in the non-cancerous tissue, but its levels are up to 10 times higher in the primary tumors.

Immunofluorescence microscopy of these OATPs on paraffin-embedded sections from SCLC tumors and non-malignant lung tissue confirms these findings (representative images are shown in Fig. 5A and B). In Fig. 5A, the green OATP staining is visible while in the merged image (Fig. 5B) green OATP, red CD34 (for endothelial cells) and blue nuclei are present. Bright green immunofluorescence staining of OATP4A1 was observed in the samples from healthy lung tissue. The OATP5A1 fluorescence staining was clearly visible in the metastases, while for OATP6A1, a rather diffuse staining in all tissue samples was visible as expected from the mRNA distribution pattern in the cell lines. Additional experiments investigating whether OATP4A1, OATP5A1, and OATP6A1 might also be expressed in blood vessels were performed. By applying an antibody against CD34 together with antibodies against OATP4A1, OATP5A1, and OATP6A1, no co-staining of CD34-positive vascular endothelial cells in the lung tissue was observed indicating absence of these OATP isoforms in these cells (Fig. 5B).

Discussion

In the present study we elucidated the mRNA expression pattern of all 11 OATPs in primary and metastatic SCLC and lung carcinoid tumor cell lines in comparison to normal non-malignant lung tissue and non-malignant human broncho-epithelial cells. Then we evaluated the effect of chemotherapeutic agents on the expression of selected OATPs. OATP4A1 was most abundant in normal lung tissue and expressed in lung cancer cell lines derived from SCLC, carcinoid and NSCLC tumors. Similar to other OATPs, it was significantly reduced in non-malignant HBE. Expression of this OATP was also previously found in lung adenocarcinomas [21], epithelial BEAS-2B cells [23], and the adenocarcinoma cell line Calu-3 [23]. Interestingly, while OATP1A2, OATP1B3, OATP4C1, OATP5A1 and OATP6A1 demonstrated higher mRNA expression levels in SCLC cell lines compared to normal lung tissue, other OATP genes, namely OATP2A1, OATP2B1, and OATP3A1 were reduced in SCLC and carcinoid tumor cell lines. Furthermore, our data also showed distinct differences in the mRNA expression pattern of OATPs between metastatic and primary tumor cell lines. This applies to OATP5A1 in which expression levels were high in cell lines derived from metastatic tumors (DMS-153 and NCI-H526) and in carcinoid cell line NCI-H835. On the other hand, OATP6A1 mRNA was found in the primary SCLC cell lines NCI-H417 and DMS-114 and in the pleural effusion cell line NCI-H69. Contrary to SCLC cells, the NSCLC cell line A549 showed a unique OATP expression pattern with preferentially OATP1B3 gene expression. This suggests possible differences in the
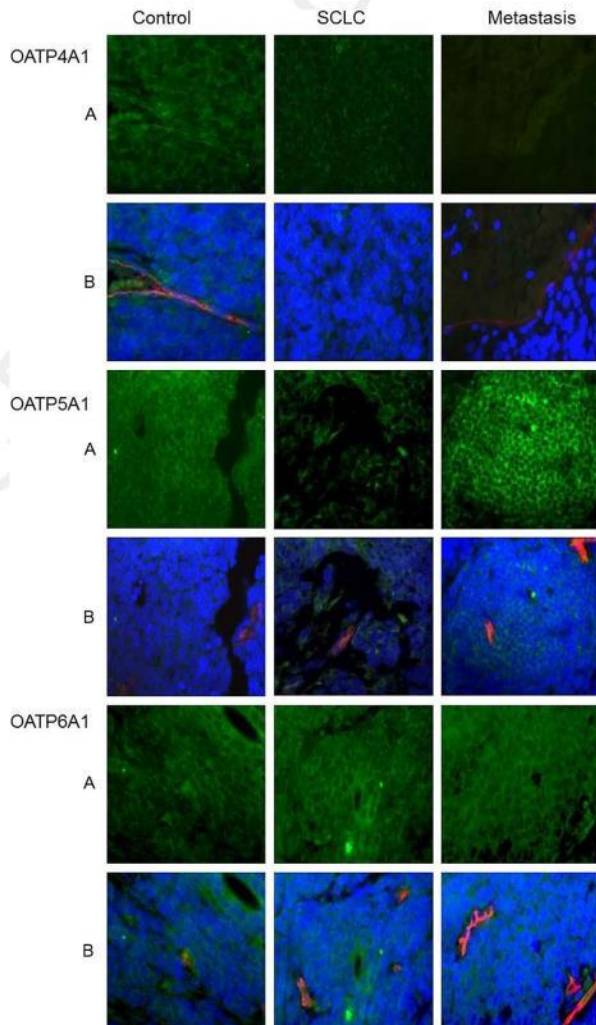

Fig. 5. Immunofluorescence staining of OATP4A1, OATP5A1 and OATP6A1 in paraffin-embedded non-malignant lung tissue (control), lung cancer sections (SCLC) and SCLC brain metastasis. 4 μm sections were probed with polyclonal rabbit anti OATP antibodies and with a mouse antibody against CD34 as endothelial cell marker. OATPs were detected by an Alexa Fluor 488 labeled anti-rabbit IgG whereas an Alexa Fluor-565 IgG was used for CD34-positive vascular endothelial cells. Sections were monitored in an automated Zeiss fluorescence microscope (Tissue FAXS) (magnification ×200). (A) Green staining for the OATPs (GFP channel) (B) overlay picture of green OATPs, red staining of vascular endothelial cells (Texas Red channel) and blue nuclei (Hoechst 33342 dye). (For interpretation of the references to color in this figure legend, the reader is referred to the web version of this article.)

uptake of OATP substrates e.g., anticancer drugs between the two tumor entities [11].

In accordance with data from the cell lines on mRNA expression and on OATP4A1, OATP5A1 and OATP6A1 levels in Western blot, OATP4A1 was more prominent in paraffin embedded sections from non-malignant lung tissue than in primary and metastatic tumors. However, its levels in the investigated tumor tissues and cells lines were still higher than those of other OATPs (OATP5A1, OATP6A1). The prominent expression of OATP4A1 in all lung samples (SCLC, carcinoid cell lines, tissue sections from primary and metastatic SCLC samples) suggests an important role for OATP4A1 in the uptake of specific substrates, such as thyroid hormones, estrone-3-sulfate, and prostaglandins into lung cancer cells. Prostaglandins are important regulators in lung cells under physiological and pathological conditions, as they control smooth muscle airway contraction [46] and modulate the inflammatory process [47]. Whether OATP4A1 might work together with lung-cell expressed OATP2A1, which is a specific uptake transporter for prostaglandins (including prostaglandin E2) [48] for their intracellular inactivation [48,49], is still unknown. Other OATP4A1 substrates are thyroid hormones and they are known to modulate tumor progression via binding the nuclear thyroid hormone receptor [50]. Thyroid hormones are the only known substrates for another OATP, namely OATP1C1, whose expression is particularly high at the blood–brain barrier [51,52]. mRNA of this OATP is also expressed at a low level in lung tissue and in lung adenocarcinoma A549 cell line, but not in SCLC tumors and cell lines. Additionally, estrogen-sulfate uptake via OATP4A1 was shown [53]. This might be important because estrone sulfate can be converted via steroid sulfatase to active 17ß-estrogen, which was found to influence pulmonary inflammation and lung cancer progression [54]. In addition to OATP4A1, other OATPs are also active in the uptake of steroid precursors, including OATP family 1 members and OATP2B1 [55,56]. The latter is also present in normal lung tissue, and in contrast to A549 cells, it is only rarely expressed in SCLC cells. Similar to OATP2B1, OATP1B3 known as tumor marker in cancer of various organs including gastrointestinal tract, breast, and prostate, was rather low expressed in SCLC. Interestingly, higher OATP5A1 mRNA levels were observed in metastatic SCLC cell lines, carcinoid- and pleural effusion-derived cells, compared to normal lung tissue. OATP5A1 immunoreactivity was also more pronounced in lung cancer metastases from SCLC patients, suggesting a role for this OATP in tumor metastasis. This assumption is supported by a recent study showing that transfection of HeLa cells with OATP5A1 induces expression of several genes involved in the regulation of differentiation and migration [24,57]. We also showed that the cancer-testis antigen OATP6A1 is present in SCLC tumor cell lines and demonstrated its presence in samples from primary SCLC and metastases, indicating that it may also be considered as a tumor marker for this lung cancer subtype [45]. To date, no substrate for human OATP6A1 has been identified, although the rat homologue was found to transport DHEA sulfate [58]. Therefore, its function is still unclear.

We also found that resistance to chemotherapy is accompanied by altered OATP mRNA expression at least in the SCLC patient treated with surgical removal of the tumor, radiation and anticancer drug therapy. In the GLC-14 cell line, isolated before therapy, only OATP4A1, but not OATP5A1 and OATP6A1, was lower than in the late stage GLC-16 and GLC-19 cell lines from the same patient. These changes were related to an increase in neurogenic differentiation as shown by the increased levels in neurogenic peptides synaptophysin and chromogranin and the epithelial marker cadherin-1. Based on this interesting finding, we also studied the expression of these OATPs in NCI-H417 and DMS-153 cells after treatment with cisplatin, etoposide and topotecan. Generally, the effects were more pronounced in the primary NCI-H-417 cells than in the metastatic cell line. Cisplatin was active to induce OATP4A1, OATP5A1 and OATP6A1 together with the neuroendocrine markers chromogranin

and synaptophysin in NCI-H417 cells. In contrast to cisplatin and etoposide, topotecan induced OATP4A1 in both cell lines, while OATP6A1 was reduced. Therefore, we further analyzed topotecan treated cell lines in Western blots. In the GLC cell lines and in the two cancer cell lines NCI-H417 and DMS-153 treated with topotecan, mRNA expression of OATP4A1, OATP5A1 and OATP6A1 correlates with protein expression. This was confirmed by quantitative microscopic image analysis of the immunohistochemical staining pattern for these OATPs in SCLC tumor samples from SCLC patients (see Fig. 4 and Table 2). So far we know that this is the first report on the protein expression of these particular OATPs in SCLC tumors.

Taken together, our data revealed a specific OATP expression pattern, with OATP4A1 being the most prominent OATP in SCLC and carcinoid cell lines and SCLC tumors. We also confirmed that OATP5A1 is highly expressed in metastatic tumor cells while OATP6A1 is present in SCLC cell lines and the tumors. Whether OATP modulation might also be observed in SCLC patients during chemotherapy is not known yet, but OATPs might function as novel biomarkers for tumor progression and the development of metastasis.

Conflict of interest

The authors declare that they have no conflict of interest.

Acknowledgements

Appendix: Supplementary material

Supplementary data to this article can be found online at doi:10.1016/j.canlet.2014.09.025.

References

[1] W.D. Travis, Update on small cell carcinoma and its differentiation from squamous cell carcinoma and other non-small cell carcinomas, Mod. Pathol. 25 (Suppl. 1) (2012) S18–S30.
[2] A.D. Elias, Small cell lung cancer: state-of-the-art therapy in, Chest 112 (1997) (1996) 251S–258S.
[3] D.R. Swarts, F.C. Ramaekers, E.J. Speel, Molecular and cellular biology of neuroendocrine lung tumors: evidence for separate biological entities, Biochim. Biophys. Acta 2012 (1826) 255–271.
[4] A. Kasprzak, M. Zabel, W. Biczysko, Selected markers (chromogranin A, neuron-specific enolase, synaptophysin, protein gene product 9.5) in diagnosis and prognosis of neuroendocrine pulmonary tumours, Pol. J. Pathol. 58 (2007) 23–33.
[5] R.L. Comis, D.M. Friedland, B.C. Good, Small-cell lung cancer: a perspective on the past and a preview of the future, Oncology (Williston Park) 12 (1998) 44–50.
[6] C. Huisman, P.E. Postmus, G. Giaccone, E.F. Smit, Second-line chemotherapy and its evaluation in small cell lung cancer, Cancer Treat. Rev. 25 (1999) 199–206.
[7] K.S. Albain, J.J. Crowley, R.B. Livingston, Long-term survival and toxicity in small cell lung cancer. Expanded Southwest Oncology Group experience, Chest 99 (1991) 1425–1432.
[8] J.B. Sørensen, K. Østerlind, Prognostic factors: from clinical parameters to new biological markers, in: P. Van Houtte, J. Klastersky, J.P. Rocmans (Eds.), Progress and Perspectives in the Treatment of Lung Cancer, Springer, Berlin, 1999, pp. 1–21.
[9] F.J. Lagerwaard, P.C. Levendag, P.J. Nowak, W.M. Eijkenboom, P.E. Hanssens, P.I. Schmitz, Identification of prognostic factors in patients with brain metastases: a review of 1292 patients, Int. J. Radiat. Oncol. Biol. Phys. 43 (1999) 795–803.
[10] C. Bosquillon, Drug transporters in the lung – do they play a role in the biopharmaceutics of inhaled drugs?, J. Pharm. Sci. 99 (2010) 2240–2255.
[11] B. Hagenbuch, C. Gui, Xenobiotic transporters of the human organic anion transporting polypeptides (OATP) family, Xenobiotica 38 (2008) 778–801.
[12] R.B. Kim, Organic anion-transporting polypeptide (OATP) transporter family and drug disposition, Eur. J. Clin. Invest. 33 (Suppl. 2) (2003) 1–5.

[13] E. Jacquemin, B. Hagenbuch, B. Stieger, A.W. Wolkoff, P.J. Meier, Expression cloning of a rat liver Na(+)-independent organic anion transporter, Proc. Natl. Acad. Sci. U.S.A. 91 (1994) 133–137.

[14] G.A. Kullak-Ublick, B. Hagenbuch, B. Stieger, C.D. Schteingart, A.F. Hofmann, A.W. Wolkoff, et al., Molecular and functional characterization of an organic anion transporting polypeptide cloned from human liver, Gastroenterology 109 (1995) 1274–1282.

[15] J. Konig, Y. Cui, A.T. Nies, D. Keppler, Localization and genomic organization of a new hepatocellular organic anion transporting polypeptide, J. Biol. Chem. 275 (2000) 23161–23168.

[16] B. Hagenbuch, P.J. Meier, Organic anion transporting polypeptides of the OATP/SLC21 family: phylogenetic classification as OATP/ SLCO superfamily, new nomenclature and molecular/functional properties, Pflugers Arch. 447 (2004) 653–665.

[17] J. Konig, Uptake transporters of the human OATP family: molecular characteristics, substrates, their role in drug-drug interactions, and functional consequences of polymorphisms, Handb. Exp. Pharmacol. (2011) 1–28.

[18] C. Fahrmayr, J. Konig, D. Auge, M. Mieth, M.F. Fromm, Identification of drugs and drug metabolites as substrates of multidrug resistance protein 2 (MRP2) using triple-transfected MDCK-OATP1B1-UGT1A1-MRP2 cells, Br. J. Pharmacol. 165 (2012) 1836–1847.

[19] B. Hagenbuch, P.J. Meier, The superfamily of organic anion transporting polypeptides, Biochim. Biophys. Acta (1609).

[20] V. Buxhofer-Ausch, L. Secky, K. Wlcek, M. Svoboda, V. Kounnis, E. Briasoulis, et al., Tumor-specific expression of organic anion-transporting polypeptides: transporters as novel targets for cancer therapy, J. Drug Deliv. 2013 (2013) 863539.

[21] I. Tamai, J. Nezu, H. Uchino, Y. Sai, A. Oku, M. Shimane, et al., Molecular identification and characterization of novel members of the human organic anion transporter (OATP) family, Biochem. Biophys. Res. Commun. 273 (2000) 251–260.

[22] K. Bleasby, J.C. Castle, C.J. Roberts, C. Cheng, W.J. Bailey, J.F. Sina, et al., Expression profiles of 50 xenobiotic transporter genes in humans and pre-clinical species: a resource for investigations into drug disposition, Xenobiotica 36 (2006) 963–988.

[23] S. Endter, D. Francombe, C. Ehrhardt, M. Gumbleton, RT-PCR analysis of ABC, SLC and SLCO drug transporters in human lung epithelial cell models, J. Pharm. Pharmacol. 61 (2009) 583–591.

[24] U. Olszewski-Hamilton, M. Svoboda, T. Thalhammer, V. Buxhofer-Ausch, K. Geissler, G. Hamilton, Organic anion transporting polypeptide 5A1 (OATP5A1) in small cell lung cancer (SCLC) cells: possible involvement in chemoresistance to satraplatin, Biomark. Cancer 3 (2011) 31–40.

[25] D.N. Carney, A.F. Gazdar, G. Bepler, J.G. Guccion, P.J. Marangos, T.W. Moody, et al., Establishment and identification of small cell lung cancer cell lines having classic and variant features, Cancer Res. 45 (1985) 2913–2923.

[26] S. Grozinsky-Glasberg, I. Shimon, H. Rubinfeld, The role of cell lines in the study of neuroendocrine tumors, Neuroendocrinology 96 (2012) 173–187.

[27] N. Pedersen, S. Mortensen, S.B. Sorensen, M.W. Pedersen, K. Rieneck, L.F. Bovin, et al., Transcriptional gene expression profiling of small cell lung cancer cells, Cancer Res. 63 (2003) 1943–1953.

[28] O.S. Pettengill, G.D. Sorenson, D.H. Wurster-Hill, T.J. Curphey, W.W. Noll, C.C. Cate, et al., Isolation and growth characteristics of continuous cell lines from small-cell carcinoma of the lung, Cancer 45 (1980) 906–918.

[29] T. Yamori, S. Sato, H. Chikazawa, T. Kadota, Anti-tumor efficacy of paclitaxel against human lung cancer xenografts, Gann 88 (1997) 1205–1210.

[30] G. Hamilton, L. Klameth, B. Rath, T. Thalhammer, Synergism of cyclin-dependent kinase inhibitors with camptothecin derivatives in small cell lung cancer cell lines, Molecules 19 (2014) 2077–2088.

[31] S. Scarpa, G. Morstyn, D.N. Carney, A. Modesti, T.J. Triche, Small cell lung cancer cell lines: pure and variant types can be distinguished by their extracellular matrix synthesis, Eur. Respir. J. 1 (1988) 639–644.

[32] S.L. Lai, H. Brauch, T. Knutsen, B.E. Johnson, M.M. Nau, T. Mitsudomi, et al., Molecular genetic characterization of neuroendocrine lung cancer cell lines, Anticancer Res. 15 (1995) 225–232.

[33] A.F. Gazdar, D.N. Carney, E.K. Russell, H.L. Sims, S.B. Baylin, P.A. Bunn Jr., et al., Establishment of continuous, clonable cultures of small-cell carcinoma of lung which have amine precursor uptake and decarboxylation cell properties, Cancer Res. 40 (1980) 3502–3507.

[34] G. Hamilton, U. Olszewski, L. Klameth, R. Ulsperger, K. Geissler, Synergistic anticancer activity of topotecan− cyclin-dependent kinase inhibitor combinations against drug-resistant small cell lung cancer (SCLC) cell lines, J. Cancer Ther. 4 (2013) 47–53.

[35] T. Takahashi, M.M. Nau, I. Chiba, M.J. Birrer, R.K. Rosenberg, M. Vinocour, et al., p53: a frequent target for genetic abnormalities in lung cancer, Science 246 (1989) 491–494.

[36] A.F. Gazdar, R.I. Linnoila, Y. Kurita, H.K. Oie, J.L. Mulshine, J.C. Clark, et al., Peripheral airway cell differentiation in human lung cancer cell lines, Cancer Res. 50 (1990) 5481–5487.

[37] M. Murias, M. Miksits, S. Aust, M. Spatzenegger, T. Thalhammer, T. Szekeres, et al., Metabolism of resveratrol in breast cancer cell lines: impact of sulfotransferase 1A1 expression on cell growth inhibition, Cancer Lett. 261 (2008) 172–182.

[38] K. Wlcek, M. Svoboda, T. Thalhammer, F. Sellner, G. Krupitza, W. Jaeger, Altered expression of organic anion transporter polypeptide (OATP) genes in human breast carcinoma, Cancer Biol. Ther. 7 (2008) 1450–1455.

[39] J. Riha, S. Brenner, M. Bohmdorfer, B. Giessrigl, M. Pignitter, K. Schueller, et al., Resveratrol and its major sulfated conjugates are substrates of organic anion transporting polypeptides (OATPs): Impact on growth of ZR-75-1 breast cancer cells, Mol. Nutr. Food Res. 58 (2014) 1830–1842.

[40] K. Wlcek, M. Svoboda, J. Riha, S. Zakaria, U. Olszewski, Z. Dvorak, et al., The analysis of organic anion transporting polypeptide (OATP) mRNA and protein patterns in primary and metastatic liver cancer, Cancer Biol. Ther. 11 (2011) 801–811.

[41] G.E. Steiner, R.C. Ecker, G. Kramer, F. Stockenhuber, M.J. Marberger, Automated data acquisition by confocal laser scanning microscopy and image analysis of triple stained immunofluorescent leukocytes in tissue, J. Immunol. Methods 237 (2000) 39–50.

[42] V. Kounnis, E. Ioachim, M. Svoboda, A. Tzakos, I. Sainis, T. Thalhammer, et al., Expression of organic anion-transporting polypeptides 1B3, 1B1, and 1A2 in human pancreatic cancer reveals a new class of potential therapeutic targets, Onco Targets Ther. 4 (2011) 27–32.

[43] D.J. Giard, S.A. Aaronson, G.J. Todaro, P. Arnstein, J.H. Kersey, H. Dosik, et al., In vitro cultivation of human tumors: establishment of cell lines derived from a series of solid tumors, J. Nat. Cancer Inst. 51 (1973) 1417–1423.

[44] H.H. Berendsen, L. de Leij, E.G. de Vries, G. Mesander, N.H. Mulder, B. de Jong, et al., Characterization of three small cell lung cancer cell lines established from one patient during longitudinal follow-up, Cancer Res. 48 (1988) 6891–6899.

[45] S.Y. Lee, B. Williamson, O.L. Caballero, Y.T. Chen, M.J. Scanlan, G. Ritter, et al., Identification of the gonad-specific antigen SLCO6A1 as a cancer/testis (CT) antigen expressed in human lung cancer, Cancer Immun. 4 (2004) 13.

[46] C.K. Billington, O.O. Ojo, R.B. Penn, S. Ito, cAMP regulation of airway smooth muscle function, Pulm. Pharmacol. Ther. 26 (2013) 112–120.

[47] M.K. McCarthy, J.B. Weinberg, Eicosanoids and respiratory viral infection: coordinators of inflammation and potential therapeutic targets, Mediators Inflamm. 2012 (2012) 236345.

[48] V.L. Schuster, Molecular mechanisms of prostaglandin transport, Annu. Rev. Physiol. 60 (1998) 221–242.

[49] V.R. Holla, M.G. Backlund, P. Yang, R.A. Newman, R.N. DuBois, Regulation of prostaglandin transporters in colorectal neoplasia, Cancer Prev. Res. 1 (2008) 93–99.

[50] L.C. Moeller, D. Fuhrer, Thyroid hormone, thyroid hormone receptors, and cancer: a clinical perspective, Endocr. Relat. Cancer 20 (2013) R19–R29.

[51] W.M. van der Deure, R.P. Peeters, T.J. Visser, Molecular aspects of thyroid hormone transporters, including MCT8, MCT10, and OATPs, and the effects of genetic variation in these transporters, J. Mol. Endocrinol. 44 (2010) 1–11.

[52] F. Pizzagalli, B. Hagenbuch, B. Stieger, U. Klenk, G. Folkers, P.J. Meier, Identification of a novel human organic anion transporting polypeptide as a high affinity thyroxine transporter, Mol. Endocrinol. 16 (2002) 2283–2296.

[53] L. Milewich, R.L. Garcia, A.R. Johnson, Steroid sulfatase activity in human lung tissue and in endothelial pulmonary cells in culture, J. Clin. Endocrinol. Metab. 57 (1983) 8–14.

[54] J.M. Siegfried, L.P. Stabile, Estrogenic steroid hormones in lung cancer, Semin. Oncol. 41 (2014) 5–16.

[55] A. Koenen, K. Kock, M. Keiser, W. Siegmund, H.K. Kroemer, M. Grube, Steroid hormones specifically modify the activity of organic anion transporting polypeptides, Eur. J. Pharm. Sci. 47 (2012) 774–780.

[56] N. Banerjee, C. Allen, R. Bendayan, Differential role of organic anion-transporting polypeptides in estrone-3-sulphate uptake by breast epithelial cells and breast cancer cells, J. Pharmacol. Exp. Ther. 342 (2012) 510–519.

[57] K. Sebastian, S. Detro-Dassen, N. Rinis, D. Fahrenkamp, G. Muller-Newen, H.F. Merk, et al., Characterization of SLCO5A1/OATP5A1, a solute carrier transport protein with non-classical function, PLoS ONE 8 (2013) e83257.

[58] T. Suzuki, T. Onogawa, N. Asano, H. Mizutamari, T. Mikkaichi, M. Tanemoto, et al., Identification and characterization of novel rat and human gonad-specific organic anion transporters, Mol. Endocrinol. 17 (2003) 1203–1215.

Resveratrol and its sulfated conjugates are substrates of organic anion transporting polypeptides (OATPs): impact on breast cancer cell growth

Juliane Riha, **Stefan Brenner**, Michaela Böhmdorfer, Benedikt Giessrigl, Marc Pignitter, Katharina Schueller, Theresia Thalhammer, Bruno Stieger, Veronika Somoza, Thomas Szekeres and Walter Jäger.

RESEARCH ARTICLE

Resveratrol and its major sulfated conjugates are substrates of organic anion transporting polypeptides (OATPs): Impact on growth of ZR-75-1 breast cancer cells

Juliane Riha[1], Stefan Brenner[1], Michaela Böhmdorfer[1], Benedikt Giessrigl[1], Marc Pignitter[2], Katharina Schueller[2], Theresia Thalhammer[3], Bruno Stieger[4], Veronika Somoza[2], Thomas Szekeres[5] and Walter Jäger[1]

[1] Department of Clinical Pharmacy and Diagnostics, University of Vienna, Vienna, Austria
[2] Department of Nutritional and Physiological Chemistry, University of Vienna, Vienna, Austria
[3] Department of Pathophysiology and Allergy Research, Center of Pathophysiology, Medical University of Vienna, Vienna, Austria
[4] Department of Clinical Pharmacology and Toxicology, University Hospital Zurich, Zurich, Switzerland
[5] Clinical Institute for Medical and Chemical Laboratory Diagnostics, Medical University of Vienna, Vienna, Austria

Scope: Resveratrol is a naturally occurring polyphenolic compound with various pharmacological activities. These effects are observed despite its low bioavailability, which is particularly caused by extensive phase II metabolism. It is unknown whether resveratrol and its metabolites can accumulate to bioactive levels in organs and tissues through protein-mediated transport mechanisms. Because organic anion transporting polypeptides (OATPs) mediate the uptake of many clinically important drugs, we investigated their role in the cellular transport of resveratrol and its major glucuronides and sulfates.
Methods and results: Uptake experiments were performed with resveratrol and its glucuronides and sulfates in OATP-expressing Chinese hamster ovary (CHO) and breast cancer (ZR-75-1) cells. The uptake rates for resveratrol in OATP1B1-, OATP1B3-, and OATP2B1-transfected Chinese hamster ovary cells were four- to sixfold higher compared to wild-type cells. Resveratrol-3-*O*-4′-*O*-disulfate was transported by OATP1B1 and OATP1B3, while resveratrol-3-*O*-sulfate was exclusively transported by OATP1B3. However, resveratrol-4′-*O*-sulfate, resveratrol-3-*O*-glucuronide, and resveratrol-4′-*O*-glucuronide did not show any affinity for these OATPs. OATP-dependent uptake of resveratrol was also confirmed in ZR-75-1 cells.
Conclusion: Our data revealed that OATPs act as cellular uptake transporters for resveratrol and its major sulfates, which must be considered in humans following oral uptake of dietary resveratrol.

Additional supporting information may be found in the online version of this article at the publisher's web-site

1 Introduction

Correspondence: Dr. Walter Jäger, Department of Clinical Pharmacy and Diagnostics, University of Vienna, A-1090 Vienna, Austria
E-mail: walter.jaeger@univie.ac.at
Fax: +43-1-4277-9555

Abbreviations: BSP, bromosulfophthalein; **CHO,** Chinese hamster ovary; **OATP,** organic anion transporting polypeptides; **WT,** wild-type

Resveratrol (*trans*-3,5,4′-trihydroxystilbene) is a naturally occurring compound found at low concentrations in grapes, berries, peanuts, and red wine [1]. Over the last decade, it has been shown that resveratrol exhibits a wide variety of biological and pharmacological properties. In several in vitro, animal models and human studies, resveratrol has been found to be active in the prevention and treatment of cancer, cardiovascular diseases, inflammation, ischemic injuries, and

neurodegenerative diseases, and resveratrol may also act as an antiobesity and antiaging compound [2]. The observed pharmacological activities of resveratrol cannot be explained by the low blood and tissue concentrations of unchanged resveratrol based on extensive metabolism in the gut and liver, leading to five to tenfold higher circulating plasma concentrations of resveratrol glucuronides and resveratrol sulfates compared with unconjugated resveratrol [3,4]. Currently, limited information is available regarding the possible benefits of resveratrol metabolites. Based on in vitro studies, resveratrol sulfates have been found to have comparable or greater potency than resveratrol against specific molecular targets, namely, COX 1 and 2, quinone reductase 1, nuclear factor κB as well as similar ability to scavenge free radicals [5–7]. Furthermore, sulfates were also very recently shown to attenuate the *Escherichia coli*-LPS-induced IL-6 and TNF-α release [8]. In contrast to resveratrol sulfates, the few published studies have shown that resveratrol glucuronides are ineffective in various human cell lines, macrophages, and HIV-1 infection [8–12]. However, the in vitro activity of resveratrol metabolites may not necessarily reflect their in vivo function given that intracellular sulfatases or ß-glucuronidases could easily convert the conjugates back to resveratrol [13]. Recent data from our laboratory have indeed shown that intracellular resveratrol-3-*O*-sulfate is readily hydrolyzed in breast tissue samples by members of the sulfatase family to regenerate parent resveratrol [13]. Monosulfate metabolites were also converted back to the parent compound in human colorectal cells [9]. The observed induction of autophagy and senescence, however, was abrogated by inclusion of a sulfatase inhibitor, which reduced intracellular resveratrol. Interestingly, cellular uptake of resveratrol-3-*O*-sulfate and resveratrol-4′-*O*-sulfate into cytoplasm of human colon cancer cells was dependent on cell line (HCEG < HCA-7 < HT-29), strongly indicating uptake transport mechanisms rather than passive diffusion [9]. An active transport for resveratrol and its conjugates is also supported by several in vitro and in vivo studies showing that the multidrug resistance-associated proteins (MRPs) namely MRP2 and MRP3 are responsible for the efflux of resveratrol glucuronides whereas breast cancer-resistance protein has been found to be the major efflux pump for native resveratrol and resveratrol sulfates [14,15]. We therefore hypothesize that resveratrol and its conjugates may accumulate to bioactive levels in cells, organs, and tissues through active transport mechanisms.

One major cellular uptake mechanism is via members of the organic anion transporting polypeptide (OATP) family [16–18]. Among the 11 human OATPs, OATP1B1 and OATP1B3 are highly expressed in the liver and mediate the uptake of numerous drugs into hepatocytes. OATP2B1 shows substantial expression in the apical membrane of enterocytes, where it contributes to the intestinal absorption of many endogenous compounds and clinically important drugs, thereby affecting drug disposition [19, 20]. Based on the structural similarity of resveratrol-3-*O*-sulfate with estrone-3-sulfate, for which OATP1B1-, OATP1B3-, and OATP2B1-mediated up-

take exists, we hypothesized that resveratrol and its conjugates might also be substrates of these OATPs. Any differences in the affinity of resveratrol glucuronides and resveratrol sulfates to these transporters might also explain the observed differences in their pharmacological activity.

Recent data from our laboratory have also shown high expression of various OATPs in human hormone receptor-positive (MCF-7 and ZR-75-1) and negative (MDA-MB-231) breast cancer cell lines [21, 22]. As pronounced resveratrol uptake into the cytoplasm was also observed in these cell lines we hypothesized that members of the OATP family may mediate intracellular resveratrol concentrations, thereby affecting cell growth.

Therefore, in the present study, we investigated the transport of resveratrol and its major metabolites, namely resveratrol-3-*O*-glucuronide, resveratrol-4′-*O*-glucuronide, resveratrol-3-*O*-sulfate, resveratrol-4′-*O*-sulfate, and resveratrol-3-*O*-4′-disulfate, in OATP1B1-, OATP1B3-, and OATP2B1-transfected Chinese hamster ovary (CHO) cells. In addition, the OATP-mediated transport of resveratrol and its correlation with cytotoxicity were also investigated in the human breast cancer cell line ZR-75-1.

2   Materials and methods

2.1   Chemicals

trans-Resveratrol was purchased from Sigma-Aldrich (Munich, Germany), and *trans*-resveratrol-3-*O*-glucuronide was obtained from Santa Cruz Biotechnology (Santa Cruz, CA, USA). *trans*-Resveratrol-3-*O*-sulfate, *trans*-resveratrol-4′-*O*-sulfate, *trans*-resveratrol-3-*O*-4′-*O*-disulfate, and *trans*-resveratrol-4′-*O*-glucuronide were synthesized as described previously [23, 24]. MeOH and water were of HPLC grade (Merck, Darmstadt, Germany). All other chemicals and solvents were commercially available and of analytical grade and were used without further purification.

2.2   Cell culture

CHO cells that were stably transfected with OATP1B1, OATP1B3, and OATP2B1 and wild-type (WT) CHO cells were provided by the University of Zurich, Switzerland and have been extensively characterized previously [25, 26]. The CHO cells were grown in DMEM supplemented with 10% FCS, 50 μg/mL L-proline, 100 U/mL penicillin, and 100 μg/mL streptomycin. The selective medium for stably transfected CHO cells additionally contained 500 μg/mL geneticin sulfate (G418) [27]. All of the media and supplements were obtained from Invitrogen (Karlsruhe, Germany). The mammalian ZR-75-1 breast cancer cell line was purchased from the American Type Culture Collection (ATCC, Rockville, MD, USA) and was maintained in RPMI medium supplemented with 10% FCS, 100 U/mL penicillin, 100 μg/mL

Mol. Nutr. Food Res. 2014, 00, 1–13

3

streptomycin, and 1% GlutaMAX. The cells were grown in T-flasks with a 25 cm^2 growth area (BD Biosciences, Franklin Lakes, NJ, USA), maintained at 37°C under 5% CO_2 and 95% relative humidity. The cells were passaged once a week and were used up to passage 55 [22].

2.3 OATP1B1 knockdown in ZR-75-1 cells via lentiviral transduction with a short hairpin RNA

For transduction, ZR-75-1 cells were plated in 24-well tissue culture plates at a density of 40 000 cells/well in 0.5 mL of growth medium. After 24 h, 250 μL of medium supplemented with 8 μg/mL polybrene (Sigma, H9268) were added. Transductions were performed by the addition of 10 μL of shRNA (Mission® Transduction Particles NM_006446, Sigma, TRCN0000043203, coding sequence CCGGGCCTTCATCTAAGGCTAACATCTCGA-GATGTTAGCCTTAGATGAAGGCTTTTTG). Twenty-four hours after transduction, the cell culture medium was changed, and 1 mL of growth medium supplemented with 1 or 5 μg/mL of puromycin (Sigma, P9620) was added to select infected cells after an additional 24 h. The obtained silencing efficiency was evaluated after 3 weeks via real-time PCR and immunofluorescence.

2.4 Real-time RT-PCR

Total RNA was extracted from cell lines using the TRIzol reagent (Invitrogen) according to the manufacturer's instructions. The concentration, purity, and integrity of the RNA samples were determined through UV absorbance and electrophoresis. Two micrograms of total RNA were reverse transcribed to cDNA using random hexamer primers and the RevertAid™ H Minus M-MuLV Reverse Transcriptase system (Fermentas, St. Leon-Rot, Germany), as recommended by the manufacturer. TaqMan® Gene Expression Assays (Applied Biosystems, Warrington, UK) were purchased for human OATP1B1. The 18S gene was used as a reference gene as previously described [21]. Multiplex quantitative real-time RT-PCR was performed in an amplification mixture with a volume of 20 μL. The target gene amplification mixture contained 10 μL of 2X TaqMan® Universal PCR Master Mix, 1 μL of the appropriate Gene Expression Assay, 1 μL of the TaqMan® endogenous control (human β-actin or 18S), 10 ng of template cDNA diluted in 5 μL of nuclease-free water and 3 μL of nuclease-free water. The thermal cycling conditions were as follows: 2 min at 50°C and 10 min at 95°C, followed by 40 cycles of 15 s at 95°C and 1 min at 60°C. Fluorescence generation due to TaqMan® probe cleavage via the 5′→3′ exonuclease activity of DNA polymerase was measured with the ABI PRISM 7700 Sequence Detection System (Applied Biosystems). All samples were amplified in triplicate. To cover the range of expected Ct values for the target mRNA, a standard curve of six serial dilutions from 50 ng to

500 pg of pooled cDNA was analyzed using Sequence Detection Software (SDS 1.9.1., Applied Biosystems). The results were imported into Microsoft Excel for further analysis. Comparable cDNA contents in the experimental samples were calculated according to the standard curve method. Relative gene expression data are given as the *n*-fold change in transcription of target genes normalized to the endogenous control. Real-time RT-PCR was performed with the following prefabricated TaqMan® Gene Expression Assays (Applied Biosystems) containing intron-spanning primer Hs00272374_m1 for OATP1B1.

2.5 Immunofluorescence

ZR-75-1 OATP1B1-knockdown cells and cells transfected with the empty vector were allowed to attach on culture slides overnight (8-Chamber Polystyrene Vessel Tissue Culture-Treated Glass Slides, BD Falcon). Formalin fixation was followed by a washing step and a blocking step (by 5% BSA). The primary antibody against OATP1B1 (OATP1B1/1B3 mMDQ mouse mAb; Acris Antibodies, Herford, Germany) was diluted 1:100, and incubation was performed for 2 h. Optimal antibody concentrations were determined by titrating serial antibody dilutions. The applied dilutions corresponded to the minimum concentration necessary to produce a positive signal. WT and OATP1B1-transfected CHO cells were used as controls. Following incubation with the secondary antibody (1:1000 dilution; Alexa Fluor® 488 Goat Anti-Mouse IgG; Invitrogen, Carlsbad, CA, USA) for 30 min, cell nuclei were stained with 0.5 μg/mL Hoechst 33342 (Sigma-Aldrich, St. Louis, MO, USA). Thereafter, the slides were rinsed with distilled water before being mounted in Mowiol 4–88 (Carl Roth, Karlsruhe, Germany). Fluorescent staining was visualized with an Axioplan 2 microscope (Carl Zeiss, Jena, Germany). Images were captured using an AxioCam HRc2 Color CCD digital camera and Axiovision 4.8 software (Carl Zeiss Vision GmbH, Aalen, Germany). To minimize background signals and to make the signal intensity and extension in different samples comparable, the exposure times for the individual antibodies were evaluated and kept constant between the samples.

2.6 Western blotting

Western blotting to confirm OATP1B1-, OATP1B3-, and OATP2B1-overexpression in transfected CHO cells was performed with membrane extracts (Pierce, Rockford, IL, USA) from these cells. WT CHO cell membrane extracts were used as controls. Protein content was determined with an assay kit from Bio-Rad Laboratories (Hercules, CA, USA) with BSA as the standard. For immunoblotting, 25 μg of protein were separated by SDS polyacrylamide gel 12% electrophoresis and transferred onto Hybond PVDF membranes. To control equal sample loading, protein on the membranes were stained

with Ponceau S. In the immunoblot, 5% nonfat dry milk in TBS/0.1% Tween 20 was used for blocking. As primary antibodies an anti-OATP1B1/1B3 mouse mAb from Acris Antibodies (BM5542) and an anti-OATP2B1 rabbit mAb from Abcam Antibodies (ab83532, Cambridge, UK) diluted 1:500 in blocking solution were applied. Peroxidase-conjugated species-specific IgGs were used as secondary antibodies (dilution 1:2000). Detection was done with an ECL detection kit from Thermo Scientific (Portsmouth, NH, USA) and Amersham Hyperfilms (GE-Healthcare, Amersham, UK).

2.7 Uptake assays in CHO cells

Transport assays were performed on 12-well plates as described in detail elsewhere [25]. Briefly, CHO cells were seeded at a density of 350 000 cells per well on 12-well plates (BD Biosciences). Uptake assays were generally performed on day 3 after seeding, when the cells had grown to confluence. Twenty-four hours before starting the transport experiments, the cells were additionally treated with 5 mM sodium butyrate (Sigma-Aldrich) to induce nonspecific gene expression [28]. Resveratrol and its sulfates were dissolved in DMSO and diluted with uptake buffer pH 7.4 (final DMSO concentration of 0.5%, which was constant in all transport experiments) to 12.5–600 μM. Control experiments contained DMSO in the medium in place of resveratrol. Prior to the transport experiment, the cells were rinsed twice with 2 mL of prewarmed (37°C) uptake buffer (116.4 mM NaCl, 5.3 mM KCl, 1 mM NaH$_2$PO$_4$, 0.8 mM MgSO$_4$, 5.5 mM D-glucose, and 20 mM Hepes; pH adjusted to 7.4). Uptake was initiated by adding 0.25 mL of uptake buffer containing the substrate. After the indicated time period at 37°C, uptake was stopped by removing the uptake solution and washing the cells five times with 2 mL of buffer (pH 7.4). The cells were then trypsinized by the addition of 100 μL of trypsin and transferred into test tubes. Next, the cell membranes were disrupted via repeated (five times) shock freezing in liquid nitrogen and thawing. Following centrifugation at 13 500 × g for 5 min, 100 μL of the supernatant was diluted with methanol/water (2:1; v/v), and aliquots (80 μL) were analyzed via HPLC [22].

As most OATPs are stimulated by an acidic pH, uptake experiments were also performed at pH 6.5 under identical conditions as mentioned above except now using acidic uptake and washing buffers.

2.8 Uptake assays in ZR-75-1 cells

Transport assays were performed on 12-well plates as described above for CHO cells. Resveratrol and its disulfate were dissolved in DMSO and were diluted with uptake buffer (pH 6.5; final DMSO concentration of 0.5%) to 12.5–400 μM. The experiments were performed in triplicate. Control experiments contained DMSO in the medium in place of resveratrol. Prior to the transport experiment, the cells were rinsed twice with 2 mL of prewarmed (37°C) uptake buffer. Uptake

was initiated by adding 0.25 mL of uptake buffer containing the substrate. After 1 min at 37°C, uptake was stopped by removing the uptake solution and washing the cells five times with 2 mL of buffer. After trypsinization, cell membranes were disrupted via repeated shock freezing in liquid nitrogen. Following centrifugation, the supernatant was diluted with methanol/water, and aliquots (80 μL) were analyzed via HPLC as described above.

2.9 Inhibition analysis

For the inhibition experiments with rifampicin and bromosulfophthalein (BSP; Sigma-Aldrich), stock solutions of these compounds were prepared in DMSO containing the indicated concentrations. CHO cells grown on 12-well plates were first washed twice with prewarmed uptake buffer (pH 7.4) and incubated for 10 min at 37°C under 5% CO$_2$ with 1 μM resveratrol or 10 μM resveratrol sulfates (resveratrol-3-O-disulfate and resveratrol-3-O-4'-O-disulfate) in the presence of the inhibitors ranging from 0.0001 to 100 μM. Control experiments were performed without BSP and rifampicin under identical conditions as mentioned above.

2.10 Metabolism studies in ZR-75-1 cells

Cells were plated on six-well plates and allowed to attach overnight. Resveratrol was dissolved in DMSO and diluted with medium (final DMSO concentration <0.1%) to a concentration of 5–100 μM. The experiments were performed under each set of conditions in triplicate. Control experiments contained DMSO in the medium in place of resveratrol. After 72 h, the medium was aspirated via suction, and aliquots (100 μL) were subsequently analyzed through HPLC. The cells were then trypsinized by the addition of 100 μL of trypsin, washed three times with phosphate buffered saline, and lysed by repeated (five times) shock freezing in liquid nitrogen and thawing. Following centrifugation at 13 500 × g for 5 min, 80 μL of the supernatant (cytoplasm) was subsequently analyzed by HPLC [22]. Additionally, the cell pellets containing the membranes were extracted with 200 μL of methanol and analyzed by HPLC for their resveratrol content. The protein concentration in the cell pellets was determined using a bicinchoninic acid protein assay kit (Pierce Science, Rockford, IL, USA), with BSA as a standard.

2.11 Cytotoxicity assay

CellTiter-Blue (Promega, Southampton, UK) is a colorimetric and fluorescent assay used to measure cell viability via nonspecific redox enzyme activity (reduction from resazurin to resorufin by viable cells). ZR-75-1 cells (50 000 cells/mL) were seeded into 96-well flat-bottomed plates and incubated for 24 h at 37°C under 5% CO$_2$. For cytotoxicity assays, the cells were incubated with various

concentrations of resveratrol (5–400 μM) for 72 h. The CellTiter-Blue (20 μL) reagent was added to the wells, and the plate was incubated for 2 h, protected from light. The absorbance was recorded for resazurin (605 nm) and resorufin (573 nm). The assay results were measured on a Tecan M200 multimode plate reader (Tecan Austria GmbH, Groedig, Austria). The absorbance was also measured in CellTiter-Blue assays in blank wells (without resveratrol) and deducted from the values from experimental wells. The viability of the treated cells was expressed as a percentage of the viability of the corresponding control cells. All experiments were repeated at least three times.

2.12 Determination of protein concentrations

Total protein was determined using the colorimetric bicinchoninic acid protein assay kit (Pierce Science) with BSA as a standard and quantification at a wavelength of 562 nm on a spectrophotometer (UV-1800, Shimadzu). Raw data were analyzed using UVProbe software (version 2.31, Shimadzu). The protein concentrations were consistent among the plates (0.150 ± 0.005 mg/well).

2.13 HPLC analysis

Resveratrol and its glucuronidated and sulfated biotransformation products were quantified by HPLC as described previously [22, 29] using a Dionex UltiMate 3000 system (Sunnyvale, CA, USA) equipped with an L-7250 injector, an L-7100 pump, an L-7300 column oven (set at 15°C), a D-7000 interface and an L-7400 UV detector (Thermo Fisher Scientific, Waltham, MA, USA) set at a wavelength of 307 nm. Calibration of the chromatogram was accomplished using the external standard method. Linear calibration curves were performed by spiking drug-free cell culture medium with standard solutions of trans-resveratrol, trans-resveratrol-3-O-sulfate, trans-resveratrol-4'-O-sulfate, trans-resveratrol-3-O-4'-O-disulfate, trans-resveratrol-3-O-glucuronide, and trans-resveratrol-4'-O-glucuronide to give a concentration range from 0.00257 to 25.7 μM (average correlation coefficients: >0.999). For this method, the lower limit of quantification for resveratrol, resveratrol sulfates and resveratrol glucuronides was 11, 13, and 25 nM, respectively. Coefficients of accuracy and precision for these compounds were <11%.

2.14 Data analysis

Kinetic analysis of the uptake of resveratrol and metabolites was performed over a substrate concentration range of 1–600 μM. Prior to these experiments, the linearity of cellular uptake over time (1, 3, and 10 min) was individually determined for WT and OATP-transfected CHO cells by using resveratrol (50 μM) as a substrate. Cellular uptake rates are presented

after normalization for the incubation time and total protein content. Net uptake rates were calculated as the difference in the uptake rate of the transfected and WT cells for each individual concentration. The data were fitted to the Michaelis–Menten model. Kinetic parameters were calculated using the Graph-Pad Prism Version 5.0 software program (GraphPad Software, San Diego, CA, USA) for Michaelis–Menten: $V = V_{max} \times S/(K_m + S)$, where V is the rate of the reaction; V_{max} is the maximum velocity; K_m is the Michaelis constant, and S is the substrate concentration. The intrinsic clearance, which is defined as the ratio V_{max}/K_m, quantifies the transport capacity. IC_{50} values were determined by plotting the log inhibitor concentration against the net uptake rate and nonlinear regression of the dataset using the equation:

$$y = \frac{a}{1 + [I/(IC_{50})s + b]}$$

in which y is the net uptake rate (pmol/μg protein/min), I is the inhibitor concentration (μM), s is the slope at the point of inversion, and a and b are the maximum and minimum values for cellular uptake. Net uptake was calculated for each inhibitor concentration as the difference in the uptake rates of the transporter-expressing and WT cell lines. Unless otherwise indicated, values are expressed as mean $\pm$ SD of three individual experiments. Significant differences from control values were determined using a using Student's paired t-test at a significance level of $p < 0.05$.

3 Results

3.1 Accumulation of resveratrol and metabolites in transfected CHO cells

To investigate whether resveratrol and its major conjugates are substrates of OATPs, uptake analysis were performed in OATP1B1-, OATP1B3-, and OATP2B1-transfected CHO cells which highly expressed these transporters in the membranes (Supporting Information Fig. 1). Uptake of resveratrol (12.5–400 μM) at pH 7.4 for all three OATPs was only linear for up to 1 min (Fig. 1). We therefore finalized all experiments at 1 min (initial linear phase). As shown in Table 1 and Fig. 2A, the initial net OATP1B1-, OATP1B3-, and OATP2B1-mediated accumulation rates (transfected-WT) for resveratrol followed Michaelis–Menten kinetics, with approximately twofold higher V_{max} values for OATP1B1 compared to OATP1B3 and OATP2B1 (V_{max}: 1100 versus 818 versus 640 pmol/mg protein/min at pH 7.4). K_m-values were the lowest for OATP1B3 (62.0 μM) and followed by OATP2B1- (88.1 μM) and OATP1B1-transfected cell lines (88.4 μM). The uptake of resveratrol-3-O-4'-O-disulfate (25–600 μM) in OATP1B1- and OATP1B3-transfected CHO cells, however, was less pronounced, showing V_{max} values of 100 and 107 pmol/mg protein/min, respectively (Fig. 2C). Interestingly, the affinity
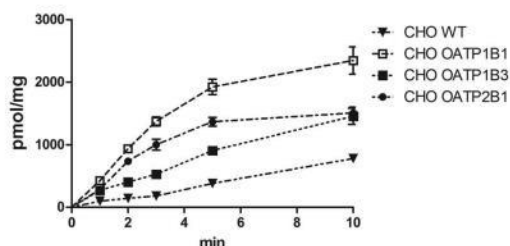
Figure 1. Time-dependent uptake of resveratrol in OATP-transfected CHO cells. The uptake of resveratrol (50 μM) after 1, 2, 3, 5, and 10 min was determined in in wild-type, OATP1B1-, OATP1B3-, and OATP2B1-transfected CHO cells at pH 7.4, 37°C. The data represent the mean ± SD of three individual determinations.

of resveratrol-3-*O*-4′-*O*-disulfate for OATP1B1 and OATP1B3 was about twofold higher with K_m-values of 37.6 and 37.5 μM compared to resveratrol. Resveratrol-3-*O*-sulfate (25–600 μM) was only taken up by OATP1B3, again with low K_m (101 μM) and V_{max} (122 pmol/mg protein/min) values. The uptake of resveratrol-4′-*O*-sulfate, resveratrol-3-*O*-glucuronide, and resveratrol-4′-*O*-glucuronide by OATP1B1-, OATP1B3-, and OATP2B1-transfected and WT CHO cells was below the detection limit (13–25 nM). As it is well known that most OATPs are stimulated by an acidic extracellular pH [27], we also performed uptake experiments at pH 6.5 with WT and OATP-transfected CHO cells. Table 1 revealed that the K_m values for the uptake of resveratrol and it sulfated conjugates were in general lower at pH 6.5 compared to pH 7.4 but only reached a level of significance for resveratrol-3-*O*-4′-*O*-disulfate by OATP1B1 and OATP1B3. V_{max} values also showed a pH dependency which was, however, less

pronounced and only significant for resveratrol uptake by OATP1B3 and OATP2B1.

3.2 Effect of OATP inhibitors on the accumulation of resveratrol and major sulfates in transfected CHO cells

To investigate whether known OATP inhibitors impact OATP1B1-, OATP1B3-, and OATP2B1-mediated resveratrol accumulation, resveratrol was quantified after incubation of 1 μM in OATP1B1-, OATP1B3-, and OATP2B1-expressing CHO cells at pH 7.4 in the absence and presence of increasing concentrations of BSP and rifampicin. The inhibition of resveratrol uptake by BSP in OATP1B3-expressing CHO cells was more potent (IC_{50}: 1.09 μM) compared to OATP1B1- and OATP2B1-expressing CHO cells (IC_{50} values: 1.39 and 1.47 μM, respectively). Rifampicin was an even more potent inhibitor of resveratrol uptake in OATP2B1 (IC_{50}: 0.48 μM) but not in OATP1B1- and OATP1B3-transfected CHO cells (IC_{50}: 1.24 and 1.34 μM, respectively). Uptake inhibition of 10 μM resveratrol-3-*O*-sulfate in OATP1B3-transfected CHO cells by BSP and rifampicin was also pronounced with IC_{50} values of 3.52 and 0.33 μM, respectively. Inhibition of resveratrol-3-*O*-4′-*O*-disulfate uptake by BSP and rifampicin resulted in even lower IC_{50} values for OATP1B1 and OATP1B3 (0.27 and 0.29 μM versus 0.25 and 0.23 μM).

3.3 OATP1B1 knockdown in ZR-75-1 cells

The PCR data from various lentiviral-transfected clones revealed an up to tenfold reduction of OATP1B1 expression in ZR-75-1 cells. The cells exhibiting the lowest expression

Table 1. pH dependency of Michaelis–Menten parameters in stably transfected CHO cells

Substrate	pH 7.4		pH 6.5	
	K_m [μM]	V_{max} [pmol/mg/min]	K_m [μM]	V_{max} [pmol/mg/min]
OATP1B1				
Res	88.4 ± 17.3	1100 ± 67.9	79.8 ± 16.9	1149 ± 74.9
3OS	n.d.	n.d.	n.d.	n.d.
DiS	**37.6 ± 5.23***	**100.3 ± 3.12***	**20.7 ± 7.38***	**83.9 ± 4.13***
OATP1B3				
Res	**62.0 ± 10.6***	**818 ± 39.3***	**42.9 ± 12.5***	**653 ± 50.4***
3OS	**101 ± 28.1***	122 ± 9.61	**80.6 ± 29.1***	120.5 ± 13.0
DiS	**37.5 ± 5.87***	**107.6 ± 3.76***	**13.5 ± 8.17***	**99.6 ± 6.19***
OATP2B1				
Res	88.1 ± 17.8	**640 ± 40.5***	77.0 ± 18.92	**990.6 ± 73.7***
3OS	n.d.	n.d.	n.d.	n.d.
DiS	n.d.	n.d.	n.d.	n.d.

Values are means ± SD of three individual determinations. The net OATP-mediated uptake values were calculated by substracting the values obtained with the wild-type CHO cells from those obtained with the stably transfected cells. Kinetic parameters were calculated by fitting the data to the Michaelis–Menten (K_m) equation with nonlinear regression. Res, resveratrol; 3OS, resveratrol-3-*O*-sulfate; DiS, resveratrol-3-*O*-4′-*O*-disulfate; n.d., not determined. K_m and V_{max} values in bold and marked with an asterisk are significantly different ($p < 0.05$) between pH 6.5 and pH 7.4.
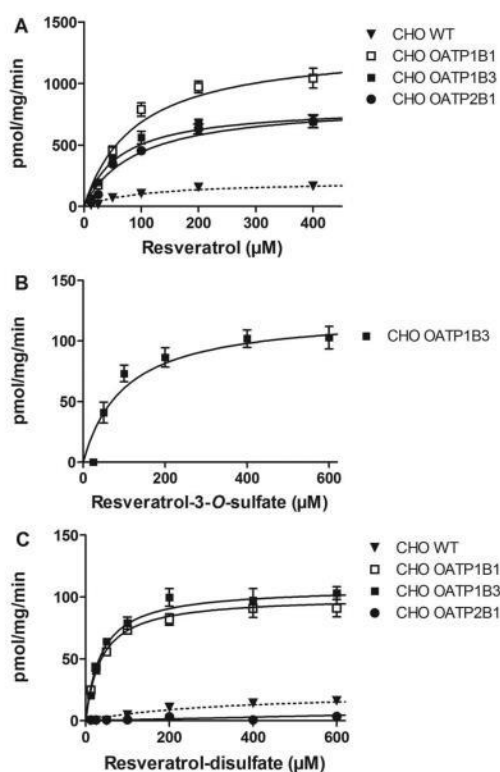
Figure 2. Uptake of resveratrol and its major sulfates in OATP-transfected and wild-type CHO cells. The uptake of resveratrol (12.5–400 μM) (A), resveratrol-3-*O*-sulfate (25–600 μM) (B), and resveratrol-3-*O*-4′-*O*-disulfate (25–600 μM) (C) by OATP1B1-, OATP1B3- and OATP2B1-transfected CHO cells and wild-type CHO cells was determined after 1 min at pH 7.4, 37°C. The data represent the mean ± SD of three individual determinations.

Figure 3. Immunofluorescent characterization of OATP1B1 in ZR-75-1 and OATP1B1 knockdown ZR-75-1 cells. Cells were grown on culture slides and stained with an antibody against OATP1B1 (green) while nuclei were visualized by Hoechst 33342 staining to give a bright blue color (see Section 2). Immunofluorescence was performed in ZR-75-1 empty vector-transfected cells (A), ZR-75-1 OATP1B1 knockdown cells (B), OATP1B1-transfected CHO cells (C), and CHO wild-type cells (D). Bright green fluorescence was seen in ZR-75-1 empty vector-transfected cells (A) and OATP1B1-transfected CHO cells (C).

of OATP1B1 (relative mRNA expression was reduced from 14.78 ± 0.26 to 1.19 ± 0.02 based on the change to the calibrator) were chosen for further experiments. Because ZR-75-1 cells do not express OATP1B3 and OATP2B1, but do express OATP1B1 [21], the expression of the OATP1B1 protein was confirmed via immunofluorescence using a specific OATP1B1/1B3 mouse mAb. Figure 3 clearly shows normal expression (bright green fluorescence) of OATP1B1 in ZR-75-1 empty vector cells (A) and extremely low expression of this transporter in ZR-75-1 OATP1B1-knockdown cells (B). OATP1B1-transfected CHO cells (C) were used as positive control, compared to WT CHO cells (D) without fluorescence.

3.4 Resveratrol accumulation in WT and ZR-75-1 OATP1B1-knockdown cells

Based on the much higher OATP1B1 mRNA level found in the WT ZR-75-1 breast cancer cell line compared to the

OATP1B1-knockdown clone, we expected that OATP1B1 expression might be directly correlated with intracellular resveratrol concentrations. For kinetic analysis, an incubation time of 1 min was selected in order to prevent cellular uptake from interference with cellular efflux mechanisms such as MRPs and breast cancer-resistance protein. Figure 4A depicts representative Michaelis–Menten plots for resveratrol uptake by WT and ZR-75-1 OATP1B1-knockdown cells, where significantly higher uptake rates and approximately twofold lower K_m values were found in the OATP1B1-expressing control cells (V_{max}: 3360 versus 2412 pmol/mg protein/min; K_m: 144

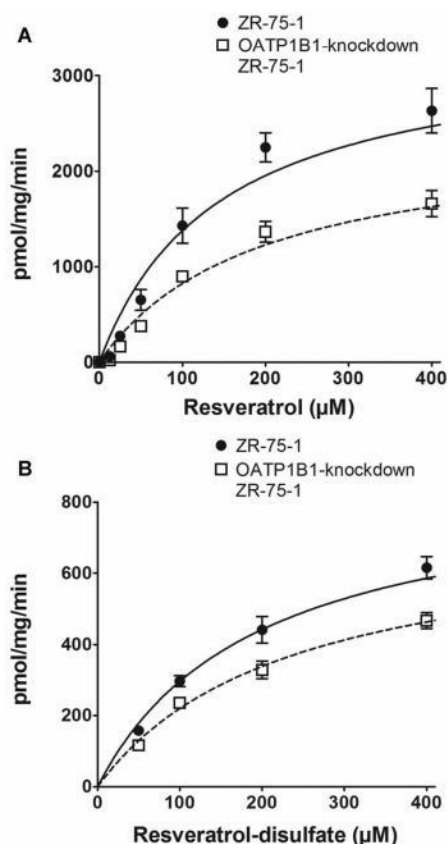8   J. Riha et al.

Mol. Nutr. Food Res. 2014, *00*, 1–13

Figure 4. Uptake of resveratrol and resveratrol disulfate in ZR-75-1 and OATP1B1 knockdown ZR-75-1 cells. The uptake of resveratrol (12.5–400 μM) (A) and resveratrol-3-*O*-4'-*O*-disulfate (12.5–400 μM) (B) in ZR-75-1 empty vector-transfected and OATP1B1 knockdown ZR-75-1 cells was determined after 1 min at pH 7.4, 37°C. The data represent the mean ± SD of three individual determinations.

Figure 5. Cytotoxicity of resveratrol and resveratrol disulfate to ZR-75-1 and OATP1B1 knockdown ZR-75-1 cells. After incubation for 72 h with 10–400 μM resveratrol (A) and resveratrol-3-*O*-4'-*O*-disulfate (B) at 37°C percent viable cells were determined (see Section 2). Dose response curves were obtained by nonlinear curve fitting using GraphPad Prism 5.0 program. The data represent the mean ± SD of three individual determinations.

versus 193 μM). Resveratrol-3-*O*-4'-*O*-disulfate, a substrate of OATP1B1, also showed higher uptake rates and a lower affinity for this transporter in ZR-75-1 cells transfected with the empty vector compared with the OATP1B1-knockdown clone (V_{max}: 870 versus 734 pmol/mg protein/min; K_m: 194 versus 234 μM). However, incubation with resveratrol-3-*O*-sulfate, which is a substrate of OATP1B3 but not of OATP1B1, did not show any differences in uptake in the two cell lines, thus strongly indicating the impact of OATP1B1 on resveratrol transport.

3.5 Cytotoxicity of resveratrol and resveratrol disulfate in ZR-75-1 OATP1B1-knockdown cells

The cytotoxicity of resveratrol in WT and OATP1B1-knockdown ZR-75-1 breast cancer cells was quantified using
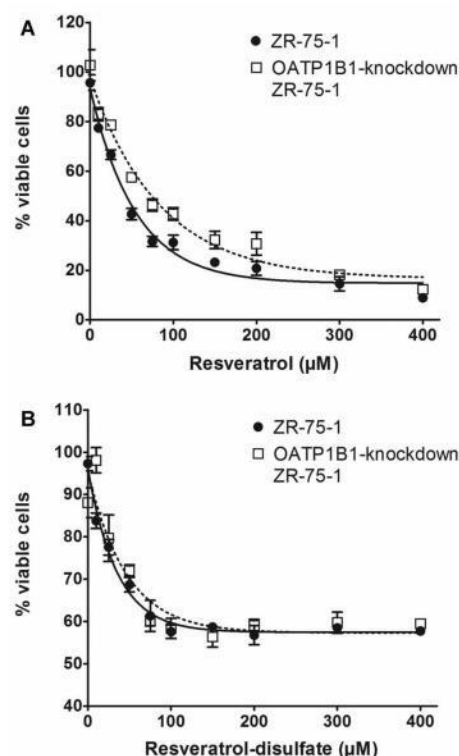
the CellTiter-Blue test kit from Promega, as described above. As shown in Fig. 5, resveratrol exhibited an approximately twofold lower IC_{50} value in control ZR-75-1 cells (37.7 μM) compared to the OATP1B1 knockdown clone (58.0 μM), supporting the importance of OATP1B1-dependent resveratrol uptake. This trend was also true for resveratrol-3-*O*-4'-*O*-disulfate, for which the IC_{25} value was lower in WT cells (6.97 μM) compared to OATP1B1-knockdown cells (9.15 μM). Due to the overall low cytotoxicity of resveratrol-3-*O*-4'-*O*-disulfate, we could not determine IC_{50} values in either cell line.

3.6 Differences in the metabolism of resveratrol and resveratrol disulfate in ZR-75-1 cells

To further evaluate the differences in resveratrol biotransformation, WT and OATP1B1-knockdown ZR 75-1 breast cancer cells were incubated for 72 h with resveratrol and
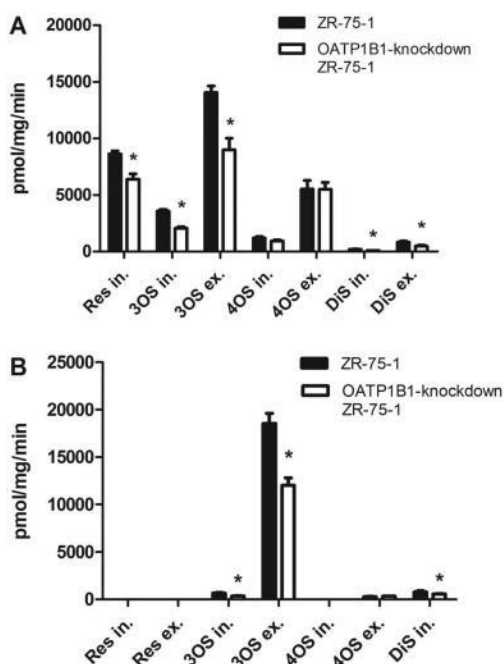
Mol. Nutr. Food Res. 2014, *00*, 1–13

9

Figure 6. Metabolism of resveratrol and resveratrol disulfate in ZR-75-1 and OATP1B1 knockdown ZR-75-1 cells. The concentrations of resveratrol, resveratrol-3-*O*-4'-*O*-disulfate as well as the formation of metabolites (DiS, resveratrol disulfate; 3OS, resveratrol-3-*O*-sulfate; and 4OS, resveratrol-4'-*O*-sulfate) were determined after incubation for 72 h with 50 μM resveratrol (A) and 50 μM resveratrol-3-*O*-4'-*O*-disulfate (B) in ZR-75-1 and ZR-75-1 OATP1B1-knockdown cells at 37°C. Concentrations were determined in the medium (ex., extracellular) and in the cytoplasm (in., intracellular). The data represent the mean ± SD of three individual determinations. Columns marked with an asterisk are significantly different ($p < 0.05$).

resveratrol-3-*O*-4'-*O*-sulfate (50 μM), and the cytoplasm and cellular supernatant were assayed to quantify resveratrol, resveratrol-3-*O*-sulfate, resveratrol 4'-*O*-sulfate, and resveratrol-3-*O*-4'-*O*-disulfate via HPLC.

As shown in Fig. 6A, the intracellular concentrations of resveratrol after incubation with 50 μM resveratrol for 72 h were significantly lower in the OATP1B1-knockdown cells compared to WT cells (6398 ± 457 versus 8620 ± 270 pmol/h/mg protein), leading to decreased formation of resveratrol-4'-*O*-sulfate (943 ± 102 versus 1215 ± 113 pmol/h/mg protein) and resveratrol-3-*O*-4'-*O*-disulfate (104 ± 12 versus 188 ± 36 pmol/h/mg protein).

In order to verify that most of resveratrol reached the cytoplasm did not remain in the membranes, cell pellets (containing the membranes) were extracted with methanol and analyzed by HPLC. Resveratrol concentrations in the cellular membranes were low (<5%) excluding any accumulation in the lipid bilayers.

As observed in the cytoplasm, resveratrol-3-*O*-sulfate was the major biotransformation product in the cellular supernatant (14 060 ± 561 pmol/h/mg protein in WT cells versus 8992 ± 1022 pmol/h/mg protein in ZR-75-1 OATP1B1-knockdown cells). Similarly, the concentrations of resveratrol-4'-*O*-sulfate and resveratrol-3-*O*-4'-*O*-disulfate were lower in ZR-75-1 OATP1B1-knockdown cells compared to WT cells (5532 ± 751 versus 5488 ± 627 pmol/h/mg protein; and 849 ± 79 versus 496 ± 83 pmol/h/mg protein).

Notably, the concentrations of resveratrol metabolites were approximately threefold higher in the medium compared to the cytosolic samples, thereby strongly indicating the occurrence of rapid cellular efflux after formation. As shown in Fig. 6B, the major metabolite following the uptake of 50 μM resveratrol-3-*O*-4'-*O*-disulfate was the deconjugation product, resveratrol-3-*O*-sulfate, followed by resveratrol-4'-*O*-sulfate. Parent resveratrol was below the detection limit of 11 nM.

4 Discussion

To identify the relevance of uptake transporters to the in vivo activity and to identify the human OATP isoforms responsible for the hepatic uptake of resveratrol and its glucuronidated and sulfated conjugates, we employed cells that stably expressed these OATPs. As shown in Fig. 2 and Table 1, resveratrol exhibited saturable uptake kinetics at pH 7.4 for OATP1B1, OATP1B3, and OATP2B1. The highest affinity was observed for OATP1B3, with a K_m of 62 μM, whereas the affinities for OATP1B1 and OATP2B1 were lower.

Interestingly, resveratrol-3-*O*-sulfate was only transported by OATP1B3 with a low affinity (K_m: 101 μM), while resveratrol-3-*O*-4'-*O*-disulfate was transported with equally high affinities by OATP1B1 (K_m: 37.6 μM) and OATP1B3 (K_m: 37.5 μM). The K_m/V_{max} value for the OATP1B1-mediated uptake of resveratrol-3-*O*-4'-*O*-disulfate was similar to that for OATP1B3 (2.67 versus 2.87 μL/min·μg) (see Table 2). Resveratrol-4'-*O*-sulfate did not show any affinity for any of the three OATPs. Notably, there was also no uptake of resveratrol-3-*O*-glucuronide or resveratrol-4'-*O*-glucuronide, indicating that resveratrol sulfates, and not glucuronides, provide the intracellular pools for resveratrol generation [9].

Based on Michaelis–Menten parameters, however, the exact contribution of OATP2B1 in the gut and of OATP1B1, OATP1B3, and OATP2B1 in the liver to the overall uptake of resveratrol and its major sulfates in humans cannot be determined because of high interindividual variability (up to tenfold) in OATP levels as determined by quantitative proteomics or by Western blotting [30–32]. Our data also suggest that OATP1B1, OATP1B3, and OATP2B1 are low-affinity transporters. Because of the low bioavailability, the portal concentration of resveratrol is probably lower than the K_m values. Indeed, administration of resveratrol (5.0 g/day) for up to 28 days to healthy volunteers showed peak plasma concentrations of 4 μM and 13 μm [33] for unconjugated resveratrol

10   J. Riha et al.

Mol. Nutr. Food Res. 2014, *00*, 1–13

Table 2. pH dependency of Michaelis–Menten parameters in stably transfected CHO cells

Substrate	pH 7.4 V_{max}/K_m [μL/min·μg]	pH 6.5 V_{max}/K_m [μL/min·μg]
OATP1B1		
Res	12.4 ± 3.07	14.4 ± 3.88
3OS	n.d.	n.d.
DiS	2.67 ± 0.45	4.05 ± 1.93
OATP1B3		
Res	13.2 ± 2.79	15.2 ± 5.82
3OS	1.21 ± 0.44	1.5 ± 0.75
DiS	2.87 ± 0.55	7.41 ± 8.27
OATP2B1		
Res	**7.26 ± 1.85***	**12.9 ± 4.07***
3OS	n.d.	n.d.
DiS	n.d.	n.d.

Values are means $\pm$ SD of three individual determinations. The net OATP-mediated uptake values were calculated by substracting the values obtained with the wild-type CHO cells from those obtained with the stably transfected cells. Kinetic parameters were calculated (see Table 1). Res, resveratrol; 3OS, resveratrol-3-*O*-sulfate; DiS, resveratrol-3-*O*-4′-*O*-disulfate; n.d., not determined. V_{max}/K_m values in bold and marked with an asterisk are significantly different ($p < 0.05$) between pH 6.5 and pH 7.4.

and resveratrol-3-*O*-sulfate, respectively. However, concentrations in the colon tissue after administration of resveratrol (1.0 g/day) for up to 8 days to patients with colorectal cancer were significantly higher with mean values of 674 μM for resveratrol and 67 μM for resveratrol-3-*O*-sufate [34] and presumably also resveratrol-3-*O*-4′-disulfate, a metabolite recently shown to be present in human plasma at the same level as resveratrol-3-*O*-sulfate [35].

Interestingly, affinity of resveratrol and its sulfates to OATPs was overall higher at pH 6.5 compared to 7.4. This is in accordance with literature data [27] also showing pH differences in the uptake of OATP substrates. As OATP2B1 is expressed in the upper part of the gut, which also shows a slightly acidic microenvironment [36] and as several literature data have shown an acid pH in the tumor environment [37, 38], pH dependency of Michaelis–Menten parameters for OATPs have to be considered in vivo.

To further demonstrate the importance of OATP1B1 for the uptake of resveratrol and its sulfates, hormone-dependent

ZR-75-1 cells that were previously shown to express high levels of OATP1B1, but not OATP1B3 and OATP2B1 [21], were incubated for 1 min with increasing concentrations of resveratrol and resveratrol-3-*O*-4′-*O*-disulfate. Indeed, the uptake of resveratrol by the ZR-75-1 OATP1B1-knockdown cells was significantly reduced compared to control cells, as indicated by higher K_m and lower V_{max} values (Fig. 4 and Table 3). Concomitant with the decreased uptake detected in ZR-75-1 knockdown cells, we also observed decreased formation of the metabolites resveratrol-4′-*O*-sulfate and resveratrol-3-*O*-sulfate after 72 h, which led to a higher IC$_{50}$ value in the cytotoxicity assay in OATP1B1-expressing WT cells (37.7 versus 58 μM; Fig. 5). As expected, we also observed lower uptake of the OATP1B1 substrate resveratrol-3-*O*-4′-*O*-disulfate in the ZR-75-1 OATP1B1-knockdown cells, which was confirmed by decreased formation of resveratrol-3-*O*-sulfate. Due to its several-fold lower cytotoxicity in breast cancer cell lines [24], the IC$_{50}$ values for resveratrol-3-*O*-4′-*O*-disulfate could not be determined in the ZR-75-1 control and OATP1B1-knockdown cells. However, the IC$_{25}$ values were again lower in WT cells (6.97 μM) compared to the OATP1B1-knockdown cells (9.15 μM). As demonstrated in a previous study, metabolite concentrations in the cellular medium were up to 15-fold higher compared to the cytoplasm, supporting the important role of ABCG2 in resveratrol sulfate efflux [22].

The observed OATP-dependent uptake of resveratrol disulfate was in agreement with recent data from Patel and co-workers [9], who found that the uptake of sulfates in human colon cancer cell lines was correlated with the expression of OATP1B3, which is high in HT-29 and HCA-7 cells, but low in HCEC cells. Indirect involvement of OATP1B1 and OATP1B3 has been reported by Gui et al. [18], who observed inhibition of OATP1B1- and OATP1B3-mediated fluorescein-methotrexate uptake by resveratrol, with an approximately twofold lower IC$_{50}$ value being found for OATP1B1 than for OATP1B3 (11 versus 23 μM).

Any variations in OATP expression may significantly alter the uptake of resveratrol and its sulfates into targeted cells and tissues, thereby strongly affecting the efficacy of treatment. Patients with low or no detectable expression of OATP1B1, OATP1B3, and OATP2B1 may therefore show decreased response rates or even no response to resveratrol. Concomitant administration of OATP inhibitors may also interfere with the uptake of resveratrol, leading to

Table 3. Michaelis–Menten parameters determined in ZR-75-1 cells

Substrate	ZR-75-1		OATP1B1 knockdown ZR-75-1	
	K_m [μM]	V_{max} [pmol/mg/min]	K_m [μM]	V_{max} [pmol/mg/min]
Resveratrol	**144 ± 34.4***	**3360 ± 281***	**192.7 ± 38.7***	**2412 ± 193***
Resveratrol-3-*O*-4′-*O*-disulfate	**194 ± 40.7***	**870 ± 68.7***	**234 ± 40.3***	**734 ± 50.2***

Values are means $\pm$ SD of three individual determinations. V_{max}/K_m values in bold and marked with an asterisk are significantly different ($p < 0.05$) between ZR-75-1 and OATP1B1 knockdown ZR-75-1 cells.

11

transporter-mediated drug/drug interactions. Our data demonstrated that BSP and rifampicin effectively inhibited resveratrol uptake in CHO cells, mediated by OATP1B1, OATP1B3, and OATP2B1 (IC_{50} values: 0.48–1.47 μM). Additional potential inhibitors include clarithromycin, erythromycin, and roxithromycin, which inhibit the uptake of pravastatin in OATP1B1- and OATP1B3-transfected HEK293 cells (showing IC_{50} values of 32–37 μM) [39]. Moreover, cyclosporin A significantly decreases the OATP1B1- and OATP1B3-mediated uptake of bosentan [26] and fexofenadine [40] in HEK293 and CHO cells. In addition to clinically applied drugs, naturally occurring flavonoids also interfere with the OATP uptake of dehydroepianstrosterone, thus indicating that they constitute a novel class of OATP1B1 modulators [12]. Ongoing studies are verifying the interactions of drugs and dietary supplements with the OATP1B1-, OATP1B3-, and OATP2B1-mediated uptake of resveratrol and its sulfates.

Whether other transporters such as OATP2A1 and OATP4C1 which are expressed in ZR-75-1 WT cells [21] are also involved in the uptake of resveratrol and its conjugates is not known yet. Possible candidates may be organic anion transporters (OATs). Besides numerous clinically used drugs, OATs are also involved in the transport of polyphenol conjugates clearly showing substrate specificity. While OAT1-overexpressing human embryonic kidney 293H cells demonstrated enhanced uptake for sulfate and glucuronide conjugates, such as quercetin-3′-O-sulfate, daidzein-7-O-glucuronide, genistein-7-O-glucuonide, and quercetin-3′-O-glucuronide, OAT3 seems to have a higher affinity for sulfates such as quercetin-3′-O-sulfate but not for the isoflavone glucuronides. [41, 42] Another candidate protein might be the sodium-dependent glucose transporter SGLT1 which was shown to be responsible for the cellular uptake of resveratrol glycoside (*trans*-piceid), but not of *trans*-resveratrol in Caco-2 cells [15]. In vascular endothelial HUVEC cells, however, Chen et al. could very recently demonstrate that resveratrol uptake involves both passive diffusion and, at least partly, an SGLT1-mediated process [43]. Active mediated uptake of resveratrol was also supported by data from Maier-Salamon et al. [44] and from Delmas and Lin [45], clearly showing that in Caco-2 and hepatoblastoma cells, resveratrol uptake was significantly higher (around 50%) at 37°C than at 4°C when protein-mediated transport should be minimal.

Contrary to previous data in Caco-2 and HUVEC cells, we could not confirm any passive diffusion mechanism for the uptake of resveratrol as uptake kinetics in WT and OATP1B1-knockout ZR-75-1 cells were saturable, strongly indicating active transport. As passive diffusion and active transport work in concert it was not possible to discriminate each part from another in our breast cancer cell model.

In conclusion, our data revealed that OATPs act as transporters for resveratrol, resveratrol-3-O-sulfate, and resveratrol-3-O-4′-O-disulfate but not for resveratrol-4′-O-sulfate and resveratrol glucuronides. The OATP-dependent uptake of resveratrol sulfates in concert with intracellular sulfatases, which rapidly deconjugate sulfates to the pharma-

cologically active parent compound, represents a key factor explaining the observed pharmacological activity of resveratrol. Future in vivo studies should focus not only on the concentration of resveratrol and its conjugates in target tissues but also on the expression levels of OATPs.

5 References

[1] Tome-Carneiro, J., Larrosa, M., Yanez-Gascon, M. J., Davalos, A. et al., One-year supplementation with a grape extract containing resveratrol modulates inflammatory-related microRNAs and cytokines expression in peripheral blood mononuclear cells of type 2 diabetes and hypertensive patients with coronary artery disease. *Pharmacol. Res.* 2013, *72*, 69–82.

[2] Maier-Salamon, A., Bohmdorfer, M., Thalhammer, T., Szekeres, T. et al., Hepatic glucuronidation of resveratrol: interspecies comparison of enzyme kinetic profiles in human, mouse, rat, and dog. *Drug Metab. Pharmacokinet.* 2011, *26*, 364–373.

[3] Urpi-Sarda, M., Jauregui, O., Lamuela-Raventos, R. M., Jaeger, W. et al., Uptake of diet resveratrol into the human low-density lipoprotein. Identification and quantification of resveratrol metabolites by liquid chromatography coupled with tandem mass spectrometry. *Anal. Chem.* 2005, *77*, 3149–3155.

[4] Walle, T., Hsieh, F., DeLegge, M. H., Oatis, J. E., Jr. et al., High absorption but very low bioavailability of oral resveratrol in humans. *Drug Metab. Dispos.* 2004, *32*, 1377–1382.

[5] Hoshino, J., Park, E. J., Kondratyuk, T. P., Marler, L. et al., Selective synthesis and biological evaluation of sulfate-conjugated resveratrol metabolites. *J. Med. Chem.* 2010, *53*, 5033–5043.

[6] Calamini, B., Ratia, K., Malkowski, M. G., Cuendet, M. et al., Pleiotropic mechanisms facilitated by resveratrol and its metabolites. *Biochem. J.* 2010, *429*, 273–282.

[7] Delmas, D., Aires, V., Limagne, E., Dutartre, P. et al., Transport, stability, and biological activity of resveratrol. *Ann. N. Y. Acad. Sci.* 2011, *1215*, 48–59.

[8] Walker, J., Schueller, K., Schaefer, L. M., Pignitter, M. et al., Resveratrol and its metabolites inhibit pro-inflammatory effects of lipopolysaccharides in U-937 macrophages in plasma-representative concentrations. *Food. Funct.* 2013, *5*, 74–84.

[9] Patel, K. R., Andreadi, C., Britton, R. G., Horner-Glister, E. et al., Sulfate metabolites provide an intracellular pool for resveratrol generation and induce autophagy with senescence. *Sci. Transl. Med.* 2013, *5*, 205ra133.

[10] Kenealey, J. D., Subramanian, L., Van Ginkel, P. R., Darjatmoko, S. et al., Resveratrol metabolites do not elicit early pro-apoptotic mechanisms in neuroblastoma cellsa. *J. Agric. Food Chem.* 2011, *59*, 4979–4986.

[11] Aires, V., Limagne, E., Cotte, A. K., Latruffe, N. et al., Resveratrol metabolites inhibit human metastatic colon cancer cells progression and synergize with chemotherapeutic drugs to induce cell death. *Mol. Nutr. Food Res.* 2013, *57*, 1170–1181.

[12] Wang, X., Wolkoff, A. W., Morris, M. E., Flavonoids as a novel class of human organic anion-transporting polypeptide OATP1B1 (OATP-C) modulators. *Drug Metab. Dispos.* 2005, *33*, 1666–1672.

[13] Miksits, M., Wlcek, K., Svoboda, M., Thalhammer, T. et al., Expression of sulfotransferases and sulfatases in human breast cancer: impact on resveratrol metabolism. *Cancer Lett.* 2010, *289*, 237–245.

[14] van de Wetering, K., Burkon, A., Feddema, W., Bot, A. et al., Intestinal breast cancer resistance protein (BCRP)/Bcrp1 and multidrug resistance protein 3 (MRP3)/Mrp3 are involved in the pharmacokinetics of resveratrol. *Mol. Pharmacol.* 2009, *75*, 876–885.

[15] Henry, C., Vitrac, X., Decendit, A., Ennamany, R. et al., Cellular uptake and efflux of trans-piceid and its aglycone trans-resveratrol on the apical membrane of human intestinal Caco-2 cells. *J. Agric. Food Chem.* 2005, *53*, 798–803.

[16] Hagenbuch, B., Gui, C., Xenobiotic transporters of the human organic anion transporting polypeptides (OATP) family. *Xenobiotica* 2008, *38*, 778–801.

[17] Kim, R. B., Organic anion-transporting polypeptide (OATP) transporter family and drug disposition. *Eur. J. Clin. Invest.* 2003, *33*(Suppl 2), 1–5.

[18] Gui, C., Obaidat, A., Chaguturu, R., Hagenbuch, B., Development of a cell-based high-throughput assay to screen for inhibitors of organic anion transporting polypeptides 1B1 and 1B3. *Curr. Chem. Genomics* 2010, *4*, 1–8.

[19] Obaidat, A., Roth, M., Hagenbuch, B., The expression and function of organic anion transporting polypeptides in normal tissues and in cancer. *Annu. Rev. Pharmacol. Toxicol.* 2012, *52*, 135–151.

[20] Svoboda, M., Riha, J., Wlcek, K., Jaeger, W. et al., Organic anion transporting polypeptides (OATPs): regulation of expression and function. *Curr. Drug Metab.* 2011, *12*, 139–153.

[21] Wlcek, K., Svoboda, M., Thalhammer, T., Sellner, F. et al., Altered expression of organic anion transporter polypeptide (OATP) genes in human breast carcinoma. *Canc. Biol. Ther.* 2008, *7*, 1452–1457.

[22] Murias, M., Miksits, M., Aust, S., Spatzenegger, M. et al., Metabolism of resveratrol in breast cancer cell lines: impact of sulfotransferase 1A1 expression on cell growth inhibition. *Cancer Lett.* 2008, *261*, 172–182.

[23] Wenzel, E., Soldo, T., Erbersdobler, H., Somoza, V., Bioactivity and metabolism of trans-resveratrol orally administered to Wistar rats. *Mol. Nutr. Food Res.* 2005, *49*, 482–494.

[24] Miksits, M., Wlcek, K., Svoboda, M., Kunert, O. et al., Antitumor activity of resveratrol and its sulfated metabolites against human breast cancer cells. *Planta Med.* 2009, *75*, 1227–1230.

[25] Gui, C., Miao, Y., Thompson, L., Wahlgren, B. et al., Effect of pregnane X receptor ligands on transport mediated by human OATP1B1 and OATP1B3. *Eur. J. Pharmacol.* 2008, *584*, 57–65.

[26] Treiber, A., Schneiter, R., Hausler, S., Stieger, B., Bosentan is a substrate of human OATP1B1 and OATP1B3: inhibition of hepatic uptake as the common mechanism of its interactions with cyclosporin A, rifampicin, and sildenafil. *Drug Metab. Dispos.* 2007, *35*, 1400–1407.

[27] Leuthold, S., Hagenbuch, B., Mohebbi, N., Wagner, C. A. et al., Mechanisms of pH-gradient driven transport mediated by organic anion polypeptide transporters. *Am. J. Physiol. Cell Physiol.* 2009, *296*, C570–C582.

[28] Palermo, D. P., DeGraaf, M. E., Marotti, K. R., Rehberg, E. et al., Production of analytical quantities of recombinant proteins in Chinese hamster ovary cells using sodium butyrate to elevate gene expression. *J. Biotechnol.* 1991, *19*, 35–47.

[29] Maier-Salamon, A., Hagenauer, B., Wirth, M., Gabor, F. et al., Increased transport of resveratrol across monolayers of the human intestinal Caco-2 cells is mediated by inhibition and saturation of metabolites. *Pharm. Res.* 2006, *23*, 2107–2115.

[30] Ohtsuki, S., Schaefer, O., Kawakami, H., Inoue, T. et al., Simultaneous absolute protein quantification of transporters, cytochromes P450, and UDP-glucuronosyltransferases as a novel approach for the characterization of individual human liver: comparison with mRNA levels and activities. *Drug Metab. Dispos.* 2012, *40*, 83–92.

[31] Prasad, B., Evers, R., Gupta, A., Hop, C. E. et al., Interindividual variability in hepatic organic anion-transporting polypeptides and P-glycoprotein (ABCB1) protein expression: quantification by liquid chromatography tandem mass spectroscopy and influence of genotype, age, and sex. *Drug Metab. Dispos.* 2014, *42*, 78–88.

[32] Nies, A. T., Niemi, M., Burk, O., Winter, S. et al., Genetics is a major determinant of expression of the human hepatic uptake transporter OATP1B1, but not of OATP1B3 and OATP2B1. *Genome Med.* 2013, *5*, 1.

[33] Brown, V. A., Patel, K. R., Viskaduraki, M., Crowell, J. A. et al., Repeat dose study of the cancer chemopreventive agent resveratrol in healthy volunteers: safety, pharmacokinetics, and effect on the insulin-like growth factor axis. *Cancer Res.* 2010, *70*, 9003–9011.

[34] Patel, K. R., Brown, V. A., Jones, D. J., Britton, R. G. et al., Clinical pharmacology of resveratrol and its metabolites in colorectal cancer patients. *Cancer Res.* 2010, *70*, 7392–7399.

[35] Burkon, A., Somoza, V., Quantification of free and protein-bound trans-resveratrol metabolites and identification of trans-resveratrol-C/O-conjugated diglucuronides—two novel resveratrol metabolites in human plasma. *Mol. Nutr. Food Res.* 2008, *52*, 549–557.

[36] Thwaites, D. T., Anderson, C. M., H+-coupled nutrient, micronutrient and drug transporters in the mammalian small intestine. *Exp. Physiol.* 2007, *92*, 603–619.

[37] Riemann, A., Ihling, A., Schneider, B., Gekle, M. et al., Impact of extracellular acidosis on intracellular pH control and cell signaling in tumor cells. *Adv. Exp. Med. Biol.* 2013, *789*, 221–228.

[38] Wojtkowiak, J. W., Verduzco, D., Schramm, K. J., Gillies, R. J., Drug resistance and cellular adaptation to tumor acidic pH microenvironment. *Mol. Pharm.* 2011, *8*, 2032–2038.

Mol. Nutr. Food Res. 2014, *00*, 1–13

13

[39] Seithel, A., Eberl, S., Singer, K., Auge, D. et al., The influence of macrolide antibiotics on the uptake of organic anions and drugs mediated by OATP1B1 and OATP1B3. *Drug Metab. Dispos.* 2007, *35*, 779–786.

[40] Matsushima, S., Maeda, K., Ishiguro, N., Igarashi, T. et al., Investigation of the inhibitory effects of various drugs on the hepatic uptake of fexofenadine in humans. *Drug Metab. Dispos.* 2008, *36*, 663–669.

[41] Wong, C. C., Botting, N. P., Orfila, C., Al-Maharik, N. et al., Flavonoid conjugates interact with organic anion transporters (OATs) and attenuate cytotoxicity of adefovir mediated by organic anion transporter 1 (OAT1/SLC22A6). *Biochem. Pharmacol.* 2011, *81*, 942–949.

[42] Wong, C. C., Akiyama, Y., Abe, T., Lippiat, J. D. et al., Carrier-mediated transport of quercetin conjugates: involvement of organic anion transporters and organic anion transporting polypeptides. *Biochem. Pharmacol.* 2012, *84*, 564–570.

[43] Chen, M. L., Yi, L., Jin, X., Xie, Q. et al., Absorption of resveratrol by vascular endothelial cells through passive diffusion and an SGLT1-mediated pathway. *J. Nutr. Biochem.* 2013, *24*, 1823–1829.

[44] Maier-Salamon, A., Bohmdorfer, M., Riha, J., Thalhammer, T. et al., Interplay between metabolism and transport of resveratrol. *Ann. N. Y. Acad. Sci.* 2013, *1290*, 98–106.

[45] Delmas, D., Lin, H. Y., Role of membrane dynamics processes and exogenous molecules in cellular resveratrol uptake: consequences in bioavailability and activities. *Mol. Nutr. Food Res.* 2011, *55*, 1142–1153.

The effect of organic anion-transporting polypeptides 1B1, 1B3 and 2B1 on the antitumor activity of flavopiridol against breast cancer cells

Stefan Brenner, Juliane Riha, Benedikt Giessrigl, Theresia Thalhammer, Michael Grusch, Georg Krupitza, Bruno Stieger, and Walter Jäger.

The effect of organic anion-transporting polypeptides 1B1, 1B3 and 2B1 on the antitumor activity of flavopiridol in breast cancer cells

STEFAN BRENNER[1], JULIANE RIHA[1], BENEDIKT GIESSRIGL[1], THERESIA THALHAMMER[2], MICHAEL GRUSCH[3], GEORG KRUPITZA[4], BRUNO STIEGER[5] and WALTER JÄGER[1]

[1]Department of Clinical Pharmacy and Diagnostics, University of Vienna, Vienna; [2]Department of Pathophysiology and Allergy Research, Center of Pathophysiology, Medical University of Vienna; [3]Department of Medicine I, Division of Cancer Research, Medical University of Vienna; [4]Clinical Pathology, Medical University of Vienna, Vienna, Austria; [5]Department of Clinical Pharmacology and Toxicology, University Hospital Zurich, Zurich, Switzerland

Abstract. The contribution of organic anion transporting polypeptides (OATPs) to the cellular uptake of flavopiridol was investigated in OATP1B1-, OATP1B3- and OATP2B1-expressing Chinese hamster ovary (CHO) cells. Uptake of flavopiridol into these cells showed typical Michaelis-Menten kinetics with much higher transport capacity for OATP1B3 compared to OATP1B1 and OATP2B1 (Vmax/Km, 33.9 vs. 8.84 and 2.41 μl/mg/min, respectively). The predominant role of OATPs was further supported by a dramatic inhibition of flavopiridol uptake in the presence of the OATP substrate rifampicin. Uptake of flavopiridol by OATPs also seems to be an important determinant in breast cancer cells. The much higher mRNA level for OATP1B1 found in wild-type compared to ZR-75-1 OATP1B1 knockdown cells correlated with higher flavopiridol initial uptake leading to 4.6-fold decreased IC_{50} values in the cytotoxicity assay (IC_{50}, 1.45 vs. 6.64 μM). Cell cycle profile also showed a clear incidence for a stronger cell cycle arrest in the G2/M phase for ZR-75-1 wild-type cells compared to OATP1B1 knockdown cells, further indicating an active uptake via OATP1B1. In conclusion, our results revealed OATP1B1, OATP1B3 and OATP2B1 as uptake transporters for flavopiridol in cancer cells, which may also apply in patients during cancer therapy.

Introduction

Flavopiridol (Alvocidib, NSC 649890, (-)-cis-5,7-dihydroxy-2-(2-chlorphenyl)-8[4-(3-hydroxy-1-methyl) piperidinyl]-4H-benzopyran-4-on) is a selective inhibitor of cyclin dependent kinases (cdk1, cdk2, cdk4 and cdk7) thereby blocking cell cycle progression at the G1 to S and G2 to M interface (1). Flavopiridol, therefore, exerts pronounced antitumor activity in a variety of cell types including human breast, prostate, hematopoietic, lung, head and neck cancer cells, and also in human tumor xenograft models including colon and prostate carcinomas (1-4). Clinical trials with flavopiridol as a single agent or in combination with anticancer drugs, including taxanes and gemcitabine (5,6), also showed tumor responses in most phase I (7,8) and phase II (9,10) studies on different types of progressive tumors refractory to conventional treatment. Furthermore, the overall response rate could be also increased when flavopiridol was administered as a single agent using a pharmacokinetically-directed schedule (8,10). However, still there was a high amount of variability in pharmacokinetics, response and toxicity which could not be explained by demographic, patients' and disease characteristics but might be caused by an altered flavopiridol accumulation in cancer cells. One factor strongly affecting anticancer drug concentrations thereby leading to altered response rates is metabolism. Indeed, recent data from our lab showed extensive glucuronidation of flavopiridol to the 5- and 7-hydroxy position in human liver microsomes by uridine diphosphate glucuronosyltransferase isoforms 1A1 and 1A9 (UGT1A1 and UGT1A9, respectively) (11). Polymorphic UGTs may therefore affect the extent of glucuronidation as well as flavopiridol disposition, activity and toxicity in a manner similar to irinotecan, a drug which shows pronounced glucuronidation (12-14). In fact, patients with diarrhea after flavopiridol treatment had a lower metabolic ratio (flavopiridol glucuronide/flavopiridol) than patients without diarrhea, indicating that systemic glucuronidation of flavopiridol is inversively associated with the risk of developing diarrhea. It is well established that overexpression of ATP-powered efflux pumps such as P-glycoprotein (P-gp), MDR1 and ABCB1, the breast cancer resistance protein BCRP (ABCG2) and the multidrug resistance protein MRP2 (ABCC2) have a great impact on intracellular concentrations of various anticancer agents. Indeed, flavopiridol was less

Correspondence to: Professor Walter Jäger, Department of Clinical Pharmacy and Diagnostics, University of Vienna, A-1090 Vienna, Austria
E-mail: walter.jaeger@univie.ac.at

Key words: flavopiridol, breast cancer, OATP, cellular uptake, transport, cell cycle inhibition

toxic in CHO cells expressing higher levels of P-gp (15) and in acute leukemia patients with high BCRP mRNA expression in the blast cells (16). MRP2 might indirectly also contribute to cellular drug concentrations as it is the main efflux transporter for flavopiridol glucuronides into bile where they can be cleaved by β-glucuronidase and reabsorbed (17). However, uptake mechanisms into tumor cells might be even more important than efflux transporters for the efficacy of anticancer drugs because they are determinants for intracellular drug concentration (18). One of the most important cellular drug uptake mechanisms in humans is via members of the organic anion-transporting polypeptide family (OATP) (19,20). To facilitate readability and understanding of this report, 'OATP' is used for both genes and proteins. OATPs are expressed in a variety of tissues (21) and tumors (22-24), where they mediate the transport of endogenous and exogenous compounds, including drugs (19,20,25). Studies have shown that uptake transporters can confer sensitivity to anticancer agents (26-30) such as the OATP1B3 substrates methotrexate and pacli-taxel (26,31). This may be therapeutically important because expression of OATP varies greatly among tumor cell lines (32). Cellular uptake of flavopiridol is facilitated by OATP1B1 in transiently transfected HEK-293 and MDCK-II cells (33). Furthermore, Ni and coworkers (33) also identified OATP1B1_rs11045819 as a polymorphic OATP1B1 variant associated with improved flavopiridol response in relapsed chronic lymphocytic leukaemia patients. However, the authors did not investigate the kinetic parameters for the cellular uptake of flavopiridol in OATP1B1-transfected cells nor did they eluci-date the impact of OATP expression on flavopiridol cytotox-icity in cancer cells. As OATPs exhibit overlapping substrate specificity, we hypothesized that additional OATPs may also contribute to the uptake of flavopiridol. In the present study, we therefore investigated the time and concentration-depen-dent transport of flavopiridol in stable OATP1B1-, OATP1B3- and OATP2B1-transfected CHO cells. Furthermore, the impact of OATP expression on cytotoxicity and cell cycle progression of flavopiridol-treated human breast cancer cells ZR-75-1 was also investigated.

Materials and methods

Materials. Flavopiridol (2-(2-chlorophenyl)-5,7-dihydroxy-8-[(3S,4R)-3-hydroxy-1-methyl-4-piperidinyl]-4-chromenone), was obtained from Sigma-Aldrich (Munich, Germany). Acetonitril and water were of HPLC grade (Merck, Darmstadt, Germany). All other chemicals and solvents were commer-cially available, of analytical grade and used without further purification.

Cell culture. Chinese hamster ovary (CHO) cells that were stably transfected with OATP1B1, OATP1B3 or OATP2B1 and wild-type CHO cells were provided by the University of Zurich, Switzerland and have been extensively previ-ously characterized (34,35). The CHO cells were grown in Dulbecco's modified Eagle's medium (DMEM) supplemented with 10% FCS, 50 μg/ml L-proline, 100 U/ml penicillin and 100 μg/ml streptomycin. The selective medium for stably transfected CHO cells additionally contained 500 μg/ml gene-ticin sulfate (G418) (36). All the media and supplements were

obtained from Invitrogen (Karlsruhe, Germany). The mamma-lian ZR-75-1 breast cancer cell line was purchased from the American Type Culture Collection (ATCC, Rockville, MD, USA) and was maintained in RPMI medium supplemented with 10% FCS, 100 U/ml penicillin, 100 μg/ml streptomycin and 1% GlutaMAX. The cells were grown in T-flasks with a 25-cm^2 growth area (BD Biosciences, Franklin Lakes, NJ, USA), maintained at 37°C under 5% CO_2 and 95% relative humidity. The cells were passaged once a week and were used up to passage 55 (37).

OATP1B1 knockdown in ZR-75-1 cells. For lentiviral trans-duction, ZR-75-1 cells were plated in 24-well tissue culture plates at a density of 40,000 cells/well in 0.5 ml of growth medium. After 24 h, 250 μl of medium supplemented with 8 μg/ml polybrene (H9268; Sigma) was added. Transductions were performed by the addition of 10 μl of shRNA (Mission® transduction particles NM_006446, Sigma, TRCN0000043203, coding sequence CCGGGCCTTCATCTAAGGCTAACA TCTCGAGATGTTAG-CCTTAG-ATGAAGGCTTTTG). Twenty-four hours after the transduction, the cell culture medium was changed, and 1 ml of growth medium supple-mented with 1 or 5 μg/ml of puromycin (P9620; Sigma) was added to select infected cells after an additional 24 h. The obtained silencing efficiency was evaluated after 3 weeks via real-time PCR and immunofluorescence (38).

Real-time RT-PCR. Total RNA was extracted from cell lines using the TRIzol reagent (Invitrogen) according to the manu-facturer's instructions. The concentration, purity and integrity of the RNA samples were determined through UV absorbance and electrophoresis. Total RNA (2 μg) were reverse transcribed to cDNA using random hexamer primers and the RevertAid™ H Minus M-MuLV Reverse Transcriptase system (Fermentas, St. Leon-Rot, Germany), as recommended by the manufac-turer. TaqMan® Gene Expression assays (Applied Biosystems, Warrington, UK) were purchased for human OATP1B1. The 18S gene was used as a reference gene, as previously described (23). Multiplex quantitative real-time RT-PCR was performed in an amplification mixture with a volume of 20 μl. The target gene amplification mixture contained 10 μl of 2X TaqMan® Universal PCR Master Mix, 1 μl of the appropriate Gene Expression Assay, 1 μl of the TaqMan® endogenous control (human β-actin or 18S), 10 ng of template cDNA diluted in 5 μl of nuclease-free water and 3 μl of nuclease free water. The thermal cycling conditions were as follows: 2 min at 50°C and 10 min at 95°C, followed by 40 cycles of 15 sec at 95°C and 1 min at 60°C. Fluorescence generation due to TaqMan® probe cleavage via the 5'-3' exonuclease activity of DNA polymerase was measured with the ABI PRISM 7700 Sequence Detection System (Applied Biosystems). All samples were amplified in triplicate. To cover the range of expected Ct values for the target mRNA, a standard curve of six serial dilutions from 50 ng to 500 pg of pooled cDNA was analyzed using the Sequence Detection Software (SDS 1.9.1.; Applied Biosystems). The results were imported into Microsoft Excel for further analysis. Comparable cDNA contents in the experi-mental samples were calculated according to the standard curve method. Relative gene expression data are given as the n-fold change in transcription of target genes normalized to

the endogenous control. Real-time RT-PCR was performed with the following prefabricated TaqMan® Gene Expression Assays (Applied Biosystems) containing intron-spanning primer Hs00272374_m1 for OATP1B1.

Immunofluorescence. ZR-75-1 OATP1B1-knockdown cells and cells transduced with the empty vector were allowed to attach on culture slides overnight (8-Chamber Polystyrene Vessel Tissue Culture-Treated Glass Slides; BD Falcon). Formalin fixation was followed by a washing step and a blocking step (by 5% BSA). The primary antibody against OATP1B1 (OATP1B1/1B3 mMDQ mouse monoclonal antibody; Acris Antibodies, Herford, Germany) was diluted 1:100, and incubation was performed for 2 h. Optimal antibody concentrations were determined by titrating serial antibody dilutions. The applied dilutions corresponded to the minimum concentration necessary to produce a positive signal. Wild-type and OATP1B1-transfected CHO cells were used as controls. Following incubation with the secondary antibody (1:1,000 dilution; Alexa Fluor® 488 goat anti-mouse IgG; Invitrogen, Carlsbad, CA, USA) for 30 min, cell nuclei were stained with $0.5~\mu g/ml$ Hoechst 33342 (Sigma-Aldrich). Thereafter, the slides were rinsed with distilled water before being mounted in Mowiol 4-88 (Carl Roth, Karlsruhe, Germany). Fluorescent staining was visualized with an Axioplan 2 microscope (Carl Zeiss, Jena, Germany). Images were captured using a AxioCam HRc2 Color CCD digital camera and AxioVision 4.8 software (Carl Zeiss Vision GmbH, Aalen, Germany). To minimize background signals and to make the signal intensity and extension in different samples comparable, the exposure times for the individual antibodies were evaluated and kept constant between the samples (38).

Cellular uptake. Transport assays were performed on 12-well plates as described in detail elsewhere (34). Briefly, CHO cells were seeded at a density of 350,000 cells/well on 12-well plates (BD Biosciences, Franklin Lakes, NJ, USA). Uptake assays were generally performed on day 3 after seeding, when the cells had grown to confluence. Twenty-four hours before starting the transport experiments, the cells were additionally treated with 5-mM sodium butyrate (Sigma-Aldrich) to induce non-specific gene expression (39). Flavopiridol was dissolved in DMSO and was diluted with uptake buffer (pH 7.4; final DMSO concentration of 0.5%) to 25-$800~\mu M$. Control experiments contained DMSO in the medium in place of flavopiridol. Prior to the transport experiment, the cells were rinsed twice with 2 ml of prewarmed (37°C) uptake buffer ($116.4~mM$ NaCl, $5.3~mM$ KCl, $1~mM$ NaH_2PO_4, $0.8~mM$ $MgSO_4$, $5.5~mM$ D-glucose and $20~mM$ Hepes; pH adjusted to 7.4). Uptake was initiated by adding 0.25 ml of uptake buffer containing the substrate. After the indicated time period at 37°C, uptake was stopped by removing the uptake solution and washing the cells five times with 2 ml of buffer (pH 7.4). The cells were then trypsinized by the addition of $100~\mu l$ of trypsin and transferred into test tubes. Next, the cell membranes were disrupted via repeated (5 times) shock freezing in liquid nitrogen and thawing. Following centrifugation at 13,500 x g for 5 min, $100~\mu l$ of the supernatant was diluted with methanol/water (2:1; v/v), and aliquots ($80~\mu l$) were analyzed via HPLC (37).

Inhibition analysis. For the inhibition experiments with rifampicin and bromosulfophthalein (BSP; Sigma-Aldrich), stock solutions of these compounds were prepared in DMSO containing the indicated concentrations. CHO cells grown on 12-well plates were first washed twice with pre-warmed uptake buffer (pH 7.4) and incubated for 10 min at 37°C under 5% CO_2 with $1~\mu M$ flavopiridol in the presence of the inhibitors ranging from 0.0001 to $100~\mu M$. Control experiments were performed without BSP and rifampicin under identical conditions as mentioned above.

Cytotoxicity assay. CellTiter-Blue (Promega, Southampton, UK) is a type of a colorimetric assay used to measure cell viability via non-specific redox enzyme activity (reduction from resazurin to resorufin by viable cells). ZR-75-1 cells (50,000 cells/ml) were seeded into 96-well flat-bottomed plates and incubated for 24 h at 37°C under 5% CO_2. For cytotoxicity assays, the cells were incubated with various concentrations of flavopiridol (5-$400~\mu M$) for 72 h. The CellTiter-Blue ($20~\mu l$) reagent was added to the wells, and the plate was incubated for 2 h, protected from light. The absorbance was recorded for resazurin (605 nm) and resorufin (573 nm). The assay results were measured on a Tecan M200 multimode plate reader (Tecan Austria GmbH, Groedig, Austria). The absorbance was also measured in CellTiter-Blue assays in blank wells (without resveratrol) and subtracted from the values from experimental wells. The viability of the treated cells was expressed as a percentage of the viability of the corresponding control cells. All experiments were repeated at least three times.

Cell cycle distribution analyses by fluorescence activated cell sorting (FACS). ZR-75-1 wild-type and OATP1B1 knockdown cells were plated on 6-well plates at a concentration of $1x10^6$ cells/ml and allowed to attach overnight. After 24- and 48-h incubation at 37°C cells were trypsinized by the addition of $100~\mu l$ of trypsin, transferred into 15-ml tubes and centrifuged (4°C, 800 rpm, 5 min) (40). The supernatant was discarded and the cell pellet washed with cold PBS (phosphate-buffered saline, pH 7.4), centrifuged (4°C, 800 rpm, 5 min), resuspended in 1-ml cold ethanol (70%) and fixed for 30 min at 4°C. After two washing steps with cold PBS, the cell pellet was resuspended in $500~\mu l$ cold PBS and transferred into a 5-ml polystyrene round bottom tube. RNAse A and propidium iodide were added to a final concentration of $50~\mu g/ml$ and incubated for 1 h at 4°C. The final cell number was adjusted between 0.5 and $1x10^6$ cells in $500~\mu l$. Cells were analyzed by the FACSCalibur flow cytometer (BD Biosciences). Cell cycle distribution was calculated with ModFid LT software (Verity Software House, Topsham, ME, USA).

Determination of protein concentrations. Total protein was determined using the colorimetric bicinchoninic acid protein (BCA) assay kit (Pierce Science, Rockford, IL, USA) with bovine serum albumin as a standard and quantification at a wavelength of 562 nm on a spectrophotometer (UV-1800; Shimadzu). Raw data were analyzed using UVProbe software (version 2.31; Shimadzu). The protein concentrations were consistent among the plates (0.150 ± 0.005 mg/well).

Table I. Uptake kinetic parameters for flavopiridol in OATP-transfected CHO and ZR-75-1 cells.

Cell lines	Km (μM)	Vmax (pmol/mg/min)	Vmax/Km (μl/min.μg)
OATP1B1 t.f. CHO	66.0±10.3	583±19.8	8.84±0.30
OATP1B3 t.f. CHO	66.8±21.3	2263±156	33.9±0.94
OATP2B1 t.f. CHO	175±25.8	422±19.9	2.41±0.03
ZR-75-1 w.t.	80.8±14.1	1876±74.0	23.2±0.90
OATP1B1 k.d. ZR-75-1	99.0±24.0	758±44.9	7.66±0.13

Values are means ± SD of 3 individual determinations. The net OATP-mediated uptake values were calculated by substracting the values obtained with the wild-type (w.t.) CHO cells from those obtained with the stably transfected cells. Kinetic parameters were calculated by fitting the data to the Michaelis-Menten (Km) equation with non-linear regression. t.f., transfected; w.t., wild-type; k.d., knockdown.

HPLC chromatography. The determination of flavopiridol was performed using a Merck 'La Chrom' System (Merck, Darmstadt, Germany) equipped with an L-7250 injector, an L-7100 pump, an L-7300 column oven (set at 37°C), a D-7000 interface, and a L-7400 UV detector (set at a wavelength at 264 nm). Chromatographic separation of flavopiridol was performed on a Hypersil BDS C18 Column (5 μM, 250 x 4.6 mm I.D.; Thermo Electron Corp.), preceded by a Hypersil BDS C18 precolumn (5 μM, 10 x 4.6 mm I.D.) at a flow rate of 1 ml/min. The mobile phase consisted of a continuous linear gradient, mixed from 10 mM ammonium acetate/acetic acid buffer, pH 7.4 (mobile phase A), and acetonitril (mobile phase B), to elute flavopiridol according to their lipophilicity. The mobile phase was filtered through a 0.45 μM filter (HVLP04700; Millipore, Vienna, Austria). The gradient ranged from 10% acetonitril (0 min) to 40% B at 15 min and linearly increased to 80% B at 17 min where it remained constant for 23 min. Subsequently, the percentage of acetonitril was decreased within 3 min to 10% in order to equilibrate the column for 9 min before application of the next sample. The sample injection volume was 80 μl. Calibration of the chromatogram was accomplished using the external standard method by spiking drug-free cell culture medium with standard solutions of flavopiridol to give a concentration range of 0.005-1 μg/ml (average correlation coefficient: >0.999). For this method the lower limit of quantification for flavopiridol was 10 ng/ml. Coefficients of accuracy and precision for this compound were <9.8%.

Data analysis. Kinetic analysis of the uptake of flavo-piridol was performed over a substrate concentration range of 25-800 μM. Prior to these experiments, the linearity of cellular uptake over time (1, 3 and 10 min) was individually determined for wild-type and OATP-transfected CHO cells by using flavopiridol (50 μM) as a substrate. Cellular uptake rates are presented after normalization for the incubation time and total protein content. Net uptake rates were calculated as the difference in the uptake rate of the transfected and wild-type cells for each individual concentration. The data were fitted to the Michaelis-Menten model. Kinetic parameters were calculated using the GraphPad Prism Version 5.0 software program (GraphPad Software, San Diego, CA, USA) for Michaelis-Menten: V = Vmax * S/(Km + S), where V is the rate of the reaction, Vmax is the maximum velocity, Km is the Michaelis
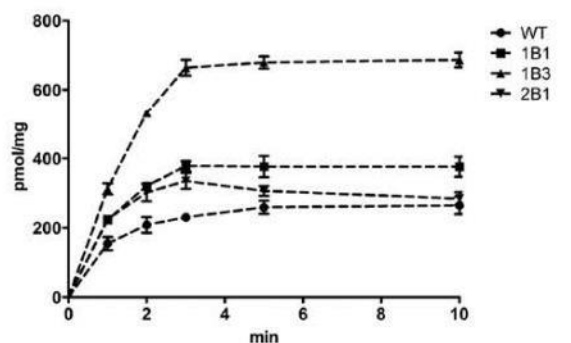

Figure 1. Time-dependent uptake of flavopiridol in OATP-transfected CHO cells. The uptake of flavopiridol (10 μM) after 1, 2, 3, 5 and 10 min was determined in wild-type and OATP1B1-, OATP1B3- and OATP2B1-transfected CHO cells at pH 7.4, 37°C. The data represent the mean ± SD of 3 individual determinations.

constant and S is the substrate concentration. The intrinsic clearance, which is defined as the ratio Vmax/Km, quantifies the transport capacity. IC_{50} values were determined by plotting the log inhibitor concentration against the net uptake rate and non-linear regression of the dataset using the equation:

$$y = \frac{a}{1 + [I/(IC_{50}) s + b]}$$

in which y is the net uptake rate (pmol/μg protein/min), I is the inhibitor concentration (μM), s is the slope at the point of inversion, and a and b are the maximum and minimum values for cellular uptake. Net uptake was calculated for each inhibitor concentration as the difference in the uptake rates of the transporter-expressing and wild-type cell lines. Unless otherwise indicated, values are expressed as mean ± SD of three individual experiments. Significant differences from control values were determined using a Student's paired t-test at a significance level of $P<0.05$.

Results

Uptake kinetics of flavopiridol in OATP transfected CHO cells. To investigate whether OATPs other than OATP1B1 contribute to flavopiridol uptake respective studies were
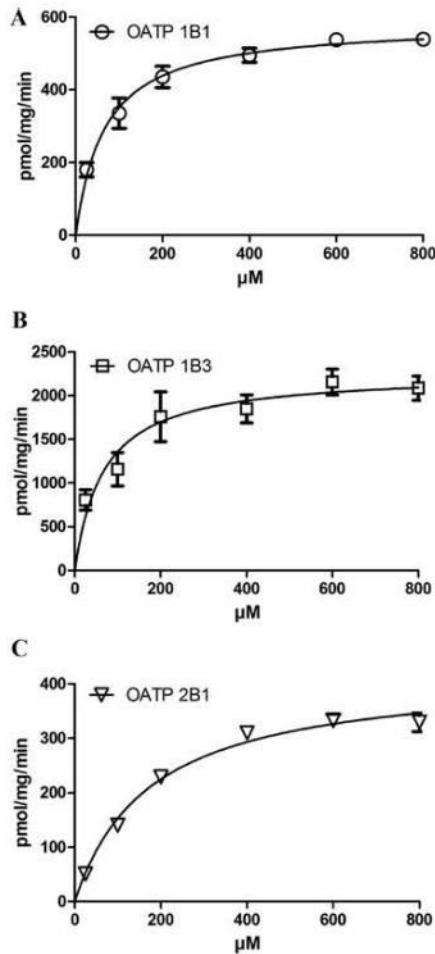
Figure 2. Uptake of flavopiridol in OATP-transfected and wild-type CHO cells. The uptake of flavopiridol (25-800 μM) by (A) OATP1B1-, (B) OATP1B3- and (C) OATP2B1-transfected CHO cells and wild-type CHO cells was determined after 1 min at pH 7.4, 37˚C. After the uptake into wild-type cells was substracted, net-OATP1B1, OATP1B3 and OATP2B1-mediated uptake was fitted to the Michaelis-Menten equation to calculate Km and Vmax values. The data represent the mean ± SD of 3 individual determinations.

Figure 3. Inhibition of flavopiridol uptake into OATP-transfected and wild-type CHO cells by rifampicin. (A) OATP1B1-, (B) OATP1B3- and (C) OATP2B1-transfected CHO cell were co-incubated with 1 μM flavopiridol and increasing concentrations of rifampicin (0.0001-10 μM) at 37˚C for 1 min (Materials and methods). Values are expressed as a percentage of vehicle control; each value represents the mean ± SD of three independent experiments.

performed in CHO cells transfected with OATP1B1, OATP1B3 and OATP2B1 using wild-type CHO cells transfected with the empty vector as controls. Western blot analysis confirmed that these cells highly expressed the respective transporters in the membranes (data not shown). Uptake of flavopiridol (25-800 μM) for all three OATPs was only linear for up to 1 min (Fig. 1). We therefore finalized all experiments at the initial linear phase. As shown in Table I and Fig. 2, the initial net OATP1B1-, OATP1B3- and OATP2B1-mediated accumulation rates (tranfected wild-type) for flavopiridol followed Michaelis-Menten kinetics, with ~4-5-fold higher Vmax values for OATP1B3 compared to OATP1B1 and OATP2B1 (Vmax, 2263 vs. 583 and 422 pmol/mg protein/min). The affinity of flavopiridol for both OATP1B1 and OATP1B3 showed very similar Km values (66.0 and 66.8 μM) but was significantly higher for OATP2B1 (175 μM).

Effect of OATP inhibitors on the accumulation of flavopiridol in transfected CHO cells. To investigate whether known OATP inhibitors impact OATP1B1-, OATP1B3- and OATP2B1-mediated flavopiridol accumulation, flavopiridol was quantified after treatment of OATP1B1-, OATP1B3- and OATP2B1-overexpressing CHO cells with 1 μM flavopiridol in the absence and presence of increasing concentrations of the known OATP inhibitors bromsulphophthalein (BSP) and rifampicin (41,42). As shown in Fig. 3 rifampicin was a potent inhibitor for flavopiridol uptake in OATP1B3- followed by OATP2B1- and OATP1B1-transfected CHO cells (IC$_{50}$ values, 1.00, 1.36 and 2.06 μM, respectively). BSP, however, did not inhibit but rather stimulated OATP-dependent flavopiridol uptake at concentrations up to 100 μM.

OATP1B1 knockdown in ZR-75-1 cells. The cells exhibiting the lowest expression of OATP1B1 (relative mRNA expression was reduced from 14.8±0.26 to 1.19±0.02) were chosen for
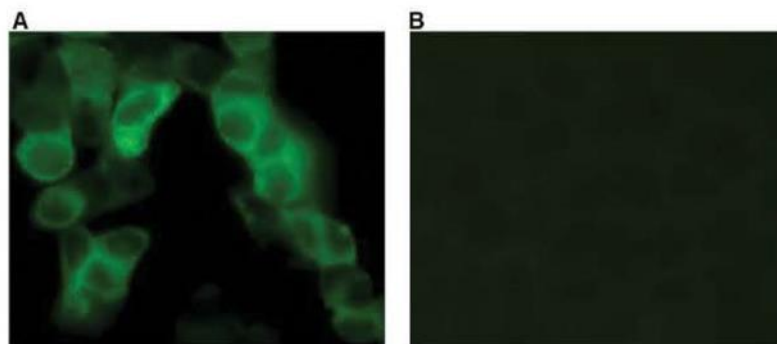
Figure 4. Immunofluorescent characterization of OATP1B1 in ZR-75-1 and OATP1B1 knockdown ZR-75-1 cells. Cells were grown on culture slides and stained with an antibody against OATP1B1 (Materials and methods). Immunofluorescence was performed in ZR-75-1 empty vector-transfected cells (A) and ZR-75-1 OATP1B1 knockdown cells (B). Bright green fluorescence was seen in ZR-75-1 empty vector-transfected cells.
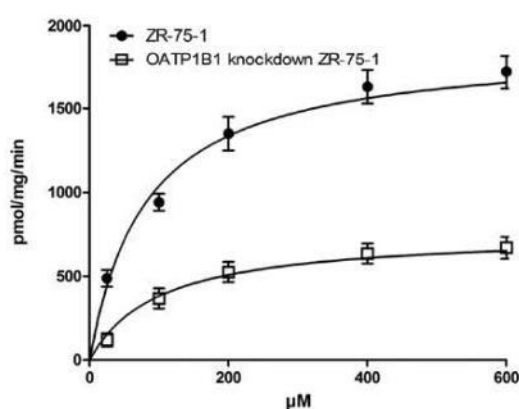

Figure 5. Uptake of flavopiridol in ZR-75-1 and OATP1B1 knockdown ZR-75-1 cells. The uptake of flavopiridol (2.5-600 μM) in ZR-75-1 empty vector-transfected and OATP1B1 knockdown ZR-75-1 cells was determined after 1 min at pH 7.4, 37˚C and the OATP-mediated uptake was fitted to the Michaelis-Menten equation to calculate Km and Vmax values. Data represent the mean ± SD of triplicate determination.

Figure 6. Cytotoxicity of flavopiridol to ZR-75-1 and OATP1B1 knockdown ZR-75-1 cells. After incubation for 72 h with 5-600 μM flavopiridol at 37˚C percent viable cells were determined (Materials and methods). Dose response curves were obtained by non-linear curve fitting using the GraphPad Prism 5.0 program. The data represent the mean ± SD of 3 individual determinations.

further experiments. Because ZR-75-1 cells express OATP1B1 (23) but not OATP1B3 and OATP2B1, the expression of the OATP1B1 protein was furthermore confirmed by immuno-fluorescence. Fig. 4 clearly shows constitutive expression (bright green fluorescence) of OATP1B1 in ZR-75-1 control cells (transfected with empty vector) (Fig. A) and suppressed protein levels of this transporter in ZR-75-1 OATP1B1-knockdown cells (Fig. B).

Uptake kinetics of flavopiridol in wild-type and OATP1B1 knockdown ZR-75-1 cells. Based on much higher OATP1B1 expression levels in wild-type ZR-75-1 breast cancer cell lines compared to OATP1B1 knockdown ZR-75-1 cells, we expected increased intracellular flavopiridol levels in the wild-type cells. For kinetic analysis, an incubation time of 1 min was chosen in order to prevent cellular uptake from interference with cellular efflux mechanisms such as MRP1 and BCRP. Fig. 5 depicts representative Michaelis-Menten kinetics for a significantly higher flavopiridol uptake (2.5-fold) by wild-type compared to OATP1B1 knockdown ZR-75-1 cells (Vmax, 1876 pmol/mg
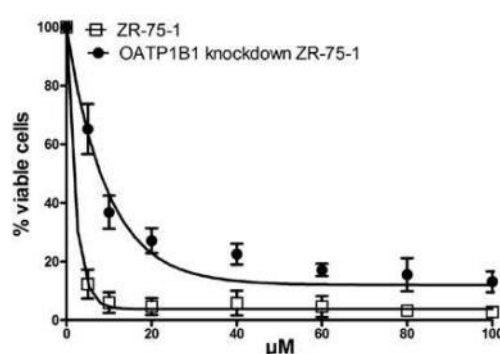
vs. 758 protein/min). Affinity of flavopiridol to OATP1B1, however, was comparable in wild-type and OATP1B1 knockdown ZR-75-1 cells (Km, 80.8 μM±14.1 and 99.0 μM±24.0) indicating that OATP1B1 knockdown did not unmask other transporters for flavopiridol.

Cytotoxicity of flavopiridol in wild-type and OATP1B1 knockdown ZR-75-1 cells. The cytotoxicity of flavopiridol against ZR-75-1 and OATP1B1 knockdown ZR-75-1 breast cancer cells was quantified using the CellTiter-Blue test kit. As shown in Fig. 6, flavopiridol was significantly less toxic in OATP1B1 knockdown (IC_{50}, 6.64 μM) than in wild-type ZR-75-1 cells (IC_{50}, 1.45 μM) underscoring that OATP1B1 is important for flavopiridol uptake.

Effect of flavopiridol on the cell cycle of ZR-75-1 wild-type and OATP1B1 knockdown cells. ZR-75-1 cells were incubated with 5 μM flavopiridol for 8, 24 and 48 h and then subjected to FACS analyses. In the absence of flavopiridol both cell lines showed a nearly identical distribution of cells in the different phases of the cell cycle (Fig. 7). Addition of flavopiridol, however, exhibited distinct effects dependent on OATP1B1 expression.
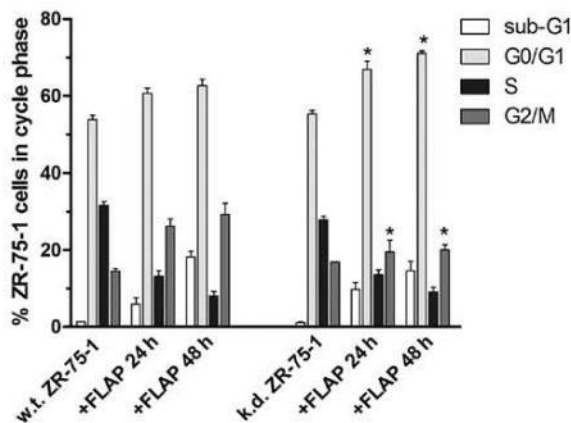
Figure 7. Analysis of cell cycle distribution in wild-type and OATP1B1 knockdown ZR-75-1 cells. ZR-75-1 cells (1×10^6 cells/ml) with flavopiridol (10 μM), harvested after 24 and 48 h, and subjected to FACS analysis. Error bars indicate ± SD, and asterisk significant alterations of cell distributions in the respective cell cycle phase compared to control (P<0.05). Experiments were performed in triplicate.

While the cell cycle of wild-type cells was inhibited in G1 and G2/M phase, OATP1B1-knockdown cells were inhibited only in G1 phase at the expense of G2/M- and S-phase cells after 24 and 48 h of flavopiridol treatment. Notably, reduced uptake of flavopiridol in OATP1B1 knockdown cells was also associated with a decreased proportion of cells in sub-G1 indicating decreased induction of apoptosis observed after 48 h of flavopiridol incubation (14.5 compared to 18.2% for wild-type cells).

Discussion

In the present study, we identified the human OATP isoforms responsible for the cellular uptake of flavopiridol and demonstrated the relevance of flavopiridol uptake for its anticancer activity. To date, the only OATP that has been characterized, by Ni et al (33), as an uptake transporter for flavopiridol is the OATP1B1. Furthermore, expression of the polymorphic variant OATP1B1_rs11045819 was associated with improved flavopiridol response in patients with chronic lymphatic leukemia (33). By systematically investigating the transport properties of flavopiridol for other OATPs using the transfected CHO cells as an in vitro model, we were able to identify OATP1B3 and OATP2B1 as additional uptake transporters for flavopiridol. As shown in Fig. 2 and Table I, flavopiridol exhibited saturable uptake kinetics for OATP1B1, OATP1B3 and OATP2B1. The affinity of flavopiridol for OATP1B1 and OATP1B3 was similar (Kms, 66.0 and 66.8 μM) but 2.6-fold lower for OATP2B1 (Km, 175 μM). Furthermore, uptake of flavopiridol into OATP1B3-transfected CHO cells was up to 5.3-fold higher (Vmax, 2263 pmol/mg/min) leading to an 3.8- and 14-fold increased transport capacity for OATP1B3 compared to OATP1B1 and OATP2B1 (Vmax/Kms, 33.9 vs. 8.84 and 2.41 μl/min/mg protein, respectively; Table I) indicating that OATP1B3 might be the far most important uptake transporter for flavopiridol followed equally by OATP1B1 and OATP2B1.

Our data also suggest that OATP1B1, OATP1B3 and OATP2B1 are low affinity transporters and that the blood concentration of flavopiridol is considerably lower than the Km values. Indeed, administration of the standard dose of flavopiridol (50 g/m^2) as a 4-h infusion dose to patients with relapsed, symptomatic CLL or small lymphocytic lymphoma (SLL) in phase I and II studies showed peak plasma concentrations of ~3 μM (43). Despite this low substrate concentration relative to the Km value, uptake of flavopiridol into cancer cells is most likely pharmacodynamically effective but slow. It should be kept in mind that the local concentrations at the cancer cells are unknown, and other parameters like local pH (36) may also affect the transport rate of the OATPs expressed in cancer cells. In addition, extrapolating in vitro results to the in vivo situation should be done with care as the absolute amount of OATP transporters in cancer cells may vary and as it is not known yet whether other transporters like OATP2A1 and OATP4C1 which are expressed in ZR-75-1 wild-type cells (23) are also involved in the uptake of flavopiridol. Other possible candidates may be organic anion transporters (OATs). Besides numerous clinically used drugs, OATs are also involved in the transport of polyphenol conjugates (44).

To further prove the importance of OATB1 for the uptake of flavopiridol, hormone-dependent ZR-75-1 cells that were previously shown to express high levels of OATP1B1, but not OATP1B3 and OATP2B1 (45), were incubated for 1 min with increasing concentrations of flavopiridol. Indeed, the uptake of flavopiridol by the ZR-75-1 OATP1B1-knockdown cells was significantly reduced compared to control cells, as indicated by lower Vmax values (Fig. 5 and Table I). Concomitant with the decreased uptake of flavopiridol detected in OATP1B1 knockdown cells, its cytotoxicity decreased 4.6-fold (Fig. 6). The pan-CDK inhibitor flavopiridol blocks the ATP pocket of CDKs and inhibits MCF-7 and MDA-MB-468 breast cancer cells simultaneously in the G1 and G2/M phases (46). Also wild-type ZR-75-1 breast cancer cells were inhibited in G1 and G2/M, whereas knockdown cells were arrested only in the G1 phase upon flavopiridol treatment. This indicated that G1-specific CDKs, such as CDK4/6, were inhibited at lower flavopiridol concentrations (which was the case in OATP1B1 knockdown cells) compared to CDKs that are specific for the G2/M phase or required for both G1 and G2 transit (i.e. CDK1 or CDK2, respectively). Furthermore, we also observed a significantly decreased proportion of cells in the sub-G1 phase (a marker for cell debris occurring throughout cell death) after 48 h of flavopiridol treatment in OATP1B1 knockdown cells. As apoptosis is known to be induced by flavopiridol (47) decreased apoptosis rates again support the role of OATP1B1-dependent flavopiridol uptake for cytotoxicity.

OATP1B1-, OATP1B3- and OATP2B1-mediated flavopiridol transport may be of clinical importance, as all three transporters are expressed in various tumor entities including colorectal, liver, ovarian, pancreatic and prostate cancer tissues (48). Any variations in OATP expression may significantly alter the uptake of flavopiridol into targeted cells and tissues, thereby strongly affecting the efficacy of treatment. Patients with low expression of wild-type OATP1B1, OATP1B3 and OATP2B1 or patients carrying polymorphic OATP alleles may therefore show decreased response. Concomitant administration of OATP inhibitors may also

interfere with the uptake of flavopiridol, leading to transporter-mediated drug/drug interactions. Our data demonstrated that rifampicin effectively inhibited flavopiridol uptake in CHO cells, mediated by OATP1B1, OATP1B3 and OATP2B1 (IC$_{50}$ values, 0.48-1.47 μM). Additional potential inhibitors include clarithromycin, erythromycin and roxithromycin, which inhibit the uptake of pravastatin in OATP1B1- and OATP1B3-transfected HEK293 cells (showing IC$_{50}$ values of 32-37 μM) (49). Moreover, cyclosporine A significantly decreases the OATP1B1- and OATP1B3-mediated uptake of bosentan (35) and fexofenadine (50) in HEK293 and CHO cells. In addition to clinically applied drugs, naturally occurring flavonoids also interfere with the OATP uptake of dehydroepiandrosterone (DHEAS), thus indicating that they constitute a novel class of OATP1B1 modulators (51). Whether all these potential OATP-dependent inhibitors interfere with the flavopiridol uptake in tumor cells is not yet known, however, care should be taken if patients use these drugs in combination with flavopiridol. Ongoing studies are verifying the interactions of drugs and dietary supplements with the OATP1B1-, OATP1B3- and OATP2B1-mediated uptake of flavopiridol.

In conclusion, our data revealed that OATP1B1, OATP1B3 and OATP2B1 act as transporters for flavopiridol; this role may also apply for the uptake of this compound into human cancer cells. Future *in vivo* studies should focus not only on the concentration of flavopiridol in target tissues but also on the expression levels of OATPs.

Acknowledgements

References

1. Carlson B, Lahusen T, Singh S, *et al*: Down-regulation of cyclin D1 by transcriptional repression in MCF-7 human breast carcinoma cells induced by flavopiridol. Cancer Res 59: 4634-4641, 1999.
2. Sedlacek HH, Czech J, Naik R, *et al*: Flavopiridol (L86 8275; NSC 649890), a new kinase inhibitor for tumor therapy. Int J Oncol 9: 1143-1168, 1996.
3. Czech J, Hoffmann D, Naik R and Sedlacek HH: Antitumoral activity of flavone L-86-8275. Int J Oncol 6: 31-36, 1995.
4. Lam LT, Pickeral OK, Peng AC, *et al*: Genomic-scale measurement of mRNA turnover and the mechanisms of action of the anti-cancer drug flavopiridol. Genome Biol 2: Research0041, 2001.
5. Reiner T, de las Pozas A and Perez-Stable C: Sequential combinations of flavopiridol and docetaxel inhibit prostate tumors, induce apoptosis, and decrease angiogenesis in the Ggamma/T-15 transgenic mouse model of prostate cancer. Prostate 66: 1487-1497, 2006.
6. Jung CP, Motwani MV and Schwartz GK: Flavopiridol increases sensitization to gemcitabine in human gastrointestinal cancer cell lines and correlates with down-regulation of ribonucleotide reductase M2 subunit. Clin Cancer Res 7: 2527-2536, 2001.
7. Byrd JC, Lin TS, Dalton JT, *et al*: Flavopiridol administered using a pharmacologically derived schedule is associated with marked clinical efficacy in refractory, genetically high-risk chronic lymphocytic leukemia. Blood 109: 399-404, 2007.
8. Phelps MA, Lin TS, Johnson AJ, *et al*: Clinical response and pharmacokinetics from a phase 1 study of an active dosing schedule of flavopiridol in relapsed chronic lymphocytic leukemia. Blood 113: 2637-2645, 2009.
9. Byrd JC, Peterson BL, Gabrilove J, *et al*: Treatment of relapsed chronic lymphocytic leukemia by 72-hour continuous infusion or 1-hour bolus infusion of flavopiridol: results from cancer and leukemia group B study 19805. Clin Cancer Res 11: 4176-4181, 2005.
10. Lin TS, Ruppert AS, Johnson AJ, *et al*: Phase II study of flavopiridol in relapsed chronic lymphocytic leukemia demonstrating high response rates in genetically high-risk disease. J Clin Oncol 27: 6012-6018, 2009.
11. Hagenauer B, Salamon A, Thalhammer T, *et al*: In vitro glucuronidation of the cyclin-dependent kinase inhibitor flavopiridol by rat and human liver microsomes: involvement of udpglucuronosyltransferases 1A1 and 1A9. Drug Metab Dispos 29: 407-414, 2001.
12. Mani S: UGT1A1 polymorphism predicts irinotecan toxicity: evolving proof. AAPS Pharm Sci 3: 2, 2001.
13. Nagar S and Blanchard RL: Pharmacogenetics of uridine diphosphoglucuronosyltransferase (UGT) 1A family members and its role in patient response to irinotecan. Drug Metab Rev 38: 393-409, 2006.
14. Innocenti F, Stadler WM, Iyer L, Ramirez J, Vokes EE and Ratain MJ: Flavopiridol metabolism in cancer patients is associated with the occurrence of diarrhea. Clin Cancer Res 6: 3400-3405, 2000.
15. Boerner SA, Tourne ME, Kaufmann SH and Bible KC: Effect of P-glycoprotein on flavopiridol sensitivity. Br J Cancer 84: 1391-1396, 2001.
16. Nakanishi T, Karp JE, Tan M, *et al*: Quantitative analysis of breast cancer resistance protein and cellular resistance to flavopiridol in acute leukemia patients. Clin Cancer Res 9: 3320-3328, 2003.
17. Jager W, Zembsch B, Wolschann P, *et al*: Metabolism of the anticancer drug flavopiridol, a new inhibitor of cyclin dependent kinases, in rat liver. Life Sci 62: 1861-1873, 1998.
18. Dobson PD and Kell DB: Carrier-mediated cellular uptake of pharmaceutical drugs: an exception or the rule? Nat Rev Drug Discov 7: 205-220, 2008.
19. Hagenbuch B and Gui C: Xenobiotic transporters of the human organic anion transporting polypeptides (OATP) family. Xenobiotica 38: 778-801, 2008.
20. Kim RB: Organic anion-transporting polypeptide (OATP) transporter family and drug disposition. Eur J Clin Invest 33 (Suppl 2): 1-5, 2003.
21. Tamai I, Nezu J, Uchino H, *et al*: Molecular identification and characterization of novel members of the human organic anion transporter (OATP) family. Biochem Biophys Res Commun 273: 251-260, 2000.
22. Muto M, Onogawa T, Suzuki T, *et al*: Human liver-specific organic anion transporter-2 is a potent prognostic factor for human breast carcinoma. Cancer Sci 98: 1570-1576, 2007.
23. Wlcek K, Svoboda M, Thalhammer T, Sellner F, Krupitza G and Jaeger W: Altered expression of organic anion transporter polypeptide (OATP) genes in human breast carcinoma. Cancer Biol Ther 7: 1452-1457, 2008.
24. Obaidat A, Roth M and Hagenbuch B: The expression and function of organic anion transporting polypeptides in normal tissues and in cancer. Annu Rev Pharmacol Toxicol 52: 135-151, 2012.
25. Mikkaichi T, Suzuki T, Tanemoto M, Ito S and Abe T: The organic anion transporter (OATP) family. Drug Metab Pharmacokinet 19: 171-179, 2004.
26. Abe T, Unno M, Onogawa T, *et al*: LST-2, a human liver-specific organic anion transporter, determines methotrexate sensitivity in gastrointestinal cancers. Gastroenterology 120: 1689-1699, 2001.
27. Okabe M, Unno M, Harigae H, *et al*: Characterization of the organic cation transporter SLC22A16: a doxorubicin importer. Biochem Biophys Res Commun 333: 754-762, 2005.
28. Ciarimboli G, Ludwig T, Lang D, *et al*: Cisplatin nephrotoxicity is critically mediated via the human organic cation transporter 2. Am J Pathol 167: 1477-1484, 2005.
29. Yonezawa A, Masuda S, Yokoo S, Katsura T and Inui K: Cisplatin and oxaliplatin, but not carboplatin and nedaplatin, are substrates for human organic cation transporters (SLC22A1-3 and multidrug and toxin extrusion family). J Pharmacol Exp Ther 319: 879-886, 2006.
30. Zhang S, Lovejoy KS, Shima JE, *et al*: Organic cation transporters are determinants of oxaliplatin cytotoxicity. Cancer Res 66: 8847-8857, 2006.

31. Svoboda M, Wlcek K, Taferner B, et al: Expression of organic anion-transporting polypeptides 1B1 and 1B3 in ovarian cancer cells: relevance for paclitaxel transport. Biomed Pharmacother 65: 417-426, 2011.

32. Okabe M, Szakacs G, Reimers MA, et al: Profiling SLCO and SLC22 genes in the NCI-60 cancer cell lines to identify drug uptake transporters. Mol Cancer Ther 7: 3081-3091, 2008.

33. Ni W, Ji J, Dai Z, et al: Flavopiridol pharmacogenetics: clinical and functional evidence for the role of SLCO1B1/OATP1B1 in flavopiridol disposition. PLoS One 5: e13792, 2010.

34. Gui C, Miao Y, Thompson L, et al: Effect of pregnane X receptor ligands on transport mediated by human OATP1B1 and OATP1B3. Eur J Pharmacol 584: 57-65, 2008.

35. Treiber A, Schneiter R, Hausler S and Stieger B: Bosentan is a substrate of human OATP1B1 and OATP1B3: inhibition of hepatic uptake as the common mechanism of its interactions with cyclosporin A, rifampicin, and sildenafil. Drug Metab Dispos 35: 1400-1407, 2007.

36. Leuthold S, Hagenbuch B, Mohebbi N, Wagner CA, Meier PJ and Stieger B: Mechanisms of pH-gradient driven transport mediated by organic anion polypeptide transporters. Am J Physiol Cell Physiol 296: C570-C582, 2009.

37. Murias M, Miksits M, Aust S, et al: Metabolism of resveratrol in breast cancer cell lines: impact of sulfotransferase 1A1 expression on cell growth inhibition. Cancer Lett 261: 172-182, 2008.

38. Riha J, Brenner S, Bohmdorfer M, et al: Resveratrol and its major sulfated conjugates are substrates of organic anion transporting polypeptides (OATPs): impact on growth of ZR-75-1 breast cancer cells. Mol Nutr Food Res 58: 1830-1842, 2014.

39. Palermo DP, DeGraaf ME, Marotti KR, Rehberg E and Post LE: Production of analytical quantities of recombinant proteins in Chinese hamster ovary cells using sodium butyrate to elevate gene expression. J Biotechnol 19: 35-47, 1991.

40. Unger C, Popescu R, Giessrigl B, et al: An apolar extract of Critonia morifolia inhibits c-Myc, cyclin D1, Cdc25A, Cdc25B, Cdc25C and Akt and induces apoptosis. Int J Oncol 40: 2131-2139, 2012.

41. Vavricka SR, Van Montfoort J, Ha HR, Meier PJ and Fattinger K: Interactions of rifamycin SV and rifampicin with organic anion uptake systems of human liver. Hepatology 36: 164-172, 2002.

42. Annaert P, Ye ZW, Stieger B and Augustijns P: Interaction of HIV protease inhibitors with OATP1B1, 1B3, and 2B1. Xenobiotica 40: 163-176, 2010.

43. Ji J, Mould DR, Blum KA, et al: A pharmacokinetic/pharmaco-dynamic model of tumor lysis syndrome in chronic lymphocytic leukemia patients treated with flavopiridol. Clin Cancer Res 19: 1269-1280, 2013.

44. Wong CC, Akiyama Y, Abe T, Lippiat JD, Orfila C and Williamson G: Carrier-mediated transport of quercetin conjugates: involvement of organic anion transporters and organic anion transporting polypeptides. Biochem Pharmacol 84: 564-570, 2012.

45. Wlcek K, Svoboda M, Thalhammer T, Sellner F, Krupitza G and Jaeger W: Altered expression of organic anion transporter polypeptide (OATP) genes in human breast carcinoma. Cancer Biol Ther 7: 1450-1455, 2008.

46. Carlson BA, Dubay MM, Sausville EA, Brizuela L and Worland PJ: Flavopiridol induces G1 arrest with inhibition of cyclin-dependent kinase (CDK) 2 and CDK4 in human breast carcinoma cells. Cancer Res 56: 2973-2978, 1996.

47. Baumann KH, Kim H, Rinke J, Plaum T, Wagner U and Reinartz S: Effects of alvocidib and carboplatin on ovarian cancer cells in vitro. Exp Oncol 35: 168-173, 2013.

48. Buxhofer-Ausch V, Secky L, Wlcek K, et al: Tumor-specific expression of organic anion-transporting polypeptides: transporters as novel targets for cancer therapy. J Drug Deliv 2013: 863539, 2013.

49. Seithel A, Eberl S, Singer K, et al: The influence of macrolide antibiotics on the uptake of organic anions and drugs mediated by OATP1B1 and OATP1B3. Drug Metab Dispos 35: 779-786, 2007.

50. Matsushima S, Maeda K, Ishiguro N, Igarashi T and Sugiyama Y: Investigation of the inhibitory effects of various drugs on the hepatic uptake of fexofenadine in humans. Drug Metab Dispos 36: 663-669, 2008.

51. Wang X, Wolkoff AW and Morris ME: Flavonoids as a novel class of human organic anion-transporting polypeptide OATP1B1 (OATP-C) modulators. Drug Metab Dispos 33: 1666-1672, 2005.

Effects of anthocyans on the expression of organic anion transporting polypeptides (OATPs) in primary human hepatocytes
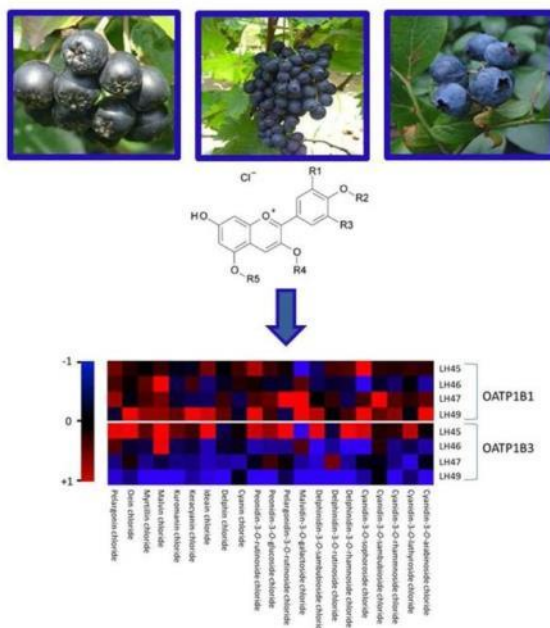
Juliane Riha, **Stefan Brenner**, Alzbeta Srovnalova, Lukas Klameth, Zdenek Dvorak, Walter Jäger and Theresa Thalhammer.

Food &
Function

Effects of anthocyans on the expression of organic anion transporting polypeptides (OATPs) in primary human hepatocytes

SCHOLARONE™
Manuscripts

254x190mm (96 x 96 DPI)

Effects of anthocyans on the expression of organic anion transporting polypeptides (OATPs) in primary human hepatocytes

Juliane Riha,[a] Stefan Brenner,[a] Alzbeta Srovnalova,[b] Lukas Klameth,[c] Zdenek Dvorak,[b] Walter Jäger[a] and Theresia Thalhammer*[d]

Affiliations:

[a] Department of Clinical Pharmacy and Diagnostics, University of Vienna, Vienna, Austria

[b] Department of Cell Biology and Genetics, Faculty of Science, Palacky University, Olomouc, Czech Republic

[c] Ludwig Boltzmann Society, Cluster for Translational Oncology, Vienna, Austria

[d] Department of Pathophysiology and Allergy Research, Center of Pathophysiology, Medical University of Vienna, Vienna, Austria,

Running Title:

Effects of anthocyans on expression of OATPs in primary human hepatocytes

Corresponding Author:

Dr. Theresia Thalhammer, Ph.D:

Department of Pathophysiology and Allergy Research, Center of Pathophysiology, Medical University of Vienna, Vienna, Austria, Tel: 0043140400/51280, Fax: 0043140400/51300, theresia.thalhammer@meduniwien.ac.at

Abstract

Anthocyans (anthocyanins and their aglycones anthocyanidins) are colorful pigments, naturally occurring in berry fruits. They exhibit many biological effects and have potent health benefits. Anthocyans are widely used as dietary supplements and the safety of products containing them is of great importance. To investigate whether anthocyans influence the expression of hepatic uptake transporters belonging to the organic anion transporting polypeptide (OATP) family, we carried out studies on primary cultures of human hepatocytes. The hepato-cellular accumulation of widely used drugs such as statins and antibiotics is mediated by the liver-specific OATP1B1 and OATP1B3 transporters, thus any interference with expression of these particular transporters might influence therapeutic outcomes. We evaluated the effects of 21 anthocyanins and their corresponding 6 anthocyanidins on the levels of OATP1B1/OATP1B3 mRNA by RT-qPCR. Changes in OATP protein levels were confirmed by western blotting. Our data show that OATP1B1 responds differently to anthocyans compared with OATP1B3. We observed the induction of OATP1B1 mRNA and protein in four hepatocyte samples by the anthocyanins malvin chloride, malvidin-3-*O*-galactoside chloride and cyanidin-3-*O*-sophoroside chloride. For OATP1B3, a reduction in the expression levels was seen with the anthocyanidin pelargonidin, and the anthocyanin delphin chloride. Although the values varied considerably between primary hepatocyte isolates from different individuals, a mean induction of OATP1B1 up to 60% and reduction of OATP1B3 gene expression by less than 25% were detected. We propose that the effects of anthocyans derived from high dose dietary supplements may have to be taken into account in patients undergoing a therapy with drugs transported by OATP1B1 and OATP1B3.

Key Words:

Anthocyans, anthocyanins, anthocyanidins, phytochemicals, OATP1B1, OATP1B3, OATP expression, human hepatocytes

Introduction

Anthocyans are a sub-group of flavonoids that exist in all tissues of higher plants as water-soluble pigments, responsible for the red, blue or purple colors of berries, grapes, apples, corn and many vegetables.[1] The broad term "anthocyan" encompasses both glycosides (termed anthocyanins) and aglycones (termed anthocyanidins). In higher plants, only anthocyanins are found, and in these, the pigment is linked to one or more sugars, often glucose, galactose, arabinose and xylose, but also to rather rare sugars including rhamnose, sophoroside or sambubioside.[2] The most common anthocyanidins are cyanidin, delphinidin, malvidin, pelargonidin, peonidin, and petunidin.[1] Many studies have demonstrated that anthocyans exhibit anti-proliferative, anti-apoptotic, anti-tumor, anti-mutagenic, anti-oxidant, anti-inflammatory and nitric oxide inhibitory effects *in vitro* that may be linked to their ability to confer important health benefits. Furthermore they are reported to reduce the incidence of diabetes, cardiovascular disease, arthritis and cancer.[1,3-6]

For the last years, public interest in the cancer chemopreventive properties of dietary constituents has increased as people have sought effective and safe diet-derived alternatives to pharmaceuticals.[7] In a study, the daily intake of anthocyanins in individuals in the U.S. has been estimated to be approximately 180-215 mg/day.[8]

Anthocyan-containing dietary supplements are available as juices, dried juice, dried fruits or water extracts, and are claimed to offer such an alternative.[9] Importantly, the dose of anthocyans in certain dietary supplements is extraordinarily high, e.g. in over-the counter drugs taken for the treatment against diarrhea (blueberry extracts, daily doses of 100-200 mg anthocyans) or against urinary tract infections (cranberry extracts, 60-225 mg per dose). However, there are no clinical studies investigating their effectiveness or potential side effects due to interactions with drug transport. For a critical review of the literature on anthocyans in dietary supplements see Espin et al., 2007.[10]

Anthocyans are metabolised in the liver,[3,11] and therefore food–drug interactions might be expected. It is of special interest to us to discover how these compounds may interact with the transport proteins that mediate the uptake of endogenous and exogenous compounds into liver cells. Two proteins, OATP1B1 and OATP1B3, members of the SLC superfamily of uptake transporters (SLC family 21) play an important role in the hepatic uptake of bilirubin, bile acids, conjugated steroids, eicosanoids and thyroid hormones, as well as xenobiotics, phytochemicals and drugs. There is considerable substrate overlap between these two OATPs, and if their substrates are co-administered, they may interfere with their transport capacity. This is especially important for drugs with a narrow

therapeutic index, such as statins, for which high concentrations in blood plasma can result in severe myopathy.[12,13] In addition to the consequences of altered substrate competition, altered levels of expression of these OATPs might also change the uptake of these therapeutics.

It has been suggested that the expression of OATP1B1 and OATP1B3 can be modified by drugs, xenobiotics and natural compounds.[14] Studies in rodents showed that activation of nuclear receptors, such as the pregnane X receptors (PXR) by natural compounds, for example the polyphenol hyperforin, and synthetic drugs such as the antibiotic rifampicin modulate the expression of OATPs.[15] However, a recent study using human hepatocytes revealed that rifampicin, although an effective stimulator of PXR, has little effect on OATP1B1 and OATP1B3 expression.[16]

To the best of our knowledge, there are no reports describing the effect of anthocyans on the expression of any OATPs in human liver cells, and so we investigated whether the levels of expression of OATP1B1 and OATP1B3 mRNA and protein are modified by common anthocyanes (21 anthocyanins and their corresponding six anthocyanidins) in human hepatocytes isolated from four healthy donors.

Materials and methods

Chemicals

Dimethyl sulfoxide (DMSO) and rifampicin (RIF) were purchased from Sigma-Aldrich (Prague, Czech Republic). The following anthocyanins and anthocyanidins were purchased from Extrasynthese (Lyon, France): peonidin-3-*O*-glucoside chloride, peonidin-3-*O*-rutinoside chloride, pelargonidin-3,5-di-*O*-glucoside chloride, pelargonidin-3-*O*-rutinoside chloride, delphinidin-3-*O*-glucoside chloride, delphinidin-3-*O*-rutinoside chloride, delphinidin-3,5-di-*O*-glucoside chloride, delphinidin-3-*O*-sambubioside chloride, delphinidin-3-*O*-rhamnoside chloride, malvidin-3-*O*-glucoside chloride, malvidin-3,5-di-*O*-glucoside chloride, malvidin-3-*O*-galactoside chloride, cyanidin-3-*O*-glucoside chloride, cyanidin-3-*O*-rutinoside chloride, cyanidin-3,5-di-*O*-glucoside chloride, cyanidin-3-*O*-sophoroside chloride, cyanidin-3-*O*-arabinoside chloride, cyanidin-3-*O*-rhamnoside chloride, cyanidin-3-*O*-galactoside chloride, cyanidin-3-*O*-sambubioside chloride, cyanidin-3-*O*-lathyroside chloride, cyanidin chloride, delphinidin chloride, malvidin chloride, peonidin chloride, petunidin chloride, and pelargonidin chloride. All other chemicals and solvents were commercially available, of analytical grade, and used without further purification.

Human hepatocytes

Human hepatocytes were isolated from human liver obtained from multiorgan donors LH45 (M, 46 years), LH46 (M, 37 years), LH47 (M, 47 years) and LH49 (M, 38 years). The tissue acquisition protocol was in accordance with the requirements stated by the local ethical commission in the Czech Republic. Long-term preserved human hepatocytes were obtained from Biopredic International (Rennes, France) as monolayer batch HEP220670 (F, 64 years).

All hepatocytes were treated in a serum-free medium for 24 h with the tested compounds and/or vehicle (DMSO; 0.1% v/v). Cultures were maintained at 37°C and 5% CO_2 in a humidified incubator.[3,17]

Quantitative reverse transcriptase polymerase chain reaction (qRT-PCR)

Total RNA was isolated using TRI Reagent® and cDNA was synthesized according to the common protocol, using M-MLV Reverse Transcriptase F-572 (Finnzymes, Thermo Scientific, Portsmouth, NH, USA) and random hexamers 3801 (Takara, Saint-Germain-en-Laye, France).[18] TaqMan® Gene Expression Assays (Applied Biosystems, Foster City, CA, USA) were purchased for OATP1B1 and OATP1B3 (containing intron-spanning primers: OATP1B1: Hs00272374_m1, OATP1B3: Hs00251986_m1). To select appropriate reference genes, the expression levels of 12 different human housekeeping mRNAs were analyzed using a geNorm reference gene selection kit with PerfectProbeTM (PrimerDesign Ltd., Southampton, UK). GAPDH (glyceraldehyde-3 phosphate dehydrogenase), YWHAZ (14-3-3 protein zeta/delta) and TOP1 (DNA topoisomerase 1) were selected as acceptable reference genes for TaqMan® q-PCR analysis of the samples as previously described.[18] Data were analyzed by the delta–delta Ct method. Results are expressed as fold-induction over DMSO-treated cells. Data were visualized as a heat map using Java TreeView.[19]

Western blotting

Total protein extracts were prepared as described elsewhere.[20] After SDS-PAGE separation and Western blot transfer, filters were probed with rabbit polyclonal antisera against OATP1B1 (rabbit polyclonal; LS-C161285; LifeSpan BioSciences, Seattle, WA, USA) or OATP1B3 (rabbit polyclonal; LS-C159033; LifeSpan BioSciences). Chemiluminescent detection was performed using a horseradish peroxidase-conjugated secondary antibody and an ECL detection kit both from Thermo Scientific (Portsmouth, NH, USA). A VersaDoc 4000MP Imaging System (Bio-Rad Laboratories

Inc., California, US) was used to capture images. As a loading control, the blots were probed to detect β-actin (data not shown).

Results

Effects of anthocyanidins on OATP expression

Initially, we elucidated the effect of the aglycones, namely the anthocyanidins cyanidin, peonidin, petunidin, pelargonidin, delphinidin, and malvidin on OATP1B1 and OATP1B3 mRNA levels in LH45, LH46, and LH47 cells. For comparison, we also used long-term preserved HEP220670 (HEP) cells derived from one donor. Cells were incubated for 24h with anthocyanidins (50 µM), and the vehicle (DMSO, 0.1% v/v), before mRNA and protein were isolated and OATP1B1 and OATP1B3 expression levels were determined.

As shown in Table 2, treatment with pelargonidin reduced OATP1B3 mRNA levels by approximately 25%. In HEP cells, no significant alterations in the mRNA expression levels were seen with any anthocyanidin.

Effects of anthocyanins on OATP expression

In the next series of experiments, the effects of 21 anthocyanins (50 µM) were tested on four different human hepatocyte cultures (LH45, LH46, LH47, LH49). The induction pattern of OATP1B1 and OATP1B3 (see heat map in Fig. 2) was highly variable between hepatocytes obtained from different donors and the effect of anthocyanins on OATP1B3 mRNA expression was more variable between the LH-cultures than it was on OATP1B1. The majority of anthocyanins increased the level of OATP1B1 mRNA in LH49 cells, whereas hardly any induction of OATP1B3 mRNA was observed in these cells.

By contrast, on using LH45 cells, OATP1B3 mRNA levels increased in response to many anthocyanins, and strong induction of OATP1B1 mRNA expression was observed after cyanidin-3-*O*-sophoroside chloride exposure, with more-moderate increases for other anthocyanins. In LH46-hepatocytes, malvin chloride caused a pronounced increase of OATP1B1 and OATP1B3 mRNA levels. In LH47 cells, increased levels of OATP1B1, but not of OATP1B3 mRNA occurred in response to cyanidin-3-*O*-sambubioside chloride, malvidin-3-*O*-galactoside chloride and pelargonidin-3-*O*-rutinoside chloride.

The mean values and minimum and maximum values for OATP1B1 and OATP1B3 mRNA levels in the LH cells are summarized in Table 3. The data indicate that the effects of anthocyanins on OATP

mRNA expression are rather moderate, revealing a maximal induction of 1.6-fold (mean values) of OATP1B1 mRNA with malvidin-3-*O*-galactoside chloride. A small, but significant increase in the mean levels of OATP1B1 mRNA was also produced by two other anthocyanins: malvin chloride (1.51-fold) and cyanidin-3-*O*-sophoroside chloride (1.38-fold). Protein levels corresponded with the mRNA response pattern in hepatocyte samples. Higher levels of immunoreactive OATP1B1 after malvidin chloride and malvidin-3-*O*-galactoside chloride treatment reflected the higher mRNA levels. Incubation with pelargonin chloride and pelargonidin-3-*O*-rutinoside chloride, which had no effect on OATP1B1 mRNA, also did not alter OATP1B1 protein levels (Fig. 3).

In contrast to OATP1B1, mean OATP1B3 mRNA expression in LH45, LH46, LH47 and LH49 cells was not significantly increased by anthocyanins (Table 3). Notably, OATP1B3 mRNA expression was reduced by nearly 20% (mean value 0.817-fold) after delphin chloride incubation. Again, OATP1B3 protein levels corresponded with the mRNA levels.

In control experiments in the hepatocytes, we also noticed that rifampicin does not induce the expression of either OATP1B1 or OATP1B3 (n-fold induction 0.74-0.99). This is not surprising, as in a previous study, rifampicin derivatives, known to be common inducers of some drug metabolising P450 enzymes (CYPs) and transporters [15,16,21], did also not show any specific upregulation of OATP mRNA.[16]

Discussion

Our investigation into the effects of 27 anthocyans on OATP1B1 and OATP1B3 expression in primary human hepatocytes revealed that these phytochemicals can indeed influence the expression of these liver-specific transporters. Interestingly, we observed induction of OATP1B1 expression, but reduction of OATP1B3 expression with some anthocyans.

In all hepatocyte cell samples tested, increases of OATP1B1 mRNA and protein levels of at least 10% occurred in response to the anthocyanins malvin chloride, malvidin-3-*O*-galactoside chloride, and cyanidin-3-*O*-sophoroside chloride. For OATP1B3 a reduction in the expression levels was seen with one anthocyanidin, pelargonidin, and one anthocyanin, delphin chloride (Table 2 and 3). Only the glycosides but not the corresponding aglycones were able to affect increases in expression, indicating that the molecule together with the sugar moiety is necessary for the stimulation. The transporters OATP1B1 and OATP1B3 mediate the intracellular accumulation of widely used drugs such as statins and chemotherapeutic agents, so our findings are important because altered expression of OATP1B1 and OATP1B3 by these dietary constituents might change the efficacy of a drug

therapy. However, it must be considered that the OATP expression pattern varies considerably between hepatocytes from individual donors[22] and those variations may have a more severe impact on the OATP-mediated cellular accumulation of drugs in patients. It is also important that in the liver, OATP1B1 is expressed in all hepatocytes throughout the lobules, whereas OATP1B3 expression is highest in hepatocytes located around the central vein.[23] This implicates that their expression in liver is regulated differently, which could also account for the different reaction of OATP1B1 and OATP1B3 to anthocyans.

In general, our data concur with previous studies on the effect of anthocyans on biotransformation pathways that showed only small effects of anthocyans on selected enzymes. Kamenickova et al. recently reported the effects of cyanidin, delphinidin, malvidin, peonidin, petunidin, pelargonidin and their most common anthocyanins on the aryl hydrocarbon receptor (AhR)–cytochrome P450 CYP1A1 pathway.[3,17] They showed, using human hepatocytes and HepG2 cells, that pelargonidin is a weak ligand/agonist of the AhR and of AhR-dependent gene expression. Pelargonidin moderately induced CYP1A1 mRNA expression in all of their primary hepatocyte cultures. Among the anthocyanins, pelargonidin-3-O-rutinoside chloride and cyanin chloride were weak inducers of CYP1A1 mRNA expression.[3,17] Studies of the effect of anthocyans on expression of CYP2C9, CYP2A6, CYP2B6, and CYP3A4 in human hepatocytes and liver microsomes did not reveal significant alterations of mRNA or protein levels.[1]

In summary, our data demonstrate that some anthocyans are capable of altering the expression of OATP1B1 and OATP1B3 in cultured primary human hepatocytes. However, the effects varied considerably among individual cell isolates. Therefore, we conclude that, within the range of commonly ingested nutritional supplements, possible effects on OATP1B1 and OATP1B3 expression may not present major problems. However, in patients under therapy with OATP substrates (e.g. statins) consequences of interaction between these OATP transporters and anthocyans taken at high doses in dietary supplements cannot be excluded.

Conflict of interest

The authors declare that they have no conflict of interest.

Acknowledgements

Table 1 Chemical structures of anthocyans
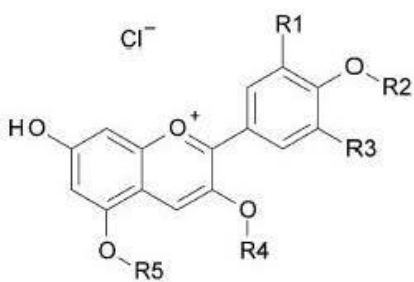
Anthocyanins	R1	R2	R3	R4	R5
Cyanidin-3-*O*-arabinoside chloride	OH	H	H	Arabinoside	H
Cyanidin-3-*O*-lathyroside chloride	OH	H	H	Lathyroside	H
Cyanidin-3-*O*-rhammmoside chloride	OH	H	H	Rhammmoside	H
Cyanidin-3-*O*-sambubioside chloride	OH	H	H	Sambubioside	H
Cyanidin-3-*O*-sophoroside chloride	OH	H	H	Sophoroside	H
Delphinidin-3-*O*-rhamnoside chloride	OH	H	OH	Rhammmoside	H
Delphinidin-3-*O*-rutinoside chloride	OH	H	OH	Rutinoside	H
Delphinidin-3-*O*-sambubioside chloride	OH	H	OH	Sambubioside	H
Malvidin-3-*O*-galactoside chloride	OCH_3	H	OCH_3	Galactoside	H
Pelargonidin-3-*O*-rutinoside chloride	H	H	OH	Rutinoside	H
Peonidin-3-*O*-glucoside chloride	OCH_3	H	H	Glucoside	H
Peonidin-3-*O*-rutinoside chloride	OCH_3	H	H	Rutinoside	H
Cyanin chloride (Cyanidin-3,5-di-*O*-glucoside chloride)	OH	H	H	Glucoside	Glucose
Delphin chloride (Delphinidin-3,5-di-*O*-glucoside chloride)	OH	H	OH	Glucoside	Glucose
Ideain chloride (Cyanidin-3-*O*-galactoside chloride)	OH	H	H	Galactoside	H
Keracyanin chloride (Cyanidin-3-*O*-rutinoside chloride)	OH	H	H	Rutinoside	H
Kuromanin chloride (Cyanidin 3-*O*-glucoside chloride)	OH	H	H	Glucoside	H
Malvin chloride (Malvidin-3,5-di-*O*-glucoside chloride)	OCH_3	H	OCH_3	Glucoside	Glucose
Myrtillin chloride (Delphinidin-3-*O*-glucoside chloride)	OH	H	OH	Glucoside	H
Oenin chloride (Malvidin-3-*O*-glucoside chloride)	OCH_3	H	OCH_3	Glucoside	H
Pelargonin chloride (Pelargonidin-3,5-di-*O*-glucoside chloride)	H	H	H	Glucoside	Glucose
Anthocyanidins					
Cyanidin chloride	OH	H	H	H	H
Delphinidin chloride	OH	H	OH	H	H
Malvidin chloride	OCH_3	H	OCH_3	H	H
Pelargonidin hloride	H	H	H	H	H
Peonidin chloride	OCH_3	H	H	H	H
Petunidin chloride	OCH_3	H	OH	H	H

Table 2 Effects of anthocyanidins on OATP1B1 and OATP1B3 mRNA levels in primary human hepatocytes treated for 24 h with tested compounds. Results are expressed as n-fold change compared to DMSO-treated cells (control). Data, normalized to the reference genes, are expressed as mean ± SD (n=3) for HEP220670 and for LH45, LH46, LH47 as means (min-max values), calculated from two separate determinations. Values in bold are significantly different (p<0.05) as assessed with the Mann-Whitney U test.

	Changes in mRNA expression				
Anthocyanidins	**LH45, LH46 and LH47**			**HEP220670**	
	OATP1B1		OATP1B3		OATP1B1	OATP1B3
Control	1.151	(0.77-1.62)	1.006	(1.00-1.01)	1.016±0.43	1.015±0.01
Cyanidin	1.027	(0.90-1.29)	0.912	(0.71-1.28)	0.782±0.15	0.929±0.38
Delphinidin	0.916	(0.54-1.39)	1.145	(0.76-1.55)	0.813±0.24	0.794±0.68
Malvidin	0.991	(0.66-1.36)	1.029	(0.72-1.63)	0.942±0.22	0.956±0.32
Pelargonidin	0.962	(0.66-1.26)	**0.756**	**(0.62-0.89)**	1.025±0.35	0.797±0.52
Peonidin	0.865	(0.70-0.98)	1.037	(0.70-1.45)	1.130±0.43	1.290±0.40
Petunidin	0.947	(0.67-1.10)	1.189	(0.70-1.97)	1.114±0.43	1.148±0.19

Table 3

Effects of anthocyanins on the levels of OATP1B1 and OATP1B3 mRNA in primary human hepatocytes LH45, LH46, LH47 and LH49 treated for 24 h with the indicated compounds. Results are expressed as n-fold changes compared to vehicle-controls. Data are mean ± SD from triplicate measurements.

Values in bold are significantly different ($p < 0.05$), determined by Mann-Whitney U test.

| Anthocyanins	Changes in mRNA expression			
	OATP1B1		OATP1B3	
Control	1.006	(1.00-1.02)	1.005	(1.00-1.01)
Cyanidin-3-*O*-arabinoside chloride	1.219	(0.66-1.92)	0.882	(0.66-1.02)
Cyanidin-3-*O*-lathyroside chloride	1.041	(0.97-1.12)	0.890	(0.55-1.40)
Cyanidin-3-*O*-rhammnoside chloride	1.078	(0.77-1.28)	0.860	(0.73-1.09)
Cyanidin-3-*O*-sambubioside chloride	1.193	(0.91-1.56)	1.026	(0.97-1.08)
Cyanidin-3-*O*-sophoroside chloride	**1.505**	**(1.14-1.72)**	1.027	(0.66-1.45)
Delphinidin-3-*O*-rhamnoside chloride	1.007	(0.83-1.18)	1.239	(0.70-1.78)
Delphinidin-3-*O*-rutinoside chloride	1.039	(0.91-1.15)	0.933	(0.69-1.24)
Delphinidin-3-*O*-sambubioside chloride	1.005	(0.81-1.38)	1.038	(0.59-1.49)
Malvidin-3-*O*-galactoside chloride	**1.606**	**(1.19-2.01)**	0.781	(0.47-1.17)
Pelargonidin-3-*O*-rutinoside chloride	1.104	(0.83-1.62)	1.107	(0.70-1.87)
Peonidin-3-*O*-glucoside chloride	1.097	(0.91-1.20)	1.051	(0.69-1.32)
Peonidin-3-*O*-rutinoside chloride	1.343	(1.04-1.82)	1.006	(0.64-1.43)
Cyanin chloride	0.993	(0.84-1.15)	0.897	(0.65-1.03)
Delphin chloride	1.066	(0.92-1.20)	**0.817**	**(0.69-0.90)**
Ideain chloride	1.065	(0.75-1.44)	0.834	(0.63-1.55)
Keracyanin chloride	1.175	(0.83-1.78)	0.864	(0.68-1.14)
Kuromanin chloride	0.981	(0.85-1.21)	0.932	(0.75-1.22)
Malvin chloride	**1.380**	**(1.13-1.86)**	1.564	(0.87-2.32)
Myrtillin chloride	1.163	(1.03-1.30)	0.926	(0.73-1.20)
Oein chloride	1.242	(0.98-1.88)	1.165	(0.73-1.97)
Pelargonin chloride	1.149	(0.91-1.30)	0.988	(0.55-1.48)

12.10.2014

References

1.   A. Srovnalova, M. Svecarova, M. Kopecna Zapletalova, P. Anzenbacher, P. Bachleda, E. Anzenbacherova and Z. Dvorak, Effects of Anthocyanidins and Anthocyanins on the Expression and Catalytic Activities of CYP2A6, CYP2B6, CYP2C9, and CYP3A4 in Primary Human Hepatocytes and Human Liver Microsomes, *J Agric Food Chem*, 2014.

2.   C. R. Welch, Q. Wu and J. E. Simon, Recent Advances in Anthocyanin Analysis and Characterization, *Curr. Anal. Chem.*, 2008, **4**, 75-101.

3.   A. Kamenickova, E. Anzenbacherova, P. Pavek, A. A. Soshilov, M. S. Denison, M. Zapletalova, P. Anzenbacher and Z. Dvorak, Effects of anthocyanins on the AhR-CYP1A1 signaling pathway in human hepatocytes and human cancer cell lines, *Toxicol. Lett.*, 2013, **221**, 1-8.

4.   R. L. Prior and X. Wu, Anthocyanins: structural characteristics that result in unique metabolic patterns and biological activities, *Free Radic. Res.*, 2006, **40**, 1014-1028.

5.   Y. Zhang, S. K. Vareed and M. G. Nair, Human tumor cell growth inhibition by nontoxic anthocyanidins, the pigments in fruits and vegetables, *Life Sci.*, 2005, **76**, 1465-1472.

6.   L. Kaume, L. R. Howard and L. Devareddy, The blackberry fruit: a review on its composition and chemistry, metabolism and bioavailability, and health benefits, *J. Agric. Food Chem.*, 2012, **60**, 5716-5727.

7.   S. Thomasset, N. Teller, H. Cai, D. Marko, D. P. Berry, W. P. Steward and A. J. Gescher, Do anthocyanins and anthocyanidins, cancer chemopreventive pigments in the diet, merit development as potential drugs?, *Cancer Chemother. Pharmacol.*, 2009, **64**, 201-211.

8.   S. Zafra-Stone, T. Yasmin, M. Bagchi, A. Chatterjee, J. A. Vinson and D. Bagchi, Berry anthocyanins as novel antioxidants in human health and disease prevention, *Mol. Nutr. Food Res.*, 2007, **51**, 675-683.

9.   L. S. Wang and G. D. Stoner, Anthocyanins and their role in cancer prevention, *Cancer Lett*, 2008, **269**, 281-290.

10.   J. C. Espin, M. T. Garcia-Conesa and F. A. Tomas-Barberan, Nutraceuticals: facts and fiction, *Phytochemistry*, 2007, **68**, 2986-3008.

11.   T. K. McGhie and M. C. Walton, The bioavailability and absorption of anthocyanins: towards a better understanding, *Mol. Nutr. Food Res.*, 2007, **51**, 702-713.

12.   B. Hagenbuch and C. Gui, Xenobiotic transporters of the human organic anion transporting polypeptides (OATP) family, *Xenobiotica*, 2008, **38**, 778-801.

13.   C. Gui, A. Obaidat, R. Chaguturu and B. Hagenbuch, Development of a cell-based high-throughput assay to screen for inhibitors of organic anion transporting polypeptides 1B1 and 1B3, *Curr. Chem. Genomics.*, 2010, **4**, 1-8.

14.   M. Svoboda, J. Riha, K. Wlcek, W. Jaeger and T. Thalhammer, Organic anion transporting polypeptides (OATPs): regulation of expression and function, *Curr. Drug Metab.*, 2011, **12**, 139-153.

15.   L. M. Aleksunes and C. D. Klaassen, Coordinated regulation of hepatic phase I and II drug-metabolizing genes and transporters using AhR-, CAR-, PXR-, PPARalpha-, and Nrf2-null mice, *Drug Metab. Dispos.*, 2012, **40**, 1366-1379.

16.   B. Williamson, K. E. Dooley, Y. Zhang, D. J. Back and A. Owen, Induction of influx and efflux transporters and cytochrome P450 3A4 in primary human hepatocytes by rifampin, rifabutin, and rifapentine, *Antimicrob. Agents Chemother.*, 2013, **57**, 6366-6369.

13

12.10.2014

17. A. Kamenickova, E. Anzenbacherova, P. Pavek, A. A. Soshilov, M. S. Denison, P. Anzenbacher and Z. Dvorak, Pelargonidin activates the AhR and induces CYP1A1 in primary human hepatocytes and human cancer cell lines HepG2 and LS174T, *Toxicol. Lett.*, 2013, **218**, 253-259.

18. K. Wlcek, M. Svoboda, T. Thalhammer, F. Sellner, G. Krupitza and W. Jaeger, Altered expression of organic anion transporter polypeptide (OATP) genes in human breast carcinoma, *Cancer Biol Ther*, 2008, **7**, 1450-1455.

19. A. J. Saldanha, Java Treeview--extensible visualization of microarray data, *Bioinformatics*, 2004, **20**, 3246-3248.

20. P. Pavek, L. Cerveny, L. Svecova, M. Brysch, A. Libra, R. Vrzal, P. Nachtigal, F. Staud, J. Ulrichova, Z. Fendrich and Z. Dvorak, Examination of Glucocorticoid receptor alpha-mediated transcriptional regulation of P-glycoprotein, CYP3A4, and CYP2C9 genes in placental trophoblast cell lines, *Placenta*, 2007, **28**, 1004-1011.

21. W. J. Burman, K. Gallicano and C. Peloquin, Comparative pharmacokinetics and pharmacodynamics of the rifamycin antibacterials, *Clin. Pharmacokinet.*, 2001, **40**, 327-341.

22. K. Wlcek, M. Svoboda, J. Riha, S. Zakaria, U. Olszewski, Z. Dvorak, F. Sellner, I. Ellinger, W. Jager and T. Thalhammer, The analysis of organic anion transporting polypeptide (OATP) mRNA and protein patterns in primary and metastatic liver cancer, *Cancer Biol. Ther.*, 2011, **11**, 801-811.

23. T. Abe, M. Unno, T. Onogawa, T. Tokui, T. N. Kondo, R. Nakagomi, H. Adachi, K. Fujiwara, M. Okabe, T. Suzuki, K. Nunoki, E. Sato, M. Kakyo, T. Nishio, J. Sugita, N. Asano, M. Tanemoto, M. Seki, F. Date, K. Ono, Y. Kondo, K. Shiiba, M. Suzuki, H. Ohtani, T. Shimosegawa, K. Iinuma, H. Nagura, S. Ito and S. Matsuno, LST-2, a human liver-specific organic anion transporter, determines methotrexate sensitivity in gastrointestinal cancers, *Gastroenterology*, 2001, **120**, 1689-1699.
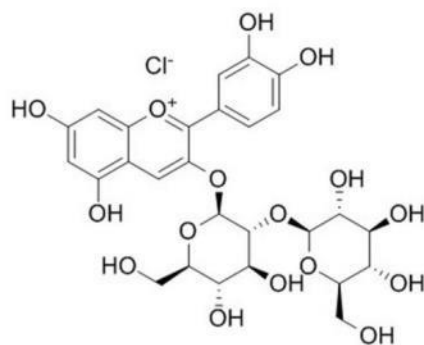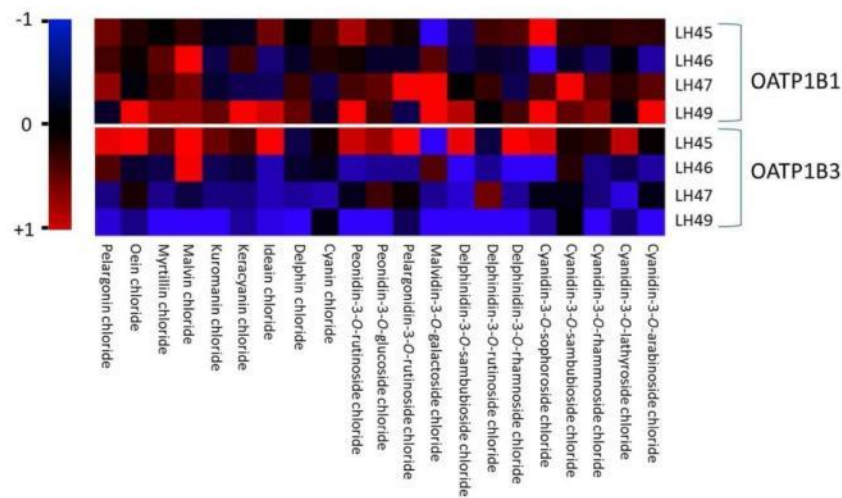
14
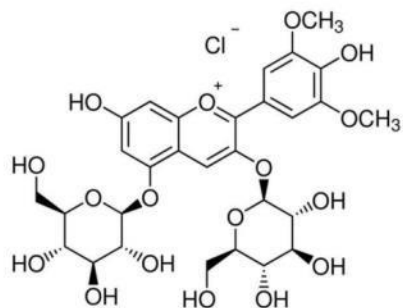
Malvin chloride

Malvidin-3-*O*-galactoside chloride
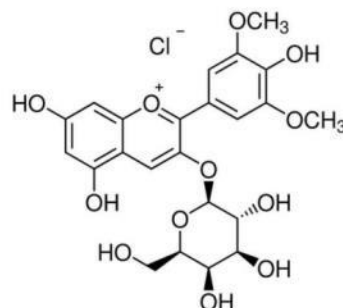
Cyanidin-3-*O*-sophoroside chloride

Chemical structures of the anthocyanins malvin chloride, malvidin-3-O-galactoside chloride and cyanidin-3-O-sophoroside chloride.
339x331mm (150 x 150 DPI)

Heat map showing mRNA expression levels for OATP1B1 and OATP1B3 in LH45, LH46, LH47 and LH49 human hepatocyte cultures. The image map (Java TreeView 19) shows the pattern of OATP gene expression as determined by TaqMan RT-PCR. Data shows upregulation (red) or downregulation (blue) of OATP mRNA after incubation with anthocyanins, compared to the median expression level (black) of DMSO-treated hepatocyte cultures.
227x136mm (150 x 150 DPI)
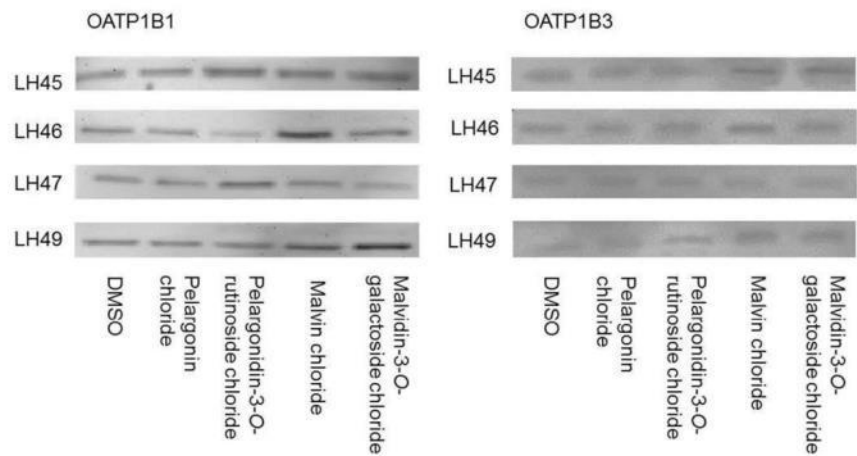
Effects of selected anthocyanins on the expression of OATP1B1 and OATP1B3 proteins in human hepatocytes. Primary human hepatocyte cultures (LH45, LH46, LH47, LH49) were incubated for 24 h with pelargonin chloride (50 µM), pelargonidin-3-O-rutinoside chloride (50 µM), malvidin chloride (50 µM), malvidin-3-O-galactoside chloride (50 µM) and DMSO (0.1% v/v) as a vehicle control. Western blots show analyses of OATP1B1 and OATP1B3 proteins in pooled samples LH45-49.
179x99mm (150 x 150 DPI)

105

Lobatin B inhibits NPM/ALK and NF-κB attenuating anaplastic-large-cell-lymphomagenesis and lymphendothelial tumour intravasation

Kiss Izabella, Unger Christine,Nguyen Huu Chi, Atanasov Atanas Georgiev, Kramer Nina, Chatuphonprasert Waranya, **Brenner Stefan**, McKinnon Ruxandra, Peschel Andrea, Vasas Andrea, Lajter Ildikó, Kain Renate, Saiko Philipp, Szekeres Thomas, Kenner Lukas, Hassler Melanie R., Diaz Rene, Frisch Richard, Dirsch Verena M., Jäger Walter, de Martin Rainer, Bochkov Valery N., Passreiter Claus M., Peter-Vörösmarty Barbara, Mader Robert M., Grusch Michael, Dolznig Helmut, Kopp Brigitte, Zupko Istvan, Hohmann Judit, Krupitza Georg;;

Lobatin B inhibits NPM/ALK and NF-κB attenuating anaplastic-large-cell-lymphomagenesis and lymphendothelial tumour intravasation

Kiss Izabella[1, 2*], Unger Christine[1*], Nguyen Huu Chi[2], Atanasov Atanas Georgiev[3], Kramer Nina[1], Chatuphonprasert Waranya[4,5], Brenner Stefan[4], McKinnon Ruxandra[3], Peschel Andrea[2], Vasas Andrea[6], Lajter Ildikó[6], Kain Renate[2], Saiko Philipp[7], Szekeres Thomas[7], Kenner Lukas[2, 8, 9], Hassler Melanie R.[2], Diaz Rene[10], Frisch Richard[10], Dirsch Verena M.[3], Jäger Walter[4], de Martin Rainer[11], Bochkov Valery N.[12], Passreiter Claus M.[13], Peter-Vörösmarty Barbara[14], Mader Robert M.[15], Grusch Michael[14], Dolznig Helmut[1], Kopp Brigitte[3], Zupko Istvan[16], Hohmann Judit[6], Krupitza Georg[2]

[1]Institute of Medical Genetics, Medical University of Vienna, Waehringer Strasse 10, A-1090 Vienna, Austria,
[2]Clinical Institute of Pathology, Medical University of Vienna, Waehringer Guertel 18-20, Austria,
[3]Department of Pharmacognosy, University of Vienna, Althanstrasse 14, A-1090 Austria,
[4]Department of Clinical Pharmacy and Diagnostics, University of Vienna, Althanstrasse 14, A-1090 Vienna, Austria,
[5]Department of Preclinic, Faculty of Medicine, Mahasarakham University, Mahasarakham, 44000 Thailand,
[6]Department of Pharmacognosy, University of Szeged, Eotvos Str. 6, H-6720 Szeged, Hungary,
[7]Department of Medical and Chemical Laboratory Diagnostics, Medical University of Vienna, Waehringer Guertel 18-20, Austria,
[8]Ludwig Boltzmann Institute for Cancer Research, LBI-CR, Waehringerstrasse 13a, 1090 Vienna, Austria,
[9]Unit of Pathology of Laboratory Animals, University of Veterinary Medicine Vienna, 1210 Vienna, Austria,
[10]Institute for Ethnobiology, Playa Diana, San José/Petén, Guatemala,
[11]Department of Vascular Biology and Thrombosis Research, Center of Biomolecular Medicine and Pharmacology, Medical University of Vienna, Schwarzspanierstraße 17, A-1090 Vienna, Austria,
[12]Institute of Pharmaceutical Sciences, University of Graz, Schubertstraße 1, A-8010 Graz, Austria,
[13]Institute of Pharmaceutical Biology and Biotechnology, Heinrich-Heine-University Düsseldorf, Universitätsstrasse 1, D-40225 Düsseldorf, Germany,
[14]Department of Medicine I, Division: Institute of Cancer Research, Comprehensive Cancer Center, Medical University Vienna, Borschkegasse 8a, A-1090 Vienna, Austria,
[15]Department of Medicine I, Comprehensive Cancer Center, Medical University Vienna, Waehringer Guertel 18-20, A-1090 Vienna, Austria,
[16]Department of Pharmacodynamics and Biopharmacy, University of Szeged, H-6720 Szeged, Hungary.

* equal contribution

Short title: Lobatin B inhibits NPM/ALK and tumour cell intravasation in vitro

Correspondence: Georg Krupitza, Institute of Clinical Pathology, Medical University of Vienna, Waehringer Guertel 18-20, A-1090, Vienna, Austria,
e-mail: georg.krupitza@meduniwien.ac.at

1

Abstract

An apolar extract of the traditional medicinal plant *Neurolaena lobata* inhibited the expression of the NPM/ALK chimera, which is causal for the majority of anaplastic large cell lymphomas (ALCLs). Therefore, an active principle of the extract, the furanoheliangolide sesquiterpene lactone lobatin B, was isolated and tested regarding the inhibition of ALCL expansion and tumour cell intravasation through the lymphendothelium.

ALCL cell lines, HL-60 cells and PBMCs were treated with plant compounds and the ALK inhibitor TAE-684 to measure mitochondrial activity, proliferation and cell cycle progression and to correlate the results with protein- and mRNA- expression of selected gene products. Several endpoints indicative for cell death were analysed after lobatin B treatment. Tumour cell intravasation through lymphendothelial monolayers was measured and potential causal mechanisms were investigated analysing NF-κB- and cytochrome P450 activity, and 12(S)-HETE production.

Lobatin B inhibited the expression of NPM/ALK, JunB and PDGF-Rβ, and attenuated proliferation of ALCL cells by arresting them in G2/M. Mitochondrial activity remained largely unaffected upon lobatin B treatment. Nevertheless, caspase 3 became activated in ALCL cells. Also HL-60 cell proliferation was attenuated whereas PBMCs of healthy donor were not affected by lobatin B. Additionally, tumour cell intravasation, which partly depends on NF-κB, was significantly suppressed by lobatin B most likely due to its NF-κB-inhibitory property.

Lobatin B, which was isolated from a plant used in ethnomedicine, targets malignant cells by at least two properties:

I)   inhibition of NPM/ALK, thereby providing high specificity in combating this most prevalent fusion protein occurring in ALCL;

II)   inhibition of NF-κB, thereby not affecting normal cells with low constitutive NF-κB activity. This property also inhibits tumour cell intravasation into the lymphatic system and may provide an option to manage this early step of metastatic progression.

Key words: Lobatin, NPM/ALK, ALCL, lymphendothelial intravasation, 3D-compound testing

List of abbreviations used

ALCL   anaplastic large cell lymphoma

ALOX   lipoxygenase A

CCID   circular chemorepellent induced defect

CYP   cytochrome P450

DCM   dichloromethane extract

EROD   ethoxyresorufin-O-deethylase

HO/PI   Hoechst 33258/propidium iodide

LEC   lymph endothelial cell

MYPT1   myosin phosphatase 1 target subunit 1

NF-κB   nuclear factor kappa B

NPM/ALK   nucleophosmin/anaplastic lymphoma kinase; the t(2;5)(p23;q35) chromosomal translocation

PARP   poly ADP-ribose polymerase

PBMC   peripheral blood mononuclear cell

PDGF-Rβ   platelet derived growth factor receptor

p21   tumour suppressor protein 21

3D   3-dimensional

12(S)-HETE   12(S) hydroxyeicosatetraenoic acid

Introduction

About 60% of currently used pharmaceutical drugs are mostly derived from natural products. Plant metabolites comprise a continuing source of new structural leads for drug discovery and development, because of the vast chemical diversity and ability to interact with multiple cellular target proteins, but only a small proportion of them have been investigated regarding their therapeutic value [1]. Also plants used in ethnomedicine are not extensively studied. Therefore, traditional medicinal plants may lead to new therapeutic compounds against a variety of hard-to-cure diseases, due to their evident benefit and safe use throughout centuries of empirical testing. Due to these reasons we recently investigated the dichloromethane (DCM) extract of *Neurolaena lobata* (L.) R.Br. ex Cass. (Asteraceae) and reported on its particular property to down-regulate the lymphoma-causing t(2;5)(p23;q35) translocation NPM/ALK [2] that gives rise to ALK-positive anaplastic large cell lymphoma (ALK+ALCL) [3]. Of particular relevance to the continuation of this study was the demonstration that the EtOH leaf extract and the dichloromethane (DCM) fraction of the methanolic leaf extract showed activity in the carrageenan-induced mouse- and rat paw oedema models (respectively) [4, 5] manifesting that the extracts still possessed active principles that were effective in intact organisms [6]. Among three furanoheliangolide sesquiterpene lactones [7] lobatin B was isolated from the DCM fraction and its activity was characterised in NPM/ALK positive ALCL lines. Lobatin B has been isolated and tested before in human cancer cell lines exhibiting strong anti-neoplastic activity [8, 9] and here we report that lobatin B inhibits NPM/ALK expression in ALCL cells. The inhibition of NPM/ALK signalling via the recently demonstrated pathway is a successful clinical approach in the treatment of NPM/ALK positive ALCL [10]. Given the youth of the vast majority of ALCL patients a careful selection of drugs is warranted to avoid the development of secondary malignancies decades after the initial treatment with genotoxic drugs, but currently the choice of ALK-specific therapies is extremely limited [11]. Therefore, we tried to elucidate the NPM/ALK-targeting properties of lobatin B. In addition, lobatin B was studied in a validated model resembling the intravasation of tumour emboli through the lymphatic vasculature, which is an early step of the metastatic process [12]. As there are currently no therapies available that prevent lymph node metastasis the inhibition of this process by lobatin B may serve as lead to develop anti-intravasative treatment concepts.

4

Methods

Plant material fine chemicals and antibodies

Extraction, isolation and quantification of *N. lobata* furanoheliangolide sesquiterpene lactones
were described by McKinnon et al. [5]. *N. lobata* compounds were dissolved and prepared in
DMSO (Sigma-Aldrich, St. Louis, MO, USA) as concentrated stock solutions. ALK-inhibitor
NVP-TAE-684 (TAE-684) was from Selleckchem (Houston, TX, USA).

CD246 anti-ALK protein mouse monoclonal antibody (mAB) and anti-nucleophosmin mouse
mAB, were purchased from Dako Cytomation (Glostrup, Denmark), PDGF-Rβ rabbit mAB
and caspase 3 polyclonal antibody (pAB) were purchased from Cell Signaling (Cambridge,
UK). PARP-1 mouse mAB, JunB rabbit pAB, JunD rabbit pAB, c-Jun rabbit pAB, and p21
rabbit pAB were purchased from Santa Cruz Biotechnology Inc. (Santa Cruz, CA, USA).
Anti-ß-actin (ascites fluid) mouse mAB was ordered from Sigma (St. Louis, MO, USA).

Cell culture

SR-786 NPM/ALK positive human ALCL (anaplastic large cell lymphoma) cells were from
DSMZ (Braunschweig, Germany), CD-417 NPM/ALK positive mouse ALCL cells were
isolated from CD4-NPM/ALK mice, HL60 (human promyelocytic leukemia cells) were
obtained from ATCC (Manassas, VA, USA). All cells were grown in RPMI 1640 medium
(Life Technologies, Carlsbad, California, USA) supplemented with 10% heat inactivated fetal
calf serum (FCS, Life Technologies, Carlsbad, California, USA), 1% L-glutamine (Lonza,
Verviers, Belgium) and 1% antibiotics (penicillin/streptomycin (PS), Sigma-Aldrich, St.
Louis, MO, USA) and maintained in a humidified atmosphere containing 5% CO_2 at 37°C.

Isolation of peripheral blood mononuclear cells (PBMCs)

With the informed consent of the donors, PBMCs were isolated from human peripheral blood
as described earlier [13].

Proliferation assay

The proliferation of SR-786, CD-417, PBMC and HL60 was determined by counting cells
with a Casy cell counter (Roche Innovatis AG, Bielefeld, Germany) as described before [2].

5

111

Western blotting

SR-786 cells were seeded at a concentration of 2 x 10^5 cells/ml and CD-417 at a concentration of 10^6 cells/ml in 6 cm dishes. After treating cells with 3 µM of *N. lobata* compounds for the indicated times, they were harvested and lysed in RIPA buffer (150 mM NaCl, 50 mM Tris pH 7.6, 1% Triton, 0.1% SDS, 0.5% Sodium deoxycholate) containing 1 mM phenylmethylsulfonyl (PSMF, Sigma-Aldrich, St. Louis, MO, USA) and 1 mM protease inhibitor mixture (PIM consists of 2 µg/ml leupeptin, 2 µg/ml aprotinin, 0.3 µg/ml benzamidine chloride and 10 µg/ml trypsin inhibitor, Sigma-Aldrich, St. Louis, MO, USA) followed by a short incubation of 5 min on ice. Lysates were treated, stored, electrophoretically separated and analysed by Western blotting as described by Unger et al. [2]. Chemiluminescence was developed by ECL detection kit (Thermo Scientific, Waltham, MA, USA) and membranes were exposed to Amersham Hyperfilms (GE Healthcare, Buckinghamshire, UK) or CL-XPosure films (Thermo Scientific, Rockford, IL, USA). Membranes were stripped in 75 ml buffer containing 4.5 ml 1M Tris-HCL pH 6.4, 7.5 ml 20% SDS, 0.5 ml β-mercaptoethanol, for 6-15 min shaking in a 55°C water bath and afterwards the membranes were washed.

Quantitative RT-PCR

SR-786 cells were seeded in a 24-well plate at a concentration of 2 x 10^5 cells/ml and incubated overnight before treatment with 3 µM of *N. lobata* compounds. For RNA preparation ReliaPrep RNA Cell Miniprep System Kit (Promega, Madison, WI) was used and RNA content was measured using a NanoDrop Fluorospectrometer (Thermo Fisher Scientific, Waltham, MA, USA). First-strand cDNA (150 ng RNA as template) was synthesised using GoScriptTM Reverse Transcription System Kit (Promega, Madison, WI).
Transcript expression was examined by real-time PCR (polymerase chain reaction) using a SYBR Green detection system (Promega, Madison, WI). For each sample, 10 µl GoTaq qPCR Master Mix (premixed solution containing GoTaq DNA polymerase, GoTaq Reaction Buffer, dNTPs and Mg^{2+}; Promega, Madison, WI) 2 µl forward primer and 2 µl reverse primer (see sequences below), 5 µl nuclease free water and 1 µl cDNA, were added to the wells of a 96-well optical reaction plate. The cycle program was: 50°C for 2 min, 95°C for 10 min to activate polymerase, 40 cycles of 95°C for 15 sec and 60°C for 1 min. (Thermocycler Primus25 advanced, Peqlab, Erlangen, Germany). The following primers were used for RT-PCR:

6

NPM/ALK (fwd: 5′-GTG GTC TTA AGG TTG AAG TGT GGT T-3′; rev: 5′-GCT TCC GGC GGT ACA CTA CTA A-3′);

nucleophosmin (fwd: 5′-TCC CTT GGG GGC TTT GAA ATA ACA CC-3′; rev: 5′-TGG AAC CTT GCT ACC ACC TC-3′);

JunB (fwd: 5′-GCT CGG TTT CAG GAG TTT GT-3′; rev: 5′-ATA CAC AGC TAC GGG ATA CGG-3′);

GAPDH (fwd: 5′- AAC AGC GAC ACC CAC TCC TC -3′; rev: 5′- CAT ACC AGG AAA TGA GCT TGA CAA -3′).

To analyse qPCR data, the Ct ($\Delta\Delta$Ct) method [14] for relative quantification of gene expression was used. To quantify relative expression of the target genes NPM/ALK, nucleophosmin and JunB the following formula was used: ΔCt = Ct target gene (NPM/ALK, nucleophosmin, JunB) – $\overline{x}$ Ct control gene (GAPDH); $\Delta\Delta$Ct = ΔCt drug treatment – $\overline{x}$ ΔCt control sample; Ratio = $2^{-\Delta\Delta Ct}$.

Cell cycle progression (FACS-analysis)

SR-786 cells were seeded in a 6-well plate at a concentration of 2×10^5 cells/ml. After 8 h of treatment, cells were harvested and centrifuged at 300 x G for 5 min at 4°C and processed as described earlier [2] and analysed on a FACS Calibur flow cytometer (BD Bioscience, Franklin Lakes, New Jersey, USA)..

Cytotoxicity, mitochondrial activity assay

To measure mitochondrial activity, CellTiter-Blue assay (Promega, Madison, WI) was used according to the manufacturer's instructions. For this, SR-786, PBMC and HL60 cells were seeded into 96-well plates at concentrations of 2×10^5, 5×10^5 and 1×10^5 cells/ml, respectively. The compounds were added at the indicated concentrations and compared to solvent-treated controls. Fluorescence was measured at 570 nm using a multi-detection reader (Synergy HT, Bio-Tek Instrument, Winooski, VT, USA).

Cell death analysis – (HO/PI staining)

Hoechst 33258 (HO) and propidium iodide (PI) double staining (Sigma-Aldrich, St. Louis, MO, USA) allows to measure cell death [15] and was performed as described earlier [2] using a fluorescence microscope equipped with a TRITC and DAPI filter (Olympus IX51, Shinjuku, Tokyo, Japan).

7

113

Caspase 3/7 activity assay

SR-786 cells were seeded in 3.5 cm dishes at a concentration of 2×10^5 cell/ml and after incubation of 1 h at 37°C cells were treated with 3 μg/ml of *N. lobata* compounds for 8, 16 and 24 h when they were analysed by the Apo-ONE Homogeneous Caspase-3/7 assay (Promega, Madison, WI) according to the manufacturer´s instructions. Fluorescence was measured by using a multi-detection reader (excitation at 499 nm and emission at 521 nm).

NF-κB transactivation assay

The transactivation of a NF-κB-driven luciferase reporter was quantified in HEK293/NF-κB-luc cells (Panomics, RC0014) as previously described [16, 17] using a GeniosPro plate reader (Tecan, Grödig, Austria). Parthenolide (Sigma–Aldrich, Vienna, Austria) was used as a positive control.

Circular chemorepellent induced defect (CCID) assay

The analysis of tumour intravasation through the lymphendothelial barrier was done as described before [12, 18-25] and CCID areas were measured using ZEN 2012 software (Zeiss, Jena, Germany). During the experiments, which were short term, we did not observe toxic effects of the tested compounds (monitored by HOPI staining) [15].

12(S)-HETE assay

MCF-7 cells were seeded in 3.5 cm dishes and grown in 2.5 ml complete MEM medium (Gibco # 10370-047). The next day, the medium was changed to FCS-free medium and cells were kept at 37°C for 24 h. Then, cells were treated with 10 μM arachidonic acid (#A3555, Sigma-Aldrich, Munich, Germany) and the indicated compounds for 24 h. The concentration of 12(S)-HETE in the cellular supernatant was measured with minor modifications as described previously [23, 24] using the 12(S)-HETE enzyme immunoassay kit (EIA, # ADI-900-050; Enzo Life Sciences, Lausen, Switzerland). Absorbance was measured with a Wallac 1420 Victor 2 multilabel plate reader (Perkin Elmer Life and Analytical Sciences).

Ethoxyresorufin-O-deethylase (EROD) assay selective for CYP1A1 activity

MCF-7 breast cancer cells were grown in phenol red-free DMEM/F12 medium (Gibco, Karlsruhe, Germany) containing 10% FCS and 1% PS (Invitrogen, Karlsruhe, Germany). Before treatment, the cells were transferred to DMEM/F12 medium supplemented with 10% charcoal-stripped FCS (PAN Biotech, Aldenbach, Germany) and 1% PS. After 24 h of

8

114

treatment CYP1A1 activity was measured with minor modifications as previously described [22]. Briefly, ethoxyresorufin (final concentration 5.0 µM, Sigma-Aldrich, Munich, Germany) was added and 0.4 ml aliquots of the medium were sampled after 180 min and the formation of resorufin was analysed by spectrofluorometry (PerkinElmer LS50B, Waltham, MA, USA) with an excitation wavelength of 530 nm and an emission wavelength of 585 nm.

Statistical analysis

For statistical analyses Excel 2003 software and Prism 5 software package (GraphPad, San Diego, CA, USA) were used. The values were expressed as mean ± SD and the Student t-test or ANOVA and Dunnett-post-test were used to evaluate statistical significance ($p < 0.05$).

9

Results

Anti-proliferative effects of *N. lobata* furanoheliangolide sesquiterpene lactones in ALCL cells

In order to explore the effects of isolated *N. lobata* compounds (**Fig. 1a**) on cell growth of ALK- positive ALCL, murine CD-417 (**Fig. 1b**) and human SR-786 cells (**Fig. 1c**), cells were treated with 1 and 3 μM lobatin B, 8β-isovaleryloxy-9α-hydroxy-calyculatolide (OH-CAL) and 8β-isovaleryloxy-9α-acetoxy-calyculatolide (OAc-CAL). A concentration of 3 μM lobatin B inhibited proliferation of murine CD-417 cells and led to their eradication after 24 h. Human SR-786 cell growth was inhibited by 1 μM lobatin B. 3 μM OAc-CAL slightly inhibited SR-786 cell growth after 24 h whereas OH-CAL did not inhibit growth of both cell lines. Hence, further experiments were performed with lobatin B to characterise the cytotoxic mechanisms and were compared to OH-CAL, which did not show anti-neoplastic effects. Interestingly, OH-CAL and OAc-CAL slightly but consistently induced the growth of CD-417 cells after 16 h of treatment.

Mitochondrial activity and cell cycle distribution upon lobatin B and OH-CAL treatment

The mitochondrial metabolism of SR-786 cells, which was measured by CellTiter-Blue assay, was only weakly affected by lobatin B and OH-CAL (**Fig. 2a**). Next, the effect of lobatin B on cell cycle distribution of SR-786 was evaluated by flow cytometric analysis (FACS). Treatment with 3 μM lobatin B for 8 h caused the accumulation of SR-786 cells in G2/M phase at the expense of cells in G1 (**Fig. 2b**). Therefore, SR-786 cells were still able to pass through S-phase upon lobatin B treatment, because no accumulation of S-phase cells was observed. We thus conclude that lobatin B inhibited proliferation by arresting SR-786 cells in G2/M. OH-CAL treatment had no effect on cell cycle distribution.

Lobatin B inhibits NPM/ALK expression in SR-786 cells

In ALCL cells the NPM/ALK chimera is driving proliferation. Therefore, it was tested whether lobatin B affected the expression of NPM/ALK. Lobatin B treatment strongly suppressed the level of NPM/ALK after 8 h and 24 h, whereas OH-CAL affected NPM/ALK expression only marginally after 24 h (**Fig. 3**). Thus, lobatin B specifically abrogated the expression of NPM/ALK and this was most likely causal for growth inhibition of SR-786 cells. Interestingly, lobatin B caused an oscillation in nucleophosmin expression and also OH-CAL suppressed nucleophosmin expression after 24 h.

10

To investigate at which stage the expression of NPM/ALK became down-regulated by lobatin B, the transcript levels were analysed. NPM/ALK- and also nucleophosmin mRNAs were reduced upon lobatin B treatment (**Fig. 4a,b**), hence giving a clue as to how lobatin B mediated the regulation of NPM/ALK, i.e. by interfering with a factor or a site regulating nucleophosmin transcription. The fact that nucleophosmin protein level remained high upon lobatin B treatment might have been due to high stability of the polypeptide. Yet, there was still a discrepancy because "inactive" OH-CAL treatment decreased the protein expression of nucleophosmin and slightly that of NPM/ALK after 24 h. Therefore, the way of transcriptional regulation of NPM/ALK by lobatin B has to be substantiated by future investigations.

The transcription of the JunB proto-oncogene was shown to be regulated by NPM/ALK [10, 26] and accordingly lobatin B treatment suppressed JunB mRNA levels (**Fig. 4c**). The Jun family of transcription factors are components of the AP-1 transcription factor complex and AP-1 (activator protein 1) is involved in cell proliferation and apoptosis [27], which provides a mechanistic link between lobatin B treatment, the down-regulation of NPM/ALK and subsequently of JunB, and the inhibition of cell proliferation/induction of apoptosis.

<u>Lobatin B affects expression of Jun family members and induces the tumour suppressor p21</u>
The expression of the Jun family members was further analysed at the protein level. JunB is the main transcription factor in the AP-1 complex induced by NPM/ALK [26, 28] and lobatin B treatment inhibited the expression of JunB protein (**Fig. 5a**) which is consistent with suppression of its mRNA. Lobatin B induced c-Jun which was strictly accompanied by an induction of p21. It was shown that c-Jun together with the ubiquitous transcription factor SP1 transactivates p21 expression [29]. On the other hand, also silencing of c-Jun by siRNA caused the upregulation of p21 and accumulation of NPM/ALK positive ALCL cells in G2/M at expense of S-phase cells [30]. Therefore, both scenarios - c-Jun induction and c-Jun inhibition - may cause p21-mediated G2/M arrest. In contrast to the observations of Leventaki et al. [30] which showed that c-Jun down-regulation is accompanied by a loss of S-phase cells, we here report that upregulation of c-Jun is accompanied by a loss of G1-phase cells. Lobatin B enhanced c-Jun protein expression in a similar way as did treatment with the DCM fraction of *N. lobata* [2]. However, the regulation of c-Jun by lobatin B remained unclear. As c-Jun can substitute for JunB the upregulation of c-Jun might be part of a compensatory feedback loop in response to JunB inhibition. Interestingly, JunD levels oscillated upon lobatin B treatment in a similar way as observed for nucleophosmin levels.

11

OH-CAL neither induced c-Jun nor p21 (**Fig. 5a**) and transiently suppressed JunB independently of NPM/ALK, because NPM/ALK remained expressed at the time point when JunB decreased. However, it is possible that just the activity of NPM/ALK, but not its expression level was compromised. This short downregulation was not substantial and had no effect on the cell cycle. Jun family members, especially JunB, promote ALCL development through transcriptional activation of PDGFR-ß as shown in an ALCL mouse model [**10**]. In the human SR-786 ALCL cell line PDGFR-ß is not expressed. Therefore, the murine CD-417 ALCL cell line was used to test the effect of lobatin B on PDGFR-ß expression. Lobatin B treatment first inhibited NPM/ALK (2 h) and subsequently JunB, and PDGFR-β was downregulated (**Fig. 5b**). Hence, lobatin B inhibited the recently discovered NPM/ALK signal transduction cascade down to the level of JunB and PDGFR-ß [**10**]. As in SR-786 cells, lobatin B induced c-Jun also in CD-417 cells.

Lobatin B triggers SR-786 cell death

Lobatin B induced cell death and more apoptotic than necrotic cells were counted by HO/PI staining (**Fig. 6a**). This was confirmed by detecting an induction of Caspase 3/7 activity within 16 h of lobatin B treatment which decreased thereafter (**Fig. 6b**). Furthermore, caspase 3 activation was confirmed by its proteolytic cleavage after 24 h and concomitant signature-type degradation of its target PARP (**Fig. 6c**). OH-CAL treatment had a minor effect on caspase 3 pre-activation. Apparently this was due to the rather similar structures of lobatin B and OH-CAL. However, OH-CAL treatment did not seriously affect the survival of SR-786 cells.

Impact of lobatin B on NPM/ALK negative cell types

To assess the specificity of lobatin B towards lymphoma cells, PBMCs from a healthy volunteer were treated with 3 µM lobatin and OH-CAL. Interestingly, the number of PBMCs increased after 8 h of lobatin B- and OH-CAL treatment (**Fig 7a**) and this was accompanied by an increased mitochondrial activity (**Fig. 7b**). Then, PBMC numbers returned to control levels after 24 h and 48 h indicating that the initially propagating cell mass was finally subjected to a reduction process, which was paralleled by a significantly reduced mitochondrial metabolism upon lobatin B treatment for 24 h. Since OH-CAL did not increase the metabolic activity after 8 h, the observed correlation between PBMC number and their mitochondrial activity (also by lobatin B treatment) was coincidental.

12

Furthermore, HL60 leukaemia cells, which do not harbour the NPM/ALK translocation, were tested to study the specificity of lobatin B towards NPM/ALK. HL60 cell number was reduced by ~60% upon lobatin B treatment (**Fig. 7a**), which severely inhibited HL60 mitochondrial metabolism (**Fig. 7b**). This showed that lobatin B exhibited additional effects beyond NPM/ALK inhibition targeting leukaemia cells but not PBMCs. Hence, the anti-proliferative effects of lobatin B were specific for neoplastic cells (i.e. lymphoma and leukaemia cells), but with a higher specificity to those cells harbouring the NPM/ALK translocation, because SR-786 cells and CD417 cells were more sensitive towards lobatin B than HL60 cells.

Specificity of the ALK inhibitor TAE-684

To estimate the impact of NPM/ALK on cell proliferation and the specificity of lobatin B regarding this mechanism SR-786 ALCL cells, ALK-negative HL60 cells, and normal PBMCs were treated with the specific NPM/ALK inhibitor TAE-684 [11] and the effect on cell proliferation was compared. TAE-786 dose dependently inhibited the proliferation of SR-786 cells but not that of HL60 and PBMCs (**Fig. 8a**). Hence, NPM/ALK is driving proliferation and TAE-684 is more specific than lobatin B regarding its property to target solely ALK. TAE-684 did not reduce the mitochondrial activity of HL60 cells but inhibited PBMC- and SR-786 mitochondrial metabolism (**Fig. 8b**). Obviously, mitochondrial activities did not correlate with cell proliferation rates and were thus independent of each other.

Lobatin B inhibits NF-κB and the intravasation of tumour spheroids through the lymphendothelial barrier

Lobatin B reduced the number of ALK-positive SR-786 lymphoma cells by downregulating NPM/ALK, and of ALK-negative HL60 leukaemia cells by an unknown mechanism. In HL60 cells NF-κB signalling is constitutively activated at high levels and counteracts monocytic differentiation [31]. NF-κB ensures cell survival by keeping up the transcription of IAPs, which are proteins intercepting caspase activity. Therefore, we tested whether NF-κB activation was inhibited by lobatin B. For this, modified HEK293 cells, which stably express NF-κB recognition sequences linked to luciferase, were treated with lobatin B to report whether NF-κB activity was modulated. Lobatin B treatment attenuated TNFα-induced luciferase expression after 4 h in a dose dependent manner and hence, NF-κB activation was suppressed (**Fig. 9a**). This may explain the susceptibility of HL60 cells to lobatin B treatment.

PBMCs remained unaffected by lobatin B treatment, because in normal cells NF-κB expression is low.

In addition to anti-apoptotic signalling NF-κB plays a significant role when tumour cells intravasate lymphendothelial barriers [18, 19]. In a validated three-dimensional co-culture model in which MCF-7 breast cancer spheroids are placed on top of lymphendothelial cell (LEC) monolayers, the tumour spheroids stimulate the retraction of adjacent LECs [20, 32, 33]. This leads to cell-free areas, so called "circular chemorepellent induced defects" (CCIDs), through which tumours intravasate lymphatics [12]. Lobatin B dose-dependently inhibited this complex pro-metastatic process resulting in significantly reduced CCID formation (**Fig. 9b**). Besides NF-κB, also ALOX12 and ALOX15, which are the major enzymes generating 12(S)-HETE ("endothelial retraction factor") [33], and cytochromes P450 (CYPs) contribute to CCID formation. Therefore, 12(S)-HETE production and CYP activity were studied by respective assays (**Fig. 9c, d**). Neither 12(S)-HETE synthesis nor CYP1A1 activity were significantly inhibited by 3 and 5 µM lobatin B.

14

Discussion

The DCM extract of *N. lobata* [7] was formerly shown to downregulate NPM/ALK, induce apoptosis in ALCL cell lines [2] and inhibit inflammation in carrageenan-induced rat paw oedema model [5]. The work presented here demonstrates that lobatin B is an active principle isolated from the DCM fraction of the methanolic extract of *N. lobata* and suppresses the NPM/ALK transcript and protein and also nucleophosmin, which, in its truncated form, is the 5-prime fusion partner of the NPM/ALK t(2;5)(p23;q35) translocation [3]. This suggested that a transcriptional mechanism responsible for nucleophosmin expression was hampered by lobatin B.

NPM/ALK was shown to induce JunB, which is a transcription factor of the tyrosine receptor kinase PDGF-Rβ [10, 26] and lobatin B inhibited the expression of JunB and PDGF-Rβ subsequently to NPM/ALK down-regulation. Interestingly, the inactive sesquiterpene lactone OH-CAL downregulated JunB independently of NPM/ALK and hence, also the effect of lobatin B on JunB might be more complex than just caused by NPM/ALK down-stream inhibition. JunB transcript suppression by OH-CAL was fairly transient and also the marginal pre-activation of caspase 3 was not sufficient to affect SR-786 cell viability. The specific effect of lobatin B on ALCL cells caused only negligible perturbations of mitochondrial activity, which is otherwise a measure for the general toxicity of a vast variety of stressors and considered as a major trigger of apoptotic cell death. The weak inhibition of mitochondrial activity was in obvious contrast to the strong inhibition of cell proliferation. This showed that growth inhibition was not due to a general toxicity that was imposed on mitochondrial function but supposedly to a more specific anti-proliferative activity. Alternatively, since lobatin B treatment caused a substantial increase in G2/M cells these cells may contain more mitochondria compensating the affected mitochondrial activity of the decreased cell number.

When activated by LPS, NF-κB-dependent expression of E-selectin [5] and TNFα [34] was inhibited by all *N. lobata* sesquiterpene lactones tested in these studies, among which were also lobatin B, OH-CAL and OAc-CAL. The α-methylene-γ-lactone ring common to all sesquiterpene lactones of *N. lobata* and also of the *bona fide* NF-κB inhibitor parthenolide was reported to cause alkylation of a cysteine residue in the activation loop of IκB kinaseβ [34, 35] thereby preventing the degradation of IκB and hence, the translocation of NF-κB into the nucleus and expression of inflammatory cytokines. Thus, the inhibition of NF-κB was responsible for the anti-inflammatory property of lobatin B in a THP-1 monocyte model and

in HUVEC [5, 24] and traditional medicine makes use of it when utilising *N. lobata* [36, 37]. Here we also demonstrated that lobatin B inhibited TNFα-induced NF-κB activation, which was most likely responsible for the toxicity towards HL60 leukaemia cells. This is in agreement with the fact that PBMCs remained unaffected by lobatin B, because in contrast to HL60 [31], under normal cell culture conditions NF-κB is not activated in PBMCs. Structurally, the anti-inflammatory activity of the sesquiterpene lactones was tied to the acetyl group at C-9 and the double bonds at C-4/5 and C-2/3 [5], but this did not correlate with the here described anti-neoplastic property, which also involved NF-κB, because OAc-CAL (acetyl group at C-9) did not inhibit proliferation.

The inhibition of NF-κB activity was shown to prevent adhesion of tumour emboli to lymphendothelial cells (LECs) [19] and this step is necessary for the subsequent retraction of the LEC barrier allowing the tumour to transmigrate. Although the structure-activity-relationship was not addressed in this investigation, blocking NF-κB activity by lobatin B or related sesquiterpenes opens a new strategy for the management of early steps of metastasis that does not exist so far.

Lobatin B specifically targets cancer cells by two independent mechanisms, inhibition of NF-κB and of NPM/ALK, and does not affect normal cells.

16

Acknowledgments

Conflicting interests

The authors do not have any conflict of interest.

17

123

References

1, Cragg GM, Newman DJ Natural products: a continuing source of novel drug leads. Biochim Biophys Acta: 2013, 1830:3670-3695.

2, Unger C, Popescu R, Giessrigl B, Laimer D, Heider S, Seelinger M, Diaz R, Wallnöfer B, Egger G, Hassler M, Knöfler M, Saleh L, Sahin E, Grusch M, Fritzer-Szekeres M, Dolznig H, Frisch R, Kenner L, Kopp B, Krupitza G The dichloromethane extract of the ethnomedicinal plant *Neurolaena lobata* inhibits NPM/ALK expression which is causal for anaplastic large cell lymphomagenesis. Int J Oncol: 2013, 42:338-348.

3, Morris SW, Kirstein MN, Valentine MB, Dittmer KG, Shapiro DN, Saltman DL, Look AT: Fusion of a kinase gene, ALK, to a nucleolar protein gene, NPM, in non-Hodgkin's lymphoma. Science 1994, 263:1281-1284.

4, de las Heras B, Slowing K, Benedí J, Carretero E, Ortega T, Toledo C, Bermejo P, Iglesias I, Abad MJ, Gómez-Serranillos P, Liso PA, Villar A, Chiriboga X: Antiinflammatory and antioxidant activity of plants used in traditional medicine in Ecuador. J Ethnopharmacol 1998, 61:161-166.

5, McKinnon R , Binder M, Zupkó I, Afonyushkin T, Lajter I, Vasas A, de Martin R, Unger C, Dolznig H, Diaz R, Frisch R, Passreiter C M, Krupitza G, Hohmann J, Kopp B, Bochkov V N: Pharmacological insight into the anti-inflammatory activity of sesquiterpene lactones from *Neurolaena lobata* (L.) R.Br. ex Cass. Phytomed, in press.

6, Butterweck V, Nahrstedt A: What is the best strategy for preclinical testing of botanicals? A critical perspective. Planta Med 2012, 78:747-754.

18

7, Passreiter CM, Wendisch D, Gondol D: Sequiterpene lactones from *Neurolaena lobata*. Phytochemistry 1995, 39:133-137.

8, Lajter I, Vasas A, Béni Z, Forgo P, Binder M, Bochkov V, Zupkó I, Krupitza G, Frisch R, Kopp B, Hohmann J: Sesquiterpenes from *Neurolaena lobata* and their antiproliferative and anti-inflammatory activities. J Nat Prod 2014, 77:576-582.

9, François G, Passreiter C, Woerdenbag H. van Looveren M: Antiplasmodial activities and cytotoxic effects of aqueous extracts and sesquiterpene lactones from *Neurolaena lobata*. Planta Med 1996, 62:126–129.

10, Laimer D, Dolznig H, Kollmann K, Vesely PW, Schlederer M, Merkel O, Schiefer AI, Hassler MR, Heider S, Amenitsch L, Thallinger C, Staber PB, Simonitsch-Klupp I, Artaker M, Lagger S, Turner SD, Pileri S, Piccaluga PP, Valent P, Messana K, Landra I, Weichhart T, Knapp S, Shehata M, Todaro M, Sexl V, Höfler G, Piva R, Medico E, Ruggeri BA, Cheng M, Eferl R, Egger G, Penninger JM, Jaeger U, Moriggl R, Inghirami G, Kenner L: PDGFR blockade is a rational and effective therapy for NPM-ALK-driven lymphomas. Nat Med 2012, 18:1699-1704.

11, Galkin AV, Melnick JS, Kim S, Hood TL, Li N, Li L, Xia G, Steensma R, Chopiuk G, Jiang J, Wan Y, Ding P, Liu Y, Sun F, Schultz PG, Gray NS, Warmuth M: Identification of NVP-TAE684, a potent, selective, and efficacious inhibitor of NPM-ALK. Proc Natl Acad Sci U S A 2007, 104:270-275.

12, Kerjaschki D, Bago-Horvath Z, Rudas M, Sexl V, Schneckenleithner C, Wolbank S, Bartel G, Krieger S, Kalt R, Hantusch B, Keller T, Nagy-Bojarszky K, Huttary N, Raab I, Lackner K, Krautgasser K, Schachner H, Kaserer K, Rezar S, Madlener S, Vonach C, Davidovits A, Nosaka H, Hämmerle M, Viola K, Dolznig H, Schreiber M, Nader A, Mikulits W, Gnant M, Hirakawa S, Detmar M, Alitalo K, Nijman S, Offner F, Maier TJ, Steinhilber D,

19

Krupitza G: Lipoxygenase mediates invasion of intrametastatic lymphatic vessels and propagates lymph node metastasis of human mammary carcinoma xenografts in mouse. J Clin Invest 2011, 121:2000-2012.

13, Popescu R, Heiss EH, Ferk F, Peschel A, Knasmueller S, Dirsch VM, Krupitza G, Kopp B: Ikarugamycin induces DNA damage, intracellular calcium increase, p38 MAP kinase activation and apoptosis in HL-60 human promyelocytic leukemia cells. Mutat Res 2011, 10:709-710.

14, Livak KJ, Schmittgen TD: Analysis of relative gene expression data using real-time quantitative PCRand the 2(-delta delta C(T)) method. Methods 2001, 25:402-408.

15, Grusch M, Polgar D, Gfatter S, Leuhuber K, Huettenbrenner S, Leisser C, Fuhrmann G, Kassie F, Steinkellner H, Smid K, Peters GJ, Jayaram HN, Klepal W, Szekeres T, Knasmüller S, Krupitza G: Maintenance of ATP favours apoptosis over necrosis triggered by benzamide riboside. Cell Death Differ 2002, 9:169-178.

16, Rozema E, Atanasov AG, Fakhrudin N, Singhuber J, Namduang U, Heiss EH, Reznicek G, Huck CW, Bonn GK, Dirsch VM, Kopp B: Selected Extracts of Chinese Herbal Medicines: Their Effect on NF-κB, PPARα and PPARγ and the Respective Bioactive Compounds. Evid Based Complement Alternat Med 2012, 983023.

17, Xie LW, Atanasov AG, Guo DA, Malainer C, Zhang JX, Zehl M, Guan SH, Heiss EH, Urban E, Dirsch VM, Kopp B: Activity-guided isolation of NF-κB inhibitors and PPARγ agonists from the root bark of Lycium chinense Miller. J Ethnopharmacol 2014, 152:470-477.

20

18, Vonach C, Viola K, Giessrigl B, Huttary N, Raab I, Kalt R, Krieger S, Vo TP, Madlener S, Bauer S, Marian B, Hämmerle M, Kretschy N, Teichmann M, Hantusch B, Stary S, Unger C, Seelinger M, Eger A, Mader R, Jäger W, Schmidt W, Grusch M, Dolznig H, Mikulits W, Krupitza G: NF-κB mediates the 12(S)-HETE-induced endothelial to mesenchymal transition of lymphendothelial cells during the intravasation of breast carcinoma cells. Brit J Cancer 2011, 105:263-271.

19, Viola K, Kopf S, Huttary N, Vonach C, Kretschy N, Teichmann M, Giessrigl B, Raab I, Stary S, Krieger S, Keller T, Bauer S, Hantusch B, Szekeres T, de Martin R, Jäger W, Mikulits W, Dolznig H, Krupitza G, Grusch M: Bay11-7082 inhibits the disintegration of the lymphendothelial barrier triggered by MCF-7 breast cancer spheroids; the role of ICAM-1 and adhesion. Brit J Cancer 2013, 108:564-569.

20, Madlener S, Saiko P, Vonach C, Viola K, Huttary N, Stark N, Popescu R, Gridling M, Vo NT, Herbacek I, Davidovits A, Giessrigl B, Venkateswarlu S, Geleff S, Jäger W, Grusch M, Kerjaschki D, Mikulits W, Golakoti T, Fritzer-Szekeres M, Szekeres T, Krupitza G: Multifactorial anticancer effects of digalloyl-resveratrol encompass apoptosis, cell-cycle arrest, and inhibition of lymphendothelial gap formation in vitro. Brit J Cancer 2010, 102:1361-1370.

21, Giessrigl B, Yazici G, Teichmann M, Kopf S, Ghassemi S, Atanasov AG, Dirsch VM, Grusch M, Jäger W, Ozmen A, Krupitza G: Effects of Scrophularia extracts on tumor cell proliferation, death and intravasation through lymphoendothelial cell barriers. Int J Oncol 2012, 40:2063-2074.

22, Viola K, Kopf S, Rarova L, Jarukamjorn K, Kretschy N, Teichmann M, Vonach C, Atanasov AG, Giessrigl B, Huttary N, Raab I, Krieger S, Strnad M, de Martin R, Saiko P, Szekeres T, Knasmüller S, Dirsch VM, Jäger W, Grusch M, Dolznig H, Mikulits W, Krupitza G: Xanthohumol attenuates tumour cell-mediated breaching of the lymphendothelial barrier and prevents intravasation and metastasis. Arch Toxicol 2013, 87:1301-1312.

21

23, Kretschy N, Teichmann M, Kopf S, Atanasov AG, Saiko P, Vonach C, Viola K, Giessrigl B, Huttary N, Raab I, Krieger S, Jäger W, Szekeres T, Nijman SM, Mikulits W, Dirsch VM, Dolznig H, Grusch M, Krupitza G: In vitro inhibition of breast cancer spheroid-induced lymphendothelial defects resembling intravasation into the lymphatic vasculature by acetohexamide, isoxsuprine, nifedipin and proadifen. Brit J Cancer 2013, 108:570-578.

24, Kopf S, Viola K, Atanasov AG, Jarukamjorn K, Rarova L, Kretschy N, Teichmann M, Vonach C, Saiko P, Giessrigl B, Huttary N, Raab I, Krieger S, Schumacher M, Diederich M, Strnad M, de Martin R, Szekeres T, Jäger W, Dirsch VM, Mikulits W, Grusch M, Dolznig H, Krupitza G: In vitro characterisation of the anti-intravasative properties of the marine product heteronemin. Arch Toxicol 2013, 87:1851-1861.

25, Teichmann M, Kretschy N, Kopf S, Jarukamjorn K, Atanasov AG, Viola K, Giessrigl B, Saiko P, Szekeres T, Mikulits W, Dirsch VM, Huttary N, Krieger S, Jäger W, Grusch M, Dolznig H, Krupitza G: Inhibition of tumour spheroid-induced prometastatic intravasation gates in the lymph endothelial cell barrier by carbamazepine: drug testing in a 3D model. Arch Toxicol 2014, 88:691-699.

26, Staber PB, Vesely P, Haq N, Ott RG, Funato K, Bambach I, Fuchs C, Schauer S, Linkesch W, Hrzenjak A, Dirks WG, Sexl V, Bergler H, Kadin ME, Sternberg DW, Kenner L, Hoefler G: The oncoprotein NPM-ALK of anaplastic large-cell lymphoma induces JUNB transcription via ERK1/2 and JunB translation via mTOR signaling. Blood 2017, 110:3374-3383.

27, Pearson JD, Lee JK, Bacani JT, Lai R, Ingham RJ: NPM-ALK and the JunB transcription factor regulate the expression of cytotoxic molecules in ALK-positive, anaplastic large cell lymphoma. Int J Clin Exp Pathol 2011, 4:124–133.

28, Mathas S, Hinz M, Anagnostopoulos I, Krappmann D, Lietz A, Jundt F, Bommert K, Mechta-Grigoriou F, Stein H, Dörken B, Scheidereit C: Aberrantly expressed c-Jun and JunB are a hallmark of Hodgkin lymphoma cells, stimulate proliferation and synergize with NF-kappa B. EMBO J 2002, 21:4104–4113.

29, Kardassis D, Papakosta P, Pardali K, Moustakas A: C-Jun Transactivates the Promoter of the Human p21WAF1/Cip1 Gene by Acting as a Superactivator of the Ubiquitous Transcription Factor Sp1. J Biol Chem 1999, 274:29572-29581.

30, Leventaki V1, Drakos E, Medeiros LJ, Lim MS, Elaenitoba-Johnson KS, Claret FX, Rassidakis GZ: NPM-ALK oncogenic kinase promotes cell-cycle progression through activation of JNK/cJun signaling in anaplastic large-cell lymphoma. Blood 2007, 110:1621-1630.

31, Kang SN, Kim SH, Chung SW, Lee MH, Kim HJ, Kim TS: Enhancement of 1,25-dihydroxyvitamin D3-induced differentiation of human leukaemia HL-60 cells into monocytes by parthenolide via inhibition of NF-kB activity. Brit J Pharmacol 2002, 135:1235-1244.

32, Uchide K, Sakon M, Ariyoshi H, Nakamori S, Tokunaga M, Monden M: Cancer cells cause vascular endothelial cell retraction via 12(S)-HETE secretion; the possible role of cancer cell derived microparticle. Ann Surg Oncol 2007, 14:862-868.

33, Honn KV, Tang DG, Grossi I, Duniec ZM, Timar J, Renaud C, Leithauser M, Blair I, Johnson CR, Diglio CA, Kimler VA, Taylor JD, Marnett LJ: Tumour cell-derived 12(S)-hydroxyeicosatetraenoic acid induces microvascular endothelial cell retraction. Cancer Res 1994, 54: 565-574.

23

34, Walshe-Roussel B, Choueiri C, Saleem A, Asim M, Caal F, Cal V, Rojas MO, Pesek T, Durst T, Arnason JT: Potent anti-inflammatory activity of sesquiterpene lactones from *Neurolaena lobata* (L.) R. Br. ex Cass., a Q'eqchi' Maya traditional medicine. Phytochemistry 2013, 92:122-127.

35, Kwok BHB, Koh B, Ndubuisi MI, Elofsson M, Crews CM: The anti-inflammatory natural product parthenolide from the medicinal herb Feverfew directly binds to and inhibits IkB kinase. Chem Biol 2001, 8:759–766.

36, Amiguet VT, Arnason JT, Maquin P, Cal V, Sanchez Vindas P, Poveda L: A consensus ethnobotany of the Q'eqchi' Maya of southern Belize. Econ Bot 2005, 59:29-42.

37, Arvigo R. Balick M: Rainforest Remedies. 2nd edn, Twin Lakes, WI: Lotus Press; 1998.

24

Figure captions

Figure 1

Anti-proliferative effects of (a) *N. lobata* compounds in (b) murine CD-417 and (c) human SR-786 cells. After 8, 16 and 24 h of treatment with 1 µM and 3 µM of lobatin B, 8β-isovaleryloxy-9α-hydroxy-calyculatolide (OH-CAL), and 8β-isovaleryloxy-9α-acetoxy-calyculatolide (OAc-CAL) cells were counted using a Casy cell counter. The relative cell number is presented as percent of control. Experiments were performed in triplicate, error bars indicate means +/- SD, and asterisks significance (p<0.05; ANOVA followed by Dunnett-post-test).

Figure 2

Potential mechanisms of proliferation inhibition by lobatin B in SR-786 cells. (a) Cells were treated with 3 µM lobatin B and OH-CAL for 8 h and 24 h, respectively, when CellTiter-Blue reagent was added and absorbance measured at 570 nm using a multi-well plate reader. The relative cell number is presented as percent of control. (b) Cell cycle distribution upon treatment with lobatin B and OH-CAL. SR-786 cells were incubated with 3 µM of either compound for 8 h and then subjected to FACS analysis. Experiments were performed in triplicate, error bars indicate means +/- SD, and asterisks significance (p<0.05; t-test).

Figure 3

Lobatin B downregulates NPM-ALK expression in SR-786. Cells were treated with 3 µM lobatin B (a) or 8β-isovaleryloxy-9α-hydroxy-calyculatolide (OH-CAL; b) for 1, 2, 8, and 24 h, harvested and subjected to Western blot analysis using the indicated antibodies. β-actin expression served as control for equal sample loading.

25

Figure 4

Quantitative PCR analysis. SR-786 cells were treated with 3 µM lobatin B for the indicated times and the mRNA expression of (a) NPM/ALK, (b) nucleophosmin, and (c) JunB was measured and normalized to GAPDH mRNA. Experiments were performed in triplicate, error bars indicate means +/- SD, and asterisks significance (p<0.05; t-test).

Figure 5

Effect of lobatin B or OH-CAL on Jun-family members, PDGFR-ß and p21 in ALK-positive ALCL cells. SR-786 cells were treated with 3 µM lobatin B (a) or 8β-isovaleryloxy-9α-hydroxy-calyculatolide (OH-CAL) (b) for 2, 4, 6, and 8 h, and CD-417 cells (c) were treated with lobatin B. Then, cells were harvested and subjected to Western blot analysis using the indicated antibodies. β-actin expression served as control for equal sample loading.

Figure 6

Apoptotic/necrotic cell death of SR-786 cells treated with *N. lobata* compounds. Cells were treated with 3 µM lobatin B and after 24 h cell death was measured by (a) HO/PI staining, which enables the identification of apoptotic and necrotic cells. (b) Cells were treated with 3 µM of lobatin B and after 8, 16 and 24 h ApoOne reagent was added and caspase 3/7 activity was measured. Experiments were performed in triplicate, error bars indicate means +/- SD, and asterisks significance (p<0.05; t-test). (c) Cells were treated with 3 µM lobatin B (left panel) and 8β-isovaleryloxy-9α-hydroxy-calyculatolide OH-CAL (right panel) for 1, 2, 8, and 24 h, harvested and subjected to Western blot analysis using the indicated antibodies. β-actin expression served as control for equal sample loading.

Figure 7

Treatment of PBMC and HL60 cells with N. lobata compounds. (a) Effects on cell number after treatment of PBMCs and HL60 cells with 3 µM lobatin B and 8β-isovaleryloxy-9α-hydroxy-calyculatolide (OH-CAL) for 8 h, 24 h and 48 h. Cell number was measured by Casy cell counter. (b) Cells were treated with 3 µM *N. lobata* compounds and after 8 h and 24 h of

26

incubation with lobatin B and OH-CAL CellTiter-Blue reagent was added and absorbance was measured at 570 nm. Experiments were performed in triplicate, error bars indicate means +/- SD, and asterisks significance (p<0.05; t-test).

Figure 8

(a) Anti-proliferative effects of TAE-684 on SR-786-, HL60 cells and on PBMCs. Cells were treated with the indicated TAE-684 concentrations for 8 h, 24 h and 48 h and then counted by Casy. (b) Effect of TAE-684 treatment on SR-786-, HL60 cells, and PBMCs mitochondrial activity. Cells were treated with 10 nM TAE-684 for 24 h and 48 h and then, CellTiter-Blue reagent was added and measured at 570 nm. Experiments were performed in triplicate, error bars indicate means +/- SD, and asterisks significance (p<0.05; ANOVA followed by Dunnett-post-test; t-test).

Figure 9

(a) Effect on NF-κB activity. HEK293-NFκB-Luc cells were stained by incubation for 1 h in serum-free medium supplemented with 2 μM Cell Tracker Green CMFDA. The cells were then reseeded in 96-well plates at a density of 4×10^4 cells/well in phenol red-free and serum-free DMEM. On the next day cells were treated with 5 μM parthenolide (Parth.) as a specific inhibitor of NF-κB, 3 μM and 5 μM lobatin B, or solvent (0.2% DMSO; Co). 1 h after treatment cells were stimulated with 2 ng/ml human recombinant TNFα for additional 4 h. The luciferase-derived signal from the NF-κB reporter was normalized by the Cell Tracker Green CMFDA-derived fluorescence to account for differences in the cell number. (b) Effect of lobatin B on the size of circular chemorepellet-induced defects (CCIDs) in LEC monolayers triggered by MCF-7 cell spheroids. Cell cultures were pre-treated for 20 min with the indicated compound concentrations and then, MCF-7 spheroids were placed on top of LEC monolayers and co-cultivated for 4 h. As control (Co) CCIDs of solvent treated (0.2% DMSO) co-cultures were measured. The CCIDs underneath 15-25 spheroids were analysed for each condition using an Axiovert microscope and Axiovision Rel. 4.5 software from Zeiss. (c) Effect on 12(S)-HETE synthesis. MCF-7 cells were seeded in 3.5 cm dishes and grown to 70% confluence and treated with 10 μM arachidonic acid together with the indicated concentrations of lobatin B for 24 h. 0.2% DMSO was used as control (Co). The 12(S)-HETE

27

concentration in the cell culture supernatant was determined by EIA. (d) Effect on CYP1A1 activity in MCF-7 cells. MCF-7 cells were kept under steroid-free conditions and treated with the indicated concentrations of lobatin B or solvent (0.2% DMSO; Co). 5 μM ethoxyresorufin were added and after 180 min the formation of resorufin was analysed, which is specific for CYP1A1 activity. Experiments were performed in triplicate, error bars indicate means +/- SD and asterisks significance ($p < 0.05$; t-test; ANOVA followed by Dunnett-post-test).

*Conflicts of Interest Statement

Conflicting interests

The authors do not have any conflict of interest.

Figure 1

a

Lobatin B   OH-CAL   OAc-CAL

b

c

Figure 2

a

b

Figure 3

SR-786

Figure 4

a

NPM/ALK

b

Nucleophosmin
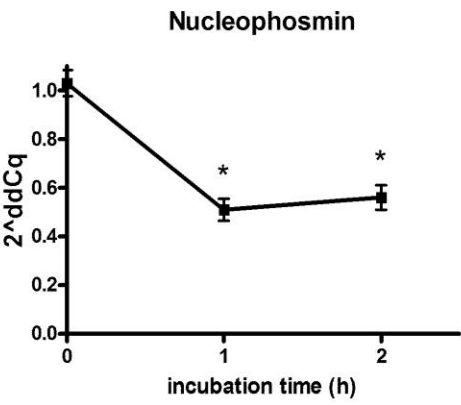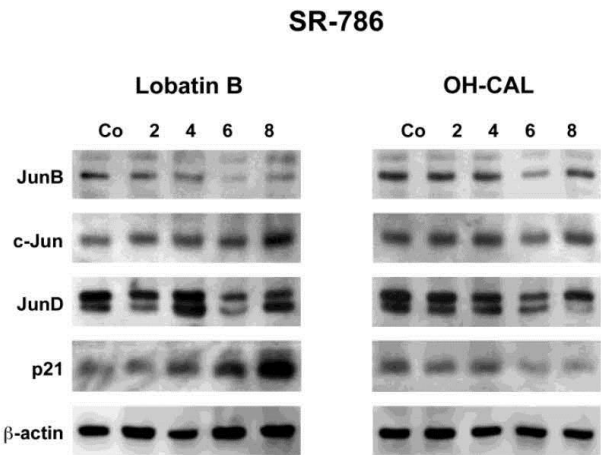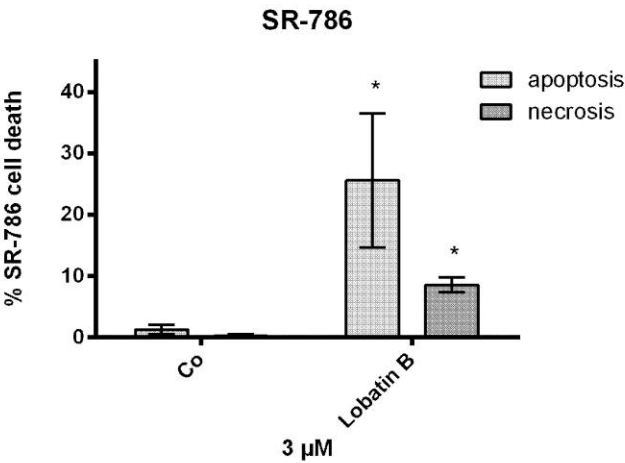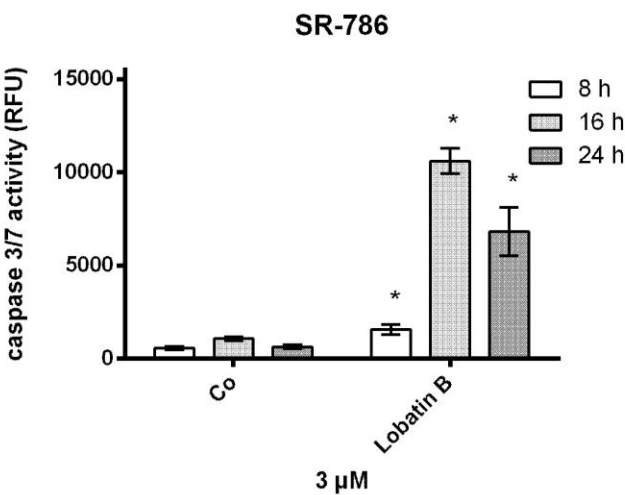

c

JunB
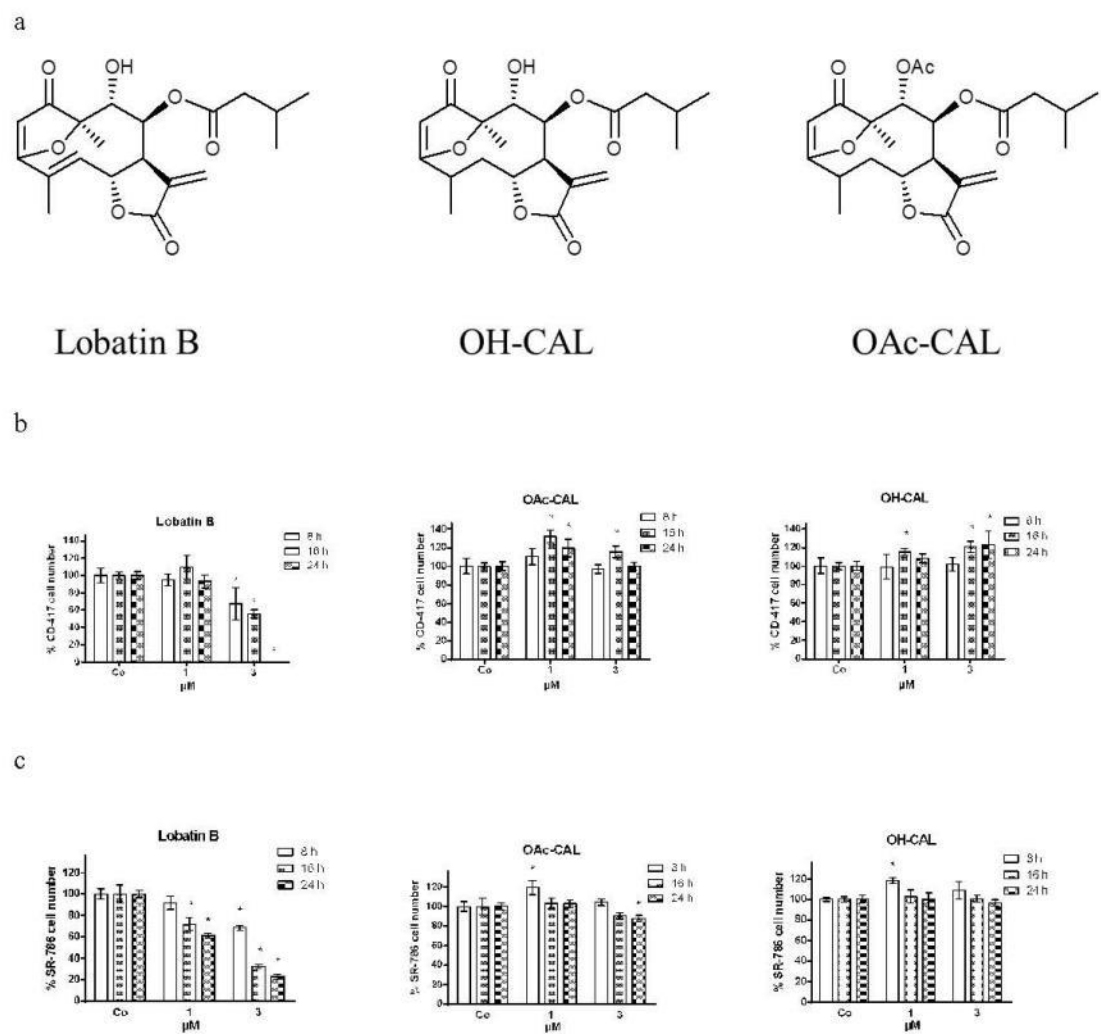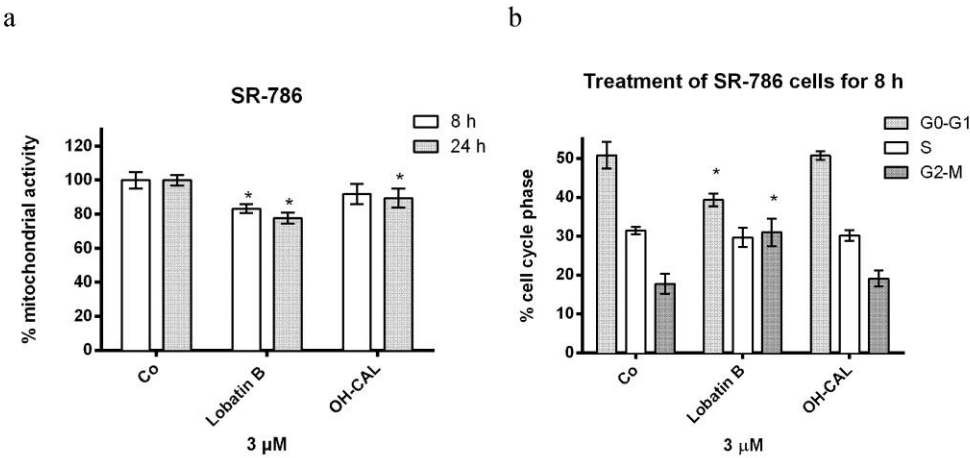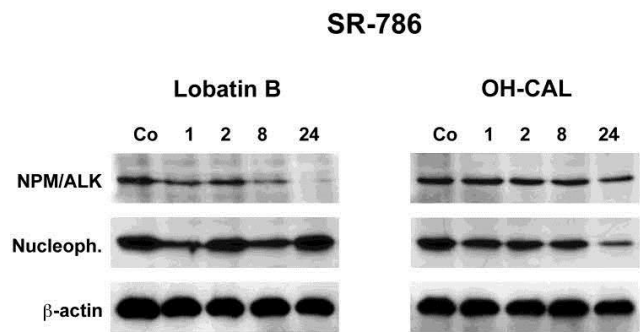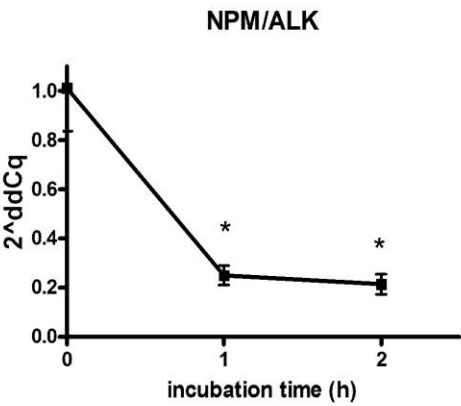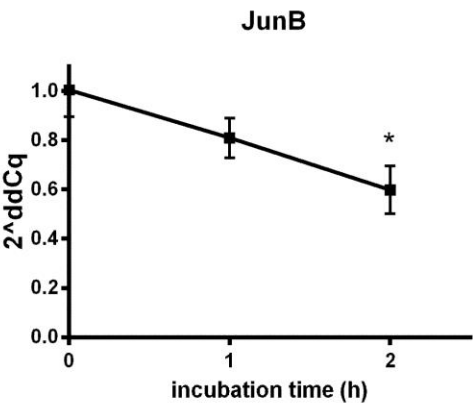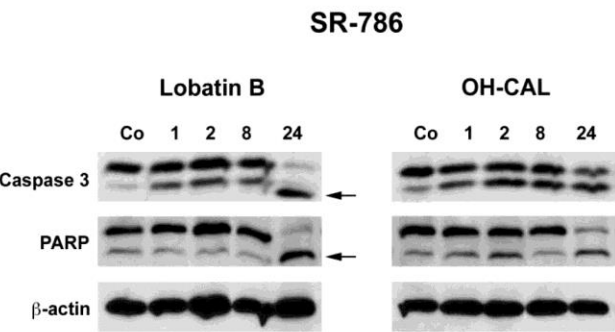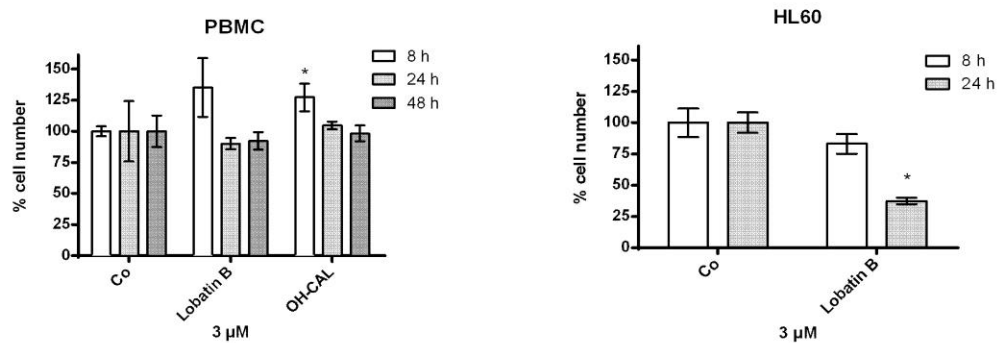
Figure 5

a

b

Figure 6

a

SR-786

b

SR-786

c

SR-786

141
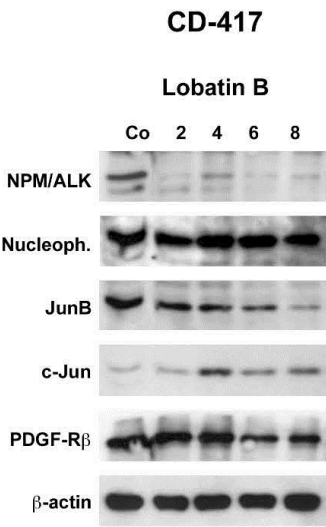
Figure 7

a

b

Figure 8

a

b

Figure 9

a

**Inhibition of NF-κB activity
by Lobatin B**

b

**Inhibition of CCID formation
by Lobatin B**

c

**Inhibition of 12(S)-HETE production
by Lobatin B**

d

**Inhibition of CYP1A1 activity
by Lobatin B**

The germacranolide sesquiterpene lactone neurolenin B of the medicinal plant Neurolaena lobata inhibits NPM/ALK-driven cell expansion and NF-κB-driven tumour Intravasation

Unger Christine, Kiss Izabella, Vasas Andrea, Lajter Ildikó, Kramer Nina, Atanasov Atanas Georgiev, Chi Nguyen Huu, Chatuphonprasert Waranya, **Brenner Stefan**, McKinnon Ruxandra, Peschel Andrea, Kain Renate, Saiko Philipp, Szekeres Thomas, Kenner Lukas, Hassler Melanie R., Diaz Rene, Frisch Richard, Dirsch Verena M., Jäger Walter, de Martin Rainer, Bochkov Valery N., Passreiter Claus M., Peter-Vörösmarty Barbara, Mader Robert M., Grusch Michael, Dolznig Helmut, Kopp Brigitte, Zupko Istvan, Hohmann Judit, Krupitza Georg
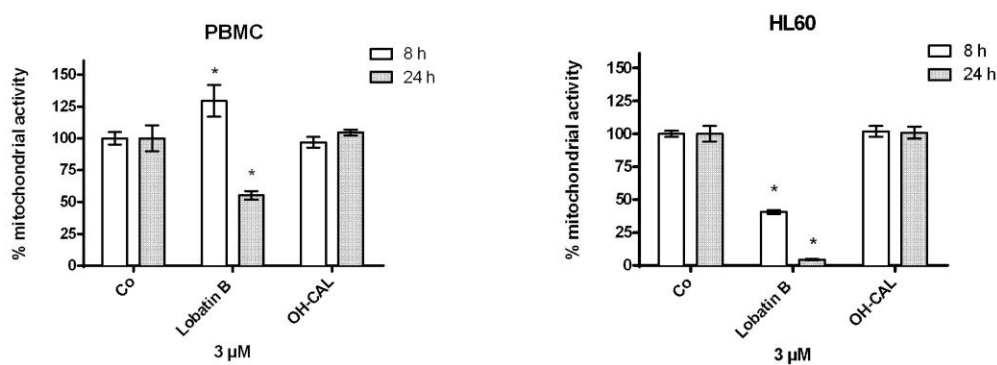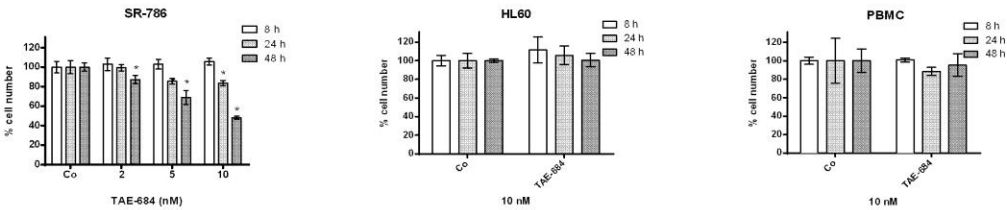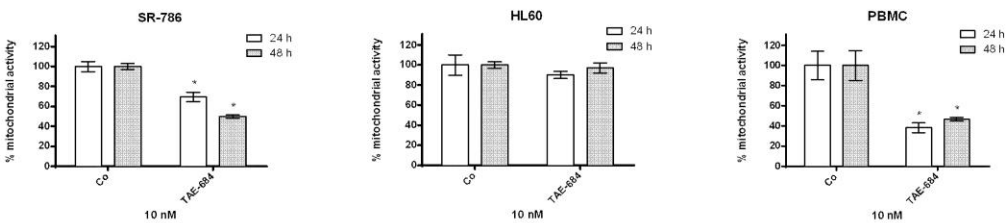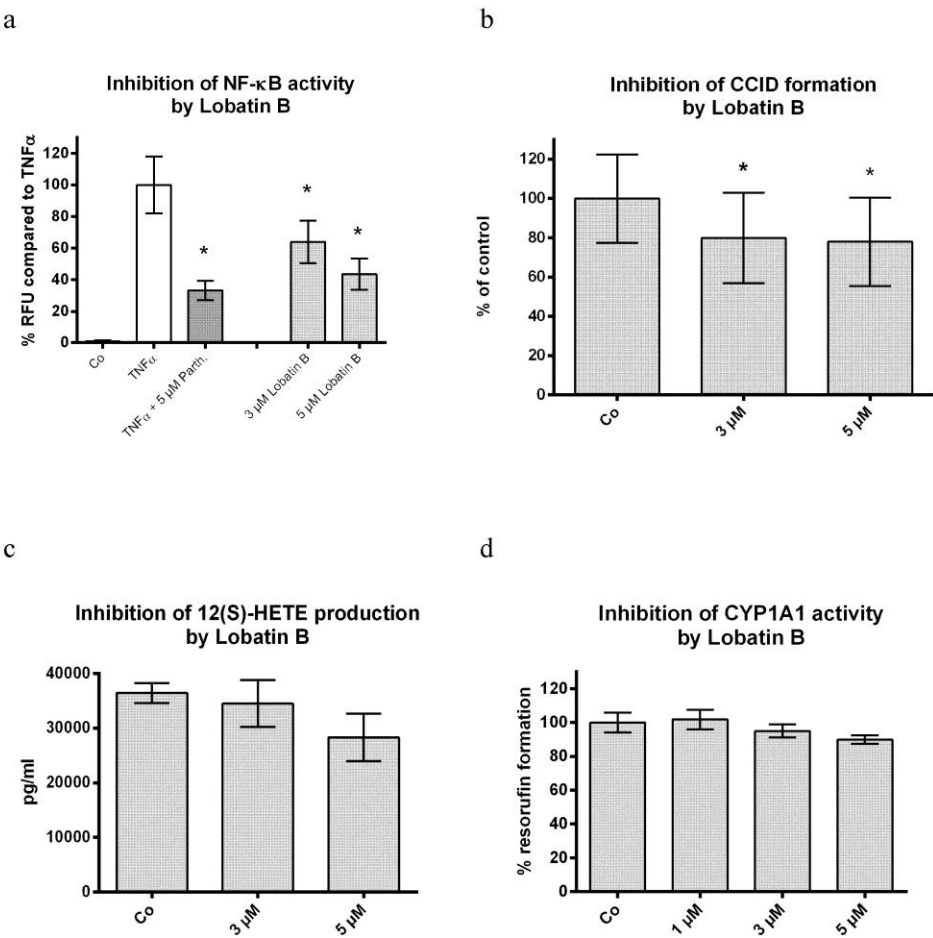
**The germacranolide sesquiterpene lactone neurolenin B
of the medicinal plant *Neurolaena lobata* inhibits NPM/ALK-driven cell expansion
and NF-κB-driven tumour intravasation**

Unger Christine[1*], Kiss Izabella[1,2*], Vasas Andrea[3], Lajter Ildikó[3], Kramer Nina[1], Atanasov Atanas Georgiev[4], Chi Nguyen Huu[2], Chatuphonprasert Waranya[5,6], Brenner Stefan[5], McKinnon Ruxandra[4], Peschel Andrea[2], Kain Renate[2], Saiko Philipp[7], Szekeres Thomas[7], Kenner Lukas[2], Hassler Melanie R.[2], Diaz Rene[8], Frisch Richard[8], Dirsch Verena M.[4], Jäger Walter[5], de Martin Rainer[9], Bochkov Valery N.[10], Passreiter Claus M.[11], Peter-Vörösmarty Barbara[12], Mader Robert M.[13], Grusch Michael[12], Dolznig Helmut[1], Kopp Brigitte[4], Zupko Istvan[14], Hohmann Judit[3], Krupitza Georg[2]

[1]Institute of Medical Genetics, Medical University of Vienna, Währinger Strasse 10, A-1090 Vienna, Austria,

[2]Clinical Institute of Pathology, Medical University of Vienna, Waehringer Guertel 18-20, Austria,

[3]Department of Pharmacognosy, University of Szeged, Eotvos Str. 6, H-6720 Szeged, Hungary,

[4]Department of Pharmacognosy, University of Vienna, Althanstrasse 14, A-1090 Vienna, Austria,

[5]Department of Clinical Pharmacy and Diagnostics, University of Vienna, Althanstrasse 14, A-1090 Vienna, Austria,

[6]Department of Preclinic, Faculty of Medicine, Mahasarakham University, Mahasarakham, 44000 Thailand,

[7]Department of Medical and Chemical Laboratory Diagnostics, Medical University of Vienna, Waehringer Guertel 18-20, Austria,

[8]Institute for Ethnobiology, Playa Diana, San José/Petén, Guatemala,

[9]Department of Vascular Biology and Thrombosis Research, Center of Biomolecular Medicine and Pharmacology, Medical University of Vienna, Schwarzspanierstraße 17, A-1090 Vienna, Austria,

[10]Institute of Pharmaceutical Sciences, University of Graz, Schubertstraße 1, A-8010 Graz, Austria,

[11]Institute of Pharmaceutical Biology and Biotechnology, Heinrich-Heine-University Düsseldorf, Universitätsstrasse 1, D-40225 Düsseldorf, Germany,

[12]Department of Medicine I, Division: Institute of Cancer Research, Comprehensive Cancer Center, Medical University Vienna, Borschkegasse 8a, A-1090 Vienna, Austria,

[13]Department of Medicine I, Comprehensive Cancer Center, Medical University Vienna, Waehringer Guertel 18-20, A-1090 Vienna, Austria,

[14]Department of Pharmacodynamics and Biopharmacy, University of Szeged, H-6720 Szeged, Hungary.

* equal contribution

Short title: Neurolenin B inhibits NPM/ALK and tumour cell intravasation in vitro

Correspondence: Georg Krupitza, Institute of Clinical Pathology, Medical University of Vienna, Waehringer Guertel 18-20, A-1090, Vienna, Austria,
e-mail: georg.krupitza@meduniwien.ac.at

1

146

Abstract

The t(2;5)(p23;q35) chromosomal translocation results in the expression of the fusion protein NPM/ALK that when expressed in T-lymphocytes gives rise to anaplastic large cell lymphomas (ALCL). In search of new therapy options the dichloromethane extract of the ethnomedicinal plant *Neurolaena lobata* was shown to inhibit NPM/ALK expression. Therefore, we isolated the active principles inhibiting tumour cell growth and tested them in ALCL cells and in a model focussing on lymph node metastasis.

NPM/ALK+ ALCL, leukaemia and breast cancer cells, and normal peripheral blood mononuclear cells (PBMCs) were treated with isolated sesquiterpene lactones and analysed for cell cycle progression, proliferation, mitochondrial activity, apoptosis, protein and mRNA expression, NF-κB and cytochrome P450 activity, 12(S)-HETE production and lymphendothelial intravasation.

In vitro treatment of ALCL by neurolenin B suppressed NPM/ALK, JunB and PDGF-Rβ expression, inhibited the growth of ALCL cells in G2/M phase, and induced apoptosis via caspase 3 without compromising mitochondrial activity (as a measure of general exogenic toxicity). Moreover, neurolenin B attenuated tumour spheroid intravasation probably through inhibition of NF-κB and CYP1A1. Hence, neurolenin B specifically targeted pro-carcinogenic mechanisms since normal PBMCs were not harmed by neurolenin B. The specific anti-cancer mechanisms of neurolenin B involved:

I) inhibition of NPM/ALK and, consequently ALCL cells were more sensitive to neurolenin B treatment than ALK-negative HL60 cells.

II) inhibition of NF-κB and hence, a mechanism by which tumours intravasate/extravasate lymphatics.

Neurolenin B may open new options to treat ALCL and to manage early metastatic processes to which no other therapies exist.

Key words: Neurolenins, NPM/ALK, ALCL, lymphendothelial intravasation, 3D-compound testing

2

Abbreviations

ALCL anaplastic large cell lymphoma

ALOX   lipoxygenase A

CCID   circular chemorepellent induced defect

CYP   cytochrome P450

DMA dichloro methane extract

EROD   ethoxyresorufin-O-deethylase

HO/PI Hoechst 33258/propidium iodide

LEC   lymph endothelial cell

MYPT1   myosin phosphatase 1 target subunit 1

NF-κB nuclear factor kappa B

NPM/ALK nucleophosmin/anaplastic lymphoma kinase; the t(2;5)(p23;q35) chromosomal

translocation

PARP poly ADP-ribose polymerase

PBMC peripheral blood mononuclear cell

PDGF-Rβ platelet derived growth factor receptor

p21 tumour suppressor protein 21

3D   3-dimensional

12(S)-HETE   12(S) hydroxyeicosatetraenoic acid

Introduction

Traditionally, plants have been used as remedies to treat and cure diseases including tumours. In fact, more than 60% of the currently used anti-cancer agents are derivatives of natural products (**Cragg and Newman 2013**). The example of vincristine (compound of *Catharanthus roseus,* the Madagaskar periwinkle) shows that a home remedy for the treatment of haemorrhage, scurvy, toothache, wounds, diabetic ulcers and hyperglycaemia (**Gidding et al. 1999**) was finally developed as a drug for the treatment of various cancer types. Hence, *C. roseus*, which was not initially used against malignancies, nevertheless contains anti-neoplastic properties. To this end we investigated the Central American plant *Neurolaena lobata* (L.) R.Br. ex Cass. (Asteraceae), which is pharmacologically active and used against ulcers, inflammatory skin disorders, malaria, ringworm, dysentery and fungal infections (**Giron et al. 1991, Amiguet et al. 2005**). Since inflammation and cancer often share similar cellular signalling pathways it was important that the dichloromethane fraction of the MeOH leaf extract and the EtOH leaf extract were inhibitory in rodent inflammation models (**McKinnon et al. in press, de Las Heras et al. 1998**), indicating that the extracts still contained *in vivo* active principles (**Butterweck and Nahrstedt 2012**).

It has recently been shown that the apolar extract of *N. lobata* inhibited the expression of the fusion onco-protein NPM/ALK (**Unger at al. 2013**), which is generated by the t(2;5)(p23;q35) translocation and responsible for the development of ALCL (**Morris et al. 1994**) occurring mostly in patients at young age. The standard combination therapy (consisting of cyclophosphamide, doxorubicine, vincristine and prednisone) does not directly target the oncogenes that are involved in ALCL (NPM/ALK, JunB, PDGFR) and is known to damage DNA. This increases the likelihood of developing secondary malignancies later in life. To provide more specificity and reducing the risk of recurrent disease and consecutive cancer synthetic inhibitors particularly targeting ALK, Critozinib and NVP-TAE-684 (**Galkin et al. 2007**), have been developed and tested in clinical trials. Here we studied natural products that interfere with NPM/ALK expression to decide about the feasibility of the development of a new drug from the isolated leads.

4

Methods

Plant material fine chemicals and antibodies

Extraction, isolation and quantification of *N. lobata* germacranolide sesquiterpene lactones
are described by **McKinnon et al. (in press)**. *N. lobata* compounds were dissolved in DMSO
(Sigma-Aldrich, St. Louis, MO, USA) as 1000-fold concentrated stock solutions. ALK-
inhibitor NVP-TAE-684 (TAE-684) was from Selleckchem (Houston, TX, USA).
CD246 anti-ALK protein mouse monoclonal antibody (mAB) and anti-nucleophosmin mouse
mAB, were from Dako Cytomation (Glostrup, Denmark), PDGF-Rβ rabbit mAB and caspase
3 polyclonal antibody (pAB) from Cell Signaling (Cambridge, UK). PARP-1 mouse mAB,
JunB rabbit pAB, JunD rabbit pAB, c-Jun rabbit pAB, and p21 rabbit pAB were from Santa
Cruz Biotechnology Inc. (Santa Cruz, CA, USA). Anti ß-actin (ascites fluid) mouse mAB was
ordered from Sigma (St. Louis, MO, USA).

Cell culture

SR-786 NPM/ALK positive human ALCL (anaplastic large cell lymphoma) cells were from
DSMZ (Braunschweig, Germany), CD-417 NPM/ALK positive mouse ALCL cells were
isolated from *CD4*-NPM/ALK mice, HL60 (human promyelocytic leukemia cells) were
obtained from ATCC (Manassas, VA, USA). All cells were grown in RPMI 1640 medium
(Life Technologies, Carlsbad, California, USA) supplemented with 10% heat inactivated fetal
calf serum (FCS, Life Technologies, Carlsbad, California, USA), 1% L-glutamine (Lonza,
Verviers, Belgium) and 1% antibiotics (penicillin/streptomycin (PS), Sigma-Aldrich, St.
Louis, MO, USA) and maintained in a humidified atmosphere containing 5% CO_2 at 37°C.

Isolation of peripheral blood mononuclear cells (PBMCs)

With the informed consent of the donors, PBMCs were isolated from human peripheral blood
by density-gradient centrifugation. 50 ml blood were collected by using a heparin
(anticoagulants, Sigma-Aldrich, St. Louis, MO, USA) coated syringe. Then, blood was
diluted with an equal volume of PBS (1x DPBS, Lonza, Verviers, Belgium) and afterwards
two parts of diluted cell suspension were carefully laid over one part Ficoll-Paque Plus (GE
Healthcare, Little Chalfont, United Kingdom) in a conical tube and centrifuged at 400 x g for
35 min without brake. The upper layer (plasma) was aspirated by leaving the white cell layer
(mononuclear cell layer-PBMC) undisturbed at the interface. PBMCs were transferred to a
new tube by trying to retrieve all cells from the interface without disturbing the red pellet

5

(erythrocytes) at the bottom of the Ficoll layer. Then, an equal volume of PBS was added to wash PBMCs. Cells were gently mixed and centrifuged at 300 x g for 7 min. The supernatant was discarded and the pellet was resuspended in PBS and centrifuged at the same conditions as before. To increase purity two further washing steps were performed at 200 x g. Finally, cells were re-suspended in culture media. All steps were performed at room temperature.

Proliferation assay

To determine which compounds of *N. lobata* inhibit proliferation, SR-786, CD-417, PBMC and HL60 were first counted by using a Casy cell counter (Roche Innovatis AG, Bielefeld, Germany). All cell lines were seeded in a 24-well plate, SR-786 at a concentration of 2×10^5 cells/ml, CD-417 cells at a concentration of 1×10^6 cells/ml, PBMC at a concentration of 5×10^5 and HL60 cells at a concentration of 1×10^5 cells/ml. Then, cells were incubated with 1 μM or 3 μM of the compounds for the indicated times. All experiments were carried out in quadruplicate.

Western blotting

SR-786 cells were seeded at a concentration of 2×10^5 cells/ml and CD-417 at a concentration of 10^6 cells/ml in 6 cm dishes. After treating cells with 3 μM of *N. lobata* compounds for the indicated times they were harvested and lysed in RIPA buffer (150 mM NaCl, 50 mM Tris pH 7.6, 1 % Triton, 0.1 % SDS, 0.5% Sodium deoxycholate) containing 1 mM phenylmethylsulfonyl (PMSF, Sigma-Aldrich, St. Louis, MO, USA) and 1 mM protease inhibitor mixture (PIM consists of 2 μg/ml leupeptin, 2 μg/ml aprotinin, 0.3 μg/ml benzamidine chloride and 10 μg/ml trypsin inhibitor, Sigma-Aldrich, St. Louis, MO, USA) followed by a short incubation of 5 min on ice. Lysates were centrifuged at 15000 x G for 20 min at 4°C to pellet un-dissolved matter. Supernatant was transferred into an Eppendorf tube and stored at -20°C until further analysis. Protein concentration was determined by Bradford assay (Protein Assay Dye reagent Concentrate, BioRad, Hercules, CA, USA). 1 μl of sample was added to 500 μl Bradford solution in a cuvette and resuspended followed by 5 min of incubation. The solution was measured at 595 nm by using a Bio-Photometer (Eppendorf, Hamburg, Germany). SDS electrophoresis, electro-transfer to PVDF and nitrocellulose membranes (Whatman, Dassel, Germany), and antibody reactions were as described by **Unger et al. (2013)**. Chemiluminescence was developed by ECL detection kit (Thermo Scientific, Waltham, MA, USA) and membranes were exposed to Amersham Hyperfilms (GE Healthcare, Buckinghamshire, UK) or CL-XPosure films (Thermo Scientific, Rockford, IL,

6

USA). In order to apply consecutive antibodies the former antibodies were stripped off the membranes. For this, membranes were placed in 75 ml stripping buffer (4.5 ml 1M Tris-HCL pH 6.4; 7.5 ml 20% SDS; 0.5 ml β-mercaptoethanol, dH$_2$O up to 75 ml) for 6-15 min shaking in a 55°C water bath and afterwards the membranes were washed. Then, free non-specific binding sites were blocked by agitating membranes in TBS/T-milk at room temperature for 1 h.

Quantitative RT-PCR

SR-786 cells were seeded in a 24-well plate at a concentration of 2 x 10^5 cells/ml and incubated overnight before treatment with 3 μM of *N. lobata* compounds. After 1, 2, 4 and 8 h cells were harvested, washed twice with cold PBS and centrifuged at 800 rpm for 5 min at 4°C. As control a sample was taken at the beginning of the experiments before the compounds were added. For RNA preparation ReliaPrep™ RNA Cell Miniprep System Kit (Promega, Madison, WI) was used according to the guidelines of the manufacturer. The concentration of the purified RNA was measured using a NanoDrop fluorospectrometer (Thermo Fisher Scientific, Waltham, MA, USA) and RNA samples were stored at -80°C until further use. The entire procedure was performed on ice. First-strand cDNA synthesis was carried out with 150 ng RNA by using GoScriptTM Reverse Transcription System Kit (Promega, Madison, WI). The cDNA was stored at -20°C for further use. Before proceeding with qPCR the reverse transcriptase was inactivated by heating samples to 70°C for 15 min. The expression of NPM/ALK, JunB and nucleophosmin transcript levels in SR-786 cells after treatment with active *N. lobata* compounds was examined by real-time PCR (polymerase chain reaction) using a SYBR Green detection system (Promega, Madison, WI). The housekeeping gene GAPDH (glyceralaldehyde 3-phosphat dehydrogenase), which is stably and constitutively expressed at high levels in most tissues and cells served as reference gene for qPCR normalisation. For each sample, 10 μl GoTaq qPCR Master Mix (premixed solution containing GoTaq DNA polymerase, GoTaq Reaction Buffer, dNTPs and Mg^{2+}; Promega, Madison, WI) 2 μl forward primer and 2 μl reverse primer (see sequences below), 5 μl nuclease free water and 1 μl cDNA, were added to the wells of a 96-well optical reaction plate. Real time PCR was carried out in quadruplicate for each cDNA template. Water instead of cDNA served as negative control. The cycle program was: 50°C for 2 min, 95°C for 10 min to activate polymerase, 40 cycles of 95°C for 15 sec and 60°C for 1 min. (Thermocycler Primus25 advanced, Peqlab, Erlangen, Germany). The following primers were used for RT-PCR:

7

NPM/ALK (fwd: 5′-GTG GTC TTA AGG TTG AAG TGT GGT T-3′; rev: 5′-GCT TCC GGC GGT ACA CTA CTA A-3′);

nucleophosmin (fwd: 5′-TCC CTT GGG GGC TTT GAA ATA ACA CC-3′; rev: 5′-TGG AAC CTT GCT ACC ACC TC-3′);

JunB (fwd: 5′-GCT CGG TTT CAG GAG TTT GT-3′; rev: 5′-ATA CAC AGC TAC GGG ATA CGG-3′);

GAPDH (fwd: 5′- AAC AGC GAC ACC CAC TCC TC -3′; rev: 5′- CAT ACC AGG AAA TGA GCT TGA CAA -3′).

To analyse qPCR data, the Ct ($\Delta\Delta$Ct) method (**Livak and Schmittgen 2001**) for relative quantification of gene expression was used. To quantify relative expression of the target genes NPM/ALK, nucleophosmin and JunB the following formula was used: ΔCt = Ct target gene (NPM/ALK, nucleophosmin, JunB) – $\bar{x}$ Ct control gene (GAPDH); $\Delta\Delta$Ct = ΔCt drug treatment – $\bar{x}\Delta$Ct control sample; Ratio = 2-$\Delta\Delta$Ct.

Cell cycle progression (FACS-analysis)

SR-786 cells were seeded in a 6-well plate at a concentration of 2×10^5 cells/ml followed by a short incubation of 1 h at 37°C. Concentrated stock solutions of *N. lobata* compounds were diluted in PBS before they were added to the cells at a final concentration of 3 μM. After 8 and 24 h of incubation at 37°C, cells were harvested and centrifuged at 800 rpm for 5 min at 4°C. Supernatants were discarded, cell pellets washed with cold PBS and centrifuged at 800 rpm for 5 min at 4°C. Pellets were re suspended in 1 ml cold 80% ethanol, and either fixed for 30 min at 4°C or stored at -20°C until further handling. After two washing steps with cold PBS (centrifugations at 600 rpm) supernatants were removed, cell pellets re suspended in 500 μl cold PBS, and transferred into a 5 ml polystyrene round bottom tube. Next, to each sample RNAse A and propidium iodide were added to a final concentration of 50 μg/ml and incubated for 2 h at 4°C and the final cell number was adjusted to 1×10^6 cells in 500 μl. Cells were analysed on a FACS Calibur flow cytometer (BD Bioscience, Franklin Lakes, New Jersey, USA). Experiments were performed in triplicate.

Cytotoxicity, mitochondrial activity assay

To evaluate mitochondrial activity and cytotoxicity, CellTiter-Blue assay (Promega, Madison, WI) was applied. HL60, SR-786 cells and PBMC were seeded into 96-well plates at concentrations of 1×10^5, 2×10^5 and 5×10^5 cells/ml, respectively, and each well was filled up to 250 μl with the cell suspensions. Compounds were added at the indicated concentrations

8

and compared to solvent-treated controls. After 8 h and 24 h 25 µl CellTiter-Blue reagent were added to each well and incubated for 120 min at 37°C until the colour changed from blue to pink. Afterwards, the 96-well plates were placed into a multi-detection reader to measure fluorescence at 570 nm (Synergy HT, Bio-Tek Instrument, Winooski, VT, USA). Experiments were done in quadruplicate. To eliminate possible background fluorescence of the medium, the mean blank value consisting of medium and CellTiter-Blue reagent was subtracted from all other measured values. The mitochondrial metabolic activity of the untreated control cells was set as 100%. All experiments were performed with an active and an inactive compound of *N. lobata* and with the ALK-inhibitor TAE-684.

Cell death analysis – (HO/PI staining)

Hoechst 33258 (HO) and propidium iodide (PI) double staining (Sigma-Aldrich, St. Louis, MO, USA) allows the determination of the cell death type, apoptosis or necrosis (**Grusch et al. 2002**). SR-786 cells were seeded in a 96-well flat bottom plate at concentrations of 2×10^5 cells/ml. Each well contained 100 µL cell suspensions and was treated with a concentration of 3 µM *N. lobata* compounds. After 24 h of incubation HO/PI were added at final concentrations of 50 µg/ml and 20 µg/ml. After 1 h of incubation at 37°C, stained cells were photographed using a fluorescence microscope (Olympus IX51, Shinjuku, Tokyo, Japan). The fluorescence microscope was equipped with a TRITC and DAPI filter. Photographs were visually examined to count the cell number and type of cell death (necrosis or apoptosis). Experiments were performed in quadruplicate.

Caspase 3/7 activity assay

The Apo-ONE Homogeneous Caspase-3/7 assay (Promega, Madison, WI) was used to monitor caspase 3/7 activation. SR-786 cells were seeded in 3.5 cm dishes at a concentration of 2×10^5 cell/ml and after incubation of 1 h at 37°C cells were treated with 3 µg/ml of *N. lobata* compounds. After 8, 16 and 24 h 25 µl of the treated cell suspension and 25 µl of untreated control were transferred into a 96-well plate. 25 µl of the substrate buffer solution (10 µl caspase substrate Z-DEVD-R110 (100X) added to 1 ml Apo-ONE Homogeneous caspase-3/7 buffer) were added to each well. The plate was agitated (300 rpm) on a shaker for 30 min and then, fluorescence was measured by using a multi-detection reader (excitation at 499 nm and emission at 521 nm). Experiments were performed in triplicate.

NF-κB transactivation assay

The transactivation of a NF-κB-driven luciferase reporter was quantified in HEK293/NF-κB-luc cells (Panomics, RC0014) as previously described (**Rozema et al. 2012, Xie LW et al. 2014**). The cells were maintained at 37°C and 5% CO_2 in Dulbecco's modified Eagle's medium (DMEM; Lonza, Basel, Switzerland) supplemented with 2 mM glutamine, 100 µg/ml hygromycin B, 100 U/ml benzylpenicillin, 100 µg/ml streptomycin, and 10% FCS. One day before the experiment, cells were stained by incubation for 1 h in serum-free medium supplemented with 2 µM Cell Tracker Green CMFDA (C2925; Invitrogen). Cells were then reseeded in 96-well plates at a density of 4×10^4 cells/well in phenol red-free and FCS-free DMEM overnight. Cells were pretreated with the indicated compounds for 30 min prior to stimulation with 2 ng/ml TNF-α (Sigma–Aldrich, Vienna, Austria) for 4 h. The final concentration of DMSO in the experiments was 0.1% or lower. An equal amount of DMSO was always tested in each experiment to assure that the solvent vehicle does not influence the results. After cell lysis the luminescence of the firefly luciferase and the fluorescence of the Cell Tracker Green CMFDA were quantified on a GeniosPro plate reader (Tecan, Grödig, Austria). The luciferase-derived signal from the NF-κB reporter was normalized by the Cell Tracker Green CMFDA-derived fluorescence to account for differences in the cell number. The known NF-κB inhibitor parthenolide (Sigma–Aldrich, Vienna, Austria) was used as a positive control.

Circular chemorepellent induced defect (CCID) assay

In the CCID assay the size of the cell-free area within the lymphendothelial cell (LEC) monolayer, which forms underneath 12(S)-HETE-secreting MCF-7 spheroids, is measured (**Madlener et al. 2010, Vonach et al. 2011, Kerjaschki et al. 2011, Giessrigl et al. 2012, Viola et al. 2013a, Viola 2013b, Kretschy et al. 2013, Kopf et al. 2013, Teichmann et al. 2014**). MCF-7 spheroids were washed in PBS, pretreated with indicated compounds for 30 min and transferred to cytotracker-stained LEC monolayers that were grown to confluence in 24-well plates (Costar 3524, Sigma-Aldrich, Munich, Germany) in 2 ml EGM2 MV medium. After 4 h of co-incubation, the CCID areas in the LEC monolayers underneath the MCF-7 spheroids were photographed using an Axiovert (Zeiss, Jena, Germany) fluorescence microscope to visualise cytotracker(green)-stained LECs underneath the spheroids. CCID areas were calculated with ZEN 2012 software (Zeiss, Jena, Germany). DMSO-treated co-cultures served as negative control. For each condition the CCID sizes of 10 or more spheroids (unless otherwise specified) were measured. During the experiments, which were

10

short term, we did not observe toxic effects of the tested compounds (monitored by HOPI staining; **Grusch et al. 2002**).

12(S)-HETE assay

The concentration of 12(S)-HETE in the cellular supernatant was measured with minor modifications as described previously (**Kretschy et al 2013, Kopf et al. 2013**). Briefly, MCF-7 cells, which were cultivated in MEM medium (Gibco # 10370-047) supplemented with 10% FCS, were seeded in 3.5 cm dishes and grown in 2.5 ml complete MEM medium. The next day, the medium was changed to FCS-free medium and cells were kept at 37°C for 24 h. Then, cells were treated with 10 μM arachidonic acid (#A3555, Sigma-Aldrich, Munich, Germany) and simultaneously with different concentrations of the indicated compounds for 24 h when the supernatants were aspirated, centrifuged at 2000 rpm at 4°C for 5 min. Then, 2.5 ml of medium samples were passed through extraction cartridges (OasisTM HLB 1cc, Waters, Milford, MA; equilibrated with 2 x 1 ml methanol, 2 x 1 ml distilled H_2O immediately before use) followed by washing of cartridges with 3 x 1 ml distilled H_2O. Bound 12(S)-HETE was eluted with 1000 μl methanol. After the evaporation of methanol with a speedvac concentrator the samples were reconstituted with 250 μl assay buffer of the 12(S)-HETE enzyme immunoassay kit (EIA, # ADI-900-050; Enzo Life Sciences, Lausen, Switzerland) and sample volumes of 100 μl each were subjected to 12(S)-HETE analysis according to the manufacturer´s instructions (**Kretschy et al 2013, Kopf et al. 2013**). Absorbance was measured with a Wallac 1420 Victor 2 multilabel plate reader (Perkin Elmer Life and Analytical Sciences).

Ethoxyresorufin-O-deethylase (EROD) assay selective for CYP1A1 activity

CYP 1A1 activity was measured with minor modifications as previously described (**Viola et al. 2013b**). Briefly, MCF-7 breast cancer cells were grown in phenol red-free DMEM/F-12 tissue culture medium (Gibco, Karlsruhe, Germany), supplemented with 10% FCS and 1% PS (Invitrogen, Karlsruhe, Germany) under standard conditions at 37°C in a humidified atmosphere containing 5% CO_2 and 95% air. Before treatment, the cells were transferred to DMEM/F-12 medium supplemented with 10% charcoal-stripped FCS (PAN Biotech, Aldenbach, Germany) and 1% PS. After 24 h of incubation with or without drugs of the indicated concentrations (which were dissolved in DMSO and diluted with medium to a final DMSO concentration < 0.1%), ethoxyresorufin (final concentration 5.0 μM, Sigma-Aldrich, Munich, Germany) was added and 0.4 ml aliquots of the medium were sampled after 180 min.

11

Negative controls contained DMSO. Experiments under each set of condition were carried out in quadruplicate. Subsequently, the formation of resorufin was analysed by spectrofluorometry (PerkinElmer LS50B, Waltham, MA, USA) with an excitation wavelength of 530 nm and an emission wavelength of 585 nm.

Statistical analysis

For statistical analyses Excel 2003 software and Prism 5 software package (GraphPad, San Diego, CA, USA) were used. The values were expressed as mean ± SD and the Student t-test or ANOVA and Dunnett-post-test were used to evaluate statistical significance ($p < 0.05$).

Results

Anti-proliferative effects of *N. lobata* germacranolide sesquiterpene lactones

ALK- positive ALCL cells (SR-786 and CD-417) were treated with 1 µM and 3 µM of lobatin A, neurolenin A, B, C and D (**Fig. 1a**), and the proliferation of human SR-786- (**Fig. 1b**) and murine CD-417 cells (**Fig. 1c**) was examined. Neurolenin B inhibited the growth of both cell lines effectively in a dose- and time-dependent manner, whereby murine CD-417 cells responded more sensitively to 3 µM neurolenin B treatment than human SR-786 cells. 3 µM neurolenin C and D inhibited cell proliferation only weakly, but lobatin A and neurolenin A showed no significant effect. Hence, further investigations were conducted with neurolenin B and compared to the closely related but least active compound, neurolenin A.

Mitochondrial activity and cell cycle distribution upon neurolenin A and B treatment

CellTiter-Blue assay was performed to evaluate the effect of neurolenin B treatment on mitochondrial metabolism. The mitochondrial activity of SR-786 cells was weakly but significantly inhibited by 3 µM neurolenin B, and interestingly, also by neurolenin A (**Fig. 2a**). Treatment of SR-786 cells with 3 µM neurolenin B for 8 h caused their accumulation in G2/M phase to the detriment of G1 cells as evidenced by FACS analysis (**Fig. 2b**). The decreased G1 fraction together with an increased cell number in G2/M implicated that cells maintained their capability to pass through S-phase despite neurolenin B treatment, whereas G2/M passage was arrested. Consequently, neurolenin B treatment blocked the cell cycle of ALK-positive ALCL in G2/M. Neurolenin A treatment showed no effect on cell cycle distribution. The effects on mitochondrial metabolism by neurolenin A and B correlated neither with cell cycle alterations nor with the inhibition of cell proliferation.

Neurolenin B modulates the expression of regulators of ALK+ALCL proliferation

It is widely accepted that the ALK translocation in ALCL cells causes enhanced proliferation and renders cells insensitive to death signals and therefore causes the expansion of the ALCL population. Hence, blocking the signalling cascade triggered by NPM/ALK is considered as a target for therapeutic intervention. To study whether neurolenin B treatment affected the expression of the NPM/ALK chimera, Western blot analysis was performed. Neurolenin B treatment caused a striking down-regulation of NPM/ALK in human SR-786 cells after 8 h

13

(**Fig. 3a**), whereas in murine CD-417 cells NPM/ALK expression was inhibited already after 4 h (**Fig. 3b**). Previous studies have shown that JunB expression is regulated by NPM/ALK (**Laimer et al. 2012, Staber et al. 2007**) and therefore, the expression of the Jun family upon neurolenin A and B treatment was analysed. JunB levels were downregulated in SR-786 and CD-417 cells by neurolenin B (after 24 h and 8 h, respectively), JunD was suppressed by neurolenin A and B after 24 h, and c-Jun by neurolenin A after 24 h, although neurolenin A had no significant effect on ALCL proliferation. This indicated that only JunB is forcing ALCL cells to replicate (**Staber et al. 2007**), which is in agreement with the fact that JunB is the major component of the AP-1 complex in ALCL cells (**Mathas et al. 2002**). Unlike neurolenin A, neurolenin B enhanced c-Jun expression without rescuing the cells from the oncolytic effects of this compound. To the contrary, c-Jun expression correlated with p21 up-regulation. It was shown that c-Jun together with SP1 transactivates p21 expression (**Kardassis et al. 1999**) and we demonstrated that increased p21 expression directly correlates with c-jun expression upon treatment with neurolenin B and the dichloro-methane extract (DME) of *N. lobata* (**Unger et al. 2013**). JunB promotes ALCL development through transcriptional regulation of PDGF-Rß (**Laimer et al. 2012**). Since PDGF-Rß is not expressed in the human SR-786 cell line, murine ALCL CD-417 cells were used to test the impact of neurolenin B on PDGF-Rß expression. The inhibition of NPM/ALK expression (after 4 h) was followed by the inhibition of JunB and PDGF-Rβ (**Fig. 3b**) according to the recently discovered NPM/ALK signal transduction cascade (**Laimer et al. 2012**). Although neurolenin A inhibited the expression of NPM/ALK, but also that of c-Jun and p21 in SR-786 cells after 24 h, this may have been the reason why neurolenin A did not attenuate the proliferation of ALCL cells. Furthermore, this indicated that neurolenin A treatment (for 24 h) disconnects JunB from the direct control by NPM/ALK.

<u>Neurolenin B decreases the NPM/ALK transcript level</u>

To elucidate at which stage NPM/ALK was regulated by neurolenin B, the mRNA level was measured in SR-786 cells. Neurolenin B decreased NPM/ALK transcripts and also JunB mRNA (**Fig. 4a, b**) consistent with the findings reported earlier (**Laimer et al. 2012, Staber et al. 2007**). Interestingly, neurolenin B induced rather than inhibited the mRNA expression of nucleophosmin (**Fig. 4c**) indicating that the 5´part of the nucleophosmin genomic sequence was not a target of neurolenin B.

<u>Apoptotic and necrotic effects of neurolenin B</u>

14

In order to examine whether neurolenin B induces cell death, Western blot analysis detecting caspase 3 activation was performed (**Fig. 5a**). After 24 h of neurolenin B treatment caspase 3 was cleaved and PARP signature-type degraded, whereas PARP and caspase 3 remained unaffected upon neurolenin A treatment. An independent assay monitoring caspase 3/7 activity confirmed the Western blot data (**Fig. 5b**). Neurolenin B treatment led to increased caspase 3/7 activity within 16 h. Cell death results were supported by HO/PI double staining. Neurolenin B treatment induced cell death, whereby significantly more apoptotic than necrotic cells were counted (**Fig. 5c**).

Impact of neurolenin B on NPM/ALK negative cell types

Neither neurolenin A nor neurolenin B treatment decreased PBMC numbers (**Fig. 6a**). Interestingly, the mitochondrial activity increased upon treatment with neurolenin B for 8 h (**Fig. 6b**) but returned to control levels thereafter. In contrast, the HL60 cell number decreased upon neurolenin B treatment (**Fig. 6a**) and also the mitochondrial activity of HL60 cells was significantly reduced after 24 h (**Fig. 6b**). Thus, also the proliferation of leukaemia cells that are not harbouring the NPM/ALK translocation was affected by neurolenin B. Sesquiterpene lactones are potent inhibitors of NF-κB (**Kwok et al. 2001**) and the permanently over-activated NF-κB pathway in HL60 cells (**Kang et al. 2009**) may have been a target of neurolenin B thereby reducing their expansion. This was a likely mechanism of neurolenin B exhibiting anti-leukaemia/lymphoma specificity but leaving normal blood cells unaffected that do not rely on NF-κB.

Effects of the specific ALK inhibitor TAE-684 in CD-417 cells

To test whether a specific ALK inhibitor performs similarly to neurolenin B, CD-417 cells were treated with TAE-684 and protein expression was investigated. We used this mouse ALCL cell line to monitor also PDGF-Rß, which is not expressed in human SR-786 cells. 10 nM TAE-684 inhibited significantly the proliferation of CD-417 cells after 24 h but induced cell growth within 8 h (**Fig. 7a**), which was also observed for neurolenin C and D (**Fig. 1**). NPM/ALK activity was down-regulated by TAE-684 treatment and consequently JunB expression was inhibited after 4 h and PDGF-Rß suppressed after 24 h (**Fig. 7b**). The NPM/ALK protein level remained unaffected, because TAE-684 interferes with the phosphorylation of ALK and thus, inhibits its activity but not its expression.

15

<u>Neurolenin B inhibits NF-κB and the intravasation of tumour spheroids through the</u>
<u>lymphendothelial barrier</u>

As mentioned above, sesquiterpene lactones inhibit NF-κB (**Kwok et al. 2001**) and this was likely the cause for the anti-proliferative effect of neurolenin B in HL60 cells (**Kang et al. 2009**). *N. lobata* is traditionally used against inflammation, which is a process involving major protagonists i.e. lipoxygenases and the transcription factor NF-κB. Moreover, lipoxygenases ALOX12/15 and NF-κB play major roles in tumour intravasation into the lymphatic vasculature and lymph node metastasis (**Kerjaschki et al. 2011, Vonach et al. 2011, Viola et al. 2013a**). Therefore, neurolenin B was tested by a luciferase assay reporting NF-κB activity and by a 12(S)-HETE immuno adsorbent assay reflecting ALOX12/15 activity, which showed that neurolenin B significantly and dose-dependently inhibited NF-κB-driven luciferase expression (**Fig. 8a**), but not 12(S)-HETE production (**Fig. 8b**). To investigate whether the NF-κB-inhibitory property of neurolenin B inhibits also the intravasation of tumour emboli through the lymphendothelial barrier we used a validated three-dimensional model consisting of MCF7 tumour cell spheroids that are co-cultivated with lymphendothelial cell (LEC) monolayers (**Viola et al. 2013b, Kopf et al. 2013, Kretschy et al. 2013, Teichmann et al. 2014**). Neurolenin B significantly inhibited the formation of "circular chemorepellent induced defects" (CCIDs) within the LEC monolayer, which are areas through which tumours transmigrate and colonise lymph nodes (**Fig. 8c**). Also CYP1A1 is a protagonist speculated to contribute to tumour intravasation (**Viola et al. 2013b, Kopf et al. 2013**) and neurolenin B inhibited CYP1A1 dose dependently (**Fig. 8d**). Hence, it is likely that neurolenin B inhibited CCID formation due to the inactivation of NF-κB and CYPs.

16

161

Discussion

The focus of this research was on studying five isolated germacranolide sesquiterpene lactones of the traditional medicinal plant *N. lobata* (**Passreiter et al. 1995**), in particular neurolenin B, regarding anti-neoplastic and anti-metastatic activities and seeking a new promising therapy for NPM/ALK positive ALCL. In an earlier study it has been reported that the DME of *N. lobata* is able to suppress NPM/ALK (**Unger et al. 2013**) and here we demonstrate that also neurolenin B downregulated NPM/ALK mRNA and protein levels. The 5′part of nucleophosmin is fused in frame to truncated ALK in the t(2;5)(p23;q35) (NPM/ALK) chromosomal translocation whereby the regulatory sequences upstream of the nucleophosmin start codon are maintained in the NPM/ALK chimera. Since neurolenin B caused an increase of nucleophosmin mRNA this implicated that this compound did not regulate nucleophosmin expression directly at the gene- or transcription factor level, but rather indirectly at various potential levels. Future studies have to focus on the details of these mechanisms. As a consequence of NPM/ALK downregulation by neurolenin B, JunB and PDGF-Rβ were subsequently inhibited, which is in agreement with the observation of **Laimer et al. (2012)**. Furthermore, neurolenin B caused the upregulation of c-Jun and p21 and this certainly contributed to the observed accumulation of cells in G2/M-phase and decrease of G1-phase cells. Induced c-Jun levels transactivate SP-1-mediated induction of p21 causing G2/M arrest of ALK+ ALCL (**Kardassis et al. 1999, Leventaki et al. 2007**). The mechanism of c-Jun upregulation by neurolenin B and by the DME of *N. lobata* (**Unger et al. 2013**) remains to be established. Interestingly, neurolenin A, which did not inhibit ALCL growth, down-regulated c-Jun and p21.

In addition to the specific NPM/ALK-targeting property of neurolenin B, which was clearly demonstrated by the downregulation of NPM/ALK transcript and protein expression, inhibition of JunB transcription and protein expression and suppression of PDGF-Rβ, it possesses also another anti-neoplastic property, which is based on the inhibition of NF-κB. The α-methylene-γ-lactone ring common to all sesquiterpene lactones of *N. lobata* and also of the *bona fide* NF-κB inhibitor parthenolide was reported to cause alkylation of a cysteine residue in the activation loop of IκB kinase β (**Kwok et al. 2001**) thereby preventing the degradation of IκB and hence, the translocation of NF-κB into the nucleus. This interferes with the transcription of NF-κB-dependent inflammatory cytokines in monocytes and endothelial cells (**Walshe-Roussel et al. 2013, McKinnon et al. in print**) and abrogates survival signals in neoplasias (**Gyrd-Hansen and Meier 2010**). The signalling cascade

17

downstream of NF-κB seems to be cell type specific, because in immune-relevant cells such as monocytes NF-κB activity was inhibited not only by neurolenin B but also by lobatin A (**Walshe-Roussel et al. 2013, McKinnon et al. in print**). Lobatin A was ineffective in inhibiting proliferation of ALCL and HL60 and therefore, for the anti-inflammatory activity of neurolenin B and lobatin A (but not for their anti-neoplastic activity) the acetyl group at C-9 is made responsible (**McKinnon et al. in press**). Whether these structures attenuate NF-κB-dependent tumour intravasation will be subject of continuing studies.

Although it remains a matter of debate whether NF-κB inhibition may also abrogate NPM/ALK expression (as one of the indirect options of neurolenin B interference), it is evident that tumour intravasation through the LEC barrier depends in part on NF-κB activity (**Vonach et al. 2011, Viola et al. 2013a**) and that neurolenin B inhibited CCID formation due to NF-κB inhibition (**Kwok et al. 2001**). Furthermore, the attenuation of HL60 leukaemia cell growth was most likely due to NF-κB inhibition (**Kang et al. 2009**) and also the use of *N. lobata* decoctions as an anti-inflammatory remedy (**Arvigo and Balick 1998**) is certainly based on this property. The specificity of neurolenin B towards lymphoma and leukaemia cells was substantiated by the unaffected mitochondrial activity of treated PBMCs, which did not compromise their viability either. Transiently, the mitochondrial activity became even elevated in PBMCs suggesting that an additional property of neurolenin B stimulated the immune system, which is consistent with the use of *N. lobata* as a remedy supporting wound healing.

Previous studies have presented sesquiterpene lactones as effective compounds against human adherent cancer cell lines such as A2780, A431, HeLa, MCF7, GLC4 and COLO 320 (**Lajter et al. 2014, Francois et al. 1996**) and neurolenin B was identified as one among the most active of the isolated and tested sesquiterpene lactones.

Altogether, our work and that of others indicate that cancer cells are specifically targeted by neurolenin B, i.e. by inhibition of NF-κB-mediated proliferation and intravasation signals and NPM/ALK/JunB-dependent survival signals, whereas normal cells that do not proliferate NF-κB-dependently are left unharmed. Hence these sesquiterpene lactones should be considered as a new therapeutic option for the treatment of malignant diseases.

18

Loss of miR-200 family in 5-fluorouracil resistant colon cancer drives lymphendothelial invasiveness in vitro

Robert Mader, Daniel Senfter, Silvio Holzner, Maria Kalipciyan, Anna Staribacher, Angelika Walzl, Nicole Huttary, Sigurd Krieger, **Stefan Brenner**, Walter Jäger, Georg Krupitza, and Helmut Dolznig

10 Curriculum Vitae

Name: Stefan Brenner
Date of birth: 1985-25-11
Place of birth: Wiener Neustadt
Nationality: Austria

Education:

1996 – 2004 BRG Gröhrmühlgasse with focus on natural sciences, Wiener Neustadt

2004 Final exam at the BRG Gröhrmühlgasse with focus on natural sciences

2004 – 2005 Military Service

2005 Inscription for the study of Pharmacy, University of Vienna

2011 Master thesis at the Department of Pharmacognosy, University of Vienna
Title: " Ausarbeitung der Monographie „Herba Anserinae" sowie Ergänzungen zu den Monographien „Flos Croci" und „Herba Herniariae" für das Österreichische Arzneibuch (ÖAB)"

2011 Graduation with distinction: Mag.pharm.

2011 Dissertation "Drug metabolising enzymes and cellular uptake transporters as key factors for the efficacy of anti-cancer agents", University of Vienna at the Department of Clinical Pharmacy and Diagnostics, as part of the Doctoral College (Initiativkolleg) : "BioProMoTION" Bioactivity Profiling and Metabolism.

Career:

2005 – 2009 Work experience at the pharmacy Heiland Apotheke, Wiener Neustadt during the summer months

WS 2010/11 study assistant for Univ. Prof. Mag. Dr. Dr. h. c. Brigitte Kopp

Tutor for undergraduate students:

Allgemeine Mikrobiologie und Hygiene
Identitäts- u. Reinheitprüfung biogener Arzneimittel (inkl.Arzneibuchanalytik)
Zellbiologische Übungen 1 des FH Studiengangs Molekulare Biotechnologie
Analytische Chemie I des FH Studiengangs Molekulare Biotechnologie

Assistant for undergraduate students:

Methoden zur Identifizierung und Charakterisierung arzneistofflief. Organismen

Identitäts- u. Reinheitprüfung biogener Arzneimittel (inkl. Arzneibuchanalytik)

Gewinnung und instrumentelle Analytik

Qualitative pharmazeutische Analytik

11 List of Publications

Stefan Brenner, Lukas Klameth, Juliane Riha, Madeleine Schölm, Gerhard Hamilton, Erika Bajna, Christoph Ausch, Angelika Reiner, Walter Jäger, Theresia Thalhammer and Veronika Buxhofer-Ausch; Specific expression of OATPs in primary small cell lung cancer (SCLC) cells as novel biomarkers for diagnosis and therapy; Cancer Lett. 2014 Oct 6. pii: S0304-3835(14)00552-7.

Juliane Riha, **Stefan Brenner**, Michaela Böhmdorfer, Benedikt Giessrigl, Marc Pignitter, Katharina Schueller, Theresia Thalhammer, Bruno Stieger, Veronika Somoza, Thomas Szekeres and Walter Jäger; Resveratrol and its major sulfated conjugates are substrates of organic anion transporting polypeptides (OATPs): impact on growth of ZR-75-1 breast cancer cells; Mol Nutr Food Res. 2014 Sep;58(9):1830-42.

Stefan Brenner, Juliane Riha, Benedikt Giessrigl, Theresia Thalhammer, Michael Grusch, Georg Krupitza, Bruno Stieger and Walter Jäger; The effect of organic anion-transporting polypeptides 1B1, 1B3 and 2B1 on the antitumor activity of flavopiridol against breast cancer cells; Int J Oncol. October 2014

Juliane Riha, **Stefan Brenner**, Alzbeta Srovnalova, Lukas Klameth, Zdenek Dvorak, Walter Jäger and Theresa Thalhammer; Effects of anthocyans on the expression of organic anion transporting polypeptides (OATPs) in primary human hepatocytes; Food Funct. Submitted October 2014

Michaela Böhmdorfer, Alexandra Maier-Salamon, Juliane Riha, **Stefan Brenner**, Martina Höferl, Walter Jäger; Interplay of drug metabolizing enzymes with cellular transporters; Wien Med Wochenschr. 2014 Sep 10

Kiss Izabella, Unger Christine,Nguyen Huu Chi, Atanasov Atanas Georgiev, Kramer Nina, Chatuphonprasert Waranya, **Brenner Stefan**, McKinnon Ruxandra, Peschel Andrea, Vasas Andrea, Lajter Ildikó, Kain Renate, Saiko Philipp, Szekeres Thomas, Kenner Lukas, Hassler Melanie R., Diaz Rene, Frisch Richard, Dirsch Verena M., Jäger Walter, de Martin Rainer, Bochkov Valery N., Passreiter Claus M., Peter-

Vörösmarty Barbara, Mader Robert M., Grusch Michael, Dolznig Helmut, Kopp Brigitte, Zupko Istvan, Hohmann Judit, Krupitza Georg; Lobatin B inhibits NPM/ALK and NF-κB attenuating anaplastic-large-cell-lymphomagenesis and lymphendothelial tumour intravasation; Cancer Lett. Submitted October 2014

Unger Christine, Kiss Izabella, Vasas Andrea, Lajter Ildikó, Kramer Nina, Atanasov Atanas Georgiev, Chi Nguyen Huu, Chatuphonprasert Waranya, **Brenner Stefan**, McKinnon Ruxandra, Peschel Andrea, Kain Renate, Saiko Philipp, Szekeres Thomas, Kenner Lukas, Hassler Melanie R., Diaz Rene, Frisch Richard, Dirsch Verena M., Jäger Walter, de Martin Rainer, Bochkov Valery N., Passreiter Claus M., Peter-Vörösmarty Barbara, Mader Robert M., Grusch Michael, Dolznig Helmut, Kopp Brigitte, Zupko Istvan, Hohmann Judit, Krupitza Georg; The germacranolide sesquiterpene lactone neurolenin B of the medicinal plant
Neurolaena lobata inhibits NPM/ALK-driven cell expansion and NF-κB-driven tumour Intravasation; Arch Toxicol. Submitted October 2014

Robert Mader, Daniel Senfter, Silvio Holzner, Maria Kalipciyan, Anna Staribacher, Angelika Walzl, Nicole Huttary, Sigurd Krieger, **Stefan Brenner**, Walter Jäger, Georg Krupitza, and Helmut Dolznig; Loss of miR-200 family in 5-fluorouracil resistant colon cancer drives lymphendothelial invasiveness in vitro; Oncogene Submitted October 2014

11.1 Poster Presentations

2012

Transport of flavopiridol by OATP1B1, OATP1B3 and OATP2B1: impact on cancer therapy, 19th International Symposium on Microsomes and Drug Oxidations, 12th European Regional ISSX Meeting, Noordwijk aan Zee, Netherlands

2013

Specific OATP expression pattern in primary small cell lung cancer (SCLC) cell lines: impact on diagnosis and therapy, 10th International ISSX Meeting, Toronto, Onatario, Canada